Metabolic and Cell Cycle Regulatory Networks in Kidney Tumours

Dissertation
zur
Erlangung der naturwissenschaftlichen Doktorwürde
(Dr. sc. nat.)

vorgelegt der
Mathematisch-naturwissenschaftlichen Fakultät
der
Universität Zürich

von

Sabine Harlander
aus
Deutschland

Promotionskomitee
Prof. Dr. Ian J. Frew
(Vorsitz und Leitung der Dissertation)
Prof. Dr. Wilhelm Krek
Dr. Nicola Zamboni
Dr. Rok Humar

Zürich 2014

Table of content

Summary

Clear cell renal cell carcinoma (ccRCC) is the most common type of renal cell carcinoma. The von Hippel-Lindau (*VHL*) tumour suppressor gene is biallelically inactivated in up to 90% of sporadic cases of ccRCC. The *VHL* gene product, pVHL, is involved in the regulation of diverse cellular processes whose dysregulation could be imagined to play a role in tumour formation. One of the best characterized functions is the post-transcriptional regulation of HIFα transcription factors which have multiple functions in diverse cellular processes. However, loss of pVHL function alone is not sufficient to cause tumour formation, indicating that additional cooperating mutations are likely to be involved in tumour initiation. We could show that mice with a combined deletion of *Vhl* and *Trp53* develop simple and atypical cysts, as well as neoplastic lesions in the kidney. However, the latency for development of cysts and tumours was one year, indicating that other mutations are most likely necessary for initiation of these lesions. Mouse embryonic fibroblasts (MEFs) as well as primary kidney cells undergo senescence upon loss of pVhl and we have shown that this effect occurs in a p53-dependent manner as in *Vhl/Trp53* negative cells the senescence phenotype is rescued. However these cells still do not have full proliferative capacity compared to *p53* null cells indicating that additional cellular responses upon loss of *Vhl* may represent transformational barriers. It remains unknown if and how metabolic alterations following loss of pVHL contribute to tumour formation.

We investigated the effects of loss of *Vhl* in MEFs on glucose and glutamine metabolism and their implications for cell transformation. We could show that *Vhl* negative, as well as *Vhl/Trp53* deficient MEFs exhibited a Hif1α-dependent Warburg-like metabolic phenotype with reduced oxygen consumption and decreased ATP generation. The impaired ATP generation appears likely to be the cause of senescence in primary *Vhl* deficient MEFs and the impaired proliferation in *Vhl/Trp53* negative cells since knockdown of *Hif1a* in these cells rescued ATP levels, senescence and proliferation. The ATP deficiency was sensed by AMPK whose activation decreased mTORC1 signalling. Thus, a selection against AMPK and/or mTORC1 may represent the additional step for tumour initiation and progression in *Vhl/Trp53* deficient cells. Multiple experiments using shRNA based knockdowns of *Tsc1*, *Tsc2*, *Stk11* or *Prkaa1* in *Vhl/Trp53* deficient MEFs were performed but could not confirm this hypothesis as none of these knockdowns promoted enhanced proliferation or transformation of these cells. In conclusion, it seems that on top of alterations of *Vhl* and *Trp53* and an activation of the mTORC1 pathway additional mutations are required for tumour initiation.

The second aim of the thesis was to elucidate if the senescence-rescued *Vhl/Trp53* null cells might use carbons derived from glutamine to fuel their demands for energy and metabolic intermediates. First experiments with metabolomic and RNA analysis could not clearly answer this question. However, Hif1α-dependent elevated levels of *Gls2* in *Vhl* and *Vhl/Trp53* deficient MEFs and kidney cells indicate a role for glutamine in *Vhl* depleted cells. Furthermore, knockdown of *Gls2* in *Vhl/Trp53* deficient MEFs enhanced the proliferation of these cells and allowed them to grow in an anchorage independent manner. Our studies suggest that Gls2 represents a barrier to transformation of *Vhl* deficient cells.

Another aim of this thesis was to identify the effect of combined loss of *Vhl* and *Rb1* on cellular senescence and cellular metabolism and its implication in tumour initiation and progression. Combined deletion of *Vhl* and *Rb1* in MEFs rescued *Vhl*-induced senescence and ATP levels and these cells were able to grow in an anchorage independent manner. Despite promising results from cell culture studies, the kidney-specific deletion of *Vhl* and *Rb1* did not lead to the breakdown of normal proliferation in mice. While $Rb1^{\Delta/\Delta}$ animals showed micro-cysts and small foci of tubular dysplasia, the additional loss of *Vhl* in fact prevented the growth of hyperplastic lesions. Potentially, additional mutations might be necessary to initiate tumour development. In this context, the combined deletion of *Vhl*, *Rb1* and *Trp53* provides promising results. Already at the age of three months neoplasms could be found, which grew in a solid or cystic pattern, some with clear cell appearance and some with nuclear atypia. This histological appearance could potentially indicate precursor lesions of ccRCC. These lesions are larger and occur at a much higher frequency about nine months earlier than the lesions that were observed in *Vhl/Trp53* null mice. It appears that combined deletion of *Vhl*, *Rb1* and *Trp53* might represent the first mouse model for ccRCC.

Zusammenfassung

Klarzellige Nierenzellkarzinome sind die häufigste Form von Nierenzellkarzinomen. Das Tumorsuppressorgen von Hippel-Lindau (*VHL*) ist in über 90% der sporadisch auftretenden klarzelligen Nierenzellkarzinome biallelisch inaktiviert. Das Proteinprodukt des *VHL* Lokus, pVHL, ist an der Regulation diverser zellulärer Prozesse beteiligt. Es wäre durchaus vorstellbar, dass die Fehlregulation dieser Abläufe eine wichtige Rolle in der Tumorentstehung spielen könnte. Die am besten charakterisierte Funktion ist die post-transkriptionelle Regulierung der HIFα Transkriptionsfaktoren, die unterschiedlichste Funktionen in einer Vielzahl von zellulären Prozessen einnehmen. Für die Tumorentstehung ist der Verlust von pVHL alleine jedoch nicht ausreichend, aller Wahrscheinlichkeit nach sind zusätzlich auftretende Mutationen daran mitverantwortlich. Wir konnten zeigen, dass Nieren von Mäusen mit einer kombinierten Inaktivierung von *Vhl* und *Trp53* einfache und atypische Zysten, sowie neoplastische Läsionen entwickeln. Die Latenzzeit für die Entwicklung dieser Zysten und Tumore beträgt jedoch ein Jahr, was darauf hindeutet, dass weitere Mutationen für die Entstehung von Läsionen notwendig sind. Die Inaktivierung von *Vhl* führt sowohl in embryonischen Fibroblasten von Mäusen (MEFs) als auch in primären Maus-Nierenzellen zu Seneszenz. Dieser Effekt ist abhängig von p53, da der seneszente Phänotyp in *Vhl/Trp53*-defizenten Zellen zumindest teilweise überwunden werden kann. Diese Zellen prolifierieren jedoch deutlich langsamer als p53-defiziente Zellen. Diese Beobachtungen deuten darauf hin, dass der Verlust von *Vhl* zu zusätzlichen zellulären Rückkopplungsmechanismen führt, die eine Transformationsbarriere darstellen können. Es ist immer noch nicht klar, ob und wie die metabolischen Veränderungen nach dem Verlust von pVHL zur Tumorentstehung beitragen.

In dieser Arbeit sollten die Auswirkungen, die der Verlust von *Vhl* auf den Glukose und Glutamin Metabolismus hat und deren Einfluss auf die zelluläre Transformation ermittelt werden. *Vhl* als auch *Vhl/Trp53* negative MEFs weisen in Abhängigkeit von Hif1α einen metabolischen Phänotyp mit reduziertem Sauerstoffverbrauch und verminderter ATP Gewinnung auf, der einem milden Warburg-Effekt gleicht. Wir vermuten, dass die verringerte Bildung von ATP der Grund für die Seneszenz in primären *Vhl* negativen Zellen sein könnte und die Proliferation in *Vhl/Trp53*-defizienten Zellen beeinträchtigt. Der Knockdown von *Hif1a* hingegen konnte das ATP-Niveau wiederherstellen und verhinderte somit die Seneszenz. Veränderungen von ATP werden in der Zelle von AMPK wahrgenommen, deren Aktivierung die Signalwirkung von mTORC1 beeinträchtigt. Die Selektion gegen AMPK und/oder mTORC1 ist möglicherweise ein weiterer Schritt der für die Initiierung und Progression von Tumoren in *Vhl/Trp53*

Knockout Zellen verantwortlich sein könnte. Verschiedene Knockdown-Experimente mit *Tsc1*, *Tsc2*, *Stk11* oder *Prkaa1* in *Vhl*/*Trp53* Knockout MEFs konnten diese Hypothese nicht weiter bestätigen, denn keiner dieser Knockdowns förderte die Proliferation oder Transformation dieser Zellen. Es scheint, dass zusätzlich zur genetischen Manipulation von *Vhl* und *Trp53* und der dauerhaften Aktivierung des mTORC1 Signalweges noch weitere Mutationen notwendig sind, um Tumore entstehen zuzulassen.

Das nächste Ziel dieser Arbeit war es, zu ermitteln, ob *Vhl*/*Trp53*-defiziente Zellen, die der Seneszenz entkommen sind, Kohlenstoff aus Glutamin verwenden, um ihren Bedarf an Energie und metabolischen Intermediaten zu decken. Erste Metabolom- und mRNA-Expressions-Analysen konnten diese Frage nicht eindeutig beantworten. Die erhöhte Hif1α-abhängige Genexpression von *Gls2* in *Vhl* und *Vhl*/*Trp53*-defizienten MEFs und Nierenzellen deutet jedoch auf eine Rolle für Glutamin in diesen Zellen hin. Des Weiteren förderte der Knockdown von *Gls2* in *Vhl*/*Trp53*-negativen MEFs deren Proliferation und ermöglichte das Wachstum ohne Oberflächenzellkontakt. Unsere Studien lassen vermuten, dass Gls2 eine Barriere für die Transformation von *Vhl* negativen Zellen darstellt.

Ein weiteres Ziel dieser Arbeit war es, die Auswirkungen, die der kombinierte Verlust von *Vhl* und *Rb1* auf die zelluläre Seneszenz und den Zellmetabolismus haben, zu ermitteln. Ausserdem untersuchen wir deren Einfluss auf die Entstehung und Weiterentwicklung von Tumoren. Die gleichzeitige Inaktivierung von *Vhl* und *Rb1* in MEFs verhinderte die durch den Verlust von *Vhl* induzierte Seneszenz. Diese Zellen zeigten einen normalisierten ATP-Spiegel und konnten ohne Oberflächenzellkontakt wachsen. Trotz vielversprechender Resultate aus den Zellkultur-Studien führte die nierenspezifische Deletion von *Vhl* und *Rb1* in Mäusen nicht zu unkontrolliertem Zellwachstum. Während $Rb1^{\Delta/\Delta}$ Tiere Mikrozysten und kleine Herde tubulärer Dysplasie aufwiesen, verhinderte die zusätzliche Deletion von *Vhl* das Wachstum wuchernder Läsionen. Dies zeigt, dass zusätzliche Mutationen für die Einleitung der Tumorentstehung notwendig sind. In diesem Zusammenhang liefert der kombinierte Verlust von *Vhl*, *Rb1* und *Trp53* vielversprechende Resultate. Bereits nach drei Monaten konnten Neoplasmen entdeckt werden, die in einem soliden oder zystischen Muster wuchsen, einige mit klarzelliger Morphologie und einige mit nuklearen Atypismen. Dieses histologische Erscheinen könnte auf Vorgänger-Läsionen von klarzelligen Nierenzellkarzinomen hindeuten. Die gesehenen Läsionen sind bereits neun Monate früher als in *Vhl*/*Trp53*-negativen Mäusen anzutreffen, sind grösser und treten häufiger auf. Möglicherweise kann die kombinierte Inaktivierung von *Vhl*, *Rb1* und *Trp53* zum ersten Mausmodel für klarzellige Nierenzellkarzinome werden.

Preface

A number of people have directly contributed to the work described in this thesis. These contributions, listed below, enabled a number of experiments to be undertaken which would not otherwise have been possible. I am extremely grateful to these people for their time and interest and have enjoyed their close collaboration.

Désirée Schönenberger, Holger Lehmann and Tomas Hejhal contributed to Chapter 2.

Tatiana Simka and Ian Frew performed the SeaHorse assays in Figure 4.2.

Nicola Zamboni and Sebastian Dubuis supervised the extraction and performed metabolomic analysis in Figure 4.4.

Désirée Schönenberger provided cDNA used for RNA analysis in Figures 4.1 and 5.3.

Joachim Albers, Michal Rajski and Tomas Hejhal provided cDNA used for RNA analysis in Figure 5.4.

Acknowledgements

First of all I would like to thank Ian Frew for all his support, guidance and supervision during my thesis. I am really grateful for the many interesting discussions and a lot of input throughout the last four years, his door was literally always open. It is really a pleasure to be part of his team and to see it growing and developing.

I greatly acknowledge the members of my PhD committee Willy Krek, Nicola Zamboni and Rok Humar for taking the time to meet and discuss my project and their constant support with new ideas.

Many thanks to the current and former members of the Frew lab for the great working atmosphere. I really appreciated the scientific and at least as much as the non-scientific support. Together Tomas (McGiver) Hejhal, Holger Lehmann and Joachim Albers could answer almost every question and solve any technical issue. Not to forget Tamara Hüsser, Mojca Adlesic and Claudia Danzer who also made my life beside science exciting and shared their work and life experience with me.

Special thanks go to Désirée Schönenberger. From the first day on I involuntarily had to share almost everything with her. But without her constant interest in my project, many helpful discussions and emergency weekend work this thesis and the time in the lab would only be half as good and awesome as it has been.

In addition I would like to thank all the former and present members of the Wenger lab for being so helpful and supportive, including technical advice and sharing of reagents and also many nice conversations.

Last but not least I would like to thank my family and friends who are far away but nevertheless always supported me with food, fun and love.

Abbreviations

4-EB-P1	eukaryotic initiation factor 4E-binding protein 1
AMPK	AMP-activated protein kinase
ccRCC	clear cell renal cell carcinoma
Cdk	cyclin dependent kinases
ECAR	extracellular acifidation rate
GAB	glutaminase B
GAC	glutaminase C
GLS	glutaminase
HIF	hypoxia inducible factor
KGA	kidney-like glutaminase
LGA	liver-like glutaminase
LKB1	serine-threonine kinase liver kinase B1
MEFs	mouse embryonic fibroblasts
mTOR	mammalian target of rapamycin
mTORC	mammalian target of rapamycin complex
OCR	oxygen consumption rate
PPP	pentose phosphate pathway
RB	retinoblastoma
RCC	renal cell carcinoma
ROS	reactive oxygen species
S6	ribosomal protein S6
S6K	ribosomal protein S6 kinase
TCA	tricarboxylic acid
TSC1	tuberous sclerosis 1 or hamartin
TSC2	tuberous sclerosis 2 or tuberin
VHL	von Hippel-Lindau

1 Introduction

1.1 Kidney cancer

Cancer is the second most frequent cause of death in the industrial world. Kidney cancers account for approximately 3% of all human cancers. Renal cell carcinomas (RCCs) are the most common type of malignancies in the kidney, accounting for over 90% of the cases. Besides hereditary cases, the common risk factors for RCC are tobacco smoking, obesity, hypertension and chronic kidney failure. Renal carcinomas arise from the epithelium of renal tubules. The majority of adult RCCs are classified as clear cell renal cell carcinomas (70%), with papillary (10-15%), chromophobe (5%) and collecting duct (< 1%) renal cell carcinomas accounting for the other subtypes (Eble et al. 2004). However, a recent update of the classifications identified five new epithelial tumour subtypes: acquired cystic disease-associated renal cell carcinoma, tubulocystic renal cell carcinoma, hereditary leiomyomatosis RCC (HLRCC) syndrome-associated RCC and clear cell papillary RCC and MiTF-translocation RCC (Srigley et al. 2013). These tumors display very distinct characteristics, leading to different prognoses and treatments within the different subtypes. The majority of RCC occur sporadically, but 2-4% of the cases are linked with inherited tumour syndromes.

1.1.1 The von Hippel-Lindau syndrome

The autosomal-dominant von Hippel-Lindau (VHL) disease is the most frequent familial renal cancer syndrome (Moch 2013). It is characterized by hemangioblastoma of the central nervous system and retina, phaeochromocytoma, pancreatic islet cell and inner ear tumours, as well as renal cysts and clear cell renal cell carcinomas (ccRCC) (Maher and Kaelin 1997). Sequencing has shown that germ-line mutations of the tumour suppressor gene *VHL*, located on chromosome 3p25, are the trigger of this disease (Seizinger et al. 1988; Latif et al. 1993). People with this syndrome inherit one defective allele of *VHL* either due to a deletion of the gene or missense or splicing defects and the remaining wild-type allele is thereafter somatically inactivated or lost (Stolle et al. 1998). This conforms to the Knudson 2-hit model, which postulates that both alleles of a tumour suppressor have to be mutated for a cell to become cancerous. Every VHL patient has an individual predisposition to different types of benign and malignant tumours based on the type of mutation that has been inherited and accordingly the treatment and prognosis will differ greatly from patient to patient. As the VHL disease has a strong genotype-phenotype correlation the families are subdivided in two groups dependent on their risk for phaeochromocytoma. Type 1 VHL disease is characterised by the complete loss of

VHL function or mutations that affect the protein folding and low risk for phaeochromocytoma. The two subtypes of type 1 have either a low risk (type 1A) or a high risk (type 1B) for renal cell carcinoma. Type 2 VHL disease displays a high risk for phaeochromocytoma and is mainly caused by missense mutations. It can be further divided dependent on its risk for renal cell carcinomas, which is low in type 2A, high in type 2B and extremely low in type 2C (Zbar et al. 1996; Hes et al. 2000; Kaelin 2002).

1.1.2 Clear cell renal cell carcinoma

Clear cell renal cell carcinomas are a typical manifestation of the inherited VHL cancer syndrome but these tumours also occur sporadically and account for the majority of cases of this disease (Foster et al. 1994; Maher and Kaelin 1997). In up to 92% of sporadic ccRCCs, the *VHL* gene is biallelically inactivated (Foster et al. 1994; Sato et al. 2013). Similarly to ccRCCs in VHL patients this occurs through an allelic deletion or loss of heterozygosity on chromosome 3p (Zbar et al. 1987) and concomitant *VHL* mutation (Gnarra et al. 1994) or promoter hypermethylation (Herman et al. 1994). Sato and colleagues also identified mutations of *TCEB1*, the gene encoding Elongin C, which is part of the pVHL-ElonginB-ElonginC complex (see section 1.1.3), in a subset of *VHL* wild type ccRCCs, thus inactivating pVHL function through another mechanism (Sato et al. 2013). Sporadic ccRCCs mainly arise as solitary cortical neoplasms with a yellow tumour surface. The appearance of the cells is caused by a high lipid and glycogen content. These cells are characterized by clear or eosinophilic cytoplasm with well-defined cell borders that is surrounded by a finely branched vascular network (Grignon and Che 2005; Moch 2013). In addition to solid ccRCCs there are some cases that show a cystic appearance. Another subtype, multilocular cystic renal cell carcinoma does not exhibit any solid tumour elements and has a complete cystic structure (Eble and Bonsib 1998; von Teichman et al. 2011).

For the development of familial and sporadic ccRCC the absence of pVHL is in most cases the initial event. According to this, the frequency of single cells or multicellular clusters with a functional loss of pVHL is extremely high in kidneys of VHL patients (Mandriota et al. 2002). Compared to the general population the frequency of cyst and tumour development in VHL patients is highly increased. However, in relation to the high number of pVHL mutated cells the frequency of cyst or tumour formation in VHL patients is very low, implying that other genetic events have to occur to induce tumourigenesis from these *VHL* mutant cells. The cell type or types that serve as the cell of origin of ccRCC is still unclear. While most evidence suggests that ccRCC most often arise from proximal tubular epithelial cells, some cases exhibit markers of distal tubules or collecting

duct cells, suggesting that epithelial cells from several different nephron segments can potentially give rise to ccRCCs (Droz et al. 1990; Paraf et al. 2000; Straube et al. 2011). Furthermore the molecular and cellular events that underlie the initiation and progression of ccRCC are still an incomplete picture. A number of studies indicate that ccRCC may arise via a cyst-dependent pathway in which cysts occur as precursor lesions or may arise directly from small solid micro-ccRCC precursor lesions (Thoma et al. 2007; Montani et al. 2010). The different ccRCC progression models are shown in Figure 1.1.

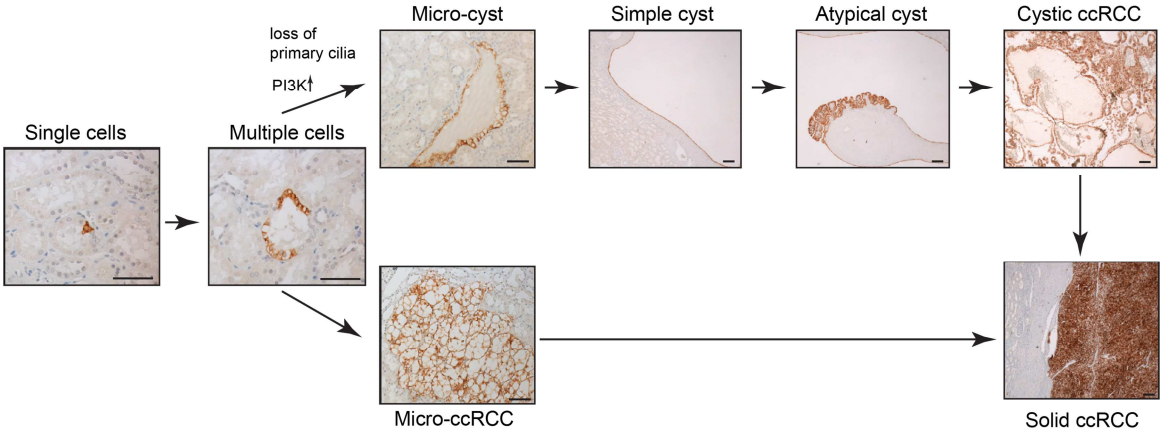

Figure 1.1: Current model of ccRCC development and progression.

Homozygous loss of *VHL* occurs frequently in VHL patients but only a small proportion of these *VHL* null cells progress into micro-cysts and the majority of *VHL* mutant cells appear to remain as single cells or as small clusters of cells. Micro-cysts are characterized by upregulated PI3K signalling and loss of the primary cilium. Cyst expansion leads to the enlargement of micro-cysts into larger simple cysts that are lined by a single epithelial layer. It is believed that some simple cysts can progress to form atypical cysts, which are characterized by regions of disorganized and multilayered epithelial growth. It is likely additional pro-proliferative mutations are needed for the development of cystic ccRCC and probably further mutations may turn cystic ccRCC into solid ccRCC. This may occur through neoplastic growth completely filling the former cystic lumen. Little is known about the mechanisms by which *VHL* null cells may progress to form micro-ccRCC lesions with a solid appearance, which may then directly go on to form solid ccRCC. In summary, it is believed that ccRCCs can form via cyst-dependent and cyst-independent precursor lesions.

1.1.3 The von Hippel-Lindau protein

The human *VHL* gene encodes a protein with two different isoforms ($pVHL_{30}$ and $pVHL_{19}$) derived from alternate translational initiation sites, both referred to as pVHL (Iliopoulos et al. 1998; Blankenship et al. 1999). pVHL has been ascribed many functions as a multipurpose adapter protein regulating a variety of transcriptional as well as other cellular processes. pVHL serves as a substrate recognition module of an E3 ubiquitin ligase complex consisting of Elongin B, Elongin C, Cullin 2 and Rbx-1 (Pause et al. 1997; Lonergan et al. 1998; Kamura et al. 1999; Lisztwan et al. 1999; Stebbins et al. 1999). This complex facilitates the proteasomal degradation of the hypoxia-inducible factor α (HIFα) transcription factors (Maxwell et al. 1999), as well as the large subunit of the RNA polymerase II complex (Rbp1) (Kuznetsova et al. 2003). pVHL also prevents the proteolytic degradation of the p53 tumour suppressor protein, an important player in cell

cycle arrest and apoptosis (Roe et al. 2006). Another function of pVHL is the inhibition of NF-κB transcription factors (Yang et al. 2007) which play a main role in regulating the immune system but are also involved in cell survival, differentiation, and proliferation (Hayden and Ghosh 2008). Additionally, pVHL supresses several cellular processes like cellular senescence (Young et al. 2008; Welford et al. 2010), aneuploidy (Thoma et al. 2009) and the transition of epithelial to mesenchymal cell characteristics (Esteban et al. 2006; Pantuck et al. 2010) and is involved in the regulation of neuronal apoptosis (Lee et al. 2005), growth factor receptor internalisation (Hsu et al. 2006), degradation of β2-adrenergic receptors (Xie et al. 2009) and canonical Wnt signalling (Chitalia et al. 2008). Furthermore, transcription-independent pVHL functions include deposition of the extracellular matrix (Ohh et al. 1998; Kurban et al. 2008) and stabilisation of the microtubule cytoskeleton (Hergovich et al. 2003), as well as maintenance of the primary cilium (Thoma et al. 2007). It seems quite possible that loss of the above mentioned pVHL functions separately or in cooperation can promote tumour initiation. So far it is still quite unclear which of the pVHL functions are important for ccRCC progression. In this thesis we mainly focused on the role of *Vhl* with regard to cell metabolism and cell cycle regulation.

To analyse the impact of *Vhl* on ccRCC progression several mouse models with a deletion of *Vhl* were generated. A germ-line mutation of *Vhl* is accompanied by embryonic lethality in homozygous animals due to failures in the vascularisation of the placenta (Gnarra et al. 1997). Heterozygous *Vhl* mutants do not develop kidney tumours even under carcinogenic conditions (Kleymenova et al. 2004). Moreover, different mouse models with a specific deletion of *Vhl* in different kidney segments like proximal tubule (Rankin et al. 2006), all nephron segments including (Schietke et al. 2012; Mathia et al. 2013) or excluding the proximal tubules (Frew et al. 2008), as well as in the thick ascending loop (Schley et al. 2011) lead to the development of cysts only in some cases and no renal tumours were ever observed. Taking these mouse studies into consideration and the fact that VHL patients have a multitude of pVHL negative cells that apparently never develop into ccRCC tumours, the loss of pVHL alone appears to be insufficient for the initiation of ccRCC and other factors and mutations are necessary for further progression of *VHL* mutated cells. ccRCC remains one of the few major human tumour types for which no autochthonous mouse model exists. One aim of this thesis was to attempt to generate such a mouse model.

1.1.4 Hypoxia-inducible factor family

As already mentioned, the best characterized function of pVHL is in effecting the oxygen-dependent degradation of HIFα transcription factors. HIFs function as a heterodimeric complex consisting of an oxygen-sensitive α-subunit (HIF1α, HIF2α and HIF3α) and a stable β-subunit (Maxwell et al. 1999; Ohh et al. 2000; Ivan et al. 2001). HIF1 and HIF2 α/β heterodimers are involved in the regulation of oxygen-regulated target genes, whereas the function for HIF3α is still unclear (Wenger et al. 2005). Under normoxic conditions HIFα is hydroxylated by a family of prolyl hydroxylases (PHD1, PDH2 and PHD3) and is therefore recognizable for the pVHL-ElonginB-ElonginC complex for proteasomal degradation (Tanimoto et al. 2000; Epstein et al. 2001; Ivan et al. 2001). Also dependent on oxygen availability is a second mechanism that inhibits HIFα via asparaginyl hydroxylation. Under normoxia and mild hypoxia, the factor inhibiting HIF (FIH) enzyme hydroxylates the C-terminus of HIFα and transcriptional co-activators like p300 and CREB binding protein (CBP) cannot be recruited (Dayan et al. 2006). With decreasing oxygen levels PHD and FIH activity is impaired, HIFα can be translocated to the nucleus where the HIFα/β complex forms and interacts with co-activators like p300 and CBP. Once HIF is stabilised it binds to a consensus hypoxia-response element (HRE) of the nuclear DNA that is conserved in hundreds of HIF target genes (Wenger et al. 2005). These genes are involved in proliferation (e.g. *TGFα*), glucose/energy metabolism (*GLUT1*, *PGK*), angiogenesis (*VEGF*, *PDGFβ*), apoptosis (*BNIP3*), differentiation (*Oct4*) and metastasis (*CXCR4*) (Gordan and Simon 2007). Many HIF target genes play important roles in various aspects of tumour biology. HIF1α and HIF2α share redundant target genes but also have unique targets that can even have opposing effects (Keith et al. 2012).

Recent evidence demonstrates the opposing effects of HIFs on oncoproteins (MYC) and tumour suppressors (p53, mTOR), both influencing cell progression on different levels (Keith et al. 2012). For example, stabilized HIF1α inhibits MYC and thus limits MYC-dependent protein synthesis, cell division and anabolic metabolism (Koshiji et al. 2004), whereas HIF2α expressing cancer cells enhance MYC activity resulting in increased cell proliferation (Gordan et al. 2007). In the development and progression of ccRCC, HIF1α and HIF2α also reveal contrasting properties, where HIF1α delays and HIF2α promotes tumour development in xenograft studies (Raval et al. 2005). In general, this reflects the different impacts of HIF1α and HIF2α function on cell proliferation. Although several studies revealed the contribution of HIF1α and HIF2α to ccRCC formation, the stabilisation of these proteins alone induced by the loss of *VHL* is not sufficient for tumour formation (Mack et al. 2003). Interestingly, a stable overexpression of HIF1α (Fu

et al. 2011), but not HIF2α (Fu et al. 2013), in kidneys was able to generate simple cysts but no further tumour development could be detected. These studies also cast new light on the contribution of the two HIFα isoforms in tumour initiation, indicating a fundamental role for HIF1α in the initiation phase. In summary, beside the loss of *VHL* and a stabilisation of HIFα, other genetic alterations are necessary for tumour initiation, and HIFα stabilisation may initially provide an environment that promotes further cancer progression only in the presence of additional mutations. In this context of the initial stages of tumour formation, we have addressed the question of which effects stabilised Hif1α and Hif2α have on the metabolism of *Vhl* deficient cells.

1.2 Cancer cell metabolism

In recent years, it has become more and more evident that alterations in cellular metabolism are common features of cancerous tissues and are sometimes even required for malignant transformation. A multitude of cancer driver mutations have been shown to also affect core metabolic signalling pathways and metabolic processes that are responsible for tumourigenesis. Cancer cells also have special needs to satisfy cell growth and proliferation. Highly proliferating cells require a huge amount of energy supported by rapid ATP generation as well as a balanced redox system and adequate amounts of macromolecular building blocks (Cairns et al. 2011).

1.2.1 Warburg effect and aerobic glycolysis

In the presence of oxygen, non-proliferating differentiated cells metabolise glucose to pyruvate that is shuttled to the mitochondria to be oxidised in the tricarboxylic acid (TCA) cycle for the production of the reducing equivalents NADH and $FADH_2$, which then maximises ATP production via oxidative phosphorylation. Under oxygen deprived conditions, pyruvate is redirected from the TCA cycle by generating lactate (Vander Heiden et al. 2009). A common characteristic of cancer cells, which Warburg already described in 1924, is increased anaerobic glycolytic metabolism (Warburg et al. 1924). Thereby, the conversion of glucose into lactate even occurs in the presence of sufficient oxygen. Warburg's first hypothesis that a defect in mitochondria caused the impaired aerobic respiration in cancer cells was later disproved by several research groups (at least for most cancer cells) (Warburg 1956; Moreno-Sánchez et al. 2007). Surprisingly, aerobic glycolysis is much less efficient at generating ATP than the oxidative TCA cycle. So why would cells choose a less efficient metabolism? Proliferating cells require a large amount of nucleotides, amino acids and lipids generated from glucose or glutamine for

replication. Directing glucose into the TCA cycle to maximise ATP production would therefore release the carbons as carbon dioxide, which are then lost for biosynthesis. However, cells using aerobic glycolysis exhibit highly increased glycolytic flux to support ATP generation and to simultaneously supply metabolic intermediates for biosynthetic processes (Vander Heiden et al. 2009; Cairns et al. 2011).

Glucose transport, aerobic glycolysis and mitochondrial respiration are regulated by the HIF1 transcription factor. HIF1 transcriptionally upregulates the glucose transporter *GLUT1* and important glycolytic enzymes including *PGK* and *LDH-A* (Semenza et al. 1994) and prevents mitochondrial respiration via *PDK1* gene upregulation, which in turn prevents metabolism of pyruvate to acetyl-CoA (see also Figure 1.2) (Kim et al. 2006; Papandreou et al. 2006). Furthermore, HIF1 controls genes that regulate proteins of the electron transport chain such as cytochrome c oxidase (Complex IV) (Fukuda et al. 2007). HIF1 also inhibits Complex I via induction of *NDUFA4L2* which is overexpressed in *VHL*-deficient cell lines and therefore decreases mitochondrial oxygenation (Tello et al. 2011). Moreover, in *VHL*-negative renal carcinoma cell lines with a constant HIF1 activity mitochondrial metabolism and biogenesis are actively repressed by inactivation of C-MYC activity (Zhang et al. 2007) and reintroduction of VHL causes increased mitochondrial electron transport complex activity and increased levels of mitochondrial DNA and respiratory chain proteins (Hervouet et al. 2007). Interestingly, increased levels of glycolytic enzymes and reduced levels of mitochondrial DNA and respiratory chain proteins have also been noted in renal cell carcinoma (Simonnet et al. 2002; Unwin et al. 2003; Meierhofer et al. 2004). Thus, there is a large amount of evidence for an involvement of pVHL in the regulation of glucose metabolism in renal cancer. However, it remains unclear if and how pVHL influences metabolism at the initial steps of cancer development. The elucidation of this question is one of the central points of this thesis.

Figure 1.2: Cell metabolism

GLUT1: Glucose transporter, HK: Hexokinase, PGI: Phosphoglucose-isomerase, PFK1: 6-Phosphofructo-1-kinase, FBP1: Fructose-1,6-bisphosphatase, PFK2: 6-Phosphofructo-2-kinase/fructose-2,6-bisphosphatase, TIGAR: TP53-inducible glycolysis and apoptosis regulator, Aldo: Aldolase, GAPDH: Glyceraldehyde-phosphate-dehydrogenase, PGK: Phosphoglycerate-kinase, PGM: Phosphoglycerate-mutase, ENO: Enolase, PK: Pyruvate-kinase, PDH: Pyruvate-dehydrogenase, LDH-A: Lactate-dehydrogenase, PDK1: Pyruvate-dehydrogenase kinase, CS: Citrate-synthase, ACL: ATP-citrate lyase, ACO: Aconitase, IDH: Isocitrate-dehydrogenase, α-KGDH: α-Ketoglutarate-dehydrogenase, SUCL: Succinate-CoA ligase, SHD: Succinate-dehydrogenase, FH: Fumarase, MDH: Malate-dehydrogenase, GLS: Glutaminase, GLUD: Glutamate-dehydrogenase, ASCT2: Glutamine transporter, PPP: Pentose phosphate pathway, TCA: tricarboxylic acid cycle. Enzymes in green are HIF1 and C-MYC target genes except of PDK1, which is an exclusive HIF1 target.

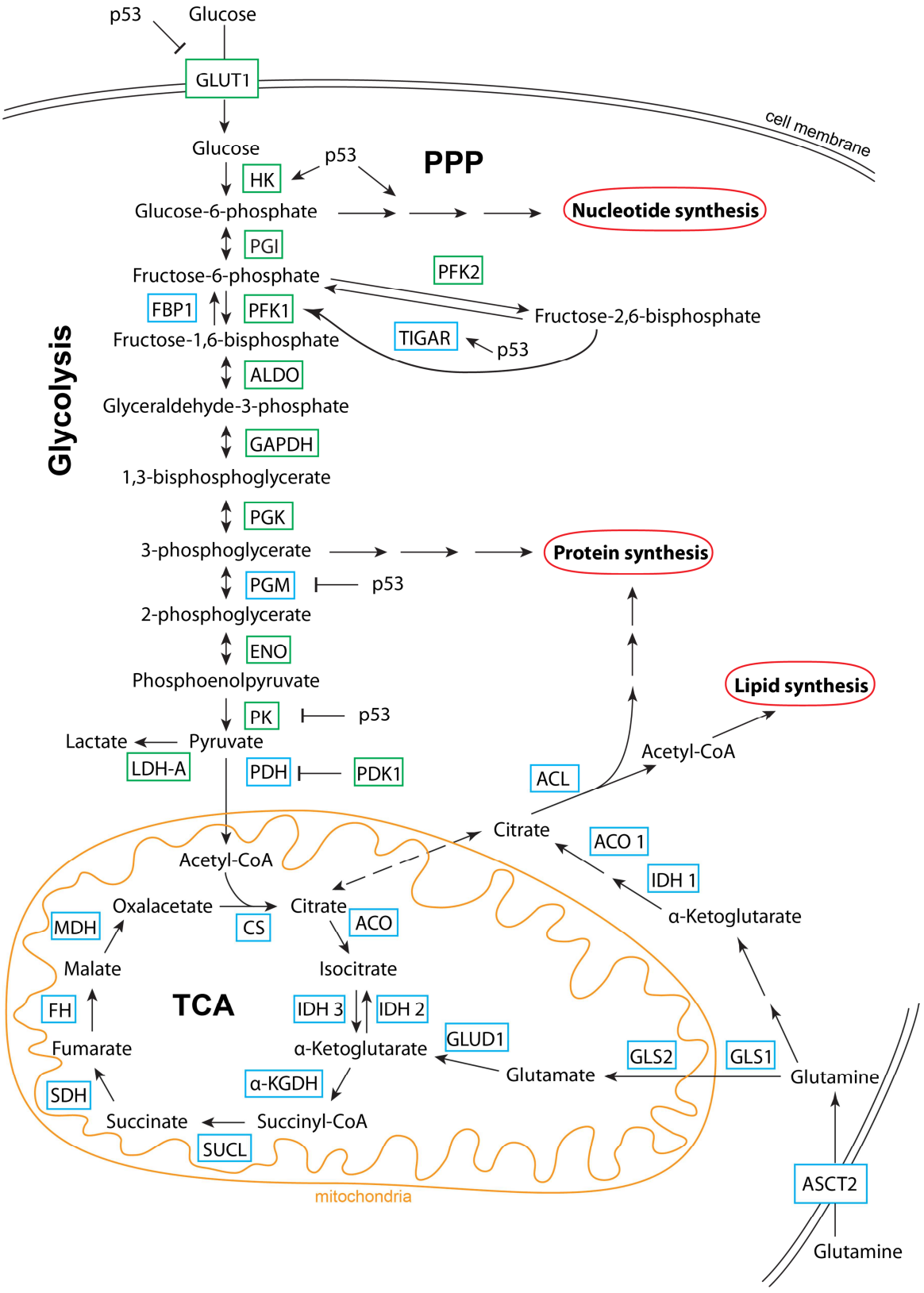

Figure 1.2: Cell metabolism

1.2.2 Glutamine metabolism

To support cell growth and division, glucose and to the same extent glutamine are catabolised to supply carbon and nitrogen, free energy and reducing equivalents. Glutamine is a non-essential amino acid and the major carrier of nitrogen between organs. In proliferating cells it is used for the synthesis of hexosamines, nonessential amino acids and nucleotides (DeBerardinis and Cheng 2010). Glutamine is also an essential precursor of glutathione that is important for cellular redox balance (Whillier et al. 2011). Glutamine-derived carbons can fuel the TCA cycle via α-ketoglutarate and oxalacetate for energy demands (DeBerardinis et al. 2008). However, in hypoxic or *VHL*-negative cancer cell lines or cells with defective mitochondria, glutamine-derived α-ketoglutarate is almost exclusively used in the reductive metabolism to generate citrate for lipid synthesis. This process is dependent on the presence of isocitrate-dehydrogenase 1 (IDH1) (cytosolic) or 2 (IDH2) (mitochondrial) (Metallo et al. 2011; Mullen et al. 2011; Filipp et al. 2012). This so-called reductive carboxylation is favoured in cells with stabilised HIF1α (Metallo et al. 2011; Wise et al. 2011; Gameiro et al. 2013). Upon HIF1α stabilisation, the activity of α-ketoglutarate dehydrogenase (α-KGDH) drops due to SIAH2 targeted ubiquitination, thus shifting glutamine from oxidative to reductive carboxylation (Sun and Denko 2014). One part of this thesis was to identify the importance of glutamine for *Vhl*-deficient cells.

1.2.3 Function of Glutaminases

The first step in glutaminolysis is the conversion of glutamine to glutamate that is performed by an enzyme called glutaminase. In mammals, the glutaminases are encoded by two different genes located on separate chromosomes (Aledo et al. 2000). The *GLS1* gene on chromosome 2 encodes the kidney-type glutaminase (KGA) (Curthoys et al. 1976), named after the organ were it was first discovered, and its splice variant glutaminase C (GAC) (Elgadi et al. 1999; Porter et al. 2002), both referred to as GLS1. KGA is formed by joining exons 1-14 and 16-19 whereas GAC only uses exons 1-15 (Marquez, Tosina 2009). The other gene *GLS2*, located on chromosome 12, encodes for two forms, liver-type glutaminase (LGA) (Aledo et al. 2000) and its longer variant glutaminase B (GAB) that is generated by alternate transcription initiation (de la Rosa et al. 2009; Martin-Rufian et al. 2012). The coding sequences of GLS1 and GLS2 show extensive similarities, however, two exons only share 62.5% and 29.4% similarity. These regions are involved in mitochondrial targeting and translocational processes (Shapiro et al. 1991; Gomez-Fabre et al. 2000). The different isoforms display variable kinetic and molecular characteristics and are expressed in a diversity of mammalian tissues and

cancer cell lines. Therefore, they are either exclusively or co-expressed with one of the other isoforms (Aledo et al. 2000; Gomez-Fabre et al. 2000; Perez-Gomez et al. 2005). So far, all isoforms have been shown to be confined to the mitochondria, with the exception that GAB can also be localised in the nucleus of brain cells, potentially as a transcriptional co-regulator (Olalla et al. 2002; Márquez et al. 2006). It seems that glutaminases have contrasting roles, especially in tumourigenesis. The expression of *GLS1* for example is regulated by C-MYC and its overexpression promotes tumour cell proliferation (Gao et al. 2009) whereas the loss of *GLS1* prevents transformation of cells (Lobo et al. 2000). However, GLS2, as a direct p53 target, mediates the tumour-suppressive effect of p53 in energy metabolism and antioxidant defence (Hu et al. 2010; Suzuki et al. 2010). In hepatocellular carcinoma, *GLS2* levels are decreased and re-expression of *GLS2* inhibits anchorage-independent cell growth and diminishes the growth of xenografts (Liu et al. 2014). It is still not yet fully understood why GLS1 and GLS2 isoenzymes that have the same catalytic ability show such differences in their biological properties. One possible explanation might be answered by the difference in response to phosphate and glutamate. GLS1 is strongly activated by phosphate and inhibited by glutamate, whereas GLS2 exhibits a considerably lower degree of phosphate dependency and no inhibition by glutamate (Curthoys and Watford 1995). In this thesis we examined a so far unknown upregulation of *Gls2* in primary mouse embryonic fibroblast and kidney cells deficient for *Vhl*.

1.2.4 Signalling pathways involved in regulation of metabolism in tumour cells

Signalling pathways are important components of the machinery that regulates cellular metabolism. Cancer cells often display a multitude of mutations in tumour suppressors and oncogenes that affect intracellular signalling pathways. These alterations in metabolism of tumour cells are important for enhanced survival and growth and enable them to respond to proliferative signals induced by oncogenic signalling pathways. These metabolic changes create a new environment that has an important impact on tumour progression, response to therapy and patient outcome (Cairns et al. 2011). Recent studies provided further verification for dysregulated metabolic pathways in sporadic ccRCC. The PI3K-AKT-mTOR pathway is mutationally activated in 26-28% of cases of ccRCC. This includes loss of function mutations of negative regulators of the pathway like *PTEN* (phosphatase and tensin homolog), *TSC1* or *TSC2* (tuberous sclerosis 1 or 2), as well as amplifications and activating mutations of positive regulators including *PIK3CA*/*B*/*G*, *RPS6KA2*/*3*/*6*, *AKT1*/*2*/*3*, *RHEB* and *MTOR*, most of them leading to

increased mTORC1 signalling (Sato et al. 2013; TCGA 2013). Further considerations for the importance of well-balanced cell homeostasis come from survival correlations. In ccRCC, decreased AMPK, decreased TCA cycle activity, an increased dependency on the pentose phosphate pathway, increased glutamine transport and increased fatty acid production are all involved in a metabolic shift that correlates with disease aggressiveness (TCGA 2013). So far it is not clear if and how these alterations are required for the initiation progression of ccRCC.

1.2.4.1 Mammalian target of rapamycin

The master regulator of cell growth and proliferation is the mammalian target of rapamycin (mTOR) that is activated by amino acid abundance and growth factor signalling, leading to the activation of protein translation and gene expression and the inhibition of autophagy (Wullschleger et al. 2006). mTOR is the catalytic component of the mTOR complexes, mTORC1 and mTORC2. Common components, besides of mTOR, are LST8/GβL and DEPTOR, which function as positive and negative regulators of the complex, respectively (Kim et al. 2003; Peterson et al. 2009). Both complexes have unique components whereas regulatory-associated protein of mTOR (RAPTOR) and Pro-rich Akt substrate (PRAS40) define mTORC1 (Hara et al. 2002; Sancak et al. 2007). mTORC2 specific components are rapamycin-insensitive companion of mTOR (RICTOR) and protein observed with RICTOR 1 and 2 (PROTOR1 and 2) and stress-activated map kinase-interacting protein 1 (SIN1) (Sarbassov et al. 2004; Pearce et al. 2007).

The most prominent and best established substrates of mTORC1 are eukaryotic initiation factor (eIF) 4E-binding protein 1 (4E-BP1) and ribosomal protein S6 kinase 1 (S6K1) (Hara et al. 1998). To control protein synthesis both proteins are able to associate with mRNAs and thus regulate mRNA translation initiation and progression. Unphosphorylated 4E-BP1 functions as a translational repressor by binding and inhibiting eIF4E, an initiation factor at the mRNA 5´-cap. Phosphorylation of 4E-BP1 by mTORC1 enables its dissociation from eIF4E and thus initiates translation. mTORC1 mediated phosphorylation of S6K1 enables its binding to or the phosphorylation of multiple proteins like ribosomal protein S6 (S6) (Ruvinsky et al. 2005), eIF4B (Holz et al. 2005), eEF2K (Wang et al. 2001), CBP80 (Wilson et al. 2000) and SKAR (Ma et al. 2008), which also affect translation initiation.

The functions of mTORC2 are less understood than those of mTORC1. Growth factors, but not nutrients, cause a response mainly through phosphorylation and activation of

AGC kinases such as AKT (or protein kinase B), protein kinase C (PKC) and serum- and glucocorticoid-regulated kinase (SGK). SGK and PKC are involved in cell survival, cell cycle progression and anabolism. mTORC2 phosphorylation of AKT primes it for further phosphorylation by PDK1 (Sarbassov et al. 2005; Garcia-Martinez and Alessi 2008; Ikenoue et al. 2008). The two mTOR complexes exhibit complicated cross-talk reactions between each other. mTORC1 affects upstream players of the PI3K-AKT signalling pathway (IRS-1 and Grb10) thus negatively regulating both mTOR complexes (Um et al. 2004; Hsu et al. 2011). Recent studies also identified a direct negative regulation of mTORC1 towards mTORC2 via phosphorylation of SIN1 through S6K. SIN1 is part of the mTORC2 complex and important for its stability and its phosphorylation by S6K leads to the dissociation of the complex (Liu et al. 2013).

The major regulatory inputs for mTORC1 are nutrients, growth factors, energy and stress. The binding of growth factors and mitogens to cognate receptors activates different pathways like the PI3K-AKT, Ras-Raf-MEK-ERK and Wnt-GSK3β axis (Manning et al. 2002). In these pathways, the TSC1/TSC2 complex takes up a key position in the regulation of mTOR (see also Figure 1.3) (Tee et al. 2002). TSC2 contains a GTPase activating protein (GAP) domain that converts RHEB (GTPase Ras homologue enriched in brain), an essential activator of mTORC1, from its active GTP-bound into an inactive GDP-bound state (Saucedo et al. 2003; Zhang et al. 2003). The phosphorylation of TSC2, also known as tuberin, by AKT, ERK or RSK inhibits its GAP function, thus promoting mTORC1 signalling (Inoki et al. 2002; Roux et al. 2004; Ma et al. 2005). Wnt signalling inhibits GSK3β that acts as a negative regulator of the mTORC1 pathway by phosphorylating and activating tuberin (Inoki et al. 2006). Tuberin also plays a key role in energy- and stress-regulated mTORC1 signalling. Alterations of cellular energy levels are sensed by AMPK, which once it is activated phosphorylates tuberin and stimulates its GAP activity towards RHEB, and suppression of mTORC1 activity (Inoki et al. 2003). Furthermore, AMPK phosphorylates RAPTOR and allows the binding of 14-3-3 proteins, enabling the inhibition of mTORC1 through allosteric mechanisms (Gwinn et al. 2008). Oxygen stress induces the expression of the *REDD1* (regulated in development and DNA damage response 1) gene via HIF1α. REDD1 promotes the release of tuberin from the inhibitory 14-3-3 proteins, enabling the formation of TSC1/TSC2 complex (Brugarolas et al. 2004; DeYoung et al. 2008). REDD1 takes up a special role in the mTOR pathway as it is part of a negative feedback loop. Thereby, HIF1α expression is mTORC1 regulated and high levels of HIF1α in turn transcribe *REDD1* which inhibits mTORC1 (Hudson et al. 2002). DNA damage suppresses mTORC1 activity through a p53-dependent activation of AMPK, whereas the overexpression of the p53 targets sestrin 1

and sestrin 2 activate AMPK (Budanov and Karin 2008). A detailed scheme is described in Figure 1.3. Considering the multitude of regulation possibilities of the TSC1/TSC2 complex it is not surprising that a mutation of those two proteins is the cause of the familial cancer syndrome TSC. Patients with this disease suffer from benign tumours called hamartomas that occur in the kidney, heart, brain, lung and skin (Orlova and Crino 2010). As mTOR occupies a key position in the regulation of cell growth and proliferation we tried to investigate its role in cells deficient for *Vhl* that undergo senescence.

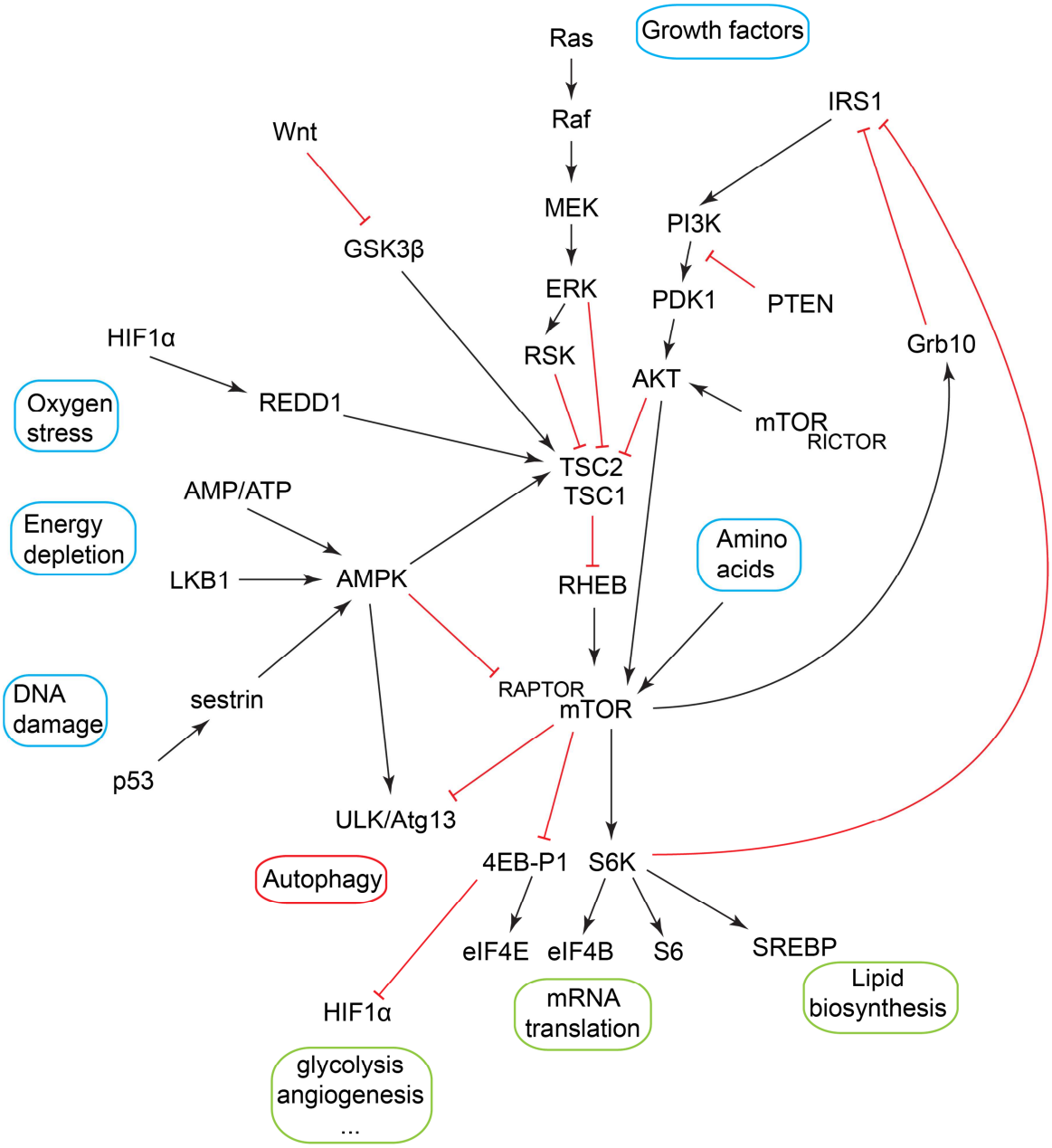

Figure 1.3: Pathways affecting mTOR signalling.

1.2.4.2 LKB1-AMPK signalling axis

1.2.4.2.1 Serine-threonine kinase liver kinase B1

The serine-threonine kinase liver kinase B1 (*LKB1* or *STK11*) is a tumour suppressor gene originally identified as the gene responsible for the inherited Peutz-Jeghers syndrome (Hemminki et al. 1998). This rare disease has a predisposition to benign intestinal hamartomatous polyps and malignancies in the gastrointestinal tract, breast, testis and ovary (Giardiello et al. 1987). Other clinical hallmarks are a melanin pigmentation of the skin and mucous membranes (Hemminki 1999). In non-small cell lung carcinoma *STK11* is one of the most commonly mutated genes (15-35%) (Sanchez-Cespedes et al. 2002), as well as in cervical carcinomas where it is somatically mutated in up to 20% of cases (Wingo et al. 2009). A recent study identified LKB1 as a tumour suppressor in sporadic cases of ccRCC whereas its underexpression seems to be important for cancer progression (Duivenvoorden et al. 2013).

There are two isoforms of LKB1 generated by alternate splicing with different C-terminal sequences, with the shorter version $LKB1_S$ lacking phosphorylation (Ser431) and farnesylation (Cys433) sites. Both forms are widely expressed but $LKB1_S$ is predominantly expressed in testis where its loss causes infertility (Towler et al. 2008; Denison et al. 2009). The LKB1 protein forms a complex with STE20-related adapter (STRAD) and scaffolding mouse 25 (MO25) proteins that are important for its activation and translocation from the nucleus to the cytoplasm (Baas et al. 2003; Boudeau et al. 2003). LKB1 is the key upstream activator of the AMP-activated protein kinase (AMPK) family including AMPKα, NUAK and MARK (Lizcano et al. 2004) and is therefore involved in controlling cell growth, energy metabolism and cell polarity (Shackelford and Shaw 2009).

1.2.4.2.2 AMP-activated protein kinase

The main energy sensor in cells is the AMP-activated protein kinase (AMPK). During stress situations such as nutrient and oxygen starvation it works as a key regulator of cellular energy metabolism by sensing increases in AMP/ATP and AMP/ADP ratios or elevated levels of Ca^{2+} (Salt et al. 1998; Marsin et al. 2000). However, other signals such as reactive oxygen species (ROS) also activate AMPK (Zmijewski et al. 2010). AMPK is a heterotrimeric kinase complex composed of a catalytic subunit (AMPKα) and two regulatory subunits (AMPKβ and AMPKγ). The subunits α and β are both encoded by two different genes (α1 or α2 and β1 or β2), whereas the γ-subunit has three responsible genes (γ1, γ2 or γ3) (Stapleton et al. 1996; Woods et al. 1996). The α-subunit contains a

serine/threonine kinase domain with a conserved threonine residue (Thr172), which upstream kinases are able to phosphorylate. This phosphorylation increases the activity of AMPK by several hundred folds (Suter et al. 2006). The γ-subunit contains four different binding sites for AMP, ADP and ATP, which regulate the status of AMPK (Xiao et al. 2007). Binding of AMP or ADP to the γ-subunit promotes phosphorylation and inhibits dephosphorylation of the Thr172 residue but only AMP is able to allosterically activate AMPK (Davies et al. 1995; Hawley et al. 1995; Xiao et al. 2011). However, ATP binds to the same sites in the γ-subunit as AMP and ADP do, antagonising all of their effects (Davies et al. 1995). The two major kinases phosphorylating AMPK are the LKB1-STRAD-MO25 complex, responsible for the above-described way of activation (Hawley et al. 2003; Woods et al. 2003; Shaw et al. 2004), as well as calcium/calmodulin-dependent protein kinase kinase-β (CaMKKβ) that is activated by elevated calcium levels in the absence of increased AMP levels (Hawley et al. 2005; Hurley et al. 2005; Woods et al. 2005).

To maintain the energy balance in cells, on the one hand AMPK activates catabolic processes to generate ATP and on the other hand inhibits energy-consuming pathways. Therefore, it is involved in regulation of glucose, protein and lipid metabolism, as well as in mitochondrial biogenesis and autophagy. Through this, AMPK promotes the uptake of glucose (through transporter Glut1 and Glut4) (Kurth-Kraczek et al. 1999; Barnes et al. 2002) and its catabolism via glycolysis (PFKFB3) (Marsin et al. 2002) including the uptake of fatty acids into the mitochondria and their breakdown in β-oxidation (ACC2) (Merrill et al. 1997) and inhibits fatty acid synthesis (ACC1) (Hardie and Pan 2002). In addition to promotion of catabolic pathways, AMPK inhibits anabolic processes such as protein synthesis. AMPK directly phosphorylates and activates TSC2 that in complex with TSC1 serves as an inhibitor of the mTORC1 complex, a key regulator of protein metabolism. TSC2 functions as a GTPase-activator protein that inhibits RHEB, an upstream activator of mTORC1 (Inoki et al. 2003). Furthermore, RAPTOR is phosphorylated by AMPK and 14-3-3 binding is induced that is responsible for mTORC1 inhibition (Gwinn et al. 2008). Together with mTORC1, AMPK also coordinates the regulation of autophagy/mitophagy. mTORC1 operates as a suppressor of ULK1 and ULK2 (Unc-51-like kinase 1 and 2) activity during nutrient-rich conditions whereas AMPK phosphorylates and activates these two proteins in response to low nutrient availability and inhibits mTORC1 directly as mentioned above and thus promotes autophagy (Chan 2009; Egan et al. 2010).

Additionally, AMPK seems to be involved in the regulation of the cell cycle. Jones and colleagues revealed that AMPK activation due to glucose deprivation induces the phosphorylation of p53 at Ser15 and an upregulation of its target gene *p21*, both involved in regulation of the cell cycle (Jones et al. 2005). In tuberin-null cells with elevated AMPK signalling the cyclin-dependent kinase inhibitor $p27^{Kip1}$ is phosphorylated by AMPK. This promotes its stabilisation as well as its sequestration to the cytoplasm and exhibits elevated levels of Cdk2 activity (Short et al. 2008; Short et al. 2010). The role of AMPK-mediated $p27^{Kip1}$ stabilisation in cell cycle is still not fully understood but phosphorylated $p27^{Kip1}$ by AMPK can also inhibit apoptosis and support autophagy (Liang et al. 2007). In this thesis we could show that the senescence phenotype of *Vhl*-deficient cells was accompanied by decreased levels of ATP. As AMPK is the energy sensor in cells we tried to investigate the role of AMPK in cells deficient for *Vhl*.

1.3 Cell cycle regulation and its link to cancer

Primary as well as transformed MEFs with a deletion of *Vhl* show signs of premature senescence or proliferation arrest, respectively (Mack et al. 2005; Young et al. 2008; Welford et al. 2010), possibly initiated by oxidative stress (Welford et al. 2010). Mack and colleagues showed that mRNA expression and protein levels of $p21^{Cip1}$ and $p27^{Kip1}$ were elevated in *Vhl* negative immortalised MEFs and fibrosarcomas caused through stabilised HIF activity, which suppressed C-MYC transcriptional repression towards *p21* and *p27* (Mack et al. 2005). Another study claimed that immortalized *Vhl* MEFs exhibited decreased levels of *Skp2* that caused stabilisation of $p27^{Kip1}$ and resulted in hypo-phosphorylated Rb in a p53- and Hif-independent manner (Young et al. 2008). The *Vhl* induced senescence seems to be dependent on functional cell cycle and senescence pathway regulators pRb (Young et al. 2008) or p53 (Welford et al. 2010). In terms of the central role pRb and p53 have in regulating cell cycle and senescence, these data provide strong evidence that during cancer progression, loss of *Vhl* activates a barrier for proliferation, which presumably has to be overcome by additional mutations in cellular checkpoints to facilitate tumour formation. Another interesting link between pVHL and cell cycle regulation is its gate keeping function in terms of contact inhibition. In renal epithelial cells pVHL is essential for the generation and maintenance of contact inhibition of cell growth (Baba et al. 2001). The loss of *VHL* in RCC cell lines causes elevated *cyclin D1* expression levels at high cell densities through stabilised HIF signalling (Bindra et al. 2002; Baba et al. 2003). Interestingly, in 40% of cases of sporadic ccRCC components of senescence and cell cycle checkpoints have genetic alterations including mutations or copy number deletions in TP53, ATM, CHEK2, MDM2, CDKN2A, E2F3 or

RB1 or copy number gains in MYC (Sato et al. 2013). These results strongly support the idea from *in vitro* studies that the loss of function of *VHL* cooperates with impaired cell cycle machinery thus leading to ccRCC development. With the generation of a mouse model we investigated the interaction between the two tumour suppressor genes *Vhl* and *Rb1*.

1.3.1 Cell cycle

Alterations in cell cycle genes are important events for cancer progression. The cell cycle is defined as the replication of DNA and the division of cells to yield two daughter cells. It is divided into mitosis (M) and interphase, while the actual cell division takes part in the M phase. The interphase consists of G1, S, and G2 phases. DNA replication occurs during S phase and is separated from the M phase by two gap phases (G1 and G2) where cells are enabled to repair DNA damage and replication errors. In G1, cells prepare for DNA synthesis whereas in G2 they prepare for mitosis. Cells that have ceased proliferation enter a silent phase called G0. The cyclin-dependent kinases (Cdk) are the key regulators of the transition between the different cell cycle phases (Malumbres et al. 2009). The Cdks are heterodimeric protein kinases containing a serine/threonine-specific catalytic core (Cdk) and regulatory binding partners called cyclins. Progression through the cell cycle requires different Cdk/cyclin complexes. For entering G1, mitogenic signals via PI3K-AKT and Ras-Raf-MEK-ERK pathways induce cyclin D (D1, D2, D3) expression, allowing the Cdk4/6-cyclin D complex to assemble (Sherr and Roberts 1999). The most recognized function of this complex is the initial phosphorylation and thus inactivation of RB family members. Inactive RB releases E2F and thus allows the transcription of cyclin E that in turn is, together with Cdk2, required for progression from G1 to S phase, causing unwinding of the double helix and DNA replication (Kelly and Brown 2000; Prasanth et al. 2004). Cdk2/cyclin E enforces RB phosphorylation and the created feedback-loop enables an irreversible G1/S transition. At the end of the S phase, when Cdk2 is no longer bound to cyclin E, it associates with cyclin A and allows completion and exit from this phase. At the same time, Cdk1 binds cyclin A that is replaced by cyclin B during transition of G2 to M (Sherr and Roberts 1999). The kinase activity of the Cdk/cyclin complex is regulated by cell cycle inhibitory proteins called Cdk inhibitors (CKI). They are divided in two subgroups, the INK4 and Cip/Kip family (Sherr and Roberts 1995). The INK4 family consists of $p16^{INK4a}$ (Cdkn2a), $p15^{INK4b}$ (Cdkn2b), $p18^{INK4c}$ (Cdkn2c) and $p14^{INK4d}$ (Cdkn2d). They bind specifically to Cdk4 and Cdk6 proteins thus preventing cyclin D association (Carnero and Hannon 1998). The Cip/Kip family includes $p21^{Cip1}$ (Cdkn1a), $p27^{Kip1}$ (Cdkn1b) and $p57^{Kip2}$ (Cdkn1c) and inactivates cyclin D-/E-/A- and B-dependent kinase complexes by binding to these complexes.

Internal as well as external signals regulate the CKIs. For example $p21^{Cip1}$ is transcriptionally controlled by p53 whereas the expression and activation of $p15^{INK4b}$ and $p27^{Kip1}$ is regulated by TGF-β (Vermeulen et al. 2003). During the cell cycle, there are several DNA damage and spindle checkpoints, to ensure an orderly process of events (Hartwell and Weinert 1989). The DNA damage checkpoints take place during transition of G1-S and G2-M phase. DNA damage occurring in G1 phase is sensed by pathways that lead to p53 activation and target genes like *p21* are transcribed. The cell cycle arrest at the G2 checkpoint can be initiated with or without p53. The Cdk kinase activity is, beside cyclins and CKIs, also controlled by phosphorylation or dephosphorylation events, protein folding and subcellular localisation (Sherr and Roberts 1999).

1.3.2 Senescence

Apoptosis and senescence can be teleologically envisaged as internal protection mechanisms that cells use to prevent uncontrolled cell proliferation. During cellular senescence, cells irreversibly arrest proliferation but are still metabolically active. The triggers of senescence are telomere shortening, DNA damage, chromatin remodelling and strong mitogenic signals (Campisi 2001). p53 and pRB are important tumour suppressors that, due to diverse stimuli, maintain pathways leading to growth arrest. These two proteins are further described in 1.3.3 and 1.3.4 respectively. The inactivation of p53 in primary MEFs is likewise sufficient for accelerated growth due to the prevention of senescence (Dirac and Bernards 2003). During senescence, E2F1, oncogenic Ras and DNA damage induce $p14^{ARF}$ ($p19^{ARF}$ in mouse) that sequesters MDM2 (mouse double minute 2 homolog), a protein involved in degradation of p53, thus activating p53 (Bringold and Serrano 2000). pRB only exists in its hypophosphorylated and thus active form in senescent cells. The Cdks that phosphorylate and inactivate pRB during cell cycle are mainly inhibited by $p16^{INK4a}$ but also $p21^{Cip1}$ and in some cases by $p27^{Kip}$. These genes are highly expressed in senescent cells and induced by oncogenes and other stress stimuli (Serrano et al. 1993; Campisi 2001; Lowe and Sherr 2003). The two different senescence pathways interact with each other at multiple levels. The above mentioned Cdk inhibitor and thus pRB activator $p21^{Cip1}$ for example is a direct target gene of p53. Furthermore, pRB prevents the degradation of p53 by binding to and inactivation of MDM2 (Campisi 2001).

1.3.3 Retinoblastoma protein

The retinoblastoma protein family consists of the three members RB1, RBL1 (p107) and RBL2 (p130). As these family members are structurally and functionally similar they have

overlapping and compensatory and in some contexts individual functions (Claudio et al. 2002). These tumour suppressors are, as already mentioned, involved in cell cycle regulation where they inhibit E2F family members in the transition of G1 to S phase by binding to them. E2F1, E2F2 and E2F3a, which act as transcriptional activators, are under the direct control of RB1 whereas E2F4 and E2F5, transcriptional repressors, are bound by RBL1 and RBL2 (Sun et al. 2007). During cell cycle progression, the function of RB is regulated by its phosphorylation status influenced by different Cdk/cyclin complexes (Buchkovich et al. 1989). Beside cell cycle modulation, RB is also involved in the induction and maintenance of cellular senescence, the regulation of apoptosis, chromosomal stability, cellular differentiation and angiogenesis (Burkhart and Sage 2008). Its special role in senescence is described in section 1.3.2. Interestingly, a recent study revealed a new role for the Rb pathway in glutamine metabolism having a direct metabolic control of ATP and macromolecular production. The loss of the complete Rb family (*Rb1*, *Rbl1* and *Rbl2*) enhanced glutamine uptake via E2F3 and the upregulation of the expression of the glutamine transporter ASCT2, increased Gls1 activity and increased glutathione synthesis (Reynolds et al. 2014). Taken together, Rb1 is important for cell cycle regulation and could be involved in cell metabolism. Therefore, we examined the effects of *Rb1* loss in *Vhl*-deficient MEFs which display a senescence phenotype.

1.3.4 p53

The tumour suppressor *TP53*, encoding p53, is the most frequently mutated gene in an enormous variety of different types of cancer (Levine and Oren 2009). p53 has a diversified range of tasks and thus occupies an important position in stress response networks. It is induced by different stress stimuli like DNA damage, hypoxia and oxygen stress. The induction of p53 facilitates DNA repair during the cell cycle and activates apoptotic or senescence responses, all being major mechanisms for tumour suppression (Levine and Oren 2009). Furthermore, recent findings suggest an important function of p53 in the regulation of the metabolic homeostasis in cells. Dependent on nutrient and oxygen availability, p53 regulates a complex network of different metabolic pathways like glycolysis (*GLUT1, HK, PGM*), oxidative phosphorylation (*SCO2*), glutaminolysis (*GLS2*), fatty acid oxidation (GAMT), nucleotide biosynthesis (G6PD), mitochondrial integrity, antioxidant response, insulin sensitivity, mTOR signalling and autophagy (LC3) (Maddocks and Vousden 2011). Thereby, p53 acts as a transcription factor and alters the expression of hundreds of genes (Menendez et al. 2009). On the other hand p53 can also operate as a transcriptional repressor (Ginsberg et al. 1991). In unstressed cells, p53 is maintained at low levels by MDM2 that acts as an E3 ligase supporting the

degradation of p53 (Freedman et al. 1999). As MDM2 is also a transcriptional target of p53 the increased activation of p53 drives the expression of its own negative regulator and creates a negative feedback loop (Wu et al. 1993). Upon DNA damage, the tumour suppressor pVHL directly acts as a positive regulator of p53. It associates with p53, leading to its stabilisation and blocking MDM2 mediated ubiquitination of p53 and its export from the nucleus (Roe et al. 2006). Besides pRB, p53 is another crucial cell cycle and senescence regulator in cells. One aim of this thesis is to understand the effects of combined *Vhl* and *p53* loss on the cell metabolism and their contribution to transformation.

1.4 Aims

This thesis has the following aims:

1. Analysis of metabolic processes, especially oxygen and nutrient sensing pathways that are dysregulated after loss of pVHL function and their implication for tumour formation.
2. Examination of the effect of combined loss of *Vhl* and *Trp53* or *Rb1* on cellular senescence and cell metabolism following loss of pVHL function.
3. Generation of a mouse model with inducible kidney epithelial cell-specific combined deletion of *Vhl* and *Rb1* to study their cooperative effects in ccRCC development.

2 Materials and Methods

2.1 Materials

2.1.1 General Chemicals

Reagent	Supplier
30% Acrylamide/Bisacrylamide Solution	Bio-Rad
Acetic acid (glacial)	Merck
Acetone	Sigma-Aldrich
Agarose, D1 low EEO	Conda
Agarose, low melting point	Sigma-Aldrich
Albumin from bovine serum	Sigma-Aldrich
Ammonium carbonate	Sigma-Aldrich
Ammonium chloride	Fluka
Boric acid	Sigma-Aldrich
Bovine serum albumin (BSA)	Invitrogen
Bromophenol blue	Sigma-Aldrich
Citric acid monohydrate	Sigma-Aldrich
Crystal violet	Sigma-Aldrich
Dimethylsulfoxide (DMSO)	Sigma-Aldrich
di-sodium hydrogen orthophosphate (Na_2HPO_4)	Sigma-Aldrich
Dithiothreitol (DTT)	Sigma-Aldrich
Entellan	Merck
Eosin 1% (aqueous)	BioSystems
Ethanol	AUL
Ethidium bromide	Sigma-Aldrich
Ethylenediamine tetra-acetic acid (EDTA) disodium salt dihydrate	Sigma-Aldrich
Formalin 10%, neutral buffered	Sigma-Aldrich
Glycerol	Sigma-Aldrich
Haematoxylin (Mayer's)	J.T.Baker
Hydrochloric acid, 32%	Sigma-Aldrich
Hydrogen peroxide	Sigma-Aldrich
Isopropanol	AUL
L-glutamine [5-C14]	Hartmann Analytic
Magnesium chloride	Sigma-Aldrich
Magnesium sulfate	Sigma-Aldrich
Methanol	AUL
Mowiol	Sigma-Aldrich
N,N,N',N'-Tetramethylethylenediamine (TEMED)	Bio-Rad
N-2-Hydroxyethylpiperazine-N'-2-ethanesulfonic acid (HEPES)	Sigma-Aldrich
NP-40	Sigma-Aldrich

Reagent	Supplier
Paraformaldehyde	Sigma-Aldrich
p-coumaric acid	Sigma-Aldrich
Phenyl-methyl-sulphonyl-fluoride (PMSF)	Sigma-Aldrich
Potassium acetate	Sigma-Aldrich
Potassium chloride	Sigma-Aldrich
Propidium iodide (PI)	Sigma-Aldrich
Protease inhibitor cocktail	Sigma-Aldrich
Protein assay Dye Reagent	Bio-Rad
Safflower oil	Migros
Sodium acetate	Sigma-Aldrich
Sodium azide	Sigma-Aldrich
Sodium chloride	Sigma-Aldrich
Sodium deoxycholate	Sigma-Aldrich
Sodium dihydrogen orthophosphate (NaH_2PO_4)	Sigma-Aldrich
Sodium Dodecyl Sulfate (SDS)	Sigma-Aldrich
Sodium hydroxide	Sigma-Aldrich
Sulforhodamine B sodium salt (SRB)	Sigma-Aldrich
SYBR FAST Universal 2X qPCR Master Mix	KapaBiosystems
SYBR Green JumpStart Taq ReadyMix	Sigma-Aldrich
Trichloroacetic acid	Sigma-Aldrich
Tris(hydroxymethyl)aminomethane (Tris base)	Sigma-Aldrich
Tris(hydroxymethyl)aminomethane hydrochloride (Tris HCl)	Sigma-Aldrich
Tri-Sodium citrate	Sigma-Aldrich
Triton X-100	Sigma-Aldrich
Tween-20	Sigma-Aldrich
Xylene	Thommen-Furler AG

2.1.2 Drugs & tissue culture reagents

Reagent	Supplier
2–Mercaptoethanol	Bio-Rad
2´,7´-dichlorodihydrofluorescein diacetate	Invitrogen
3,3,5 Triiodothyronine (T3)	Sigma-Aldrich
Acridine Orange 10-nonyl bromide	Sigma-Aldrich
Ampicillin	Sigma-Aldrich
Apo-Transferrin (TF), human	Sigma-Aldrich
Calcium chloride	Sigma-Aldrich
Collagenase Type II	Gibco
Cycloheximid	Sigma-Aldrich
D-glucose	Sigma-Aldrich
DMEM without L-methionine, L-cystine	Sigma-Aldrich
DMEM/F12	Sigma-Aldrich

Reagent	Supplier
Dulbecco's Modified Eagle Medium (DMEM)	Sigma-Aldrich
Epidermal Growth factor (EGF), murine	PeproTech
Fetal Calf Serum (FCS)	Biochrome AG
HBSS	Gibco
Hepatocyte Growth factor (HGF)	PeproTech
HEPES 1M	Sigma-Aldrich
Hydrocortisone (HC)	Sigma-Aldrich
Insulin, human	Sigma-Aldrich
Kanamycin	Sigma-Aldrich
L-Glutamine	Sigma-Aldrich
Luria Bertani Bouillon medium	Sigma-Aldrich
Met-[S35]-label (SCIS-103)	Hartmann Analytics
Penicillin/Streptomycin	PAA
Phosphate Buffered Saline (PBS)	Biochrome Ag
Polybrene (Hexadimethrine Bromide)	Sigma-Aldrich
Prostagladin E1 (PGE1)	Sigma-Aldrich
Puromycin	InvivoGen
S.O.C. medium	Invitrogene
Sodium bicarbonate	Sigma-Aldrich
Sodium bicarbonate	Sigma-Aldrich
Tamoxifen	Sigma-Aldrich
Trypsin EDTA	Gibco
Trypsin inhibitor, soybean	Gibco

2.1.3 Kits

Name	Supplier
ABC Kit (PK6100)	Vectorstain
Avidin/Biotin Blocking Kit (SP 2001)	VectorLaboratories
CellTiter-Glo Luminescent Cell Viability Assay	Promega
CSA detection kit	Dako
DAB Substrate Kit (SK-4100)	VectorLaboratories
GenElute Mammalian Genomic DNA Miniprep Kit	Sigma-Aldrich
Glucose assay Kit II	Biovision
Lactate assay Kit II	Biovision
NucleoBond Xtra Midi	Macherey-Nagel
NucleoSpin RNA kit	Macherey-Nagel
Ready-To-Go You-Prime First-Strand Beads	GE Healthcare

2.1.4 Antibodies

Name	Vendor	Order number	Source	Dilution	Application
β-Actin (AC-74)	Sigma-Aldrich	A2228	Mouse	1:1000	WB
Acetyl-CoA-Carboxylase	Cell Signaling Technologies	3662	Rabbit	1:1000	WB
Phospho-Ser79-Acetyl-CoA-Carboxylase	Cell Signaling Technologies	3661	Rabbit	1:1000	WB
AMPKα (F6)	Cell Signaling Technologies	2793	Mouse	1:1000	WB
AMPKα1 (Y365)	Abcam	ab32047	Rabbit	1:1000	WB
AMPKα2 (Y365)	Abcam	ab3760	Rabbit	1:1000	WB
Phospho-Thr172-AMPKα	Cell Signaling Technologies	2535	Rabbit	1:1000	WB
4E-BP1 (53H11)	Cell Signaling Technologies	9644	Rabbit	1:1000	WB
Phospho-Thr37/46-4E-BP1	Cell Signaling Technologies	2855	Rabbit	1:1000	WB
GLS2	Novus Biologicals	NBP1-54773	Rabbit	1:500	WB
GLS2 R471	Abcam	AP6650b	Rabbit	1:500	WB
Hamartin	Cell Signaling Technologies	4906	Rabbit	1:1000	WB
HIF1α (H1α67)	Novus Biotechnologies	NB-100-105	Mouse	1:20000	IHC
HIF1α	Novus Biotechnologies	NB-100-479	Rabbit	1:1000	WB
HRP anti-mouse	ThermoScientific	31430	Goat	1:1000	IHC
LDH-A (N-14)	Santa Cruz Biotechnology	Sc-27230	Goat	1:1000	WB
LKB1 (D60C5)	Cell Signaling Technologies	3047	Rabbit	1:1000	WB
p53	Leica Microsystems	NCL-p53-CM5p	Rabbit	1:1000	WB
Phospho-Ser15-p53	Cell Signaling Technologies	9284	Rabbit	1:500	WB
PDK-1	Enzo Life Sciences	ADI-KAP-PK112-D	Rabbit	1:1000	WB
Retinoblastoma Protein (G3-245)	BD Biosciences	554136	Mouse	1:1000 1:7000	WB IHC
S6 ribosomal protein	Cell Signaling Technologies	2217	Rabbit	1:1000	WB
Phospho-Ser240/244-ribosomal S6 protein	Cell Signaling Technologies	2215	Rabbit	1:1000	WB
p70 S6 kinase (49D7)	Cell Signaling Technologies	2708	Rabbit	1:1000	WB
Phospho-Thr389-p70 S6 kinase (1A5)	Cell Signaling Technologies	9206	Rabbit	1:1000	WB

Name	Vendor	Order number	Source	Dilution	Application
Tuberin (D57A9)	Cell Signaling Technologies	3990	Rabbit	1:1000	WB
VHL (FL-181)	Santa Cruz Biotechnologies	Sc-5575	Rabbit	1:100	WB

2.1.5 Oligonucleotide sequences

Name	Sequence	Application
Control band Cre fwd	ATA ATG CCT TTC CTC AGT AAA CCA G	Genotyping
Control band Cre rew	GGA TCC CAT TAC AGA TGG TTG TG	Genotyping
Ksp.Cre1.3 fwd	AGG TTC GTG CAC TCA TGG A	Genotyping
Ksp.Cre1.3 rev	TCG ACC AGT TTA GTT ACC C	Genotyping
Rb1 fwd	GGC GTG TGC CAT CAA TG	Genotyping
Rb1 rev	AAC TCA AGG GAG ACC TG	Genotyping
Trp53 fwd	GCC CTC TCT TAT CGC CAG AT	Genotyping
Trp53 rev	GCT TAT GGG CTT CTC CAA ACT	Genotyping
Vhl fwd	GGA GTA GGA TAA GTC AGC TG	Genotyping
Vhl rev	GTA CAC CTG AGA GCG GCT TC	Genotyping
Aco1 fwd	ACT CAA GAT ACG GAC GCT TAC C	RT-qPCR
Aco1 rev	GTT GCA TGA CAT TCC AAT TCA GG	RT-qPCR
Aco2 fwd	ATC GAG CGG GGA AAG ACA TAC	RT-qPCR
Aco2 rev	TGA TGG TAC AGC CAC CTT AGG	RT-qPCR
Asct2 fwd	CAT CAA CGA CTC TGT TGT AGA CC	RT-qPCR
Asct2 rev	CGC TGG ATA CAG GAT TGC GG	RT-qPCR
Gls1 fwd	AGT TGT CCC CAA CGT CAT GGG C	RT-qPCR
Gls1 rev	AGT CCA ATG GTC CAA AGG AAT GC	RT-qPCR
Gls2 A fwd	GCA CTC GGA TCA TGA CGC CTC AC	RT-qPCR
Gls2 A rev	TTG GAC CAT GCG CTG CAT CTT G	RT-qPCR
Gls2 B fwd	CGT CCG GTA CTA CCT CGG T	RT-qPCR
Gls2 B rev	TGT CCC TCT GCA ATA GTG TAG AA	RT-qPCR
Gls2 C fwd	CAG AGG GAC AGG AGC GTA TC	RT-qPCR
Gls2 C rev	TTC TTT CGG AAT GCC TGA GTC	RT-qPCR
Gls2 D fwd	TCA GGC ATT CCG AAA GAA GTT T	RT-qPCR
Gls2 D rev	CAG AAG GGG ATC TTC GTG TGG	RT-qPCR
Glud1 fwd	CCC AAC TTC TTC AAG ATG GTG G	RT-qPCR
Glud1 rev	AGA GGC TCA ACA CAT GGT TGC	RT-qPCR
Glut1 fwd	GCT TAT GGG CTT CTC CAA ACT	RT-qPCR
Glut1 rev	GGT GAC ACC TCT CCC ACA TAC	RT-qPCR
Got1 fwd	GCG CCT CCA TCA GTC TTT G	RT-qPCR

Name	Sequence	Application
Got1 rev	ATT CAT CTG TGC GGT ACG CTC	RT-qPCR
Got2 fwd	GGA CCT CCA GAT CCC ATC CT	RT-qPCR
Got2 rev	GGT TTT CCG TTA TCA TCC CGG TA	RT-qPCR
Hif1a fwd	TGCTCATCAGTTGCCACTTC	RT-qPCR
Hif1a rev	CCTCATGGTCACATGGATGA	RT-qPCR
Hif2a fwd	CTG ATG GCC AGG CGC ATG ATG	RT-qPCR
Hif2a rev	CTG ATG GCC AGG CGC ATG ATG	RT-qPCR
Idh1 fwd	ATG CAA GGA GAT GAA ATG ACA CG	RT-qPCR
Idh1 rev	GCA TCA CGA TTC TCT ATG CCT AA	RT-qPCR
Idh2 fwd	GGA GAA GCC GGT AGT GGA GAT	RT-qPCR
Idh2 rev	GGT CTG GTC ACG GTT TGG AA	RT-qPCR
Ldha fwd	TGG CTT TCC CAA AAA CCG AGT	RT-qPCR
Ldha rev	CCA TCA GGT AAC GGA ACC GC	RT-qPCR
Lga fwd	GCC AGA TGG TTC AAA GAG GAG G	RT-qPCR
Lga rev	GTG GTG AAC TTG TGG ATA GGG	RT-qPCR
Mdm2 fwd	AGG AGA TGT GTT TGG AGT CCC	RT-qPCR
Mdm2 rev	CTC AGC GAT GTG CCA GAG TC	RT-qPCR
p21 fwd	CCT GGT GAT GTC CGA CCT G	RT-qPCR
p21 rev	CCA TGA GCG CAT CGC AAT C	RT-qPCR
Pdk1 fwd	AGG ATC AGA AAC CGG CAC AAT	RT-qPCR
Pdk1 rev	GTG CTG GTT GAG TAG CAT TCT A	RT-qPCR
Pfkfb3 fwd	CAA CTC CCC AAC CGT GAT TGT	RT-qPCR
Pfkfb3 rev	TGA GGT AGC GAG TCA GCT TCT	RT-qPCR
Pgk1 fwd	TGG AGC CAA CTC CGT TGT C	RT-qPCR
Pgk1 rev	CAG GCA TTC TCG ACT TCT GGG	RT-qPCR
Prkaa1 fwd	TCG GCA CCT TCG GGA AA	RT-qPCR
Prkaa1 rev	GTT GAG TAT CTT CAC AGC CAC TTT ATG T	RT-qPCR
Prkaa2 fwd	CGC CTC TCA TCG CAG ACA	RT-qPCR
Prkaa2 rev	CTT GGG CTT CGT TGT GTT GA	RT-qPCR
Rb1 fwd	TGC ATC TTT ATC GCA GCA GTT	RT-qPCR
Rb1 rev	GTT CAC ACG TCC GTT CTA ATT TG	RT-qPCR
S12 fwd	GAA GCT GCC AAA GCC TTA GA	RT-qPCR
S12 rev	AAC TGC AAC CAA CCA CCT TC	RT-qPCR
Stk11 fwd	TTG GGC CTT TTC TCC GAG G	RT-qPCR
Stk11 rev	CAG GTC CCC CAT CAG GTA CT	RT-qPCR
Tigar fwd	GCC TGG AGG AGA GAC AGT TG	RT-qPCR
Tigar rev	TCC AAC AGG GAA AAC CTC TG	RT-qPCR
Trp53 fwd	GCG TAA ACG CTT CGA GAT GTT	RT-qPCR
Trp53 rev	TTT TTA TGG CGG GAA GTA GAC TG	RT-qPCR
Vhl fwd	CAG CTA CCG AGG TCA TCT TTG	RT-qPCR
Vhl rev	CTG TCC ATC GAC ATT GAG GGA	RT-qPCR

2.1.6 Plasmids and lentiviral vectors

Name	Reference	Vendor
pLKO.1-*Vhl*	gift from Krek lab	
pLKO.1-ns	10879	Addgene
psPAX2	10879	Addgene
pMD2.G	12259	Addgene
pLKO.1-*Tsc1*	NM_022887.3-462s21c1	Sigma-Aldrich
pLKO.1-*Tsc2*	NM_011647.2-1874s21c1	Sigma-Aldrich
pLKO.1-*Gls1*	NM_001081081.2-983s21c1	Sigma-Aldrich
pLKO.1-*Gls2*	NM_001033264.1-2135s1c1	Sigma-Aldrich
pLKO.1-*Stk11*	NM_011492.1-1189s1c1	Sigma-Aldrich
pLKO.1-*Stk11*	NM_011492.1-783s1c1	Sigma-Aldrich
pLKO.1-*Stk11*	NM_011492.1-1585s1c1	Sigma-Aldrich
pLKO.1-*Stk11*	NM_011492.1-736s1c1	Sigma-Aldrich
pLKO.1-*Prkaa1*	XM_139298.4-1540s1c1	Sigma-Aldrich
pLKO.1-*Prkaa1*	XM_139298.4-1396s1c1	Sigma-Aldrich
Adeno-Cre-GFP	Vector Biolabs	1700
Adeno-GFP	Vector Biolabs	1060

2.2 Cell infection

2.2.1 Bacterial strains and media

Plasmid DNA was grown in the bacterial strain Mach1-T1^{R}. S.O.B. medium and Luria Bertani Bouillon medium was used for growth of bacteria.

2.2.2 Transformation of bacterial cells with plasmid DNA

The plasmid DNA was added to 100 µl of chemically competent bacteria thawed on ice. The DNA/cell mix was incubated on ice for 30 minutes and then heated for 45 seconds at 42°C without shaking. Afterwards, cells were placed on ice for 2 minutes followed by addition of room temperature S.O.C. medium. Cells were incubated at 37°C for 1 hour at 300 rpm in a shaking incubator. Finally, transformation mix was plated onto pre-warmed agar plates containing appropriate antibiotics (100 µg/ml ampicillin or 50 µg/ml kanamycin), and incubated at 37°C overnight.

2.2.3 Isolation of plasmid DNA

For small-scale preparations, 2 ml of an overnight bacterial culture were centrifuged at 12000 rpm for 5 minutes. DNA was isolated using GenElute Mammalian Genomic DNA Miniprep Kit according to manufacturer´s protocol.

For large-scale preparations, 200 ml of an overnight bacterial culture were centrifuged at 4500 rpm for 10 minutes. DNA was isolated using NucleoBond Xtra Midi Kit according to the manufacturer's instructions. Following resuspension in TE buffer (Tris 1 mM, EDTA 10 mM, pH 8), DNA concentration was determined by absorbance at 260 nm.

2.2.4 Adenoviral vectors

Adenoviruses - Type 5 (dE1/E3) expressing Cre recombinase + GFP (Adeno-Cre) or GFP only (Adeno-GFP) was amplified in HEK-293 cells, cultured in DMEM mix (10% FCS, 2 mM glutamine, 10 kU/ml penicillin, 10 mg/ml streptomycin). The cells were infected with adenoviral stock at 80% confluency. Infection was allowed to proceed until 80-90% of the cells were rounded up and floating or loosely attached to the tissue culture dish. Adenovirus-containing cells were typically harvested 2-3 days after infection and centrifuged at 300 rpm for 5 minutes. Cell pellets were resuspended in PBS, frozen in liquid nitrogen and thawed again in a 37°C water bath. Freezing and thawing steps were repeated twice. Cell lysates were centrifuged at 2900 rpm for 15 minutes at room temperature to pellet the cell debris. The supernatant containing viral particles was aliquoted and stored at -80°C.

2.2.5 Lentiviral vectors

Lentiviral vectors were produced using calcium phosphate-mediated transfection of HEK-293T cells. The cells were maintained in DMEM supplemented with 10% FCS, 2 mM glutamine, 10 kU/ml penicillin, 10 mg/ml streptomycin. Transfection was performed when 50-70% of the plate surface was covered with cells. The medium was replaced with fresh DMEM two hours before transfection. The following transfection mix for one 15 cm dish was prepared in a 50 ml conical tube: 23 µg transfer vector plasmid, 15 µg packaging plasmid: psPAX2, 8 µg amphotropic VSV-G envelope: pMD2.G (Morita et al. 2000), 660 µl of 0.1x TE, 420 µl of H_2O and 375 µl of 1 M $CaCl_2$. 1.5 ml of 2x HEBS (0.05 M HEPES, 0.28 M NaCl, pH 7) was added drop wise under agitation. The precipitate was left at room temperature for 15 minutes and then added drop wise to the cells. After 16 hours the medium was aspirated and 14 ml of fresh DMEM was slowly added. The

medium containing lentiviral particles was harvested twice every 24 hours. The supernatants were cleared by centrifugation at 500 rpm for 5 minutes and filtered using a 0.45 µm filter unit. Aliquots of lentiviral vectors were stored at -80°C.

2.2.6 Viral Titer determination

For lentiviral titration $5x10^4$ cells were seeded per 6-well plate the day before infection. The next day the virus was diluted in DMEM $1:10^3$, $1:10^4$ and $1:10^5$ and added to the cells together with polybrene (4 µg/ml). 24 hours later the viral supernatant was removed and the cells were split 1:4 in triplicates on 6-well plates. Two days after infection, puromycin selection (2 µg/ml) was performed for 7-10 days. To visualize colony growth, the plates were stained with crystal violet (0.3% crystal violet in 70% methanol) at room temperature. After 1 hour, cells were washed in tap water and air dried. The viral titer corresponds to the number of colonies present at the highest dilution that still contains colonies, multiplied by the dilution factor and by two, to account for the twofold increase of cells during the transduction period and the 1:4 splitting.

2.2.7 Virus infection of cells

For lentiviral infection cells were counted and infected with virus of MOI 3. Polybrene (4 µg/ml) was supplemented to the media. After 16 hours the media was replaced with fresh DMEM. Two days after infection, puromycin selection (2 µg/ml) was performed for at least two days before continuing with experiments.

2.3 Cell culture

2.3.1 Isolation and culturing of mouse embryonic fibroblasts

Mouse embryonic fibroblasts (MEFs) were isolated from embryos of relevant floxed strains at day E13.5. After dissecting away the head, internal organs and spinal cord the remaining tissue was minced with a razorblade, incubated for 15 minutes at 37°C in trypsin EDTA, dispersed in growth media (DMEM supplemented with 10% fetal calf serum (FCS), 2 mM glutamine, 10 kU/ml penicillin, 10 mg/ml streptomycin and 200 µM β-mercaptoethanol) and plated on a 10 cm dish. Cells were split 2-3 days later into two 15 cm dishes and after a further 2-3 days they were frozen at passage 2. Cells were cultured in conventional cell culture incubators at atmospheric oxygen or at 5% oxygen. For low oxygen concentrations (1% oxygen) cells were cultured in an oxygen glove-box incubator ($INVIVO_2$ 400, Ruskinn).

2.3.2 Isolation and culturing of epithelial kidney cells

Kidneys were dissected from two month-old floxed mice. After removing the capsule under sterile conditions, kidneys were mashed with a razor blade on ice and digested in collagenase II solution at 37°C for 30 minutes. The cell suspension was filtered through a 70 µm cell strainer and washed in HBSS + 5% FCS. Erythrocytes were lysed for 1 minute using standard ACK buffer. Cells were re-suspended in complete K-1 culture medium (Dulbecco's modified Eagle's medium (DMEM):Hams F12) (50:50), supplemented with 0.5% fetal calf serum, 2 mM glutamine, 10 kU/ml penicillin, 10 mg/ml streptomycin, hormone mix (5 µg/ml insulin, 1.25 ng/ml prostaglandin E_1 (PGE_1), 34 pg/ml triiodothyronine, 5 µg/ml transferrin, 1.73 ng/ml sodium selenite, and 18 ng/ml of hydrocortisone) and 25 ng/ml epidermal growth factor (EGF). Cells were counted and seeded at a density of $1x10^6$ cells on standard 10 cm plastic tissue culture plates. After 5-6 days in culture, cells were infected with adenoviruses expressing GFP (Adeno-GFP) or Cre-GFP (Adeno-Cre).

2.3.3 Proliferation assays

For MEF proliferation assays, cells were seeded at densities of either $2x10^5$ or $3x10^5$ cells per 6 cm dish in triplicate dishes and counted after three days before reseeding at the same density for the next passage. All proliferation assays shown in all Figures are representative of at least three independent experiments.

For primary kidney cells, a Sulforhodamine B (SRB) colometric assay was performed (Vichai and Kirtikara 2006). Cells were cultured in K-1 medium containing 10% fetal calf serum for two days before seeding for the SRB assay. $2x10^3$ cells per well were seeded and fixed with 5% (wt/vol) trichloroacetic acid at the indicated time points, followed by staining with 0.057% (wt/vol) SRB solution and air drying. SRB was solubilized by incubation in 10 mM Tris base solution (pH 10.5) and OD was measured at 540 nm in a microplate reader (Anthos Lucy 3).

2.3.4 Transformation assays

For colony forming assays, testing the immortalization capacity, 5000 cells were seeded per 10 cm plate. After ten days, cells were washed with PBS and stained with crystal violet (0.3% crystal violet in 70% methanol) at room temperature. After 1 hour, cells were washed with tap water and air dried.

For soft agar assays, 2% low melting temperature agarose was dissolved in ddH_2O and mixed 1:1 with 2x DMEM mix (20% FCS, 4 mM glutamine, 20 kU/ml penicillin, 20 mg/ml streptomycin, pH 7.4). 1 ml solution was distributed per well of a 12-well plate and allowed to set at room temperature. For the middle layer, 0.8% low melting agarose was dissolved in ddH_2O and mixed 1:1 with 2x DMEM mix containing $1x10^5$ cells per genotype. Subsequently, 1 ml cell suspension was distributed in triplicates (final cell number: $2.5x10^4$ per well), and allowed to set for 30 minutes at room temperature. Finally, the layers were covered with 0.5 ml normal medium to prevent dehydration.

For primary kidney cells, 2x K-1 medium (31.2 g/l DMEM/F12, 2.4 g/l sodium bicarbonate, 20% FCS, 20 kU/ml penicillin, 20 mg/ml streptomycin, 5 µg/ml insulin, 1.25 ng/ml prostaglandin E_1 (PGE_1), 34 pg/ml triiodothyronine, 5 µg/ml transferrin, 1.73 ng/ml sodium selenite, and 18 ng/ml of hydrocortisone, pH 7.4) was used instead of 2x DMEM mix.

For anchorage independent growth assays, $1x10^5$ cells were seeded in untreated polystyrene plates to reduce cell attachment. Medium was changed by filtering the cells in cell strainers (pore size 40 – 100 µm).

2.3.5 Starvation assays

For starvation experiments $2.5x10^5$ (for 24 hour starvation) or $3x10^5$ (for 2 and 6 hours starvation) cells were seeded the day before. Cells were washed twice with PBS and appropriate media was added. After 2, 6 or 24 hours cells were trypsinised and the cellular ATP levels were determined as characterized below (2.4.1) and cells were harvested for Western blotting (see section 2.6). The used media was DMEM supplemented with 10 kU/ml penicillin and 10 mg/ml streptomycin and the ingredients shown in the table below.

	glucose	glutamine	FCS
low glucose	1 g/l	2 mM	10%
no glucose	-	2 mM	10%
no glutamine	4.5 g/l	-	10%
low FCS	4.5 g/l	2 mM	1%

To prepare medium with lower amino acid content, normal DMEM media without glutamine was diluted with the corresponding volume of amino-acid-free DMEM (0.2 g/l

$CaCl_2$, 0.1 mg/l $Fe(NO_3)_3$, 0.2 g/l $MgSO_4$, 0.4 g/l KCl, 3.7 g/l $NaHCO_3$, 6.4 g/l NaCl, 0.125 g/l NaH_2PO_4, 4.5 g/l glucose, 40% Vitamin solution, 10% dialysed FCS, 10 kU/ml penicillin and 10 mg/ml streptomycin).

2.4 Cellular and biochemical assays

2.4.1 ATP measurements

Cells were trypsinised, counted (Beckman counter Vi-Cell XR and Z2) and $1.5x10^5$ cells were resuspended in 75 µl PBS and 75 µl buffer (CellTiter-Glo Luminescent Cell Viability Assay, Promega). Cells were lysed for 10 minutes at room temperature and distributed as technical triplicates in an opaque 96-well plate. Luminescence signal was detected with a microplate reader (Anthos Lucy 3). Student's t-test was performed for statistical analysis.

2.4.2 Glutamine uptake

To determine glutamine uptake in cells, $1x10^5$ cells per 6-well plate were seeded in triplicates. The next day cells were incubated for 20 minutes with DMEM (10% FCS, 2 mM glutamine, 10 kU/ml penicillin, 10 mg/ml streptomycin) supplemented with 1µM [U-$^{14}C_5$]-glutamine. Cells were washed twice with ice-cold PBS, lysed for 1 hour with lysis buffer (0.2% SDS; 0.2 M NaOH) and radioactivity was measured by scintillation counting with the Tri-Carb B2910TR Liquid Scintillation Analyzer (PerkinElmer).

2.4.3 Protein synthesis assay

For the detection of protein synthesis cells were incubated for 1 hour in methionine depleted media (DMEM w/o methionine and cysteine supplemented with 10% dialysed FCS, 2 mM glutamine, 10 kU/ml penicillin and 10 mg/ml streptomycin) and for another hour in DMEM containing 20 µCi L-[^{35}S]-methionine (70%)/ L-[^{35}S]-cysteine (25%). As a negative control cells were incubated in the same media supplemented with 10 µg/ml cycloheximid. Cells were washed twice in ice-cold PBS and lysed in buffer containing 10 mM Hepes/KOH (pH 8), 1.5 mM $MgCl_2$, 10 mM KCl and 0.5% NP-40 supplemented with EDTA-free protease inhibitors for 15 minutes on ice. Lysates were centrifuged for 15 minutes and the protein concentration was determined by Bradford protein assay. The total protein (15 µg) was precipitated by 10% trichloroacetic acid, washed twice in ice-cold acetone and radioactivity was measured by scintillation counting with the Tri-Carb B2910TR Liquid Scintillation Analyzer (PerkinElmer).

2.4.4 Extracellular flux and mitochondrial oxygen consumption

The Seahorse Bioscience XF^e96 Extracellular Flux Analyzer (Seahorse Bioscience, North Billerica, MA, USA) was used for the measurement of mitochondrial oxygen consumption and extracellular acidification in MEFs. Therefore $5x10^4$ cells were seeded per well in 12 wells of XF^e 96-well cell culture microplates in 200 µl of DMEM and incubated overnight (14–16 hours) at 37°C in 21% CO_2. The next day the growth medium was replaced with 175 µl of bicarbonate-free DMEM (25 mM glucose, 110 mg/l sodiumpyruvate, 2 mM glutamine, pH 7.4) pre-warmed at 37°C. Before starting the assay procedured cells were preincubated at 37°C for 1 hour for degassing. For the measurement of oxygen consumption rate (OCR) and extracellular acidification rate (ECAR) 5 cycles of mix/wait/measure times of 3/3/3 minutes were used. The protein abundance was determined via Bradford assay.

2.4.5 Metabolomics

For metabolomic analysis $1x10^5$ cells were seeded in triplicates on a 6-well plate. When cells reached 80% confluency the plates were washed twice with prewarmed wash solution (75 mM $(NH_4)_2CO_3$ pH 7.4, 37°C) and frozen by slowly immersing the plate in liquid nitrogen. The plates were stored at -80°C until further analysis. For cell extraction 700 µl prewarmed extraction solution (70% EtOH, 75°C) was added to each well of the plates and were placed on a heating block at 75°C. The closed plates were shaked for 3 minutes on the heating block. After removing the solution, another 700 µl prewarmed extraction solution was added to the plates and gently agitated for further 2 minutes. The extracts were pooled and stored at -80°C until further analysis. Quantification of metabolites was performed on an Agilent 6550 QTOF instrument by flow injection analysis time-of-flight mass spectrometry (Fuhrer et al., 2011). All samples were injected in duplicates. Ions were annotated based on their accurate mass and the Human Metabolome Database reference list allowing a tolerance of 0.001 Da (Wishart et al., 2013). Unknown ions and those annotated as adducts were discarded.

2.4.6 FACS analysis

For the detection of mitochondrial content in MEFs FACS analysis were used. After trypsinising, cells were washed twice in pre-warmed PBS and incubated for 30 minutes at 37°C with 100 nM NAO (mitochondria) in PBS with 10% FCS. Samples were analysed by flow cytometry using FACSCanto II machines. Data were quantitated using WinMDI software.

2.5 Real time PCR-analysis

Total RNA was prepared from cultured cells or from powdered tissue of whole kidneys using NucleoSpin RNA kit and cDNA synthesis was done with random hexadeoxynucleotide primers and Ready-To-Go You-Prime First-Strand Beads. The real-time PCR analysis of cDNA was performed with SYBR Green JumpStart Taq ReadyMix and used primers listed above (2.1.5).

2.6 Western blotting

Protein extracts from cultured cells were prepared by washing the cells twice with cold PBS and lysing in RIPA buffer (50 mM Tris–HCl at pH 7.5, 150 mM sodium chloride, 1% NP-40, 1% sodium deoxycholate, 0.1% SDS, 2mM EDTA, 1 mM sodium fluoride, 1 mM Na_3VO_4, 1 mM PMSF, 1 mM dithiothreitol, 1:100 Protease Inhibitor Cocktail).

For the preparation of nuclear extracts cells were washed once in PBS and subsequently incubated for 20 minutes on ice in lysis buffer (10 mM HEPES, KOH pH 7.9, 10 mM KCl, 0.1 mM EDTA, 0.1 mM EGTA, 1:100 Protease Inhibitor Cocktail, and 1 mM PMSF) followed by addition of NP-40 to a final concentration of 0.1%, vortexing and spinning at 5000 rpm. The nuclear pellet was extracted for 20 minutes on ice with frequent agitation in protein extraction buffer (400 mM NaCl, 20 mM HEPES, KOH pH 7.9, 1 mM EDTA, 1mM EGTA, 1:100 Protease Inhibitor Cocktail, and 1 mM PMSF). To remove insoluble material the lysates were centrifuged at 14000 rpm and 4°C for 10 minutes.

For mitochondrial extracts cells were lysed in TES buffer (25 mM Tris/HCl, 0.2 mM EDTA, 0.33 M sucrose, pH 8) supplemented with 1:100 Protease Inhibitor Cocktail. Cells were than homogenized with a 1 ml syringe with a 29 gauge needle for 8-10 strokes. The solution was centrifuge at 1000 rpm for 10 minutes at 4°C. The supernatant was centrifuged again at 12000 rpm for 10 minutes at 4°C. The pellet contained the crude mitochondrial fraction, the supernatant the cytosolic fraction. Afterwards, the pellet was washed twice with TES buffer, resuspended in RIPA buffer and kept at −80°C until further analysis.

Using the Bradford protein assay cleared protein lysates were quantitated using bovine serum albumin as a standard. Prior to use, samples were boiled for 5 minutes at 95°C. Proteins were run on 6–15% acrylamide gels, transferred to nitrocellulose membranes and visualized by semi-dry immunoblotting with antibodies described above (2.1.4). The signal was detected using the Fujifilm Luminescent Image Analyzer LAS4000 mini.

2.7 Mouse maintenance

2.7.1 Mouse strains

Rb1$^{fl/fl}$ (Marino et al. 2000), *Vhl*$^{fl/fl}$ (Haase et al. 2001), *Trp53*$^{fl/fl}$ (Jonkers et al. 2001) mice were crossed with Ksp1.3-Cre-ER^{T2} (Patel et al. 2008) mice to generate Ksp1.3-Cre-ER^{T2}; *Vhl*$^{fl/fl}$; *Rb1*$^{fl/fl}$; *Trp53*$^{fl/fl}$, Ksp1.3-Cre-ER^{T2}; *Vhl*$^{fl/fl}$; *Rb*$^{fl/fl}$, Ksp1.3-Cre-ER^{T2}; *Rb*$^{fl/fl}$; *Trp53*$^{fl/fl}$, Ksp1.3-Cre-ER$^{T2\ Tg/+}$; *Rb1*$^{fl/fl}$. Previously described Ksp1.3-Cre/+; *Vhl*$^{fl/fl}$ (Frew et al. 2008) and Ksp1.3-Cre/+; *Trp53*$^{fl/fl}$ (Wild et al. 2012) mouse strains were interbred to generate Ksp1.3-Cre/+; *Vhl*$^{fl/fl}$; *Trp53*$^{fl/fl}$ mice. Non-Cre transgenic littermate mice served as controls for all cohorts. SCID/Beige mice (C.B-17/IcrHsd-Prkdc^{scid} Lyst^{bg-J}) were obtained from Harlan Laboratories (USA). Wild type cells were isolated from C57BL/6 embryos (Janvier Labs (USA)).

2.7.2 Genotyping

Ear biopsies were digested for 15 minutes at 95°C in lysis buffer (25 mM NaOH, 0.2 mM EDTA, pH 12) and thereafter neutralised with the same amount of neutralisation buffer (40 mM Tris-HCl, pH 5). The PCR reaction was carried out according to standard procedures using JumpStart Taq DNA polymerase and the primers shown in table 2.1.5. The DNA was analyzed on 1.5% agarose gels in SBE buffer (5 mM NaOH buffered with boric acid, pH 8.5).

2.7.3 Tamoxifen treatment

Ksp1.3-Cre/ER^{T2} transgenic mice were administered tamoxifen for induction of Cre/loxP recombination. Tamoxifen was dissolved in 100% ethanol and diluted 10-fold in corn oil to a final concentration of 20 mg/ml. Mice were injected intra peritoneal with tamoxifen (4 mg/40 g body weight) at P35 for 5 consecutive days and at P11 only once. To induce recombination in newborn mice, nursing dams were injected with tamoxifen (4 mg/40 g body weight) on post-partum days 2-4. Non-Cre transgenic littermate mice served as controls for all cohorts.

2.7.4 Xenograft assay

3-5x10^6 cells were detached with Accutase and resuspended in 70 µl DMEM. Cells were placed in a pre-cooled 30 gauge syringe and mixed with 70 µl ice cold matrigel. Syringes were kept on ice to avoid hardening of matrigel. SCID/Beige mice were anaesthetized by inhalation of 2% isofluorane using oxygen as carrier gas, shaved at both flanks and cells

were slowly injected subcutaneously. Mice were euthanized the latest when xenograft size reached a size of 1 cm^3. The xenograft was fixed in 10% formalin and processed as described below (2.8).

2.8 Tissue collection and procedure

Mouse tissues were immersion-fixed in 10% formalin at 4°C overnight and stored in 70% ethanol. After dehydration in serial dilutions (3 hours 70% EtOH, 2 hours 80% EtOH, 2 hours 90% EtOH, 2 hours 96% EtOH, 2 hours 100% EtOH, 2 hours xylene, 3 hours paraffin at 65°C), organs were embedded in paraffin and cut into 5 µm sections and fixed on polysine glass slides (VWR).

2.9 Histological analysis

2.9.1 Haematoxylin and Eosin (H&E) staining

Tissue sections were de-waxed for 3 minutes in xylene and hydrated for 2 minutes each in serial dilutions of ethanol washes (100%, 95%, 70%). Nuclei were stained for 4 minutes in haematoxylin and dipped three times in 0.3% acid alcohol for differentiation. Proteins were stained for 8 minutes in 1% eosin solution. Finally, specimen were dehydrated for 2 minutes in serial ethanol dilutions (70%, 95%, 100%), 3 minutes in xylene and mounted in entellan.

2.9.2 Immunohistochemistry

Tissue sections were de-waxed in xylene and hydrated in series of ethanol washes (10 minutes xylene, 100 % EtOH, 95% EtOH and 5 minutes in 70% EtOH) and washed for 5 minutes in PBS-T (137 mM NaCl, 2.7 mM KCl, 19 mM Na_2HPO_4, 1.7 mM KH_2PO_4, pH 7.4, 0.3% Triton X-100). For antigen retrieval, slides were cooked for 5 minutes at 110°C in 0.1 M citrate buffer (pH 6) using a standardized pressure cooker (HistosPro, Milestone). Next, specimens were incubated in peroxidase blocking solution (3% H_2O_2 in 10% methanol) for 30 minutes, circled with a hydrophobic pen and incubated in protein blocking solution (PBS, supplemented with 10% goat serum, 0.3% Triton X-100, 1 drop avadin per 250 µl solution). Primary antibodies were diluted in PBS, containing 10% goat serum, 0.3% Triton X-100 and 1 drop biotin solution per 250 µl blocking buffer) and sections were incubated overnight at 4°C. Biotinylated secondary antibodies were diluted (10% goat serum in PBS) and applied for 1 hour at room temperature. Sections were washed and subsequently incubated in TBS (20 mM Tris, 150 mM NaCl, pH 7.6) for

10 minutes. For complex formation, 1 drop Avadin DH and 1 drop biotinylated horseradish peroxidase were mixed in 2.5 ml TBS 30 minutes prior to use, and solution was applied for 1 hour at room temperature. Next, specimen were washed in TBS and incubated in 50 mM Tris (pH 7.6). 3,3'-diaminobenzidine (DAB) was used as a chromogen according to the manufacturer's instructions. Finally, the specimens were counterstained with hematoxylin solution for 30 seconds, dehydrated in serial ethanol dilutions (1 minute 70% EtOH, 2 minutes 95% EtOH and 100% EtOH, 3 minutes in Xylene) and mounted in entellan. All incubations were performed in a humidified chamber. Between incubations, sections were washed three times for 5 minutes in PBS, unless otherwise stated.

Immunohistochemistry targeting Hifα and Rb1 proteins was performed using the Dako Catalyzed Signal Amplification (CSA) kit according to the manufacturer's instruction. The following changes were included in the protocol: After peroxidase block, specimen were incubated for 15 minutes in Avadin solution (TBS, supplemented with 1% BSA, 0.1% Tween-20, 2 drops Avadin solution per 250 µl solution), followed by 15 minutes biotin solution (TBS, containing 1% BSA, 0.1% Tween-20 and 2 drops biotin solution per 250 µl solution). For washing, standard TBS-T (50 mM Tris, 150 mM NaCl, 0.1% Tween-20) was used before primary antibody incubation, whereas high salt TBS-T (0.05 M Tris-HCl pH 7.6 containing 0.3 M NaCl and 0.1% Tween-20) was used afterwards. Rehydration of sections, antigen retrieval and counterstaining was performed as described above.

3 Combined mutation of *Vhl* and *Trp53* causes renal cysts and tumours in mice

During the initial part of my PhD work I participated in a project that analysed the effects of deletion of *Vhl* and *Trp53* in the epithelium of mouse kidneys and genital-urinary tract. This publication forms the first Results chapter and several conclusions are relevant for the rationale and understanding of the results presented in the subsequent Results chapters. In summary, these studies revealed that double deletion of *Vhl* and *Trp53* causes the formation of simple cysts, atypical cysts and neoplasms in the kidneys, and deletion in the epithelia of the genital urinary tract leads to dysplasia and tumour formation. Mouse embryonic fibroblasts undergo senescence when the *Vhl* gene is deleted. We discovered that this phenotype is rescued by the co-deletion of *Trp53*. The loss of *Vhl* and *Trp53* results in the immortalisation but not in the transformation of these cells. The growth of *Vhl* deficient cells is largely independent of oxygen concentrations. Personally I answered the question that the culturing of these cells in 5% compared to 21% oxygen leads to a partial but not full restoration of proliferative capacity (Figure 1G and 1H of (Albers et al. 2013)) and performed several experiments relating to analyses of MEFs deficient for *Vhl* and/or *Trp53*. Due to these findings all of the following experiments described in this thesis were performed at 5% oxygen in a cell culture incubator.

Research Article
Kidney cysts and tumours in *Vhl/Trp53* mutant mice

TRANSPARENT PROCESS OPEN ACCESS EMBO Molecular Medicine

Combined mutation of *Vhl* and *Trp53* causes renal cysts and tumours in mice

Joachim Albers[1,2†], Michal Rajski[1,3†], Désirée Schönenberger[1†], Sabine Harlander[1,2,3†], Peter Schraml[4], Adriana von Teichman[4], Strahil Georgiev[5], Peter J. Wild[2,4], Holger Moch[2,4], Wilhelm Krek[2,5], Ian J. Frew[1,2,3]*

Keywords: ccRCC; cyst; p53; *VHL*

DOI 10.1002/emmm.201202231

Received November 02, 2012
Revised March 08, 2013
Accepted March 12, 2013

The combinations of genetic alterations that cooperate with von Hippel–Lindau (*VHL*) mutation to cause clear cell renal cell carcinoma (ccRCC) remain poorly understood. We show that the *TP53* tumour suppressor gene is mutated in approximately 9% of human ccRCCs. Combined deletion of *Vhl* and *Trp53* in primary mouse embryo fibroblasts causes proliferative dysregulation and high rates of aneuploidy. Deletion of these genes in the epithelium of the kidney induces the formation of simple cysts, atypical cysts and neoplasms, and deletion in the epithelia of the genital urinary tract leads to dysplasia and tumour formation. Kidney cysts display a reduced frequency of primary cilia and atypical cysts and neoplasms exhibit a pro-proliferative signature including activation of mTORC1 and high expression of Myc, mimicking several cellular and molecular alterations seen in human ccRCC and its precursor lesions. As the majority of ccRCC is associated with functional inactivation of *VHL*, our findings suggest that for a subset of ccRCC, loss of p53 function represents a critical event in tumour development.

INTRODUCTION

Clear cell renal cell carcinoma (ccRCC) accounts for approximately 80% of kidney tumours and thereby approximately 2.5% of all types of human malignancy. The von Hippel–Lindau (*VHL*) tumour suppressor gene is mutated, deleted or epigenetically silenced in up to 85% of all sporadic cases of ccRCC (Maher, 2013). Germline inheritance of a single mutant allele of *VHL* gives rise to the dominantly inherited VHL familial cancer syndrome which predisposes not only to the formation of ccRCC, but also to cystic lesions in the kidney and pancreas as well as to diverse types of tumours in the central nervous system, eye, ear, pancreas, adrenal gland, epididymis and broad ligament (Kaelin, 2002).

The pVHL protein has been ascribed several distinct biochemical activities and implicated in the regulation of diverse cellular processes, dysregulation of any or all of which could be envisaged to play important roles in tumour formation (Frew & Krek, 2007). Two lines of evidence however suggest that loss of pVHL function alone is insufficient for tumour initiation in the kidney. Kidneys of patients with an inherited *VHL* mutation frequently display cystic lesions as well as ccRCC. Since some pVHL-deficient proliferative cysts contain micro-foci of ccRCC, it is believed that, at least in some cases, cysts represent a precursor lesion in the evolution of malignant ccRCC (Lubensky et al, 1996; Walther et al, 1995). Detailed analysis of regions of normal histology in these kidneys revealed that VHL patient kidneys likely contain many thousands of individual isolated cells that are null for pVHL function (Mandriota et al, 2002; Montani et al, 2010). pVHL-deficient cysts and ccRCC apparently arise infrequently in comparison to the total frequency of *VHL* mutation. Secondly, heterozygous deletion of the mouse homologue of the *VHL* gene, *Vhl* (previously referred to as *Vhlh*), in the entire mouse (Haase et al, 2001), or

(1) Institute of Physiology, University of Zurich, Zurich, Switzerland
(2) Competence Center for Systems Physiology and Metabolic Diseases, ETH Zurich and University of Zurich, Zurich, Switzerland
(3) Zurich Center for Integrative Human Physiology, University of Zurich, Zurich, Switzerland
(4) Institute of Surgical Pathology, University Hospital Zurich, Zurich, Switzerland
(5) Institute of Molecular Health Sciences, ETH Zurich, Zurich, Switzerland
***Corresponding author:** Tel: +41 44 635 5004; Fax: +41 44 635 6814; E-mail: ian.frew@access.uzh.ch

†These authors contributed equally to this work.

homozygous deletion under the control of kidney-specific Cre transgenes, does not lead to proliferative dysregulation or tumour formation in the kidney (Frew et al, 2008b; Rankin et al, 2006). Multiple genetic mutations appear to be required to cause proliferation and transformation of pVHL-deficient cells.

Genes that are mutated at high frequency in diverse human epithelial tumours, including *PTEN*, *EGFR*, *ERBB2*, *BRAF*, *RAS* family genes, *RB1* and *APC*, are either not mutated or are mutated at relatively low frequencies (<10%) in ccRCC. Rather, ccRCC frequently (41%) harbour mutations in the chromatin remodelling gene *PBRM1* (Varela et al, 2011) and in several genes involved in histone modification (Dalgliesh et al, 2010) and protein ubiquitination and de-ubiquitination (Guo et al, 2012; Pena-Llopis et al, 2012). Several chromosomal regions are frequently amplified or deleted and numerous genes are frequently hypermethylated in ccRCC (Maher, 2013), implying that there may be many different combinations of genetic alterations that can cooperate with loss of *VHL* function to cause tumour formation. Our previous studies demonstrate that low-frequency mutations could be functionally important in ccRCC formation; co-deletion of *Vhl* and *Pten* in the mouse kidney led to the formation of proliferative cysts, mimicking the precursor lesions of ccRCC that arise in human VHL patients (Frew et al, 2008b). Several studies, including data presented herein, have shown that *TP53* is mutated in a subset of ccRCC (http://cancer.sanger.ac.uk/cosmic). We demonstrate that combined mutation of *Vhl* and *Trp53* causes dysregulation of cellular proliferation in primary mouse embryo fibroblasts (MEFs) and kidney epithelial cells and results in the formation of kidney cysts and neoplastic lesions in kidneys as well as tumours in genital tract organs.

RESULTS

TP53 mutations occur in sporadic ccRCCs

We sequenced the entire *VHL* gene and exons 5–8 of the *TP53* gene in 54 cases of sporadic ccRCC (Table 1). As expected, missense or truncating *VHL* mutations were observed in 73% of the tumours. Immunohistochemistry for the HIF1α-inducible proteins CA9 and Glut1, and for HIF1α itself, revealed moderate or strong expression of at least one of these markers in all but two of the tumours, verifying the well-described hypoxic signature associated with loss of function of pVHL. *TP53* mutations that affected the coding region were detected in 5 (9%) tumours, all of which are either previously described pathogenic mutations or are predicted to be pathogenic. One tumour harboured both *VHL* and *TP53* mutations, while the other four *TP53* mutant tumours were wild-type for *VIIL*. While methylation analyses for the *VHL* gene were not possible in these samples, it is likely that pVHL expression may be silenced in these tumours as they showed very high immunohistochemical staining for the HIFα target genes. In agreement with our data, the COSMIC database (http://cancer.sanger.ac.uk/cosmic) lists 30 of 209 (14.4%) tumours that display *TP53* coding region mutations. Unfortunately the *VHL* mutation status of these tumours is in most cases unknown. Thus, *TP53* is mutated in a significant fraction of sporadic ccRCCs.

Trp53 mutation allows immortalisation of *Vhl* mutant primary mouse embryo fibroblasts

We first utilized primary MEFs to investigate potential cooperative interactions of the mouse *Vhl* and *Trp53* genes in proliferative control. Deletion of *Vhl* in primary and transformed MEFs induces proliferation arrest and/or the onset of premature senescence (Mack et al, 2005; Welford et al, 2010; Young et al, 2008). Consistent with these findings, lentiviral-mediated shRNA knockdown of *Vhl* led to rapid loss of proliferative capacity of wild-type MEFs (Fig 1A). In contrast, *Vhl* knockdown had no anti-proliferative effect on $Trp53^{-/-}$ MEFs (Fig 1C). Interestingly, while efficient reduction of pVHL protein was maintained throughout the duration of the experiment in wild-type cells (Fig 1B), the extent of knockdown rapidly diminished with increasing passage in $Trp53^{-/-}$ cells (Fig 1D), suggesting that there is a proliferative selection for those cells in which the knockdown occurs less efficiently. To attempt to overcome this problem of selection, MEFs from wild-type, $Vhl^{fl/fl}$, $Trp53^{fl/fl}$ and $Vhl^{fl/fl}Trp53^{fl/fl}$ mice were infected with adenovirus expressing GFP (Adeno-GFP) as control or with adenovirus expressing a Cre-GFP fusion protein (Adeno-Cre) to delete the floxed genes. *Vhl* knockout MEFs rapidly lost proliferative capacity whereas *Vhl/Trp53* double deletion allowed proliferation, albeit at a slower rate of proliferation than *Trp53* deletion alone (Fig 1E). Consistent with a rescue of senescence, *Vhl/Trp53* double null cells retained the appearance of proliferating cells while *Vhl* deletion caused an enlarged, flattened cell morphology characteristic of senescence (Supporting Information Fig 1). None of the gene deletions allowed the formation of colonies in soft agar, demonstrating that the cells are immortalized but not transformed. Western blotting 4 days after infection confirmed the high efficiency of gene deletion but after approximately 20–30 days of continuous proliferation, a significant restoration of pVHL expression was evident in the $Vhl^{fl/fl}Trp53^{fl/fl}$ Cre-infected cell population (Fig 1F), suggesting a mixed cell population in which *Vhl* null cells have a proliferative disadvantage in comparison to an initially rare population of pVHL-expressing cells (see results below).

In light of recent findings showing that senescence induced by loss of *Vhl* can be rescued by culturing cells at 2 or 5% oxygen (Welford et al, 2010), we conducted a series of experiments in which cells were grown at 5% oxygen. We observed a reproducible but only partial restoration of proliferative capacity following *Vhl* knockout (Fig 1G) when cells were cultured either in a glove box incubator to ensure constant oxygen tension throughout the experiment or in a conventional oxygen incubator where cells were briefly exposed to 21% oxygen every 3 days during passaging. In either incubator, wild-type MEFs did not enter senescence within 50 days of culture at 5% oxygen but typically entered senescence after about 10–12 days at 21% oxygen, verifying our culture system against published data (Parrinello et al, 2003). In light of this partial rescue of proliferation of *Vhl* mutant cells, all subsequent proliferation

Table 1. *VHL* and *TP53* mutations and CA9, GLUT1 and HIF1α immunohistochemistry in sporadic cases of human ccRCC

pT	*VHL* sequencing			Immunohistochemistry			*TP53* sequencing			
	Exon 1	Exon 2	Exon 3	CA9	Glut1	HIF1α	Exon 5	Exon 6	Exon 7	Exon 8
3	–	–	A207CfsX49	2	0	0	–	–	–	–
3b	–	T124RfsX5	–	2	2	1	–	–	–	–
3	–	H115SfsX17	–	2	1	0	–	–	–	–
3b	N78S	–	–	2	2	1	n.a.	–	–	–
3b	–	–	–	1	2	0	K139K	–	–	–
3a	–	V155CfsX4	–	2	0	2	–	–	–	–
3b	–	–	–	1	0	n.a.	Q165X	–	–	–
3	–	–	–	2	1	1	n.a.	–	–	–
3b	–	–	R167_V170del	2	2	2	–	–	–	–
3a	–	–	–	1	1	1	–	–	–	–
3b	P99QfsX60	–	–	2	2	1	–	R213R	–	–
3b	S68T	–	–	2	2	0	–	–	–	–
3a	–	–	–	0	1	0	–	–	–	–
3	S65T	–	–	2	2	0	–	–	–	–
3a	–	–	I180V	2	2	2	–	–	–	–
3	–	V130F	–	2	1	0	–	–	L257L	–
3b	–	L153TfsX21	–	2	1	1	–	R142R	–	–
4	–	–	V170D	2	2	1	–	–	–	–
3a	–	–	L158V	2	n.a.	0	–	–	–	–
3a	–	–	H191H	2	2	0	–	P219L	–	–
3a	–	–	–	2	2	0	H179L	–	–	–
3a	–	W117R	–	2	2	2	–	–	–	–
3b	–	–	R161P	0	0	1	–	–	–	–
4	Y98X	–	–	0	2	1	–	–	–	–
3a	T100SfsX59	–	–	2	2	2	–	–	–	–
4	–	–	–	0	2	n.a.	–	–	–	–
3a	–	–	–	2	2	0	–	–	–	–
3	L101P	–	–	2	2	0	–	–	–	–
3a	–	–	–	2	2	1	–	–	–	–
3a	Y112D	–	–	n.a.	n.a.	0	–	–	–	–
3b	D92AfsX36	–	–	2	2	0	–	–	–	–
3b	V62CfsX5	–	–	1	n.a.	0	–	–	–	–
3	–	–	–	1	2	0	–	–	–	–
3b	c.340 + 1G>T	–	–	2	2	0	–	–	–	–
3	S65L	–	–	2	2	1	–	–	–	–
3	–	c.341-2A>G	–	2	2	0	–	–	–	–
3a	–	–	–	2	2	1	–	–	–	–
4	S68X	–	–	2	2	0	–	–	–	–
3b	Y98N	–	–	2	1	0	–	R213R	–	–
3b	S68X	–	–	2	2	0	–	–	–	–
3b	R107VfsX45	–	–	2	2	1	–	–	–	–
3b	Q73X	–	–	0	2	0	–	–	–	R273C
3a	–	–	R161X	2	n.a.	1	–	–	–	–
3b	–	–	V181KfsX14	n.a.	n.a.	0	–	–	–	–
3	n.d.	n.d.	n.d.	2	2	0	–	–	–	–
3	n.d.	n.d.	n.d.	2	2	0	–	–	–	–
3	n.d.	n.d.	n.d.	2	2	1	–	–	–	–
3	n.d.	n.d.	n.d.	0	1	1	–	–	–	–
3	n.d.	n.d.	n.d.	2	2	2	–	–	–	–
3	n.d.	n.d.	n.d.	0	1	1	–	–	–	–
2	n.d.	n.d.	n.d.	2	1	1	–	–	–	–
4	n.d.	n.d.	n.d.	2	2	0	–	1bp ins*	–	–
3	n.d.	n.d.	n.d.	1	2	1	–	–	–	–
3	n.d.	n.d.	n.d.	2	1	1	–	–	–	–

Grey shading highlights a mutation that causes a coding alteration. Amino acid alterations are shown by single letter code, del = deletion, fs = frame shift, X = new stop codon, n.a. = not analysable, n.d. = not determined, * = bp insertion not identifiable, 0 = no staining, 1 = moderate staining, 2 = strong staining.

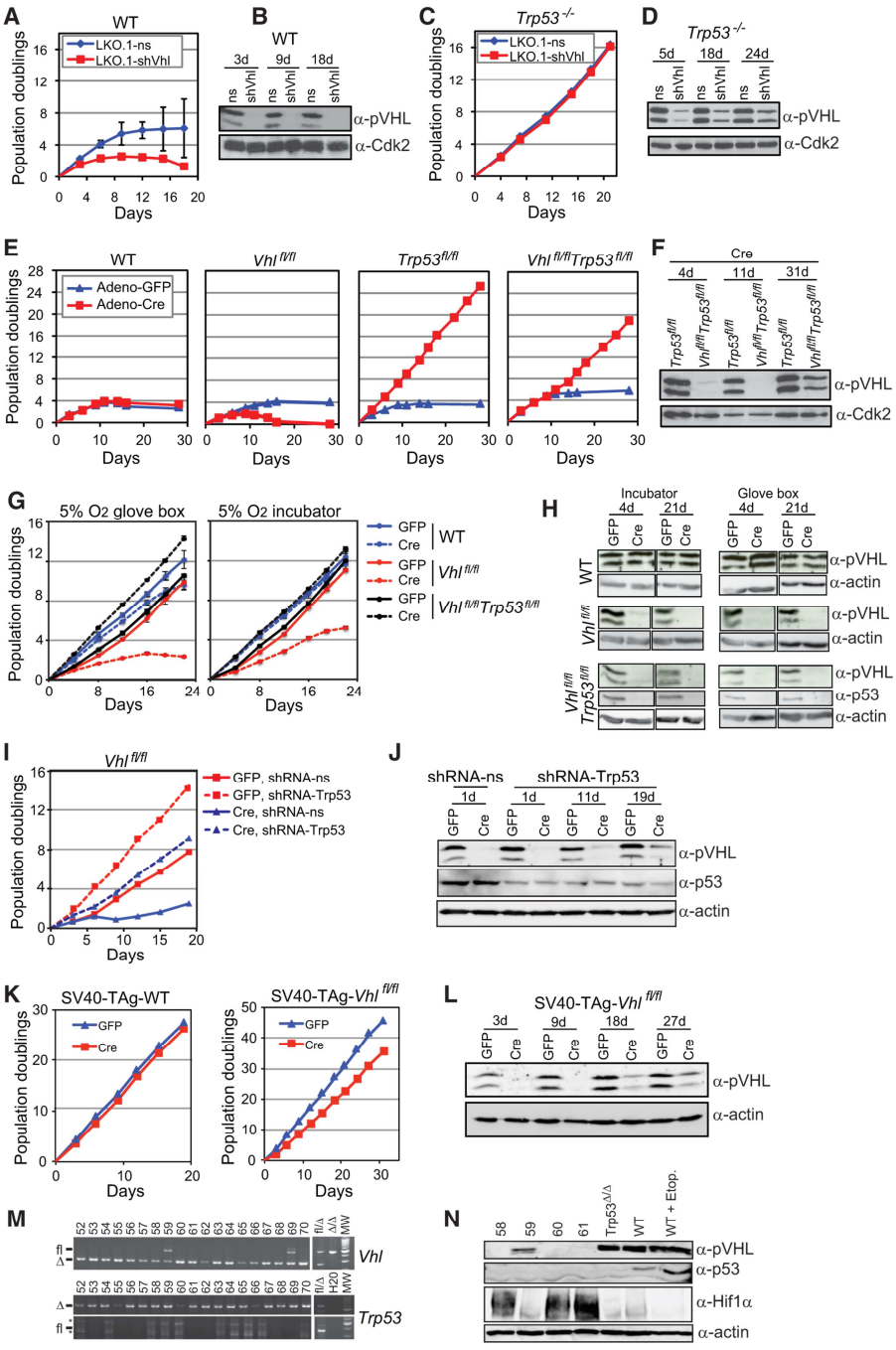

Figure 1.

experiments were conducted at 5% oxygen in a conventional incubator.

To permit comparison of proliferation rates in an isogenic background, we knocked down *Trp53* in $Vhl^{fl/fl}$ MEFs. *Trp53* knockdown rescued the proliferation defect of *Vhl* knockout (Adeno-Cre treated) cells but these cells proliferated more slowly than control (Adeno-GFP treated) cells with *Trp53* knockdown alone (Fig 1I). The *Vhl* knockout/*Trp53* knockdown cultures became enriched with pVHL-expressing cells over time (Fig 1J). A similar reduction in proliferation rate (Fig 1K) and passage-dependent enrichment of pVHL-expressing cells in the cell population (Fig 1L) was also observed in cultures where *Vhl* was deleted from $Vhl^{fl/fl}$ MEFs that had been transformed with SV40 Large T-Antigen to simultaneously inactivate both the p53 and pRB-dependent cell cycle checkpoints. Thus, loss of pVHL compromises cellular proliferation in MEFs in a manner independent of the p53 and pRB cell cycle checkpoints.

Given the strong selection against pVHL-expressing cells in bulk population experiments, we performed experiments using single cells to definitively address the question of whether *Vhl*/*Trp53* double null cells are truly immortalized. While wild-type MEFs undergo cellular senescence when plated as single cells, *Trp53* null cells form colonies allowing the generation of immortalized cell lines founded from single cells. Two days after infection of $Vhl^{fl/fl}Trp53^{fl/fl}$ primary MEFs with Adeno-Cre, cells were plated at a density of 0.5 cells/well in six 96-well plates. Cell lines were generated over a period of 6 weeks and genotyped to detect the floxed or deleted *Vhl* allele, allowing a retrospective assessment of the genotype of the initiating cell of the cell line. From a theoretical maximum of 288 cell lines, 135 cell lines were generated. One hundred and thirty-three of these harboured homozygous deletion of *Vhl*, while two were heterozygous for the floxed and deleted allele (Fig 1M). All cell lines showed homozygous deletion of the floxed *Trp53* gene (Fig 1M). Western blotting of a subset of these cell lines confirmed the PCR genotyping results (Fig 1N). Thus, *Trp53* deletion efficiently allows immortalization of *Vhl* null MEFs. It is likely that the rare cells in which only one floxed *Vhl* allele (but both floxed *Trp53* alleles) has undergone Cre-mediated recombination have a proliferative advantage over the *Vhl*/*Trp53* null cells, allowing them to accumulate over time in bulk populations.

Trp53 mutation rescues proliferation of *Vhl* mutant primary renal epithelial cells

To investigate the cooperative effects of combined *Vhl* and *Trp53* deletion in a disease-relevant cell type we cultured primary mouse renal epithelial cells from the various floxed mouse strains at 5% oxygen and deleted *Vhl* and/or *Trp53* using Adeno-Cre or using Adeno-GFP as control (Fig 2A). While long-term assays of renal epithelial cell behaviour are not possible due to the epithelial to mesenchymal transition that occurs over time, in short term assays we observed that deletion of *Vhl* inhibited the proliferation of renal epithelial cells and co-deletion of *Trp53* rescued this inhibition of proliferation (Fig 2B). Unlike in MEFs, cultures of *Trp53* or *Vhl/Trp53* null renal epithelial cells formed colonies when plated at single cell density with very low efficiency (<1%), and did not grow in soft agar, demonstrating that these cells are not immortalized or transformed.

Enhanced rates of aneuploidy in *Trp53* and *Vhl/Trp53* mutant MEFs

One driving force in the evolution of tumours is aneuploidy. Loss of pVHL, through an uncharacterized mechanism, results in lower levels of the mitotic checkpoint protein Mad2, which alone causes a moderate elevation of levels of aneuploidy but when combined with reduction in expression of another mitotic spindle checkpoint protein, CENP-E, induces a dramatic increase in aneuploidy (Thoma et al, 2009). Here we confirm that deletion (Fig 3A) or knockdown (Fig 3B) of *Vhl* causes a reduction of Mad2 protein expression. Loss of *Trp53* function in MEFs also causes higher levels of aneuploidy and polyploidy and has been shown to result in aberrantly elevated expression levels of the checkpoint proteins Aurora A (Mao et al, 2007), Mad2 and separase (Pati et al, 2004). Western blotting of

◀ **Figure 1. *Trp53* mutation allows immortalized proliferation of *Vhl* null MEFs.**

A,C. Proliferation assays of wild-type (A) and $Trp53^{-/-}$ (C) MEFs following infection with pLKO.1 lentiviruses expressing a non-silencing sequence (ns) or shRNA directed against *Vhl* (shVhl).

B,D. Western blotting analysis for pVHL in cells from A and C at the time points (number of days after infection) indicated. Immunoblotting using an antibody against Cdk2 served as a loading and transfer control.

E. Proliferation assays of wild-type, $Vhl^{fl/fl}$, $Trp53^{fl/fl}$ or $Vhl^{fl/fl}Trp53^{fl/fl}$ MEFs following infection with adenoviruses expressing GFP (GFP) or Cre-GFP (Cre).

F. Western blotting analysis of $Trp53^{fl/fl}$ and $Vhl^{fl/fl}Trp53^{fl/fl}$ MEFs in E at the indicated time points. Immunoblotting using an antibody against actin served as a loading and transfer control.

G. Proliferation assays of wild-type, $Vhl^{fl/fl}$ and $Vhl^{fl/fl}Trp53^{fl/fl}$ MEFs in 5% oxygen.

H. Western blotting analysis of cells from G at the indicated timepoints.

I. Proliferation assays of $Vhl^{fl/fl}$ MEFs infected with GFP or Cre and lentiviruses expressing an empty miR30 shRNA (shRNA-ns) or miR30-format shRNA directed against *Trp53* (shRNA-Trp53).

J. Western blotting analysis of cells from I at the indicated time points.

K. Proliferation assays of SV40 T-antigen transformed WT and $Vhl^{fl/fl}$ MEFs following GFP or Cre infection.

L. Western blotting analysis of SV40-TAg-$Vhl^{fl/fl}$ from K at the indicated timepoints.

M. Cell lines (52–70) derived from Cre-infected $Vhl^{fl/fl}Trp53^{fl/fl}$ MEFs genotyped for floxed (fl) and deleted (Δ) *Vhl* and *Trp53* alleles. Samples with known *Vhl* and *Trp53* genotypes served as controls, MW: molecular weight markers, * non-specific bands.

N. Western blotting analysis of clones 58–61 for pVHL, p53 and Hif1α, confirming the loss of p53 expression and presence and functionality of pVHL expression in clone 59. Lysates from *Trp53* null MEFs, wild-type MEFs or wild-type MEFs treated with etoposide (10 μM, 6 h) served as controls for the p53 protein.

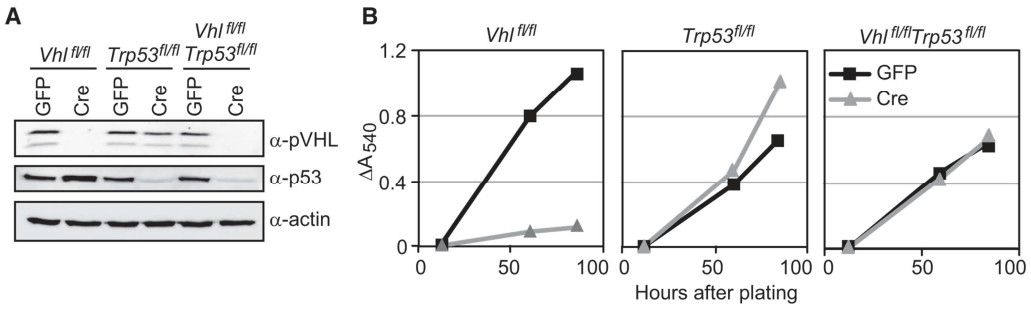

Figure 2. *Trp53* deletion rescues proliferative defects of *Vhl* null primary kidney epithelial cells.

A. Western blotting analysis of primary kidney epithelial cell cultures derived from $Vhl^{fl/fl}$, $Trp53^{fl/fl}$ or $Vhl^{fl/fl}Trp53^{fl/fl}$ mice 3 days after infection with adenoviruses expressing GFP or Cre.

B. Proliferation of cells from A assessed using an SRB assay to detect increase in total protein content of the culture over time.

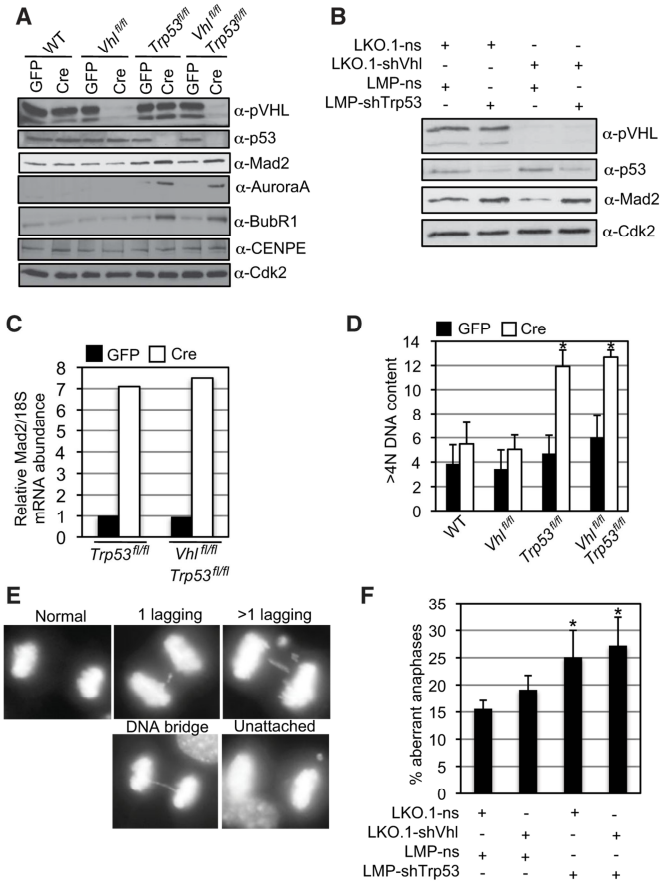

Figure 3. High rates of aneuploidy in *Trp53* and *Vhl/Trp53* null MEFs.

A. Western blotting analysis of wild-type, $Vhl^{fl/fl}$, $Trp53^{fl/fl}$ or $Vhl^{fl/fl}Trp53^{fl/fl}$ MEFs infected with adenoviruses expressing GFP (GFP) or Cre-GFP (Cre).

B. Western blotting analysis of wild-type MEFs infected with combinations of pLKO.1 lentiviruses expressing a non-silencing sequence (ns) or shRNA directed against *Vhl* (shVhl) and LMP retroviruses expressing a non-silencing sequence (ns) or shRNA directed against *Trp53* (shTrp53).

C. Real-time quantitative PCR analysis of Mad2 mRNA abundance normalized to 18S mRNA abundance in GFP and Cre infected $Trp53^{fl/fl}$ and $Vhl^{fl/fl}Trp53^{fl/fl}$ MEFs.

D. Frequency of cells with greater than 4N DNA content as assessed by flow cytometric analysis. Results represent mean ± SD of triplicate samples and * represents statistically significant differences between GFP and Cre treated cells of the same genotype (Student's *t*-test, $p < 0.01$).

E. Depiction of a normal anaphase and examples of anaphases showing a range of chromosome segregation defects.

F. Anaphases of cells from B were scored five days after infection according to the scheme shown in E and the percentage of aberrant anaphases calculated. Data represent mean ± SD of triplicate samples (in each $n > 120$ anaphases were counted) and * represents statistically significant differences to cells infected with both ns vectors (Student's *t*-test, $p < 0.01$).

Trp53$^{fl/fl}$ cells infected with Adeno-Cre (Fig 3A) revealed elevated expression levels of Aurora A and Mad2, as well as elevated expression of BubR1, another spindle checkpoint protein, but no change in the expression levels of CENP-E. To our knowledge this is the first report of this effect of p53 on BubR1. Since double mutation of *Mad2* and *Trp53* has been shown to lead to dramatic levels of aneuploidy (Burds et al, 2005), we investigated whether the combined effects of loss of *Vhl* and *Trp53* on the expression of various mitotic spindle checkpoint proteins would have a similar effect. However, *Vhl/Trp53* double knockout (Fig 3A) or double knockdown (Fig 3B) cells displayed higher than normal levels of Mad2. This was presumably due to the elevation in mRNA abundance of *Mad2* in *Trp53* and *Vhl/Trp53* knockout MEFs (Fig 3C), consistent with previous observations that p53 represses *Mad2* mRNA expression (Pati et al, 2004), overriding the effect of loss of *Vhl* in reducing Mad2 expression. Thus, in terms of the expression of several proteins whose levels regulate spindle checkpoint function, *Vhl/Trp53* double null cells are similar to *Trp53* null cells. Functional studies supported this idea. Flow cytometry revealed that cultures of *Trp53* null MEFs accumulated polyploid cells at the same frequency as cultures of *Vhl/Trp53* double null MEFs (Fig 3D). To directly monitor the integrity of the mitotic spindle checkpoint in an isogenic background we performed lentiviral-mediated knockdown of *Vhl* and/or *Trp53* in MEFs and performed fluorescence microscopy to detect aberrant anaphases that are characterized by the presence of lagging or unattached chromosomes or DNA bridges (Fig 3E). Knockdown of *Vhl* led to a slightly increased rate of aberrant anaphases (Fig 3F), *Trp53* knockdown and *Vhl/Trp53* double knockdown both led to a statistically significant increase in the frequency of aberrant anaphases in comparison to control knockdowns, but the two genotypes were not significantly different from one another (Fig 3F).

In summary, while there appear to be no cooperative genetic effects of loss of *Vhl* and *Trp53* function on aneuploidy, *Trp53* mutation in a *Vhl* mutant background may enhance aneuploidy, which may be relevant for tumourigenesis.

Deletion of *Vhl* and *Trp53* in mouse kidney and genital–urinary tract epithelia causes dysplasia and tumour formation

To investigate the consequences of combined deletion of *Vhl* and *Trp53* in epithelial tissues *in vivo*, *Vhl*$^{fl/fl}$ and *Trp53*$^{fl/fl}$ mice were interbred with *Ksp1.3-Cre* transgenic mice to generate *Ksp1.3-Cre*; *Vhl*$^{fl/fl}$ (Frew et al, 2008b), *Ksp1.3-Cre*; *Trp53*$^{fl/fl}$ (Wild et al, 2012) and *Ksp1.3-Cre*; *Vhl*$^{fl/fl}$; *Trp53*$^{fl/fl}$ mice, hereafter referred to as Vhl$^{\Delta/\Delta}$, Trp53$^{\Delta/\Delta}$ and Vhl$^{\Delta/\Delta}$Trp53$^{\Delta/\Delta}$ mice respectively. In the kidney, the *Ksp1.3-Cre* transgene induces gene deletion in the epithelial cells at the urinary pole of the glomerulus, distal tubules, loops of Henle, collecting ducts and also very infrequently in proximal tubular cells. Expression of this transgene in the Wolffian and Müllerian ducts during development also leads to gene deletion in the epithelia of the renal pelvis, ureter, vesicular glands, epididymis, vas deferens and endometrium.

Vhl$^{\Delta/\Delta}$Trp53$^{\Delta/\Delta}$ mice were sub-viable, with approximately 25% of mice dying within the first 3 months of life and with subsequent deaths in an apparently stochastic manner as the mice aged. Autopsy of these mice failed to reveal any obvious cause of death and no tumours were evident in any of the dead mice. This fact complicated the accrual of large cohorts of aged mice. Nonetheless, in combination with previously published analyses (Frew et al, 2008a,b) we analysed cohorts of mice at the following ages: 2–3 months (Vhl$^{\Delta/\Delta}$, $n=8$; Trp53$^{\Delta/\Delta}$, $n=7$; Vhl$^{\Delta/\Delta}$Trp53$^{\Delta/\Delta}$ $n=6$), 4–8 months (Vhl$^{\Delta/\Delta}$, $n=6$; Trp53$^{\Delta/\Delta}$, $n=10$; Vhl$^{\Delta/\Delta}$Trp53$^{\Delta/\Delta}$ $n=10$) and 11–13 months (Vhl$^{\Delta/\Delta}$, $n=9$; Trp53$^{\Delta/\Delta}$, $n=10$; Vhl$^{\Delta/\Delta}$Trp53$^{\Delta/\Delta}$ $n=17$). Littermate mice that were negative for the *Ksp1.3-Cre* transgene served as controls for all of these cohorts.

As previously described, kidneys of Trp53$^{\Delta/\Delta}$ mice developed normally and showed no histological abnormalities within 18 months of age (Wild et al, 2012). Similarly to Vhl$^{\Delta/\Delta}$ mice (Frew et al, 2008b), Vhl$^{\Delta/\Delta}$Trp53$^{\Delta/\Delta}$ mice developed a hydronephrosis phenotype of unknown cause but otherwise showed no defects in the structure of the nephrons at early ages. Mutation of *Trp53* in combination with *Vhl* led to a similar accumulation of nuclear HIF1α and HIF2α in tubular epithelia to that seen in *Vhl* single mutant mice (Supporting Information Fig 2). By 5 months of age small clusters of disorganized cells (Fig 4F) or micro-cysts (not shown) could infrequently be observed in the double knockout mice but not in either of the single mutant mice or control mice, suggestive of a breakdown in normal proliferative control in these cells. In comparison to the normal histological appearance of kidneys from 11- to 13-month-old control and single *Vhl* and *Trp53* mutant mice, kidneys of 13 out of 17 Vhl$^{\Delta/\Delta}$Trp53$^{\Delta/\Delta}$ mice aged 11–13 months mice displayed multiple hyperproliferative lesions (Fig 4G) and mild focal lymphoplasmacellular inflammation. Sections through the midline of 24 kidneys from these mice revealed 399 cysts ranging in diameter from 100 μm to 1 mm. Three hundred and forty-nine of these were lined by a single layered cuboidal epithelium (simple cyst) (Fig 4H) while 50 cysts showed multilayered micro-papillary epithelial growths projecting into the lumen (atypical cyst) (Fig 4I). Some larger cysts showed signs of regression, bleeding, cholesterol accumulation and foam cell macrophage infiltration. An additional 16 neoplastic lesions (diameter 250 μm to 1 mm) were also observed (Fig 4J and K). These lesions were non-invasive, displayed an increased mitotic index, low nuclear grade (Fig 4L) and cells grew either in a micro-papillary (Fig 4J) or solid (Fig 4K and L) growth pattern. Tumour cells typically showed weak cytoplasmic eosin staining (Fig 4L), similar to, but to a lesser extent than, the clear cell morphology seen in human ccRCC. Approximately half of the neoplasms were growing into a cystic space (Fig 4J) whereas the other lesions presented as a solid mass (Fig 4K and L). It was not possible to distinguish whether these latter lesions may represent completely filled cysts or whether they have arisen as a cyst-independent neoplasm. Epithelial cells lining simple and atypical cysts (Fig 4N and O) and neoplastic cells (Fig 4P) displayed frequent labelling for the proliferation marker Ki67. Simple cysts, atypical cysts and neoplasms all displayed high nuclear immunoreactivity for

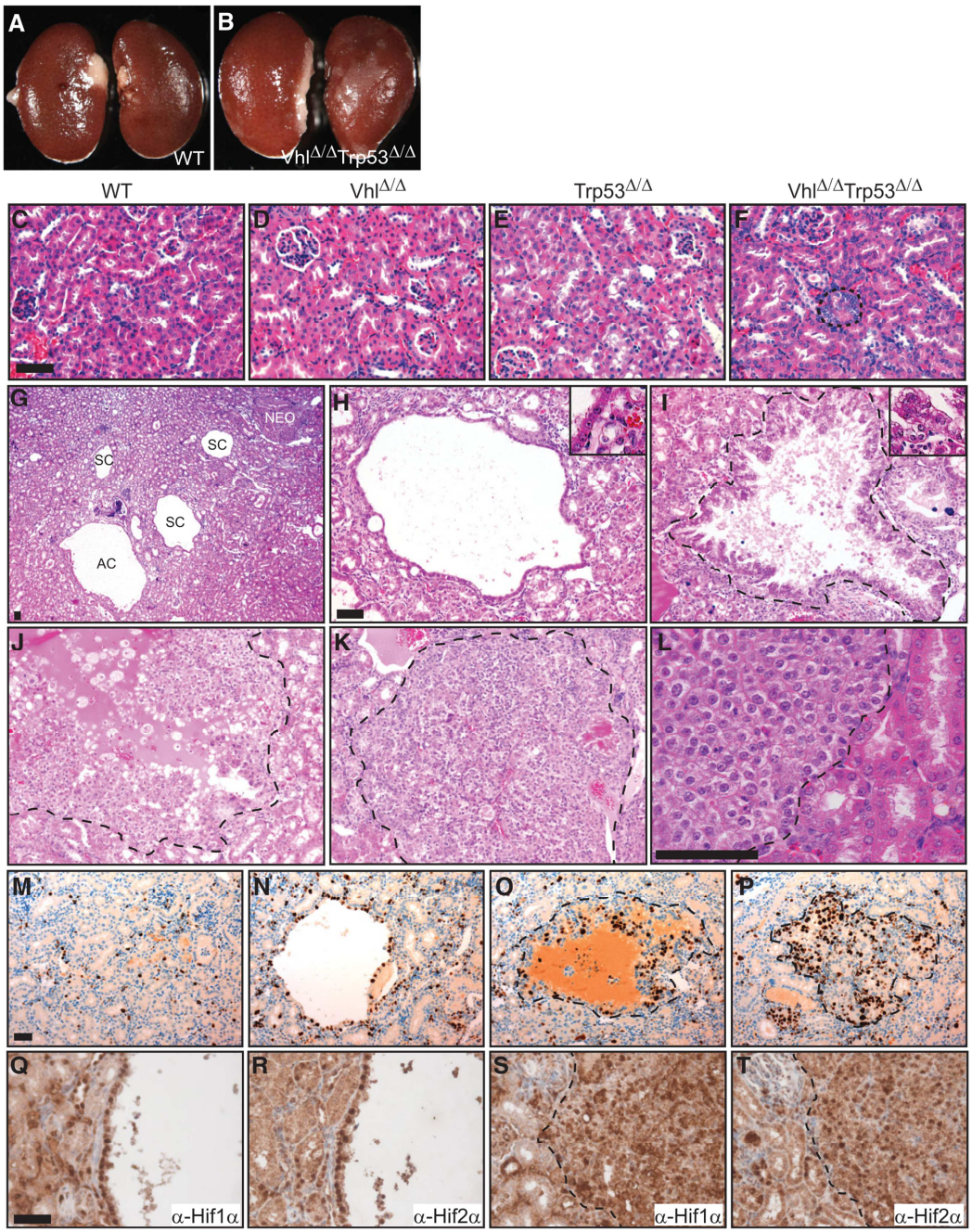

Figure 4.

HIF1α and HIF2α (Fig 4Q–T) verifying that these lesions are derived from *Vhl* null cells. While it is not possible to assay for loss of p53 protein by immunohistochemistry due to the fact that p53 is not detectable in normal kidney cells, PCR genotyping of laser capture micro-dissected simple cysts, atypical cysts and neoplasms demonstrated that the recombined *Trp53* and *Vhl* alleles were present in cells in these lesions (Supporting Information Fig 3). The non-recombined *Trp53* floxed and *Vhl* floxed alleles were also detected, likely due to presence of wild-type ($Vhl^{fl/fl}$;$Trp53^{fl/fl}$) stromal, inflammatory or vascular cells in these lesions.

Immunohistochemical staining using antibodies against NaPi2 (proximal), NCC (distal), THP (thick ascending loop of Henle) and AQP2 (collecting ducts) to mark different tubule segments revealed that most simple cysts express one of these markers (Supporting Information Fig 4), demonstrating that cysts arise from different nephron segments. Very rarely, remnants of the glomerulus could be observed in simple cysts (data not shown), suggesting that these cysts had arisen from the tubular epithelium at the urinary pole of the glomerulus. However, atypical cysts and neoplasms were always negative for all of the tubular markers (Supporting Information Fig 4), preventing assessment of the tubular segment of origin of these lesions and suggesting that the transition to tumour formation involves some degree of de-differentiation. Unlike the findings reported for some precursor lesions in human VHL patient kidneys (Esteban et al, 2006), *Vhl* mutant cystic lesions and neoplasms in the mouse retain expression of the epithelial marker E-cadherin and do not display the mesenchymal marker vimentin (Supporting Information Fig 5).

Thus, *Vhl* and *Trp53* double deletion does not automatically cause proliferative dysregulation of kidney epithelial cells *in vivo* but eventually leads to the evolution of lesions that appear to follow a pathway of simple cyst to atypical cyst to neoplasm that is similar to the proposed disease progression model in kidneys of patients with an inherited *VHL* mutation. Given the apparent morphological similarities and overlapping spectrum of development of atypical cysts and neoplasms, these lesions were grouped together and considered as being distinct from simple cysts in the analyses in the remainder of this study.

$Vhl^{\Delta/\Delta}Trp53^{\Delta/\Delta}$ mice also displayed a variety of dysplasias and tumours in the genital–urinary tract. Deletion of *Trp53* alone caused a moderate disorganisation of the epithelia in epididymal tubules, predominantly in tubules of the corpus and cauda of the epididymis, with an age-dependent accumulation of aberrant nuclei and multi-nucleated cells (Wild et al, 2012, Supporting Information Fig 6E). Epididymides from $Vhl^{\Delta/\Delta}Trp53^{\Delta/\Delta}$ mice appeared externally normal in the first months of life (Supporting Information Fig 6B) but histological analysis of aged cohorts revealed that they displayed a qualitatively more severe phenotype of nuclear abnormalities than the $Trp53^{\Delta/\Delta}$ mice (Supporting Information Fig 6F). At 11–13 months of age, the epididymides of all male $Vhl^{\Delta/\Delta}Trp53^{\Delta/\Delta}$ mice, but not of control or single mutant mice, displayed benign growths (Supporting Information Fig 6H). These growths were predominantly due to squamous metaplasia (Supporting Information Fig 6I) and extensive epithelial dysplasia (Supporting Information Fig 6J). These lesions are histologically identical to those arising in $Vhl^{\Delta/\Delta}Pten^{\Delta/\Delta}$ mice (Frew et al, 2008a). Epididymides also frequently displayed fibrosis, inflammation, foreign body reactions and metaplastic stromal changes, likely as a result of the blockage of tubules by dysplasia and squamous metaplasia. One mouse developed an epididymal clear cell papillary cystadenoma (Supporting Information Fig 7A) that appeared histologically identical to the cystadenomas that arise at high frequency in patients with an inherited *VHL* mutation. Vesicular glands of $Vhl^{\Delta/\Delta}Trp53^{\Delta/\Delta}$ mice (Supporting Information Fig 6L), but not of $Vhl^{\Delta/\Delta}$ or $Trp53^{\Delta/\Delta}$ mice (not shown), were malformed. In contrast to the normal single layered epithelium, vesicular glands of $Vhl^{\Delta/\Delta}Trp53^{\Delta/\Delta}$ mice displayed a disorganized epithelium characterized by multiple convoluted layers of epithelial cells and the formation of gland-like structures (Supporting Information Fig 6P). This phenotype increased in severity with age and two mice exhibited carcinomas in the vesicular gland (Supporting Information Fig 7C). The uterus in all genotypes developed normally (Supporting Information Fig 6R) and displayed a normal organisation of lumenal and glandular endometrial epithelium (Supporting Information Fig 6V). In older $Vhl^{\Delta/\Delta}Trp53^{\Delta/\Delta}$ mice, small foci of disorganized and multilayered epithelial cells could frequently be observed. Consistent with this, one mouse developed a high-grade carcinoma of the endometrium (Supporting Information Fig 7E) and another a high-grade squamous carcinoma of the

◀ **Figure 4. $Vhl^{\Delta/\Delta}Trp53^{\Delta/\Delta}$ mice develop kidney cysts and neoplasms.** C–F and Q–T are all the same magnification, H–K are the same magnification, M–P are the same magnification. Scale bars depict 50 μm. Dotted lines indicate the boundary of normal tissue and atypical cysts or neoplasms.

A,B. Normal external appearance of kidneys from 6 month-old $Vhl^{\Delta/\Delta}Trp53^{\Delta/\Delta}$ mice.

C–F. Histological appearance of cortex of kidneys from 6 month-old wild-type (C), $Vhl^{\Delta/\Delta}$ (D), $Trp53^{\Delta/\Delta}$ (E) and $Vhl^{\Delta/\Delta}Trp53^{\Delta/\Delta}$ (F) mice. The dotted region outlined in F is an example of an abnormal cluster of cells.

G. Example of lesions arising in the cortex of a kidney from a 1-year-old $Vhl^{\Delta/\Delta}Trp53^{\Delta/\Delta}$ mouse. AC: atypical cyst, SC: simple cyst, NEO: neoplasm.

H–K. Examples of lesions found in kidneys of one year-old $Vhl^{\Delta/\Delta}Trp53^{\Delta/\Delta}$ mice; simple tubular cyst (H), atypical cyst (I), neoplasm with cystic precursor (J) and solid neoplasm (K). Insets in H and I show high magnification of the cystic epithelium.

L. High magnification of a solid neoplasm showing clear cell morphology and low nuclear grade.

M–P. Representative Ki67 stainings of histologically normal epithelium (M), a simple cyst (N), an atypical cyst (O) and a neoplasm (P) in $Vhl^{\Delta/\Delta}Trp53^{\Delta/\Delta}$ mouse kidneys.

Q,R. Anti-HIF1α and anti-HIF2α immunohistochemistry of serial sections of a simple cyst.

S,T. Anti-HIF1α and anti-HIF2α immunohistochemistry of serial sections of a neoplastic lesion.

upper cervix (Supporting Information Fig 7G). One mouse displayed a high-grade carcinoma that most likely arose in the urothelium of the renal pelvis and which had also metastasized to the lungs and liver (Supporting Information Fig 7I).

Collectively, these findings demonstrate that mutation of the *Vhl* and *Trp53* tumour suppressor genes ultimately causes dysregulation of epithelial cell proliferation and the evolution of dysplastic and malignant lesions in multiple tissues in mice.

Cooperating pathways in tumour formation in *Vhl/Trp53* double mutant mice

Since we have previously shown a connection between loss of the primary cilium and cyst formation in VHL disease (Frew et al, 2008b; Thoma et al, 2007), we examined whether epithelial cells lining simple cystic lesions that arise in *Vhl/Trp53* double mutant mice displayed a similar loss of primary cilia. Visualising the primary cilium using an antibody against acetylated tubulin revealed that only 40% of cystic epithelial cells but almost 90% of cells in non-cystic tubules displayed a primary cilium (Fig 5A and B). Since only non-proliferating cells exhibit a primary cilium we asked if this reduction in cilia frequency was simply due to the increased proliferation of cystic epithelial cells by staining for Ki67, which labels proliferating cells in all cell cycle stages. On average, 18% of cystic epithelial cells stained positively for Ki67 (Fig 5C), a far lower frequency than the frequency of cells lacking a cilium. Indeed, dual colour immunofluorescence staining experiments revealed that many Ki67 negative cystic cells lacked primary cilia (Fig 5A) demonstrating that the loss of the primary cilium is likely a consequence of loss of pVHL and not an indirect consequence of cellular proliferation and might therefore be causal to cyst formation. Neoplasms displayed a mixed phenotype with respect to cilia, some displayed a very high frequency of ciliated cells (Fig 5D), some displayed an intermediate frequency (Fig 5E) and some were almost completely devoid of cilia (Fig 5F).

We have previously demonstrated that one pathway to cilia loss involves both inactivation of pVHL and inhibition of GSK3β (Frew et al, 2008b; Thoma et al, 2007), which can occur via hyperactivation of the PI3K signalling pathway (Frew et al, 2008b). However, immunohistochemical staining using antibodies against phospho-Thr37/46-4E-BP1 (P-4EBP1) (Fig 6G–I) and phospho-Ser240/244-ribosomal S6 protein (P-S6) (Fig 6J–L), two sensitive and robust downstream markers of activation of the PI3K-mTORC1 signalling pathway, revealed that only about 6–8% of simple cysts displayed mTORC1 pathway

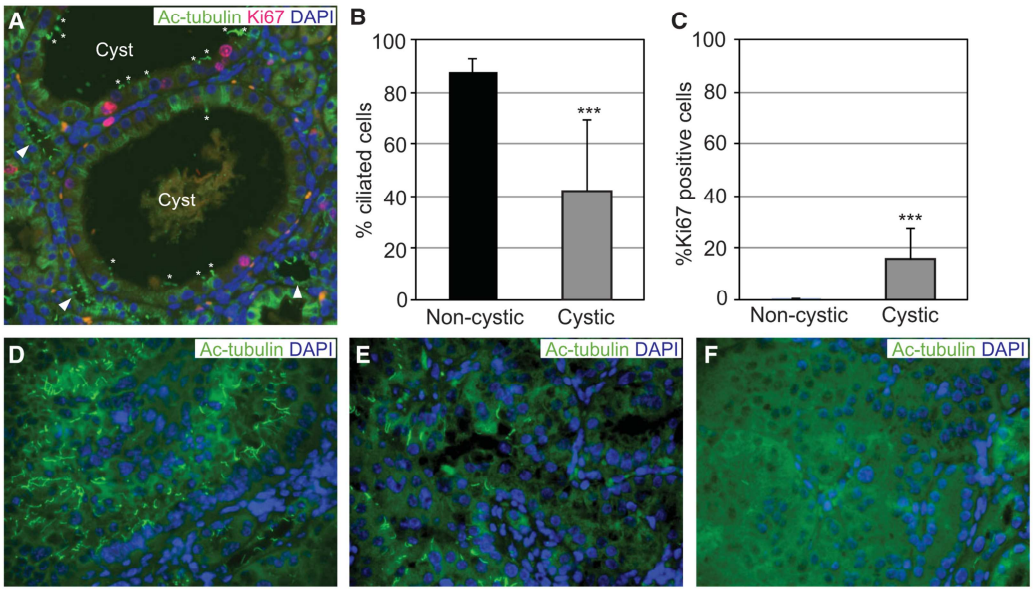

Figure 5. Reduced frequency of primary cilia in cysts.

A. Immunofluorescence staining of formalin-fixed paraffin embedded tissue for acetylated tubulin (green) to mark primary cilia, Ki67 (red) to mark proliferating cells and DAPI (blue) to mark nuclei in a cortical section of kidney from a $Vhl^{\Delta/\Delta}Trp53^{\Delta/\Delta}$ mouse. Arrowheads point to adjacent normal tubules showing a normal frequency of ciliated cells and * highlight primary cilia in cysts. Note the high frequency of Ki67 negative cells that lack a primary cilium.

B,C. Quantification of percentage of epithelial cells displaying a primary cilium (B) or staining for Ki67 (C) in non-cystic tubules ($n = 18$) or simple cysts ($n = 39$) in $Vhl^{\Delta/\Delta}Trp53^{\Delta/\Delta}$ mice. Mean and SD is shown, $^{***}p < 0.001$ Student's *t*-test.

D–F. Examples of neoplasms displaying varying frequencies of primary cilia.

activation above levels seen in histologically normal tubules in the same mice (Fig 6P). Interestingly, atypical cysts and neoplasms were almost always strongly positive for both of these markers (Fig 6P). Approximately half of all simple cystic lesions and almost all atypical cysts or neoplasms displayed elevated levels of the pro-proliferative Myc protein (Fig 6M–P). Thus, multilayered or papillary growth of *Vhl/Trp53* mutant cells into the lumen of cysts or growth as a solid neoplasm correlates with the acquisition of the pro-proliferative signature of mTORC1 activation and Myc expression.

DISCUSSION

We show that *TP53* is mutated in a subset of sporadic human ccRCCs and demonstrate genetically that *Trp53* mutation allows *Vhl* null MEFs to escape senescence and proliferate in an immortalized manner. We also show that combined deletion of *Vhl* and *Trp53* in mice results in the formation of simple and atypical cysts, as well as neoplastic lesions in kidneys and causes tumours to form in other genital tract tissues.

The long latency of tumour formation observed in mice (1 year) is consistent with our primary cell culture data showing that *Vhl/Trp53* mutation causes immortalization but not transformation of MEFs. These findings clarify previous contradictory reports concerning the role of p53 in regulating senescence following loss of *Vhl* in mouse fibroblasts (Welford et al, 2010; Young et al, 2008). *Vhl* null cells nonetheless exhibit a lower proliferation rate than *Vhl* wild-type cells, even in the background of loss of the p53 and pRB cell cycle checkpoints, implying that there may be additional cellular responses that represent barriers that prevent full transformation of *Vhl/Trp53* mutant cells. We suggest that the increase in aneuploidy observed in *Vhl/Trp53* null MEFs might potentially represent a mechanism that could contribute to cellular transformation and tumour evolution *in vivo*.

Our findings strengthen the model derived from studies of human VHL patients that ccRCCs can form via cyst-dependent and cyst-independent pathways (Fig 6Q). *Vhl/Trp53* mutant mice develop an apparent spectrum of cystic lesions beginning with simple cysts lined by a single layer of epithelial cells, followed by atypical cysts that display micro-papillary epithelial growths that project into the lumen of the cyst and finally cysts that are almost entirely filled with neoplastic growth. About half of the neoplasms are a solid mass of cells, preventing assessment of whether they arise via a cystic precursor lesion or not. *Vhl/Trp53* neoplastic lesions display several features of human ccRCC including clear cell-like changes, HIFα stabilisation and high rate of proliferation, but differ in that they exhibit a low nuclear grade and do not invade surrounding tissue. The lack of a capsule surrounding the neoplasms and absence of extra-renal metastases speaks against a malignant ccRCC lesion. *Vhl/Trp53* mutant neoplasms also frequently grow in a micro-papillary pattern, akin to papillary renal cell carcinomas. While the precursor lesions of human renal carcinomas are poorly characterized in general, in papillary type I and type II tumours the size of the lesion is the sole definitive distinguishing criteria. Lesions smaller than 5 mm are classified as adenomas and larger lesions are carcinomas (Eble et al, 2004). Taking the relative sizes of the human and mouse kidney into account, many of the neoplasms in our model would be classified as carcinomas under this definition. Because of the mixed features of the *Vhl/Trp53* null neoplasms we classify these tumours simply as renal neoplasms, rather than as a specific sub-type of renal cell carcinoma.

Epithelial cells lining simple cystic lesions display a reduced frequency of primary cilia, similar to cysts in human VHL patients (Thoma et al, 2007), further supporting the involvement of pVHL in maintenance of primary cilia and suppression of cyst formation. However, in contrast to *Vhl/Pten* mutant mice (Frew et al, 2008b), in *Vhl/Trp53* mutant mice, these simple cysts do not display evidence of over-activation of the PI3K signalling pathway or inactivating phosphorylation of GSK3β (unpublished observations), implying that there may be other unidentified pathways that cooperate with pVHL in maintenance of the primary cilium. In contrast to simple cysts, atypical cysts and neoplasms display hyperactivation of mTORC1 signalling. Since both lesions are characterized by disorganized patterns of cellular growth it is noteworthy that mTORC1 activation has been shown to induce a translational program that promotes cellular invasion (Hsieh et al, 2012). Hyperactivation of mTORC1 predicts poor outcome in ccRCC patients and mTORC1 inhibitors show clinical efficacy against ccRCC (Hudes, 2009). Atypical cysts and neoplasms almost invariably also display high levels of Myc protein. Upregulation of *MYC* expression is common in ccRCC and amplification of *MYC* predicts poor outcome in human ccRCC patients (Monzon et al, 2011; Tang et al, 2009). The combination of *Vhl/Trp53* double mutation with a pro-proliferative signature of mTORC1 activation and high Myc expression therefore correlates with the transition to a neoplastic state.

While approximately 1 in 10 ccRCC tumours harbour *TP53* mutations, in many epithelial malignancies the *TP53* mutation frequency is much higher (50–90%). In ccRCC, several mechanisms have been proposed to act to compromise p53 function, potentially alleviating the selective pressure for *TP53* mutation or deletion during tumour formation. USP10 normally de-ubiquitinates p53 in response to DNA damage, opposing the action of Mdm2 and allowing p53 protein accumulation (Yuan et al, 2010). Interestingly, 90% of ccRCC express lower than normal levels of USP10, possibly leading to reduced p53 activation (Yuan et al, 2010). pVHL itself has been implicated as a factor important for full p53 activation by promoting the recruitment of the p300 acetylase and ATM kinase to p53 (Roe et al, 2006). Knockdown of *VHL* expression reduced p53 activity in response to DNA damage and reintroduction of pVHL expression in *VHL*-deficient RCC cells enhanced damage-induced activation of p53 (Roe et al, 2006). Downstream of loss of pVHL function, activation of HIFα transcription factors may also act to compromise p53 activity. The hypoxia-inducible *PAX2* gene is a transcriptional repressor of *TP53* and is highly upregulated in *VHL* mutant cells and ccRCCs (Luu et al, 2009; Stuart et al, 1995). Elevated HIF2α levels in *VHL*-mutant ccRCC are proposed to induce growth factor expression leading firstly

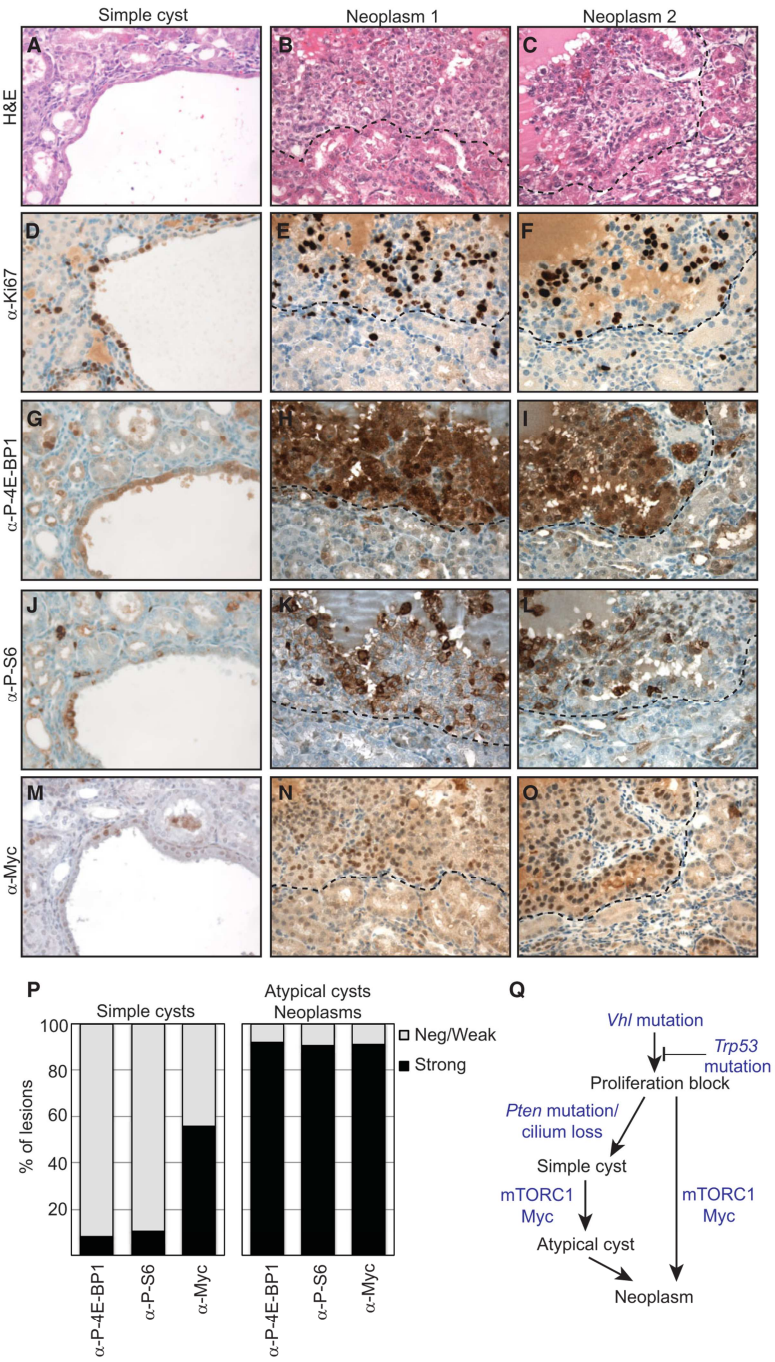

Figure 6.

to the AKT-mediated phosphorylation of HDM2, promoting its ability to degrade p53 (Roberts et al, 2009) or secondly to the suppression of formation of reactive oxygen species which reduce p53 activation (Bertout et al, 2009). *PBRM1* is mutated in 41% of ccRCCs (Varela et al, 2011) and has been shown to be necessary for induction of senescence by p53 (Burrows et al, 2010), thus potentially abrogating part of p53's tumour suppressing activity in the kidney. In our hands however, knockdown of *Pbrm1* failed to alleviate proliferative arrest following *Vhl* knockout in MEFs (unpublished observations). Similarly, *SETD2* is mutated in a small fraction of ccRCCs (Dalgliesh et al, 2010) and has been suggested to regulate a subset of p53 target genes (Xie et al, 2008). Thus, p53 function may either be lost by mutation or compromised by other mechanisms in a large proportion of *VHL*-negative ccRCCs.

It will be important to clarify when *TP53* mutations arise during the process of tumour initiation and progression. In this regard, a study of four ccRCCs utilized deep sequencing of the tumour DNA population to reconstruct the molecular evolutionary history of the tumours (Gerstung et al, 2012). In one of these tumours a single *TP53* truncation mutation was present at about one-fifteenth the frequency of a single *VHL* frameshift mutation, implying that the *TP53* mutation was an event that occurred secondarily to an initiating *VHL* mutation and that it resulted in the formation of a *VHL/TP53* double mutant subclone of the tumour cell population. This finding supports the notion that genetic cooperation between *VHL* and *TP53* mutations promotes tumour progression. Similar analyses of larger numbers of ccRCC samples from different stages of disease progression would test how representative this initial finding is for ccRCCs in general.

In summary, we present strong evidence to support the idea that loss of function of *VHL* and *TP53* is a *bone fide* tumour promoting combination and describe a mouse model that recapitulates many of the steps involved in the formation of *VHL* mutant kidney tumours in humans.

MATERIALS AND METHODS

Mouse genetics

Previously described *Ksp1.3-Cre/+*; $Vhl^{fl/fl}$ (Frew et al, 2008b) and *Ksp1.3-Cre/+*; $Trp53^{fl/fl}$ (Wild et al, 2012) mouse strains were interbred to generate *Ksp1.3-Cre/+*; $Vhl^{fl/fl}$; $Trp53^{fl/fl}$ mice. Non-Cre transgenic littermate mice served as controls for all cohorts. Wild-type cells were isolated from C57BL/6 embryos.

Analyses of human ccRCCs

Tissue samples were from the University Hospital of Zurich (Zurich, Switzerland). The study was approved by the local ethics commission (reference number StV 38-2005). Haematoxylin and eosin stained sections of all paraffin embedded ccRCC specimens were reviewed by H.M. DNA extraction and *VHL* sequencing were performed as previously described (von Teichman et al, 2011). The primers used for PCR and sequencing of *TP53* exons 5–8 are listed in Supporting Information Table S1. PCR was performed with 40 cycles consisting of denaturation at 94°C for 45 s, annealing at 58°C for 45 s and extension at 72°C for 45 s. *VHL* and *TP53* mutations were validated by an independent PCR and sequence analysis. Paraffin sections (2.5 μm) were treated using Ventana Benchmark XT (Tuscon, AZ, USA) or BOND-MAX (Leica Microsystems, Wetzlar, Germany) automated systems. Immunostainings for CAIX, GLUT1 and HIF1α were performed as recently described (Dahinden et al, 2010; Luu et al, 2009). Nuclear HIF1α and membranous CAIX, GLUT1 expression were defined positive if at least 5% of tumour cells showed weak (+1) or strong (+2) staining.

Assays of MEFs

MEFs were isolated from relevant floxed strains and aliquots were frozen at passage 2. $Trp53^{-/-}$ MEFs were a kind gift from Scott Lowe. Cells were cultured either in conventional cell culture incubators at atmospheric oxygen or at 5% oxygen or were cultured in a darkened oxygen glove-box incubator ($INVIVO_2$ 400, Ruskinn) at 5% oxygen in which medium and PBS were equilibrated for 2 h prior to splitting of cells to ensure that cells were exposed to constant oxygen tension throughout the experiment. For proliferation assays, cells were seeded at densities of either 2×10^5 or 3×10^5 cells per 6 cm dish in triplicate dishes and counted after 3 days before reseeding at the same density for the next passage. All proliferation assays shown in the Figures are representative of at least three independent experiments. Wild-type and $Vhl^{fl/fl}$ MEFs were transformed by transfection with a plasmid expressing SV40 large T-Antigen (Addgene, pBSSVD2005) and pools of cells that formed colonies after plating at low density were harvested to generate cell lines. Cells were infected with adenoviruses expressing GFP (Vector Biolabs, 1060) or Cre-GFP (Vector Biolabs, 1700), retroviruses (LMP) expressing non-silencing hairpin or miR30-shRNA against *Trp53* (Dickins et al, 2005), lentiviruses (LKO.1) expressing non-silencing hairpin (Addgene, 10879) or shRNA against *Vhl* (Open Biosystems, TRC0000009735) (Thoma et al, 2007). For lentiviral-mediated knockdown of *Trp53*, we generated a vector (pLenti X1 Puro DEST, Addgene 17297) containing the U6 promoter (derived from pENTR/pSM2 (U6), Addgene 17387) driving expression of a previously described (Dickins et al, 2005) miR30 format shRNA against *Trp53* (1224) or expressing an empty (ns) miR30 backbone. Infections were followed after 48 h by puromycin selection (4 μg/ml) where appro-

Figure 6. mTORC1 activation and Myc expression signature in atypical cysts and neoplasms.

A–O. Serial sections of a simple cyst (A,D,G,J,M) and two neoplasms (B,E,H,K,N and C,F,I,L,O) stained with H&E (A–C) or stained immunohistochemically for Ki67 (D–F), phospho-Thr37/46-4E-BP1 (G–I), phospho-Ser240/244-ribosomal S6 protein (J–L) or Myc (M–O). Dotted lines indicate the boundary of normal tissue and neoplasms.

P. Quantification of the percentage of simple cysts ($n = 68–185$) or atypical cysts and neoplasms ($n = 34–51$) that display higher levels (strong) of staining than adjacent normal tissue in the same section (negative/weak).

Q. Model summarising the proposed sequence of morphological and molecular alterations involved in formation of ccRCC. For details see the Discussion Section.

The paper explained

PROBLEM:

The cooperating genetic events that lead to the formation of clear cell renal cell carcinoma (ccRCC), the most frequent form of kidney cancer in humans, remain unclear. While the vast majority of familial and sporadic forms of ccRCC harbour biallelic inactivation of the von Hippel–Lindau tumour suppressor gene (*VHL*), loss of *VHL* function alone in humans and in mice is insufficient to cause kidney tumour formation. It is presumed that other genetic events must cooperate with loss of *VHL* to cause ccRCC but these cooperating mutations remain poorly understood.

RESULTS:

Here we identify loss of function mutations in *TP53* in a subset of sporadic human ccRCCs and show that kidney-specific combined deletion of *Vhl* and *Trp53* leads to the formation of cysts and tumours in mice, recapitulating the precursor lesions and cellular and molecular alterations that are involved in the formation of *VHL* mutant ccRCC in humans.

IMPACT:

These findings provide the first demonstration that secondary genetic alterations can cooperate with loss of *VHL* to cause kidney tumour formation and implicate *TP53* mutations in the pathogenesis of a subset of human ccRCC.

priate. Genotyping for the floxed or recombined *Vhl* and *Trp53* alleles were performed as described (Biju et al, 2004; Jonkers et al, 2001). Flow cytometry (Frew et al, 2002) and counting of aberrant anaphases (Burds et al, 2005) were performed as described.

Real-time PCR

Real-time PCR was performed as described (Frew et al, 2008b) using the following primer pairs: *18S rRNA* (5′-TGGCCGACCATAAACGATGCC-3′, 5′-TGGTGGTGCCCTTCCGTCAAT-3′), *Mad2* (5′-GTGGCCGAGTTTTTCT-CATTTG-3′, 5′-AGGTGAGTCCATATTTCTGCACT-3′).

Kidney epithelial cell proliferation assays

Kidneys were dissected from 2-month-old floxed mice. After removing the capsule under sterile conditions, kidneys were mashed with a razor blade on ice and digested in collagenase II (Gibco) and soya trypsin inhibitor (Gibco) solution at 37°C for 30 min. The cell suspension was filtered through a 70 μm cell strainer and washed in HBSS + 5% FCS. Erythrocytes were lysed for 1 min using standard ACK buffer. Cells were resuspended in complete K-1 culture medium [Dulbecco's modified Eagle's medium (DMEM):Hams F12] (50:50), supplemented with 0.5% foetal calf serum, hormone mix [5 μg/ml insulin, 1.25 ng/ml prostaglandin E_1 (PGE_1), 34 pg/ml triiodothyronine, 5 μg/ml Apo-transferrin, 1.73 ng/ml sodium selenite and 18 ng/ml of hydrocortisone] and 25 ng/ml epidermal growth factor (EGF). Cells were counted and seeded at a density of 1×10^6 cells on standard 100 mm plastic tissue culture plates. After 5–6 days in culture, cells were infected with adenoviruses expressing GFP (Vector Biolabs, 1060) or Cre-GFP (Vector Biolabs, 1700). Sulforhodamine B (SRB) proliferation assay was performed in 96-well format as described (Vichai & Kirtikara, 2006). Briefly, primary kidney epithelial cells were cultured in K-1 medium containing 10% foetal calf serum for 2 days before seeding for the SRB assay. 2×10^3 cells per well were seeded and fixed in 5% w/v trichloracetic acid at the indicated time points. Cells were stained in 0.057% w/v SRB solution and air dried. SRB was solubilized by incubation in 10 mM Tris base solution (pH 10.5) and OD was measured at 540 nm in a micro-plate reader.

Antibodies, Western blotting, immunofluorescence and immunohistochemistry

Western blotting, immunohistochemistry or immunofluorescence were conducted using previously described methods (Frew et al, 2008b) and the antibodies against the following epitopes: Acetylated tubulin (Sigma, #T6793), Actin (Sigma-Aldrich, A2228), AQP2 (Wagner et al, 2008), Aurora A (Abcam, ab13824), BubR1 (BD Biosciences, 612502), CDK-2 (Santa Cruz, sc-163-g), Cenp-E (Meraldi et al, 2004), E-cadherin (Abcam, ab11512), phospho-Thr37/46-4E-BP1 (Cell Signaling Technology, #2855), HIF1α (Novus Biologicals, NB100-105), HIF2α (Pollard et al, 2007, PM8), Ki67 (DakoCytomation, TEC-3), Mad2 (Bethyl Laboratories, A300301A), Myc (Epitomics, Y69), p53 (Novocastra, NCL-p53-CM5p), NaPi2 (Custer et al, 1994), NCC (Millipore, AB3553), phospho-Ser240/244-ribosomal S6 protein (Cell Signaling Technology, #2215), THP (Santa Cruz Biotechnology, sc-20631), $pVHL(m)_{CT}$ antibody (Hergovich et al, 2003), pVHL (Santa Cruz, sc-5575), Vimentin (Cell Signaling Technology, #5741).

Author contributions

IJF and WK designed the study, IJF, JA, MR, DS, SH, PS, AvT and SG conducted and analysed the experiments, PJW and HM performed histopathological analyses and the manuscript was written by IJF with the assistance of all authors.

Acknowledgements

This work was supported by grants to I.J.F. from SNF Förderungsprofessur (PP00P3_128257) and ERC Starting Grant (260316), to J.A. from the European Community's Seventh Framework Programme (FP7/2007-2013) under grant agreement no. 246539, and to W.K. from the SNF. We are grateful to Johannes Loffing and Jürg Biber for providing antibodies and to the Centre for Microscopy and Imaging Analysis, University of Zurich for assistance with laser capture microdissection.

Supporting Information is available at EMBO Molecular Medicine online.

The authors declare that they have no conflicts of interest.

For more information

For information about the VHL Family Alliance for patients with inherited VHL disease:

http://www.vhl.org

For general information about kidney cancer subtypes and treatments:

http://www.cancer.gov/cancertopics/types/kidney

For information about the genetic mutations that have been found in ccRCC:

http://www.sanger.ac.uk/perl/genetics/CGP/cgp_viewer?action=study;study_id=321

http://www.sanger.ac.uk/genetics/CGP/Studies/Renal/

http://www.sanger.ac.uk/perl/genetics/CGP/cosmic?action=bysite&s=4&hn=carcinoma&sn=kidney&sh=clear_cell_renal_cell_carcinoma

References

Bertout JA, Majmundar AJ, Gordan JD, Lam JC, Ditsworth D, Keith B, Brown EJ, Nathanson KL, Simon MC (2009) HIF2alpha inhibition promotes p53 pathway activity, tumor cell death, and radiation responses. Proc Natl Acad Sci USA 106: 14391-14396

Biju MP, Neumann AK, Bensinger SJ, Johnson RS, Turka LA, Haase VH (2004) Vhlh gene deletion induces Hif-1-mediated cell death in thymocytes. Mol Cell Biol 24: 9038-9047

Burds AA, Lutum AS, Sorger PK (2005) Generating chromosome instability through the simultaneous deletion of Mad2 and p53. Proc Natl Acad Sci USA 102: 11296-11301

Burrows AE, Smogorzewska A, Elledge SJ (2010) Polybromo-associated BRG1-associated factor components BRD7 and BAF180 are critical regulators of p53 required for induction of replicative senescence. Proc Natl Acad Sci USA 107: 14280-14285

Custer M, Lotscher M, Biber J, Murer H, Kaissling B (1994) Expression of Na-P(i) cotransport in rat kidney: localization by RT-PCR and immunohistochemistry. Am J Physiol 266: F767-F774

Dahinden C, Ingold B, Wild P, Boysen G, Luu VD, Montani M, Kristiansen G, Sulser T, Buhlmann P, Moch H, *et al* (2010) Mining tissue microarray data to uncover combinations of biomarker expression patterns that improve intermediate staging and grading of clear cell renal cell cancer. Clin Cancer Res 16: 88-98

Dalgliesh GL, Furge K, Greenman C, Chen L, Bignell G, Butler A, Davies H, Edkins S, Hardy C, Latimer C, *et al* (2010) Systematic sequencing of renal carcinoma reveals inactivation of histone modifying genes. Nature 463: 360-363

Dickins RA, Hemann MT, Zilfou JT, Simpson DR, Ibarra I, Hannon GJ, Lowe SW (2005) Probing tumor phenotypes using stable and regulated synthetic microRNA precursors. Nat Genet 37: 1289-1295

Eble JN, Sauter G, Epstein JI, Sesterhehn IA (2004) *World Health Organisation Classification of Tumours: Pathology and Genetics of Tumours of the Urinary System and Male Genital Organs*. Lyon: IARC Press

Esteban MA, Tran MG, Harten SK, Hill P, Castellanos MC, Chandra A, Raval R, O'Brien TS, Maxwell PH (2006) Regulation of E-cadherin expression by VHL and hypoxia-inducible factor. Cancer Res 66: 3567-3575

Frew IJ, Dickins RA, Cuddihy AR, Del Rosario M, Reinhard C, O'Connell MJ, Bowtell DD (2002) Normal p53 function in primary cells deficient for Siah genes. Mol Cell Biol 22: 8155-8164

Frew IJ, Krek W (2007) Multitasking by pVHL in tumour suppression. Curr Opin Cell Biol 19: 685-690

Frew IJ, Minola A, Georgiev S, Hitz M, Moch H, Richard S, Vortmeyer AO, Krek W (2008a) Combined VHLH and PTEN mutation causes genital tract cystadenoma and squamous metaplasia. Mol Cell Biol 28: 4536-4548

Frew IJ, Thoma CR, Georgiev S, Minola A, Hitz M, Montani M, Moch H, Krek W (2008b) pVHL and PTEN tumour suppressor proteins cooperatively suppress kidney cyst formation. EMBO J 27: 1747-1757

Gerstung M, Beisel C, Rechsteiner M, Wild P, Schraml P, Moch H, Beerenwinkel N (2012) Reliable detection of subclonal single-nucleotide variants in tumour cell populations. Nat Commun 3: 811

Guo G, Gui Y, Gao S, Tang A, Hu X, Huang Y, Jia W, Li Z, He M, Sun L, *et al* (2012) Frequent mutations of genes encoding ubiquitin-mediated proteolysis pathway components in clear cell renal cell carcinoma. Nat Genet 44: 17-19

Haase VH, Glickman JN, Socolovsky M, Jaenisch R (2001) Vascular tumors in livers with targeted inactivation of the von Hippel-Lindau tumor suppressor. Proc Natl Acad Sci USA 98: 1583-1588

Hergovich A, Lisztwan J, Barry R, Ballschmieter P, Krek W (2003) Regulation of microtubule stability by the von Hippel-Lindau tumour suppressor protein pVHL. Nat Cell Biol 5: 64-70

Hsieh AC, Liu Y, Edlind MP, Ingolia NT, Janes MR, Sher A, Shi EY, Stumpf CR, Christensen C, Bonham MJ, *et al* (2012) The translational landscape of mTOR signalling steers cancer initiation and metastasis. Nature 485: 55-61

Hudes GR (2009) Targeting mTOR in renal cell carcinoma. Cancer 115: 2313-2320

Jonkers J, Meuwissen R, van der Gulden H, Peterse H, van der Valk M, Berns A (2001) Synergistic tumor suppressor activity of BRCA2 and p53 in a conditional mouse model for breast cancer. Nat Genet 29: 418-425

Kaelin WG, Jr (2002) Molecular basis of the VHL hereditary cancer syndrome. Nat Rev Cancer 2: 673-682

Lubensky IA, Gnarra JR, Bertheau P, Walther MM, Linehan WM, Zhuang Z (1996) Allelic deletions of the VHL gene detected in multiple microscopic clear cell renal lesions in von Hippel-Lindau disease patients. Am J Pathol 149: 2089-2094

Luu VD, Boysen G, Struckmann K, Casagrande S, von Teichman A, Wild PJ, Sulser T, Schraml P, Moch H (2009) Loss of VHL and hypoxia provokes PAX2 up-regulation in clear cell renal cell carcinoma. Clin Cancer Res 15: 3297-3304

Mack FA, Patel JH, Biju MP, Haase VH, Simon MC (2005) Decreased growth of Vhl−/− fibrosarcomas is associated with elevated levels of cyclin kinase inhibitors p21 and p27. Mol Cell Biol 25: 4565-4578

Maher ER (2013) Genomics and epigenomics of renal cell carcinoma. Semin Cancer Biol 23: 10-17

Mandriota SJ, Turner KJ, Davies DR, Murray PG, Morgan NV, Sowter HM, Wykoff CC, Maher ER, Harris AL, Ratcliffe PJ, *et al* (2002) HIF activation identifies early lesions in VHL kidneys: evidence for site-specific tumor suppressor function in the nephron. Cancer Cell 1: 459-468

Mao JH, Wu D, Perez-Losada J, Jiang T, Li Q, Neve RM, Gray JW, Cai WW, Balmain A (2007) Crosstalk between Aurora-A and p53: frequent deletion or downregulation of Aurora-A in tumors from p53 null mice. Cancer Cell 11: 161-173

Meraldi P, Draviam VM, Sorger PK (2004) Timing and checkpoints in the regulation of mitotic progression. Dev Cell 7: 45-60

Montani M, Heinimann K, von Teichman A, Rudolph T, Perren A, Moch H (2010) VHL-gene deletion in single renal tubular epithelial cells and renal tubular cysts: further evidence for a cyst-dependent progression pathway of clear cell renal carcinoma in von Hippel-Lindau disease. Am J Surg Pathol 34: 806-815

Monzon FA, Alvarez K, Peterson L, Truong L, Amato RJ, Hernandez-McClain J, Tannir N, Parwani AV, Jonasch E (2011) Chromosome 14q loss defines a molecular subtype of clear-cell renal cell carcinoma associated with poor prognosis. Mod Pathol 24: 1470-1479

Parrinello S, Samper E, Krtolica A, Goldstein J, Melov S, Campisi J (2003) Oxygen sensitivity severely limits the replicative lifespan of murine fibroblasts. Nat Cell Biol 5: 741-747

Pati D, Haddad BR, Haegele A, Thompson H, Kittrell FS, Shepard A, Montagna C, Zhang N, Ge G, Otta SK, *et al* (2004) Hormone-induced chromosomal instability in p53-null mammary epithelium. Cancer Res 64: 5608-5616

Pena-Llopis S, Vega-Rubin-de-Celis S, Liao A, Leng N, Pavia-Jimenez A, Wang S, Yamasaki T, Zhrebker L, Sivanand S, Spence P, *et al* (2012) BAP1 loss defines a new class of renal cell carcinoma. Nat Genet 44: 751-759

Pollard PJ, Spencer-Dene B, Shukla D, Howarth K, Nye E, El-Bahrawy M, Deheragoda M, Joannou M, McDonald S, Martin A, *et al* (2007) Targeted inactivation of fh1 causes proliferative renal cyst development and activation of the hypoxia pathway. Cancer Cell 11: 311-319

Rankin EB, Tomaszewski JE, Haase VH (2006) Renal cyst development in mice with conditional inactivation of the von Hippel-Lindau tumor suppressor. Cancer Res 66: 2576-2583

Roberts AM, Watson IR, Evans AJ, Foster DA, Irwin MS, Ohh M (2009) Suppression of hypoxia-inducible factor 2alpha restores p53 activity via Hdm2 and reverses chemoresistance of renal carcinoma cells. Cancer Res 69: 9056-9064

Roe JS, Kim H, Lee SM, Kim ST, Cho EJ, Youn HD (2006) p53 stabilization and transactivation by a von Hippel-Lindau protein. Mol Cell 22: 395-405

Stuart ET, Haffner R, Oren M, Gruss P (1995) Loss of p53 function through PAX-mediated transcriptional repression. EMBO J 14: 5638-5645

Tang SW, Chang WH, Su YC, Chen YC, Lai YH, Wu PT, Hsu CI, Lin WC, Lai MK, Lin JY (2009) MYC pathway is activated in clear cell renal cell carcinoma and essential for proliferation of clear cell renal cell carcinoma cells. Cancer Lett 273: 35-43

Thoma CR, Frew IJ, Hoerner CR, Montani M, Moch H, Krek W (2007) pVHL and GSK3beta are components of a primary cilium-maintenance signalling network. Nat Cell Biol 9: 588-595

Thoma CR, Toso A, Gutbrodt KL, Reggi SP, Frew IJ, Schraml P, Hergovich A, Moch H, Meraldi P, Krek W (2009) VHL loss causes spindle misorientation and chromosome instability. Nat Cell Biol 11: 994-1001

Varela I, Tarpey P, Raine K, Huang D, Ong CK, Stephens P, Davies H, Jones D, Lin ML, Teague J, *et al* (2011) Exome sequencing identifies frequent mutation of the SWI/SNF complex gene PBRM1 in renal carcinoma. Nature 469: 539-542

Vichai V, Kirtikara K (2006) Sulforhodamine B colorimetric assay for cytotoxicity screening. Nat Protoc 1: 1112-1116

von Teichman A, Comperat E, Behnke S, Storz M, Moch H, Schraml P (2011) VHL mutations and dysregulation of pVHL- and PTEN-controlled pathways in multilocular cystic renal cell carcinoma. Mod Pathol 24: 571-578

Wagner CA, Loffing-Cueni D, Yan Q, Schulz N, Fakitsas P, Carrel M, Wang T, Verrey F, Geibel JP, Giebisch G, *et al* (2008) Mouse model of type II Bartter's syndrome. II. Altered expression of renal sodium- and water-transporting proteins. Am J Physiol Renal Physiol 294: F1373-F1380

Walther MM, Lubensky IA, Venzon D, Zbar B, Linehan WM (1995) Prevalence of microscopic lesions in grossly normal renal parenchyma from patients with von Hippel-Lindau disease, sporadic renal cell carcinoma and no renal disease: clinical implications. J Urol 154: 2010-2014; discussion 2014–2015

Welford SM, Dorie MJ, Li X, Haase VH, Giaccia AJ (2010) Renal oxygenation suppresses VHL loss-induced senescence that is caused by increased sensitivity to oxidative stress. Mol Cell Biol 30: 4595-4603

Wild PJ, Ikenberg K, Fuchs TJ, Rechsteiner M, Georgiev S, Fankhauser N, Noske A, Roessle M, Caduff R, Dellas A, *et al* (2012) p53 suppresses type II endometrial carcinomas in mice and governs endometrial tumour aggressiveness in humans. EMBO Mol Med 4: 808-824

Xie P, Tian C, An L, Nie J, Lu K, Xing G, Zhang L, He F (2008) Histone methyltransferase protein SETD2 interacts with p53 and selectively regulates its downstream genes. Cell Signal 20: 1671-1678

Young AP, Schlisio S, Minamishima YA, Zhang Q, Li L, Grisanzio C, Signoretti S, Kaelin WG, Jr (2008) VHL loss actuates a HIF-independent senescence programme mediated by Rb and p400. Nat Cell Biol 10: 361-369

Yuan J, Luo K, Zhang L, Cheville JC, Lou Z (2010) USP10 regulates p53 localization and stability by deubiquitinating p53. Cell 140: 384-396

4 Metabolic profiling of *Vhl* negative cells

4.1 Introduction and Aims

The initial event in sporadic as well as hereditary ccRCC is the biallelic inactivation of the tumour suppressor protein pVHL. pVHL is involved in the regulation of diverse cellular processes whose dysregulation could be imagined to play a role in tumour formation (Frew and Krek 2007). Amongst other functions, the loss of *VHL* stabilises HIFα transcription factors which have multiple functions in proliferation, angiogenesis, apoptosis, invasion, metastasis and glucose metabolism (Gordan and Simon 2007). The HIF transcription factors are key regulators of glycolysis and oxidative phosphorylation, inducing the Warburg effect, characterised by increased glucose uptake and excretion as lactate at the expense of entry of pyruvate into the mitochondria for metabolism in the TCA cycle. This form of metabolism is a less efficient way of producing ATP but more importantly glucose breakdown via glycolysis provides the building blocks necessary for macromolecule biosynthesis that supports cellular proliferation (Vander Heiden et al. 2009).

Despite the diverse pathways that VHL and HIF regulate, mouse studies demonstrated that neither the loss of *Vhl* nor the activation of Hif1α or Hif2α could induce the formation of tumours in mouse kidneys. Most likely other mutations have to occur on top of the deletion of *Vhl* to promote cancer development (Frew et al. 2008; Fu et al. 2011; Fu et al. 2013). Recent studies provided new insights in common mutations in ccRCC. Interestingly, besides VHL dysregulation, no other mutations occur with such a high frequency in sporadic ccRCC. However, some well-known tumour suppressors or oncogenes are mutated, but with a much lower frequency. These studies showed that it is more likely that whole pathways are dysregulated. In sporadic ccRCC the PI3K-AKT-mTOR axis is mutated in up to 28% of cases, leading to increased mTORC1 signalling. As mTOR is the key regulator of cell growth and proliferation it is perhaps not surprising that mutations in this pathway occur frequently in ccRCC (Sato et al. 2013).

In this chapter we sought to define the effects of loss of *Vhl* in mouse embryonic fibroblasts (MEFs) on the metabolism of glucose and glutamine as a model for the initial genetic event in ccRCC progression, namely the mutation of *VHL* in an otherwise genetically normal cell. We investigated how this is mediated by the stabilisation of the Hif1α and Hif2α transcription factors. Furthermore, we tried to determine the importance of dysregulated metabolic processes after loss of pVHL function on cell proliferation and their implication for tumour formation.

4.2 Results

4.2.1 Warburg-like phenotype in *Vhl* and *Vhl/Trp53* deficient cells

We focused our first analyses on the metabolism of glucose via glycolysis and oxidative phosphorylation. To address this question, the expression levels of several known Hif1α target genes that are enzymes in these metabolic pathways were analysed in $Vhl^{fl/fl}$ as well as in the senescence rescued $Vhl^{fl/fl}$ $Trp53^{fl/fl}$ MEFs. This latter genotype was important as it allowed us to rule out that gene expression changes are a result of general effects of senescence rather than specific effects of loss of *Vhl*. Cells were infected with adenovirus expressing GFP as control (Adeno-GFP) or expressing Cre recombinase (Adeno-Cre) to induce deletion of the floxed genes. In both genotypes the genes *Glut1*, *Pfkfb3*, *Pgk1*, *Ldha* and *Pdk1* showed a higher expression after the deletion of *Vhl* (Figure 4.1A, B). The gene products Glut1, Pfkfb3 and Pgk1 are involved in inducing glycolysis and Lda-A and Pdk1 prevent glucose from entering the TCA cycle. This effect is due to the loss of *Vhl* as control cells ($Trp53^{fl/fl}$ and wild-type) did not show any alterations (Figure 4.1C, D). Analyses of $Vhl^{fl/fl}$ $Hif1a^{fl/fl}$, $Vhl^{fl/fl}$ $Hif2a^{fl/fl}$ and $Vhl^{fl/fl}$ $Hif1a^{fl/fl}$ $Hif2a^{fl/fl}$ MEFs revealed that the upregulation of these genes is dependent on Hif1α activity but not on Hif2α activity (Figure 4.1E-G).

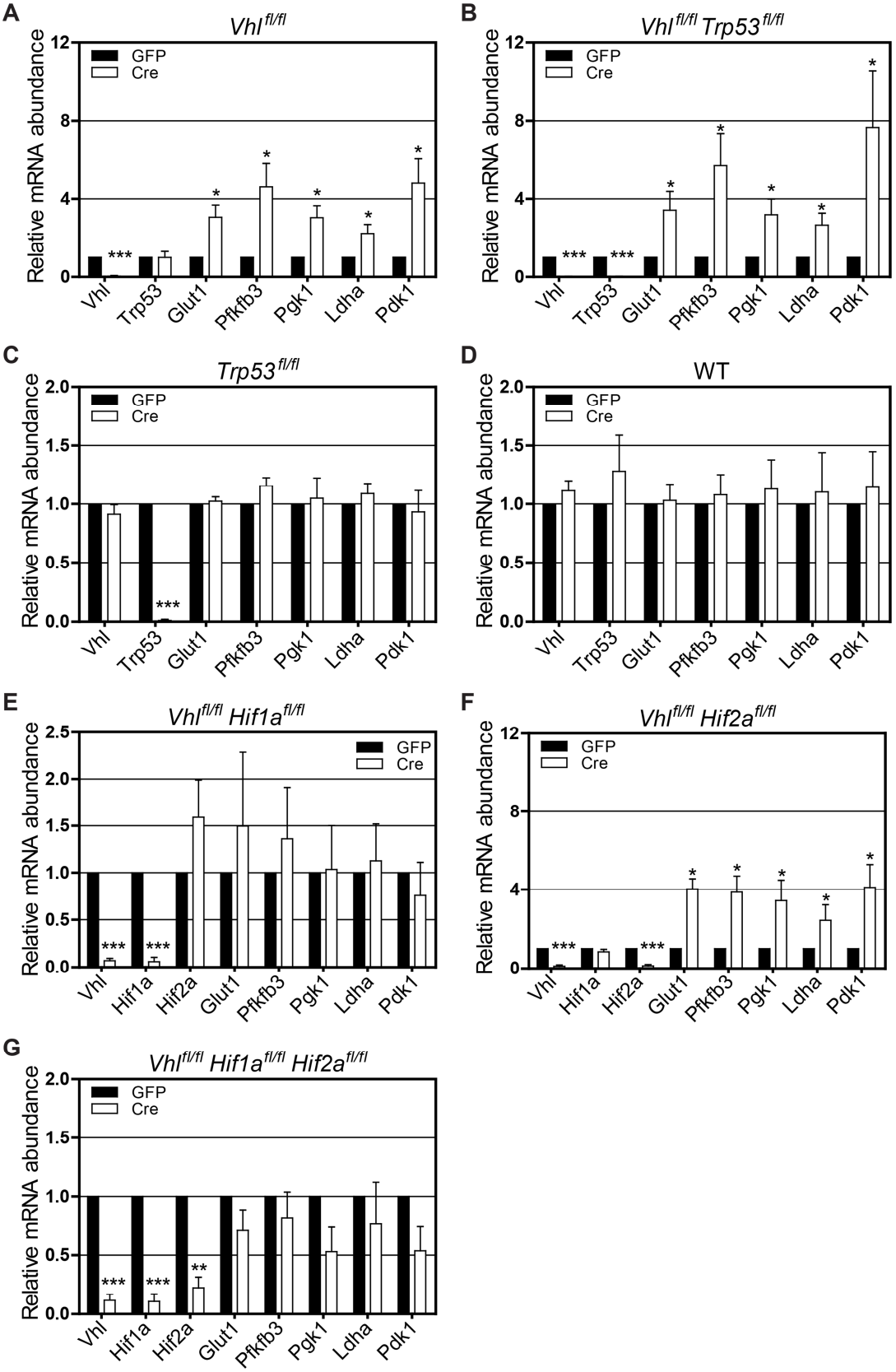

Figure 4.1: Upregulation of glycolytic genes in Vhl negative MEFs is dependent on *Hif1a* but not on *Hif2a*.

A-G Real-time quantitative PCR analysis of Hif1α target genes. mRNA abundance was normalized to *S12* mRNA abundance in *Vhl*$^{fl/fl}$ (A), *Vhl*$^{fl/fl}$ *Trp53*$^{fl/fl}$ (B), *Trp53*$^{fl/fl}$ (C), wild-type (D), *Vhl*$^{fl/fl}$ *Hif1a*$^{fl/fl}$ (E), *Vhl*$^{fl/fl}$ *Hif2a*$^{fl/fl}$ (F) and *Vhl*$^{fl/fl}$ *Hif1a*$^{fl/fl}$ *Hif2a*$^{fl/fl}$ (G) MEFs infected with adenoviruses expressing GFP (GFP) or Cre-GFP (Cre) (Student´s t-test, *$p < 0.05$, **$p < 0.01$, ***$p < 0.001$).

The upregulation of glycolytic genes in *Vhl* negative cells could be confirmed with elevated protein levels of Ldh-A and Pdk1 (Figure 4.2A). These findings suggested that *Vhl* deficient MEFs would exhibit an upregulation of glycolytic flux to lactate and a decrease of entry of pyruvate into the mitochondria for metabolism by oxidative phosphorylation. In both *Vhl* and *Vhl/Trp53* mutant cells the acid efflux (ECAR) (Figure 4.2B) as well as the amount of lactate released into the media (Figure 4.2C) and glucose uptake (Figure 4.2D) were significantly increased. In parallel to the ECAR measurement, the oxygen consumption rate (OCR) was detected as a readout of mitochondrial respiration. OCR was highly decreased in *Vhl* negative cells (Figure 4.2E). This effect was not due to a reduction in the mitochondrial content (Figure 4.2G, H). If these results are considered together, a clear shift from oxidative phosphorylation towards aerobic glycolysis is visible. Since oxidative phosphorylation of glucose-derived carbons represents the major source of cellular ATP, we predicted that ATP levels may be affected in *Vhl* mutant cells. Indeed, the ATP levels in $Vhl^{fl/fl}$ as well as in $Vhl^{fl/fl}$ $Trp53^{fl/fl}$ MEFs were significantly decreased (Figure 4.2F). The fact that the ATP levels were not restored in *Vhl/Trp53* deficient cells indicates that a mechanism other than senescence has to be responsible for this. Parallel studies in our laboratory showed that the decreased levels of ATP are entirely dependent on *Hif1a* and not on *Hif2a* (data not shown, Désirée Schönenberger), consistent with the effects of gene deletion on glycolytic gene expression in these cells (Figure 4.1E-F). Thus, Hif1α activation in MEFs causes a Warburg-like shift in glucose metabolism with a small increase in glucose uptake and metabolism to lactate but a large drop in oxidative phosphorylation that leads to a deficiency in ATP production.

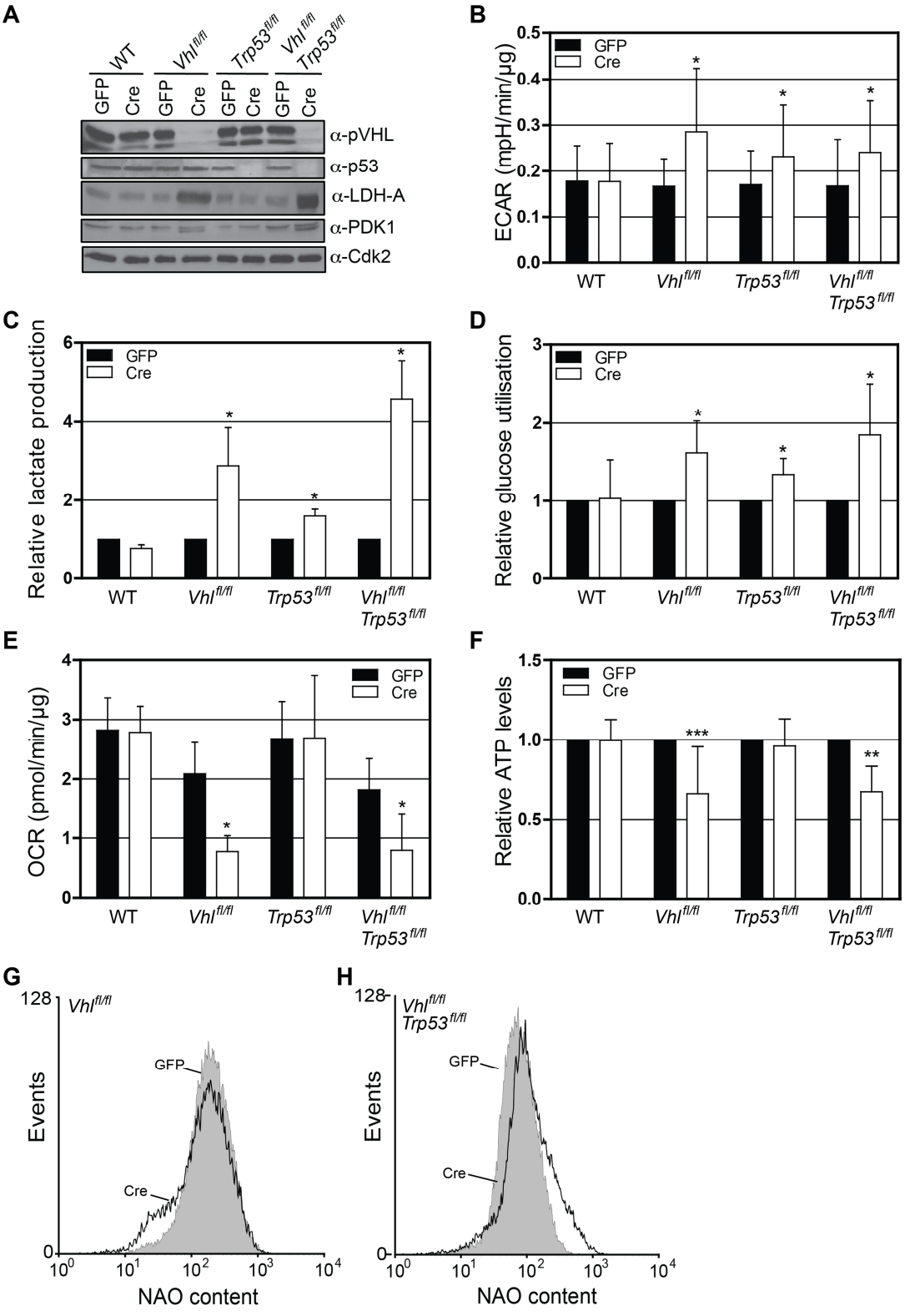

Figure 4.2: Warburg-like metabolism in *Vhl* negative MEFs causes ATP deficiency.

A Western blotting analysis of wild-type, *Vhl*$^{fl/fl}$, *Trp53*$^{fl/fl}$ and *Vhl*$^{fl/fl}$ *Trp53*$^{fl/fl}$ MEFs infected with adenoviruses expressing GFP or Cre.

B-F Measurements of glycolytic parameters in wild-type, *Vhl*$^{fl/fl}$, *Trp53*$^{fl/fl}$ and *Vhl*$^{fl/fl}$ *Trp53*$^{fl/fl}$ MEFs: (B) extracellular acidification rate (ECAR), (C) relative lactate production, (D) glucose utilisation, (E) oxygen consumption rate (OCR) and (F) relative ATP levels (Student´s t-test, *$p < 0.05$, **$p < 0.01$, ***$p < 0.001$).

G, H FACS analysis of *Vhl*$^{fl/fl}$ (G) and *Vhl*$^{fl/fl}$ *Trp53*$^{fl/fl}$ (H) MEFs using NAO as a dye for quantification of mitochondria.

During glycolysis the cytosolic balance of NAD^+/NADH ratio is shifted as the metabolism of glucose to pyruvate also generates NADH. In cells with a low rate of glycolysis the regeneration of NAD^+ in the cytosol can occur through malate-aspartate shuttles but in highly proliferating cells with highly increased glycolysis this mechanism of NAD^+ generation are likely saturated (Locasale and Cantley 2011). Therefore, other mechanisms like reduction of pyruvate to lactate are required to regenerate NAD^+ from NADH. We were now wondering if increased glycolysis in *Vhl* deficient cells affects the levels of NAD^+ and its reduced form NADH. Interestingly, NAD^+ as well as NADH levels were increased in *Vhl* negative cells, but the ratio of NAD^+/NADH did not differ compared to control cells (Figure 4.3A, C). The levels of NADH in *Vhl/Trp53* and *Trp53* negative MEFs were slightly increased, resulting in a decrease in the ratio of NAD^+/NADH (Figure 4.3B-D). In skeletal muscle cells an activation of AMPK could increase the amount of NAD^+ and also the ratio NAD^+/NADH (Canto et al. 2009). The activation of AMPK in *Vhl* deficient cells will be discussed in the following paragraph (4.2.2).

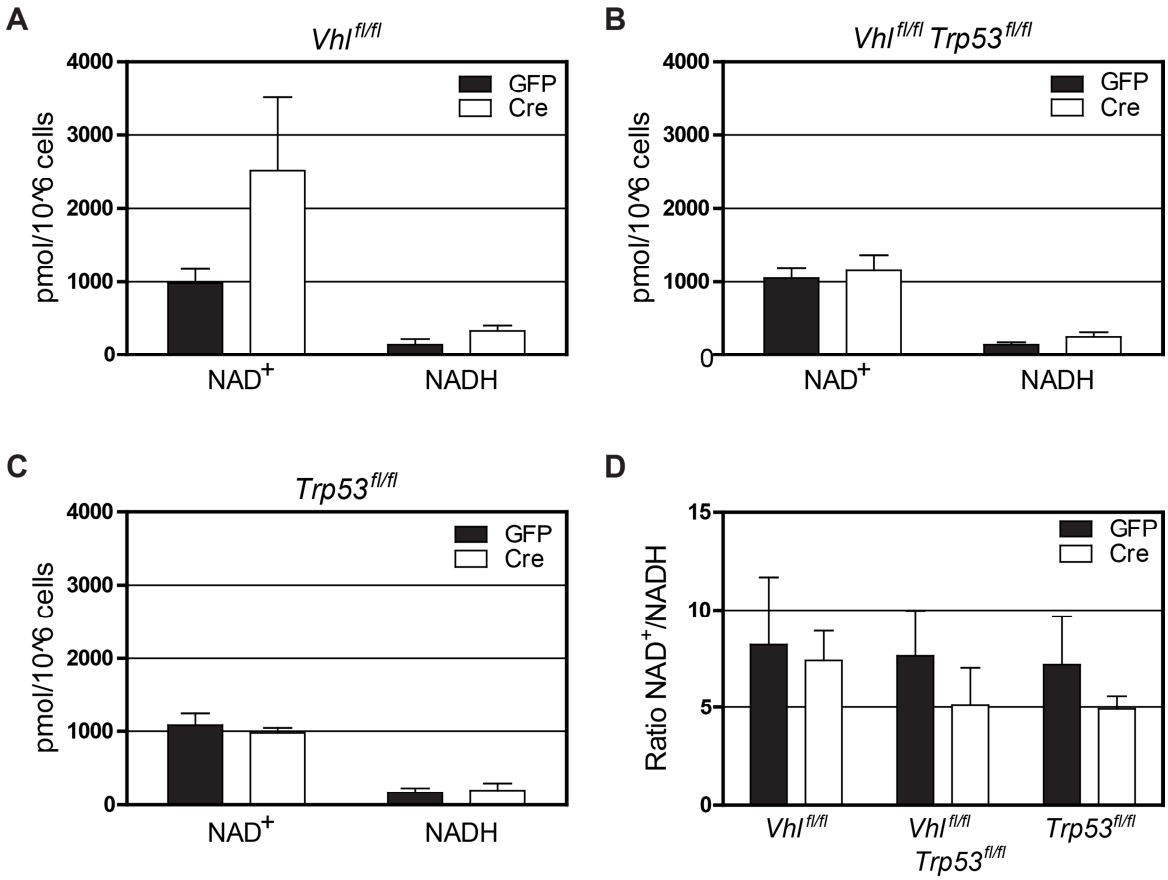

Figure 4.3: Increased levels of NAD^+ and NADH in *Vhl* deficient MEFs.

A-D Intracellular NAD^+ and NADH levels of *Vhl*$^{fl/fl}$, *Vhl*$^{fl/fl}$ *Trp53*$^{fl/fl}$ and *Trp53*$^{fl/fl}$ MEFs infected with adenoviruses expressing GFP or Cre.

In order to gain deeper insights into metabolic changes of *Vhl* deficient cells and to better understand integrated metabolic responses we performed mass spectrometry-based metabolomic analyses. With this technique it is possible to simultaneously monitor and quantify the abundance of hundreds of intracellular metabolites like cofactors, energy equivalents and primary metabolites (Fuhrer et al. 2011). For these experiments, we used wild-type, $Vhl^{fl/fl}$, $Trp53^{fl/fl}$ and $Vhl^{fl/fl}$ $Trp53^{fl/fl}$ primary MEFs treated with adenovirus expressing GFP or GFP-Cre. For the analysis knockout cells were compared to control cells (Adeno-GFP treated). These experiments yielded rather inconsistent results between replicates and independent experiments, complicating analyses. The only partially consistent changes observed were that *Vhl* and *Vhl/Trp53* deficient cells compared to their control cells showed an increase of intermediates of the pentose phosphate pathway. However, in different experiments not always the same intermediates could be detected and also the detected amount varied (Figure 4.4). Another problem was the detection of baseline differences in wild-type GFP treated compared to wild-type Cre treated cells and also in various experiments the profiles differed quite a lot. Furthermore, the intensity of the detected peaks was much lower than expected. Despite several trials these problems could not be solved satisfyingly and this experimental approach was not further pursued.

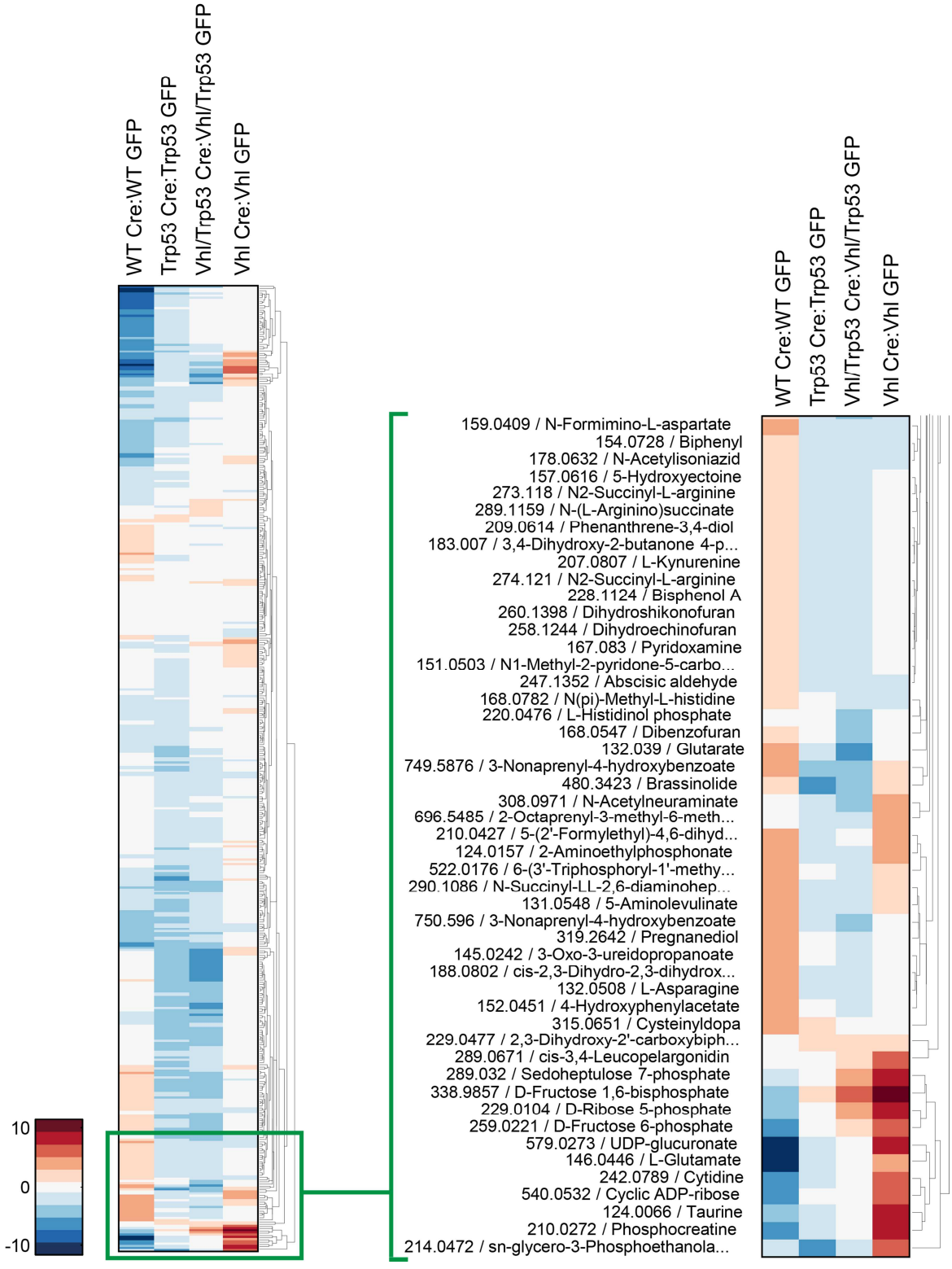

Figure 4.4: Deficiency of *Vhl* increases pentose phosphate pathway intermediates.

Tree-chart of metabolomic profiling of wild-type, *Trp53*$^{fl/fl}$, *Vhl*$^{fl/fl}$ and *Vhl*$^{fl/fl}$ *Trp53*$^{fl/fl}$ MEFs infected with adenoviruses expressing GFP or Cre.

4.2.2 Activation of AMPK in *Vhl* negative MEFs

The energy status in cells is sensed by the AMP-activated protein kinase (AMPK) due to changes in the ratio of AMP to ATP that are caused by metabolic stresses like hypoxia, ischemia and oxidative and hyperosmotic stresses. Activated AMPK is responsible for the activation of catabolic processes like glycolysis and fatty acid synthesis and the inhibition of anabolic events including lipid, protein and glycogen synthesis (Hardie 2004). As the levels of ATP were decreased in *Vhl* knockout cells, the activation status of AMPK was examined via detection of the phosphorylation status of Thr172. Despite observing consistently decreased ATP levels in *Vhl* negative cells (Figure 4.2F), AMPK was clearly activated in some experiments (Figure 4.5A, B) but not in others (Figure 4.5C) although the knockout efficiency for *Vhl* was very consistent. One possible explanation for this inconsistency could be that unknown factors, which are not directly associated with the loss of *Vhl,* also impact the phosphorylation status of AMPK.

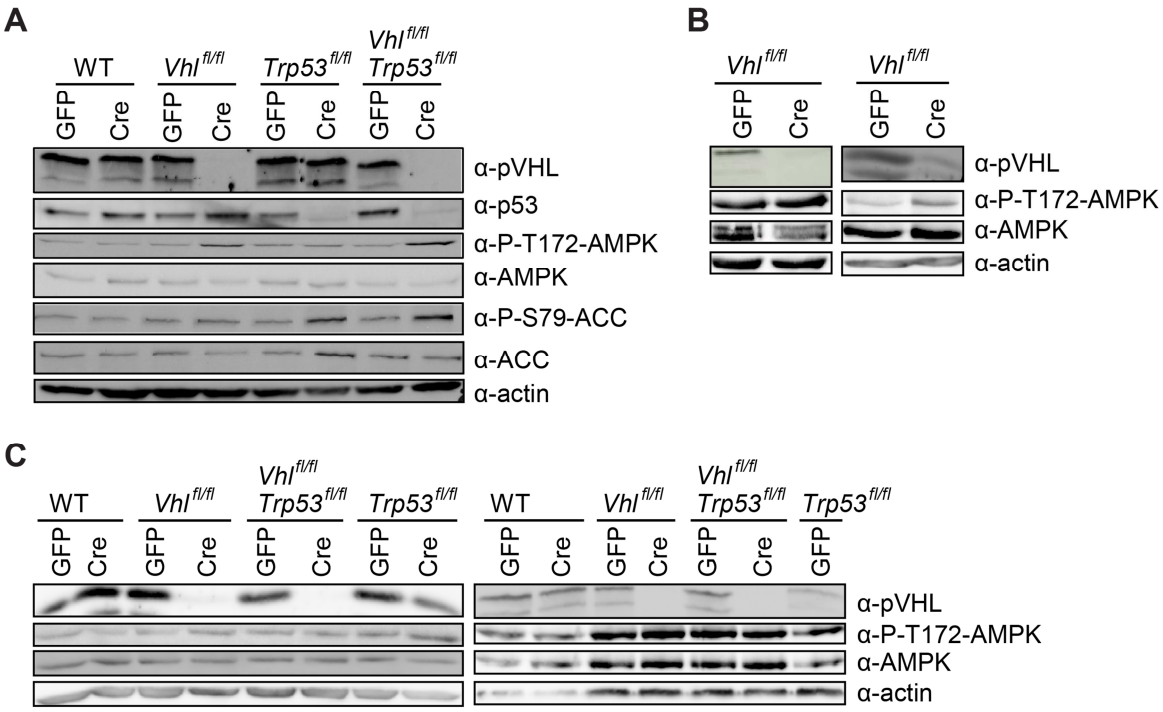

Figure 4.5: Activation of AMPK in *Vhl* deleted MEFs is inconsistent.

A-C Western blotting analysis of multiple independent experiments using wild-type, *Vhl*$^{fl/fl}$, *Trp53*$^{fl/fl}$ and *Vhl*$^{fl/fl}$ *Trp53*$^{fl/fl}$ MEFs infected with adenoviruses expressing GFP or Cre.

To attempt to understand these inconsistent phosphorylation events, different starvation experiments were performed in *Vhl* negative cells. We hypothesised that the induction of additional stress might help to answer the question of which factors have a further effect on the ATP levels and the activation of AMPK. We further hypothesised that *Vhl* deficient cells might be hypersensitive to metabolic changes induced by starvation, for example, they may be highly dependent on glucose or glutamine for energy production. Therefore,

Vhl$^{fl/fl}$ and *Vhl*$^{fl/fl}$ *Trp53*$^{fl/fl}$ MEFs were starved for two or six hours of glucose or glutamine. Surprisingly, the ATP levels in all *Vhl* deficient cells were rescued due to the withdrawal of glucose at both time points, contrary to our initial expectations. This may possibly be due to activation of other metabolic pathways that allow ATP generation from glycogen stores or fatty acids, or potentially from the induction of autophagy. Glutamine deprivation for six hours moderately decreased ATP levels in wild type cells and also caused a similar moderate decrease in *Vhl* deficient cells (Figure 4.6A, C). Glucose deprivation in general increased the amount of phosphorylated AMPK but the deletion of *Vhl* had no additional effect (Figure 4.6B, D).

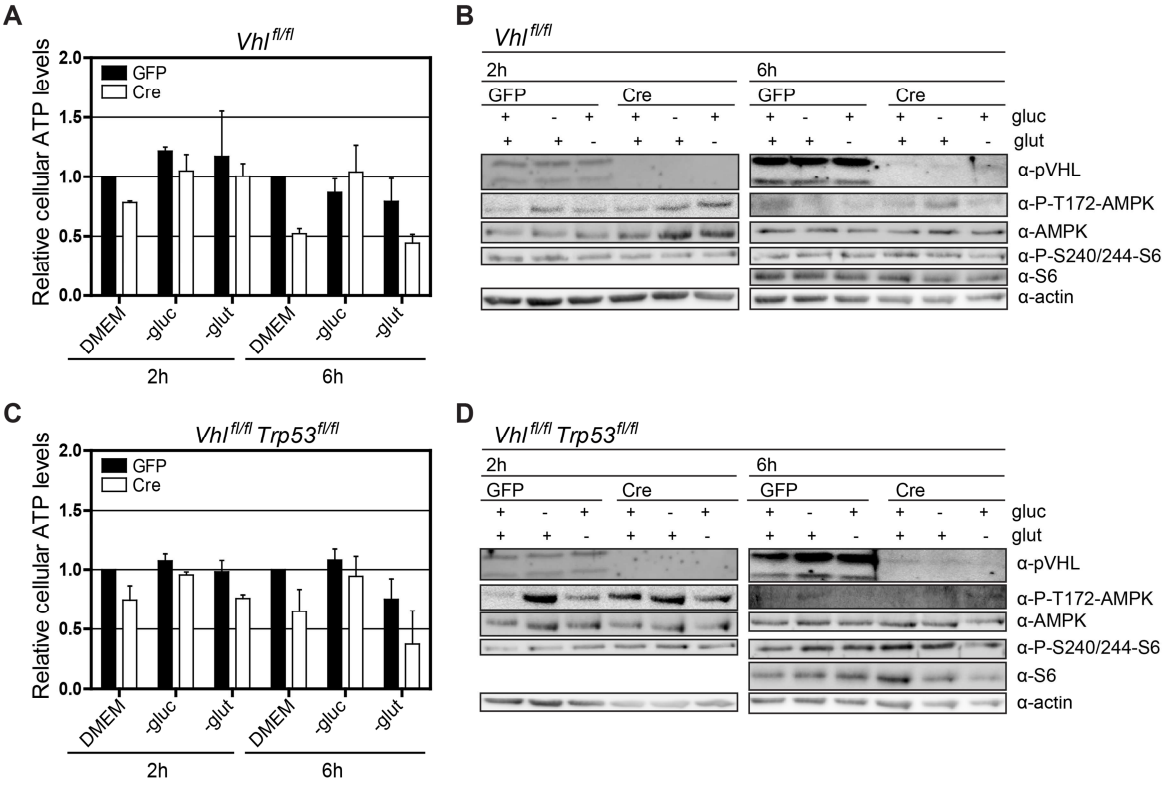

Figure 4.6: *Vhl* deficient cells are not sensitised to glucose or glutamine starvation.

A, C Cellular ATP levels of *Vhl*$^{fl/fl}$ and *Vhl*$^{fl/fl}$ *Trp53*$^{fl/fl}$ MEFs infected with adenoviruses expressing GFP or Cre starved of glucose or glutamine for 2 or 6 hours.

B, D Western blotting analysis of cells from (A) and (C).

Prolonged (24 hour) glucose or glutamine starvation of Adeno-GFP and Adeno-Cre treated *Vhl*$^{fl/fl}$, *Vhl*$^{fl/fl}$ *Trp53*$^{fl/fl}$ and control cells (*Trp53*$^{fl/fl}$ and wild-type) showed decreased ATP levels in all genotypes but *Vhl* negative cells were not more sensitive to glutamine starvation (Figure 4.7A-D). In addition, *Vhl/Trp53* knockout cells that were exposed for 24 hours to media with reduced glucose, FCS or amino acids were analysed. However, neither the ATP levels (Figure 4.7E) nor the phosphorylation status of AMPK (Figure 4.7F) was further affected in any of these conditions. Energy stress-activated AMPK inhibits the mTORC1 pathway (Inoki et al. 2003; Gwinn et al. 2008) thus mTORC1

targets including ribosomal protein S6 or 4E-BP1 might be expected to show lower phosphorylation levels in *Vhl* deficient cells. However, after short term starvation (two and six hours) no changes in the phosphorylation states of these proteins could be observed (Figure 4.6B, D). Furthermore, in Adeno-GFP and Cre treated cells a starvation for 24 hours reduced phosphorylation levels of S6 protein only due to glucose withdrawal but this did not correlate with the phosphorylation levels of AMPK (Figure 4.7F). Taking the obtained results together, none of the performed experiments could explain the inconsistent phosphorylation pattern of AMPK.

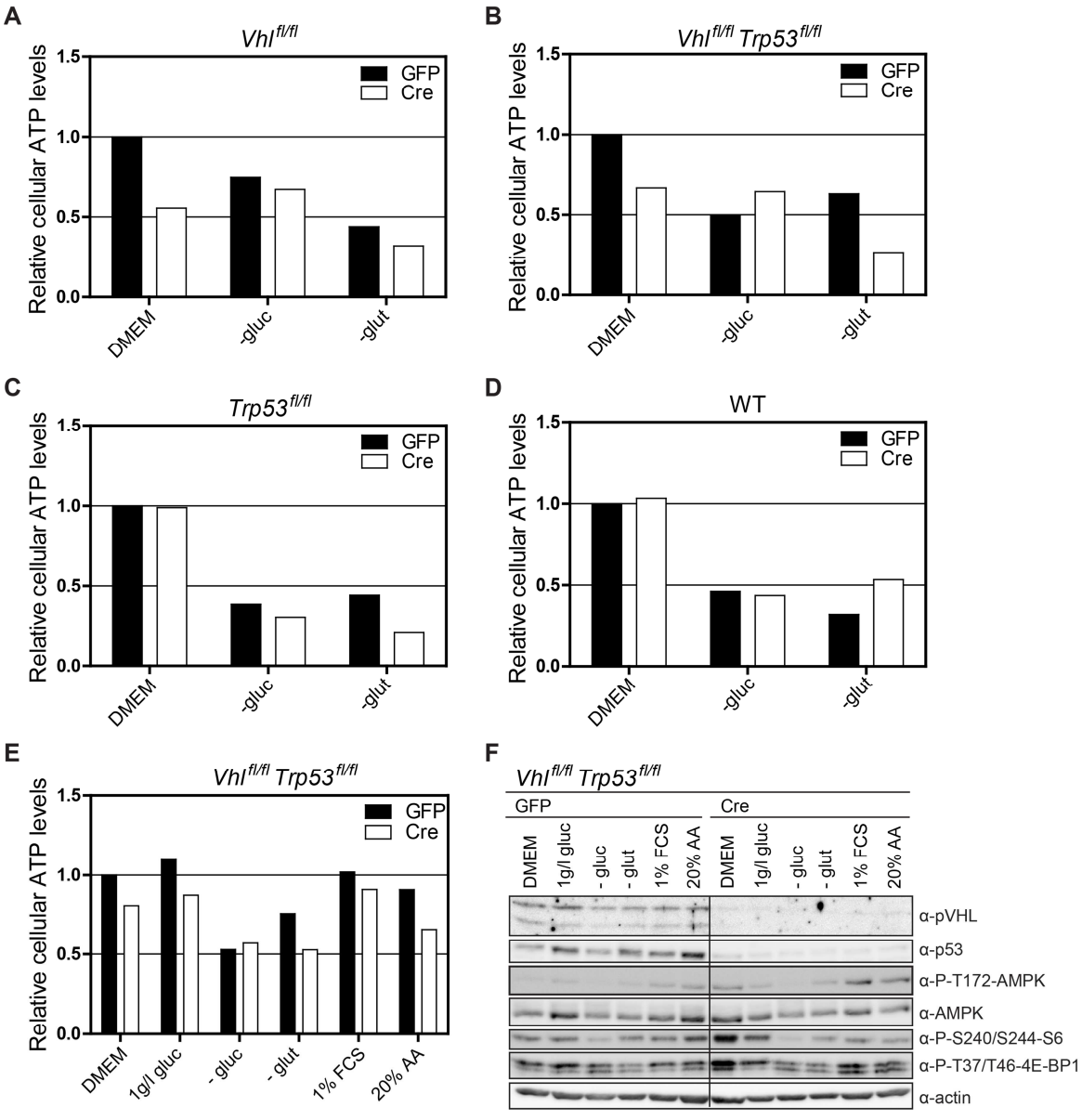

Figure 4.7: Long-term glucose or glutamine starvation reduces cellular ATP levels.

A-D Cellular ATP levels of *Vhl*$^{fl/fl}$ (A), *Vhl*$^{fl/fl}$ *Trp53*$^{fl/fl}$ (B), *Trp53*$^{fl/fl}$ (C) and wild-type (D) MEFs infected with adenoviruses expressing GFP or Cre. Cells were starved for 24 hours of glucose or glutamine.

E Cellular ATP levels of *Vhl*$^{fl/fl}$ *Trp53*$^{fl/fl}$ MEFs infected with GFP or Cre. Cells were treated for 24 hours with normal DMEM, DMEM with: 1g/l glucose, no glucose, no glutamine, 1% FCS or 20% amino acids.

F Western blotting analysis of cells from (E).

4.2.3 Loss of *Vhl* does not activate p53

One downstream target of AMPK is the tumour suppressor p53 that is also activated due to cellular damage or stress and induces cell cycle responses like apoptosis or growth arrest. AMPK phosphorylates and activates p53, which in turn induces cell cycle arrest in the G1/S phase of the cell cycle and this is accompanied by an upregulation of the p53 target gene *p21* (Jones et al. 2005). Since we initially observed that *Vhl* deletion induces senescence that is genetically dependent on *Trp53*, we hypothesised that energy deficiency may activate AMPK to induce p53 activity and thereby induce senescence. In *Vhl* deficient primary MEFs with activated AMPK, slightly increased protein levels of p53 as well as of phosphorylated p53 could be observed. However, there was no change in the protein level of $p21^{Cip}$ (Figure 4.8A). Wild-type MEFs that were infected with an adenovirus expressing Cre also showed increased phosphorylation levels of p53 (Figure 4.8A, B) and this was not further induced by knockdown of *Vhl* (Figure 4.8B). These findings argue that the observed induction of p53 phosphorylation may result from DNA damage induced by Cre activity (Loonstra et al. 2001). The results from protein analyses could be confirmed with data from quantitative RNA analyses where the p53 target genes *Mdm2*, *p21* and *Tigar* were not induced in cells with deleted *Vhl* (Figure 4.8C-E). Altogether, these results demonstrated that the deletion of *Vhl* in MEFs and the resulting activation of AMPK did not induce a p53 response. The induction of p53 was rather likely to be a consequence of Cre expression, which has previously been shown to cut genomic DNA non-specifically and cause DNA damage (Loonstra et al. 2001).

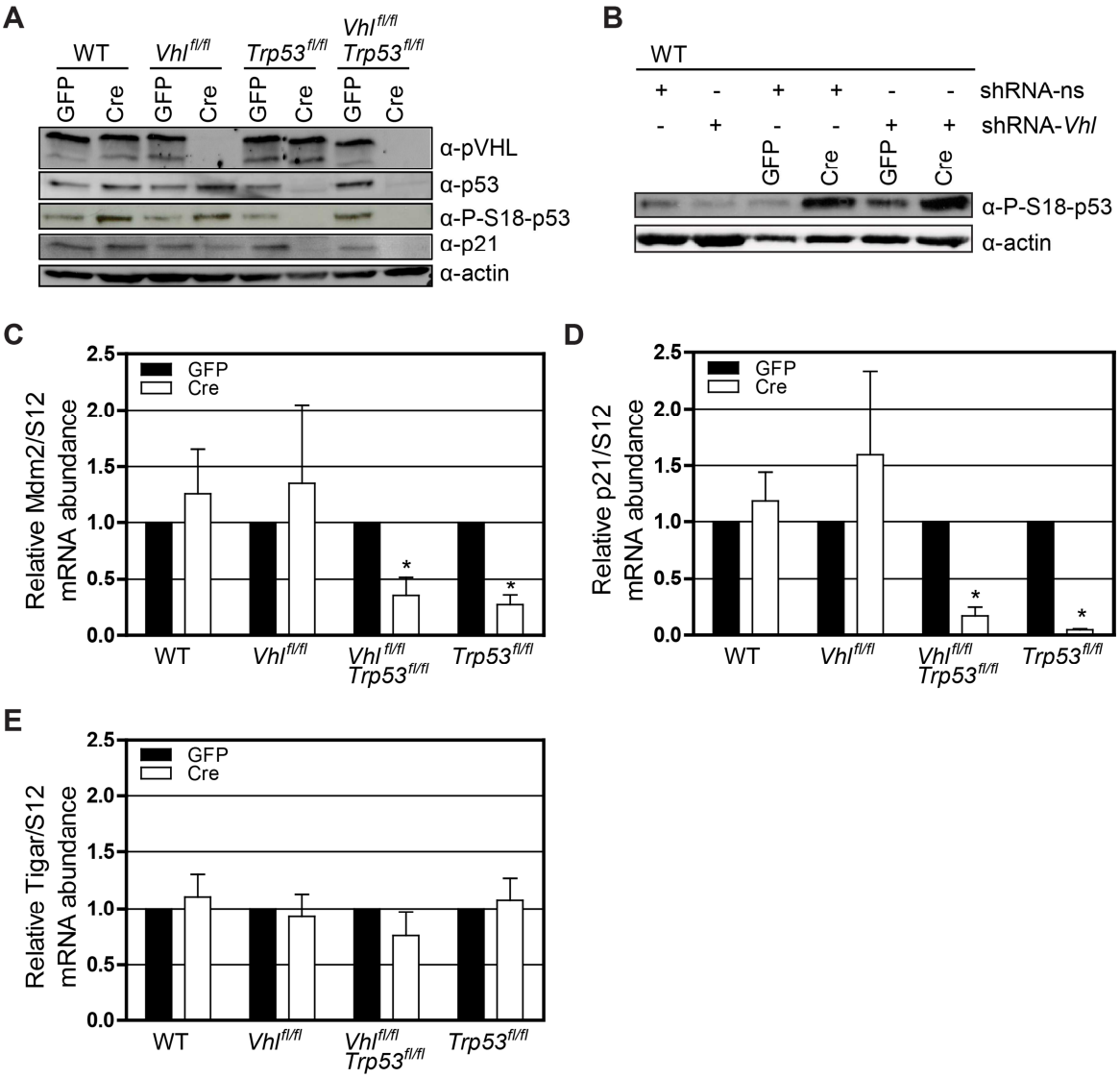

Figure 4.8: Absence of p53 induction in *Vhl* knockout cells.

A Western blotting analysis of wild-type, *Vhl*$^{fl/fl}$, *Trp53*$^{fl/fl}$ and *Vhl*$^{fl/fl}$ *Trp53*$^{fl/fl}$ MEFs infected with adenoviruses expressing GFP or Cre.

B Western blotting analysis of wild-type MEFs infected with GFP or Cre and/or lentiviruses expressing an empty pLKO.1 shRNA (shRNA-ns) or pLKO.1 shRNA directed against *Vhl* (shRNA-*Vhl*).

C-E Real-time quantitative PCR analysis of *Mdm2* (C), *p21* (D) and *Tigar* (E) mRNA abundance normalized to *S12* mRNA abundance in GFP or Cre infected wild-type, *Vhl*$^{fl/fl}$, *Vhl*$^{fl/fl}$ *Trp53*$^{fl/fl}$ and *Trp53*$^{fl/fl}$ MEFs (Student´s t-test, *$p < 0.05$).

4.2.4 Deletion of *Vhl* alone is not enough for consistent downregulation of the mTORC1 pathway

Another target of AMPK is the mTORC1 complex that regulates cell growth by integrating nutrient and growth factor-derived signals to control protein synthesis. AMPK indirectly inhibits mTORC1 via phosphorylation of TSC2 (Inoki et al. 2003), a GTPase upstream of mTORC1 or directly by phosphorylation of RAPTOR (Gwinn et al. 2008), which is part of the mTORC1 complex (see also Figure 1.3). As a readout for the activity of the mTORC1 complex its downstream targets ribosomal protein S6 kinase (S6K) and ribosomal protein

S6, which are phosphorylated when mTORC1 is active (Ruvinsky et al. 2005), were analysed. In *Vhl* negative cells a slight reduction of phosphorylated S6K and S6 protein could be observed when AMPK was activated, indicating an inhibition of mTORC1 signalling. Since decreased levels of total protein levels of S6K and S6 were observed, we wondered if protein synthesis could be affected due to the loss of *Vhl* (Figure 4.9A, B). To address this question, a ^{35}S-methionine incorporation assay was performed, which could detect a mild decrease of protein synthesis in *Vhl* knockout cells (Figure 4.9C, D). However, since these cells exhibit a slower rate of proliferation, it is possible that the reduced level of protein synthesis may be a consequence, rather than a cause, of the proliferation rate. As mentioned before, activated AMPK could not be observed in all analysed samples. The same was true for the decreased phosphorylation status of S6K and S6 protein that could also not be observed in all analysed samples from independent experiments (Figure 4.6B, D; Figure 4.7F). Again, we hypothesise that one or several unknown factors are influencing AMPK activity, which made further studies of potential downstream phenotypes very difficult.

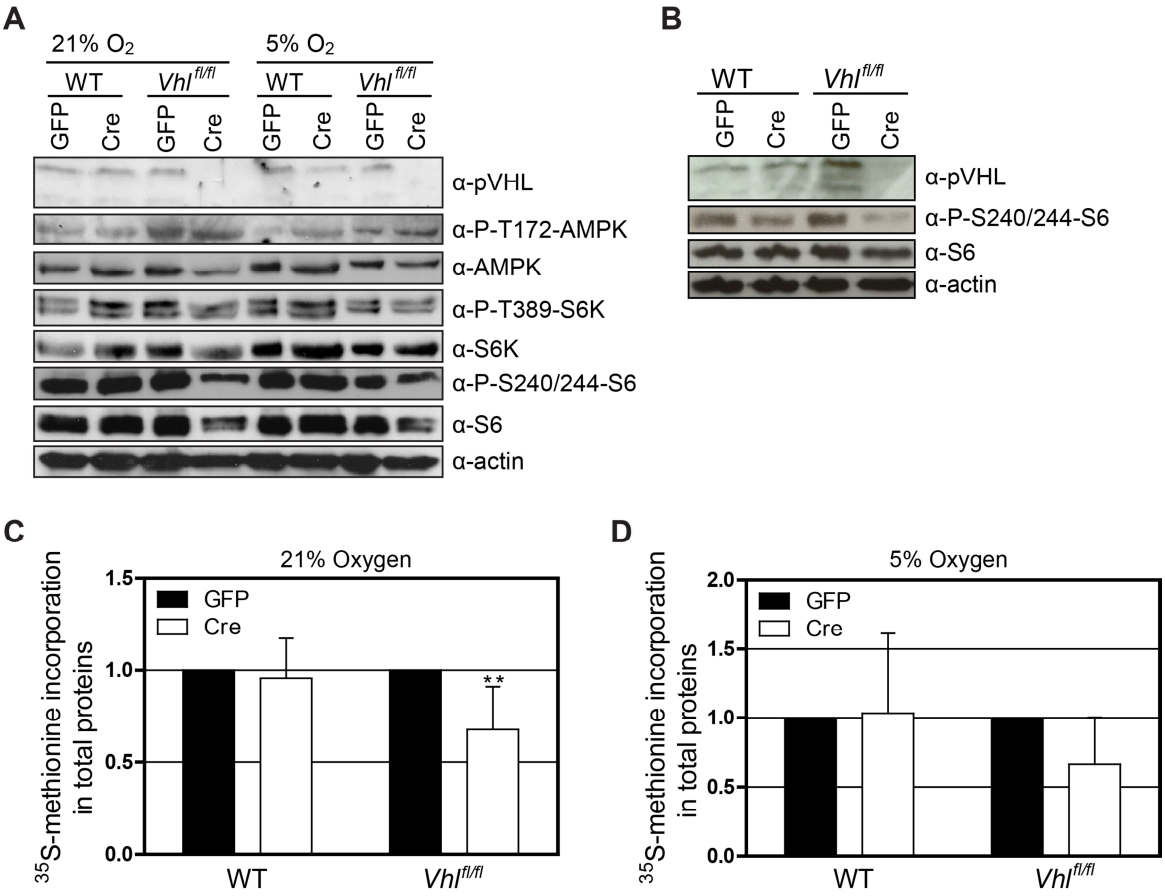

Figure 4.9: Downregulation of activated S6 and protein synthesis in cells with loss of *Vhl*.

A, B Western blotting analysis of wild-type and *Vhl*$^{fl/fl}$ MEFs infected with adenoviruses expressing GFP or Cre.

C, D Measurement of protein synthesis of wild-type and *Vhl*$^{fl/fl}$ MEFs infected with GFP or Cre by incorporation of ^{35}S-methionine (Student´s t-test, *$p < 0.05$, **$p < 0.01$).

4.2.5 Induction of mTORC1 via loss of *Tsc2* is insufficient for transformation

An important conclusion of our analyses of the proliferation of *Vhl/Trp53* mutant MEFs was that these cells are immortalised but proliferate more slowly than *Trp53* null MEFs. We have also recently shown that the inhibitory effects on proliferation through loss of *Vhl* are mediated by Hif1α activation (Désirée Schönenberger, data not shown). We therefore wondered whether Hif1α-mediated metabolic changes could cause energy stress, AMPK activation and downregulation of the mTORC1 pathway, leading to lowered rates of proliferation.

A natural self-protection of cells against excessive proliferation signals is the inhibition of the mTORC1 pathway via multiple feedback mechanisms. Additional mutations in pathways involved in cell proliferation might help to overcome the inhibition of the mTORC1 pathway, thus allowing uncontrolled cell growth. In ccRCC, multiple components of the PI3K-AKT-mTOR pathway are altered (TCGA 2013). The tumour suppressor genes *TSC1* and *TSC2*, encoding hamartin and tuberin, form a complex that antagonises the mTORC1 pathway (Tee et al. 2002). AMPK operates on different levels as a counterpart of mTORC1. For example it phosphorylates and thus activates tuberin (also see Figure 1.3) (Inoki et al. 2003). To further address the question if suppression of the mTOR pathway is a barrier for prolonged proliferation, a knockdown of *Tsc1* or *Tsc2* in *Vhl/Trp53* deficient cells was introduced. Studies in our laboratory showed that knockdown of *Tsc1* or *Tsc2* causes *Trp53*-dependent senescence (Ana Filipa Gonçalves, data not shown) and *Tsc1* or *Tsc2* knockdown in *Vhl* deficient MEFs completely prevented cellular proliferation. In contrast, *Tsc1* or *Tsc2* were able to be knocked down in *Vhl/Trp53* double mutant fibroblasts but this did not increase the proliferative rate of these cells (Figure 4.10A, B), despite activation of the mTORC1 pathway, indicated by increased levels of phosphorylated ribosomal protein S6 and 4E-BP1 (Figure 4.10C). A way to measure cellular immortalisation is the so-called colony formation assay in which immortalised cells, but not primary MEFs display the ability to proliferate to form colonies when plated at low density. In wild-type cells low cell density seeding causes a premature senescence program. We showed that *Vhl/Trp53* null MEFs are immortalised (Albers et al. 2013). *Vhl/Trp53* null cells with a knockdown of *Tsc1* or *Tsc2* were still able to form colonies in this assay (Figure 4.10D). Neither the additional loss of *Tsc1* nor of *Tsc2* caused a transformation of the *Vhl/Trp53* negative cells as the cells were unable to grow in a soft agar assay (data not shown). While *Tsc1* or *Tsc2* knockdown increased ATP levels in wild-type cells, there was no rescue of the low levels of ATP in *Vhl/Trp53* null cells (Figure 4.10E). In summary, although the loss of *Tsc1* or

Tsc2 induces activation of the mTORC1 pathway, the additional loss of *Vhl* and *Trp53* is not sufficient for a transformation of primary MEFs.

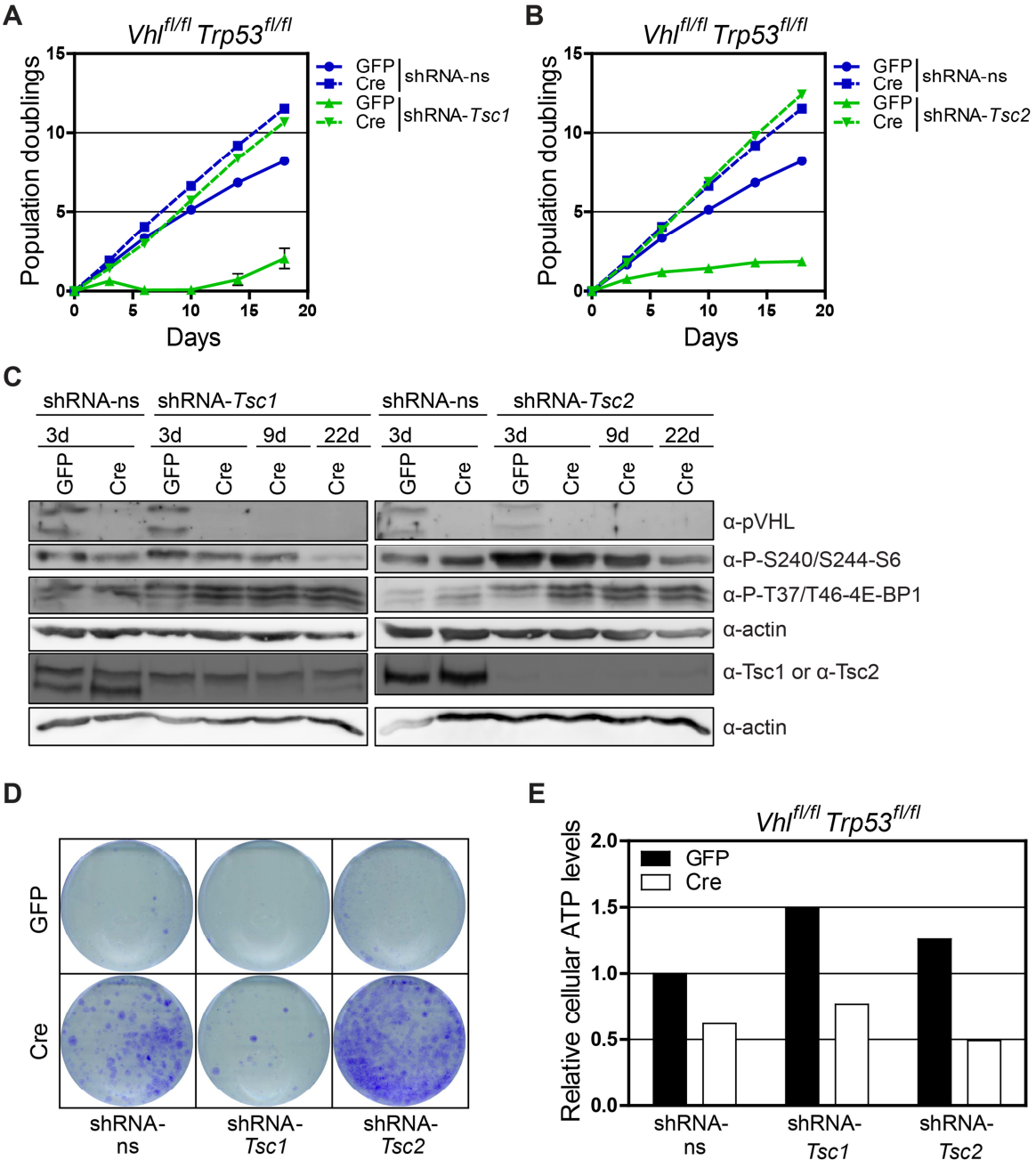

Figure 4.10: Deletion of *Tsc1* or *Tsc2* has no further proliferative effect on *Vhl/Trp53* deficient cells.

A, B Proliferation assay of *Vhl*$^{fl/fl}$ *Trp53*$^{fl/fl}$ MEFs infected with adenoviruses expressing GFP or Cre and lentiviruses expressing an empty pLKO.1 shRNA (shRNA-ns) or pLKO.1 shRNA directed against *Tsc1* or *Tsc2* (shRNA-*Tsc1* or *Tsc2*).

C Western blotting analysis of cells from (A) and (B) at indicated time points.

D Immortalisation assay of cells from (A) and (B).

E Cellular ATP levels of cells from (A) and (B) 6 days after adenovirus infection.

4.2.6 Loss of *Lkb1* does not cooperate genetically with loss of *Vhl* to cause transformation

Since AMPK affects multiple cellular processes, other pathways in addition to regulation of mTORC1 signalling might be more relevant for the potential AMPK-mediated proliferation suppression following *Vhl* deletion. We therefore tested the idea that AMPK activation in general may represent a proliferation barrier in *Vhl* deficient cells. Alternatively, it could also be envisaged that loss of *Vhl* causes a metabolic stress and that AMPK activity is necessary to coordinate the cellular metabolic responses to this stress. The absence of correct AMPK activation could therefore be imagined to be protective and be necessary for the survival or proliferation of *Vhl* deficient cells. To better understand the effects of AMPK activation in *Vhl* deficient cells we knocked down the kinase that phosphorylates and activates AMPK in metabolic stress situations. The serine/threonine kinase LKB1 was originally identified as a tumour suppressor that is mutated in the Peutz-Jeghers hereditary cancer syndrome (Hemminki et al. 1998; Jenne et al. 1998). Recent studies have suggested that LKB1 might also act as a tumour suppressor in some sporadic cases of ccRCC (Duivenvoorden et al. 2013). Knockdown experiments of *Stk11*, the gene encoding Lkb1, were performed in $Vhl^{fl/fl}$ $Trp53^{fl/fl}$ primary MEFs treated with Adeno-Cre using four different shRNA hairpins. Unexpectedly, the hairpins behaved differently. Two of the *Stk11* knockdowns (hairpin A and C) in *Vhl/Trp53* deficient cells created a proliferative advantage whereas the other two hairpins (B and D) inhibited proliferation (Figure 4.11A, E). The reason for these phenotypic differences is not related to different knockdown efficiencies as protein and RNA abundance of Lkb1 was reduced similarly by all four hairpins (Figure 4.11C, D, F). Anchorage independent proliferation was measured by seeding cells in uncoated plates to reduce cell attachment. Interestingly, anchorage independent growth was only possible with hairpin C in *Vhl/Trp53* deficient cells (Figure 4.11G) and these cells were able to form tumours in a xenograft assay (data not shown). However, since we could observe this effect only in cells infected with one of four hairpins and the different hairpins behaved differently in the proliferation assays it is impossible to draw conclusions from this experimental approach and the cooperative effects in transformation likely reflect an off-target effect of hairpin C.

Figure 4.11: *Lkb1* knockdown has inconsistent effects on *Vhl/Trp53* knockout MEFs.

A, E Proliferation assay of $Vhl^{fl/fl}$ $Trp53^{fl/fl}$ MEFs infected with adenoviruses expressing GFP or Cre and lentiviruses expressing an empty pLKO.1 shRNA (shRNA-ns) or four different pLKO.1 shRNAs directed against *Stk11* (shRNA-*Stk11* A-D).

B, F Western blotting analysis of cells from (A and E) at indicated time points.

C, D Real-time quantitative PCR analysis of *Stk11* (C) and *Vhl* (D) mRNA abundance normalized to *S12* mRNA abundance in cells from (A).

G Anchorage independent growth of cells from (A). Scale bar 50 µm.

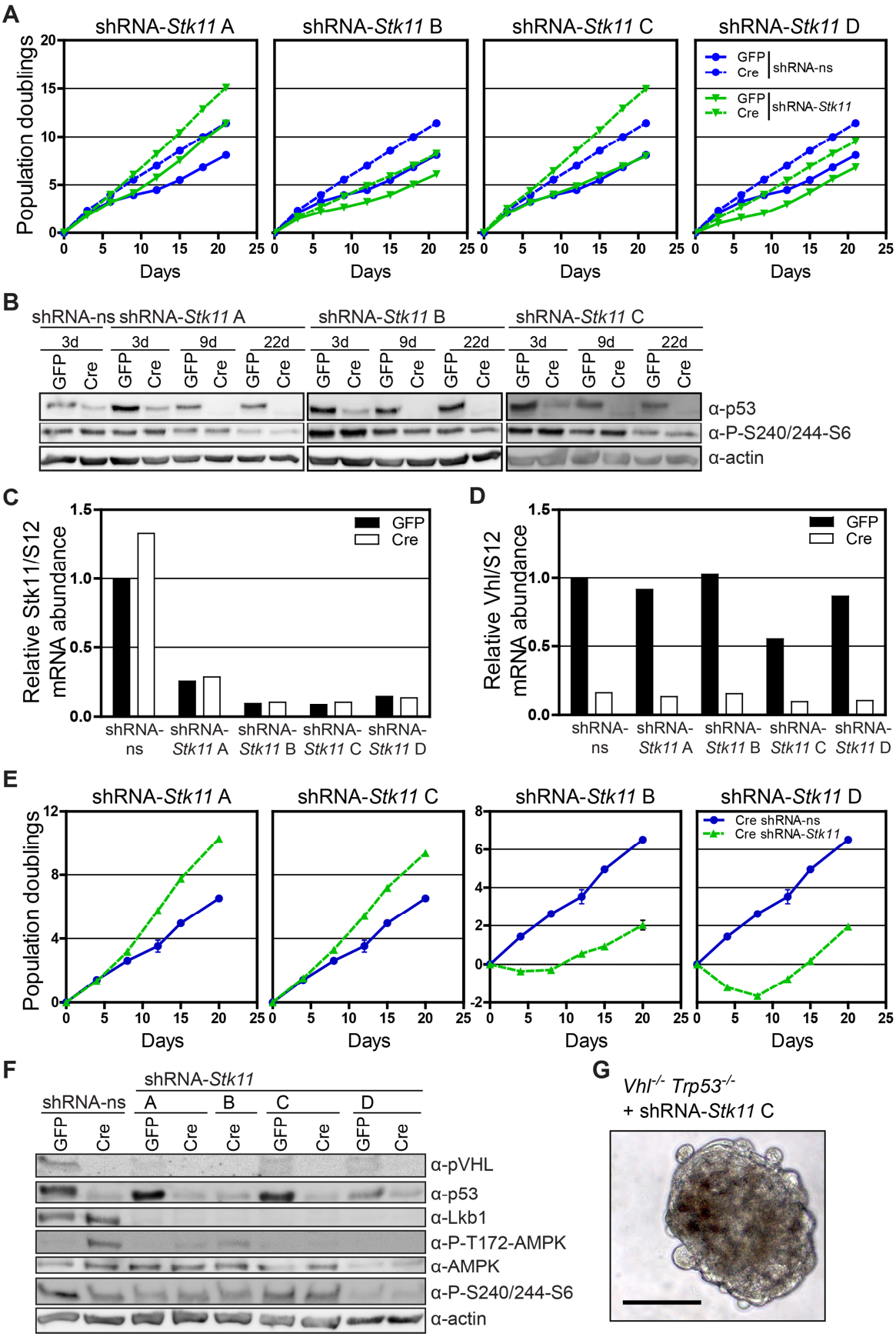

Figure 4.11: *Lkb1* knockdown has inconsistent effects on *Vhl/Trp53* knockout MEFs.

4.2.7 Combined loss of pVhl and AMPK is insufficient to transform cells

The AMPK enzyme is composed of three subunits. AMPKα1 and AMPKα2 are the catalytically active subunits in different complexes, encoded by *Prkaa1* and *Prkaa2*, respectively (Stapleton et al. 1996). As an alternative approach to inhibiting AMPK activation by silencing *Lkb1*, we also directly examined the effects of genetic loss of AMPK on cellular behaviour of *Vhl* knockdown cells. SV40-T Antigen immortalised *Prkaa1*-null, *Prkaa2*-null or *Prkaa1/2*-null MEFs were used and a shRNA against *Vhl* was introduced. The proliferation pattern of these cells did not significantly differ with or without *Vhl*, only the *Prkaa2*-null cells showed a slight reduction in proliferative capacity (Figure 4.12A). A limiting factor in these experiments is that over time, as the cells are repeatedly passaged, all of the *Vhl* knockdown cultures became enriched with pVHL-expressing cells (Figure 4.12B). This phenomenon of selection against efficient *Vhl* knockdown is described in Chapter 3. Interestingly, even though the knockdown of *Vhl* was initially very efficient, there were no effects on ATP levels (Figure 4.12C). One potential explanation for this might be related to findings in Chapter 6 in which we could show that loss of Rb1 function is sufficient to rescue the ATP deficiency in *Vhl* deficient cells. Since SV40-T Antigen inhibits both p53 and Rb protein functions, it could be that the transformed background of the AMPK-deficient MEFs provides a rescue of the ATP phenotype, making these cells an inappropriate model to study genetic interactions between loss of *Vhl* and loss of *Prkaa1/2*.

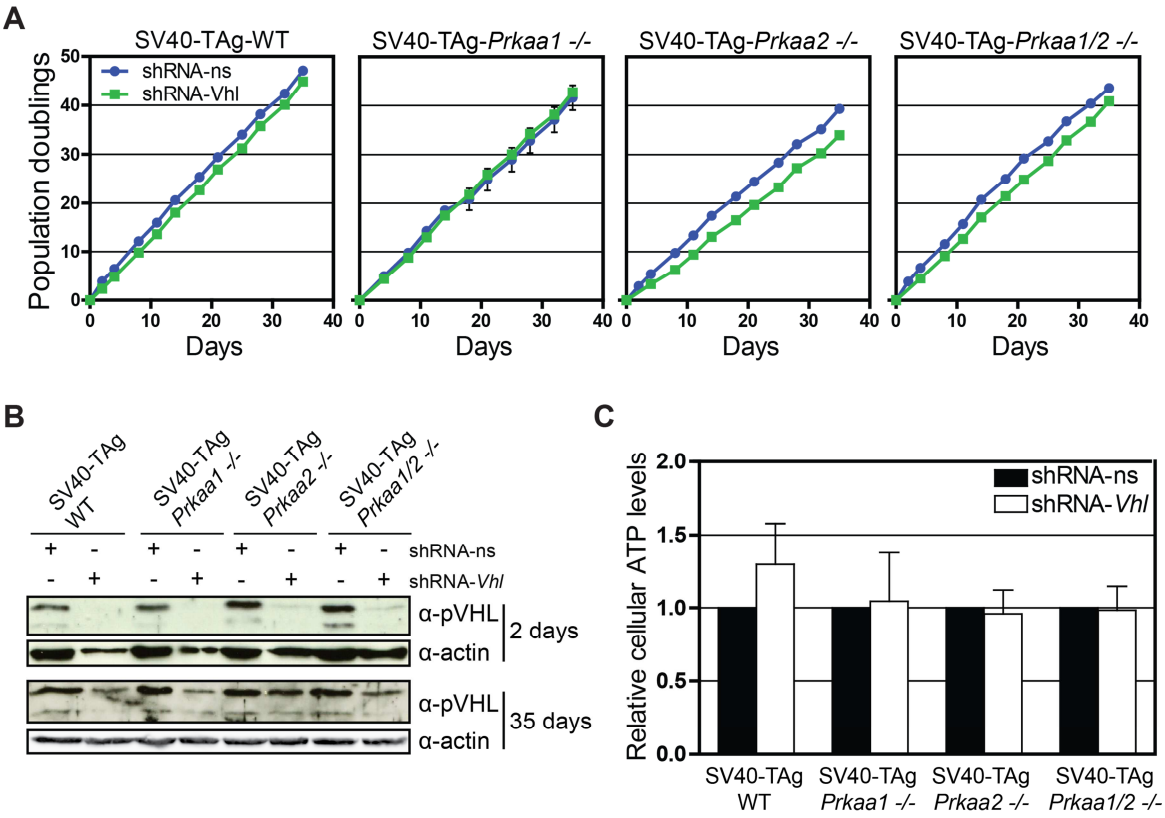

Figure 4.12: Knockdown of *Vhl* in AMPK negative cells is not enough for reduction of ATP levels.

A Proliferation assay of SV40-TAg WT, *Prkaa1 -/-*, *Prkaa2 -/-*, *Prkaa1/2 -/-* MEFs infected with lentiviruses expressing an empty pLKO.1 shRNA (shRNA-ns) or pLKO.1 shRNA directed against *Vhl* (shRNA-*Vhl*).

B Western blotting analysis of cells from (A) at indicated time points.

C Cellular ATP levels of cells from (A) 6 days after lentiviral infection.

To attempt to better address how the loss of AMPK affects *Vhl*-deficient cells, primary MEFs instead of SV40-T Antigen immortalised MEFs were used. *Vhl/Trp53* negative MEFs were infected with shRNAs to induce the knockdown of *Prkaa1*, which was reduced to about 25-50% of normal levels (Figure 4.13D). The knockdown of *Prkaa1* decreased the proliferation rate of control cells (Adeno-GFP treated) dramatically (Figure 4.13A) showing that AMPKα1 activity is necessary for the proliferation of wild-type cells. In *Vhl/Trp53* negative MEFs the knockdown of *Prkaa1* resulted in a growth disadvantage at the beginning of the proliferation curve, but the cells could at least partially recover over time (Figure 4.13A). The reduced ATP levels following *Vhl/Trp53* knockout were not further affected by the knockdown of *Prkaa1* (Figure 4.13E). The isoform of AMPKα that is most highly abundantly expressed in MEFs is AMPKα1 (Phoenix et al. 2012), (Figure 4.14A and Figure 4.13F). The knockdown of *Prkaa1* was not compensated by elevated levels of *Prkaa2* expression in control or in *Vhl/Trp53* negative MEFs (Figure 4.14B and Figure 4.13F). In summary these results point out that the loss of *Prkaa1* in combination with *Vhl/Trp53* deletion is not sufficient to enhance cellular proliferation, nor does it significantly compromise the ability of these cells to survive the metabolic alterations that are caused by loss of *Vhl*.

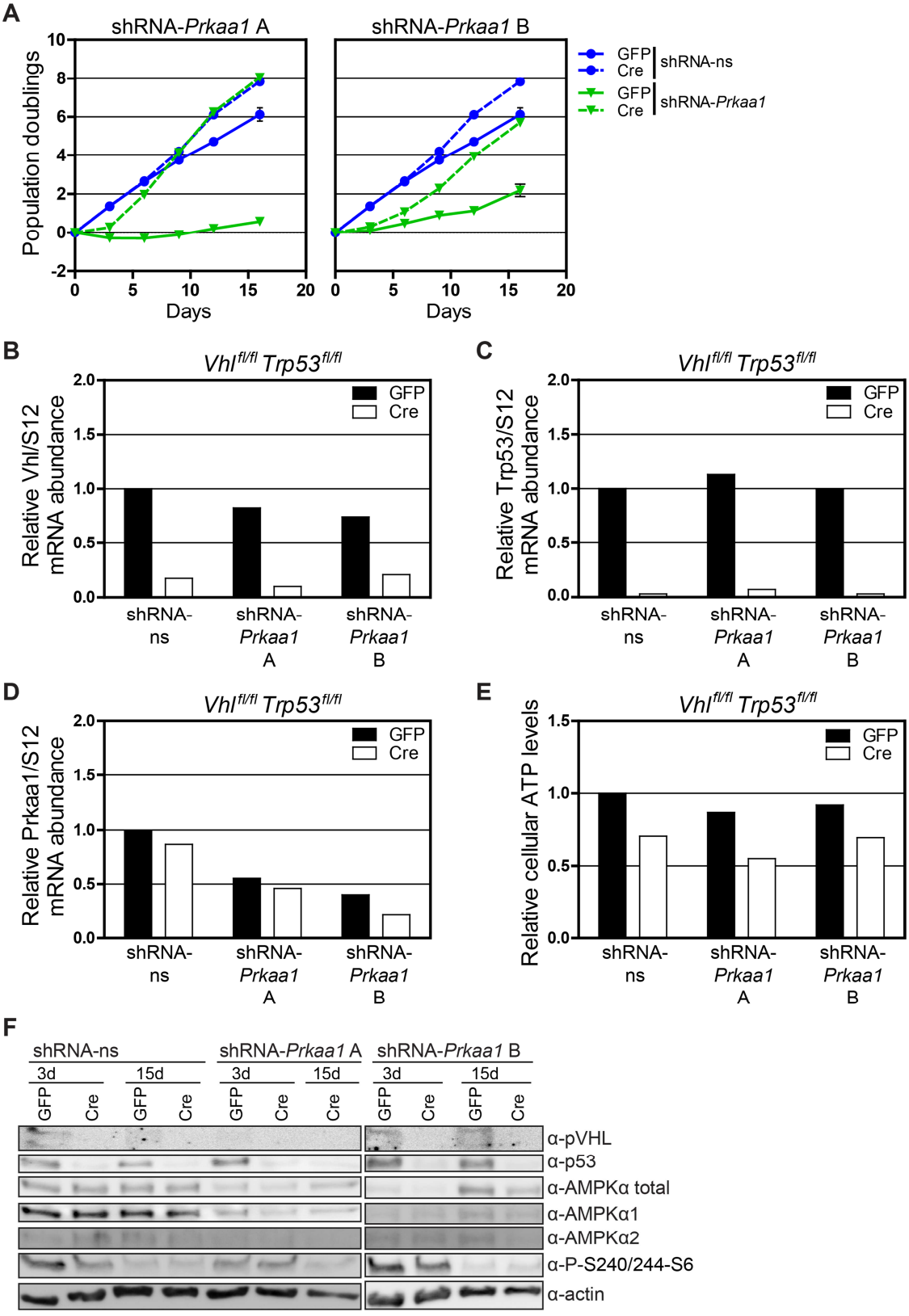

Figure 4.13: No pro-proliferative effect of *Prkaa1* loss on *Vhl/Trp53* deficient cells.

A Proliferation assay of *Vhl*$^{fl/fl}$ *Trp53*$^{fl/fl}$ MEFs infected with adenoviruses expressing GFP or Cre and lentiviruses expressing an empty pLKO.1 shRNA (shRNA-ns) or two different pLKO.1 shRNAs directed against *Prkaa1* (shRNA-*Prkaa1* A or B).

B-D Real-time quantitative PCR analysis of *Vhl* (B), *Trp53* (C) and *Prkaa1* (D) mRNA abundance normalized to *S12* mRNA abundance in cells from (A).

E Cellular ATP levels of cells from (A) 6 days after adenovirus infection.

F Western blotting analysis of cells from (A) at indicated time points.

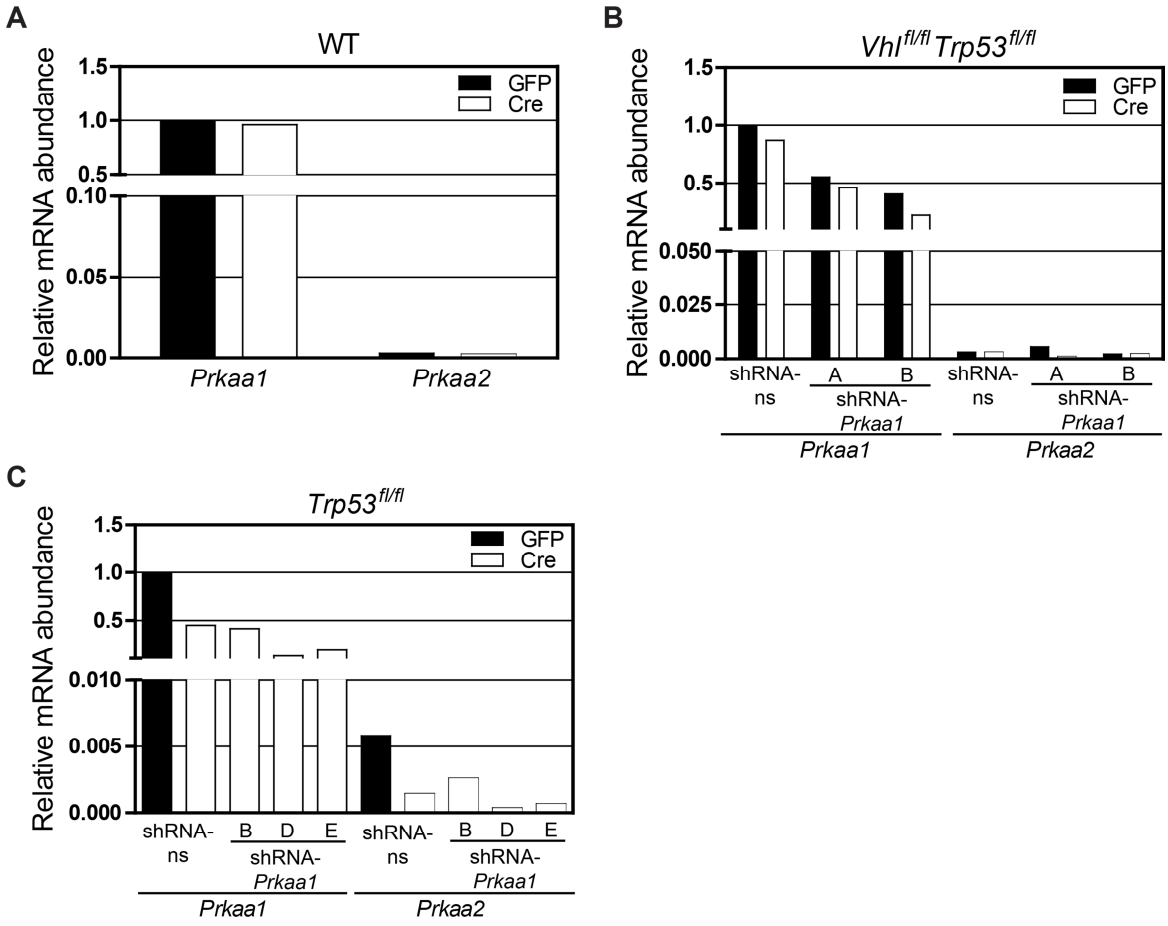

Figure 4.14: Knockdown of *Prkaa1* does not increase *Prkaa2* mRNA levels.

A Real-time quantitative PCR analysis of wild-type MEFs infected with adenoviruses expressing GFP or Cre. The measured mRNA abundance of *Prkaa1* and *Prkaa2* was normalized to *S12* mRNA abundance.

B, C Real-time quantitative PCR analysis of *Vhl*$^{fl/fl}$ *Trp53*$^{fl/fl}$ (B) and *Trp53*$^{fl/fl}$ (C) MEFs infected with GFP or Cre and lentiviruses expressing an empty pLKO.1 shRNA (shRNA-ns) or different pLKO.1 shRNAs directed against *Prkaa1* (shRNA-*Prkaa1* A-D). The mRNA abundance of *Prkaa1* and *Prkaa2* was normalized to *S12* mRNA abundance.

4.3 Discussion

Mouse embryonic fibroblasts as well as primary kidney cells undergo senescence when *Vhl* is deleted. Work described in this thesis contributed to the discovery that this effect occurs in a p53-dependent manner as in *Vhl*/*Trp53* negative cells the senescence phenotype is rescued and cells proliferate in an immortalised manner. Interestingly, cells deficient for *Vhl* proliferate slower than *Vhl* positive cells even when cell cycle regulators like p53 and pRb are mutated. These observations indicate that additional cellular responses to loss of *Vhl* may represent barriers to transformation of primary cells and perhaps might represent barriers to tumour formation in vivo (Albers et al. 2013). So far it is still unknown if and how metabolic alterations following loss of pVHL contribute to tumour formation and whether these alterations may represent transformational barriers

or alternatively whether they may enable cellular transformation. One aim of this thesis was to define the effects of loss of *Vhl* in MEFs on the metabolism of glucose and glutamine as a model for the initial genetic event in ccRCC progression, namely the mutation of *VHL* in an otherwise genetically normal cell. We investigated how this is mediated by the stabilisation of the Hif1α and Hif2α transcription factors.

In this thesis it could be shown that *Vhl* negative, as well as *Vhl/Trp53* deficient MEFs exhibited a Hif1α-dependent Warburg-like metabolic phenotype with elevated expression of glycolytic genes, a small increase in glucose uptake and metabolism to lactate but a large decrease in oxidative phosphorylation (Figure 4.1 and 4.2). Since the rate of glycolytic flux was not increased to an extent that would compensate for decreased ATP production by mitochondrial oxidation, these cells exhibited lowered levels of ATP. *Vhl* and *Vhl/Trp53* deficient MEFs both showed low ATP levels, indicating that this decrease is not simply a consequence of the senescence phenotype as *Vhl/Trp53* knockout cells escape senescence. The impaired ATP generation might be one contributing factor to the initiation of senescence in primary *Vhl* deficient MEFs and impaired proliferation in *Vhl/Trp53* negative MEFs since knockdown of *Hif1a* rescued ATP levels and rescued senescence and proliferation (Désirée Schönenberger, unpublished data). Several studies in different *VHL*-deficient ccRCC cancer cell lines revealed HIF1α and/or HIF2α-dependent regulation of glucose transport, aerobic glycolysis and mitochondrial respiration and showed that restoration of VHL increased cellular ATP levels, arguing that the MEF model accurately reflects at least some of the metabolic features of ccRCC cells (see also section 1.2.1) (Papandreou et al. 2006; Langbein et al. 2008; Chan et al. 2011). However, compared to the MEFs that we used which harbour exactly defined mutations, these ccRCC cell lines have a complex genetic background with additional mutations that emerged during tumour development. These mutations potentially brought further advantages that allowed these cells to deal with metabolic limitations imposed by constitutive HIFα activity and enabled them to form tumours. For example, in sporadic ccRCC, mutations could be detected leading to overexpressed C-MYC or activation of the PI3K-AKT-mTOR pathway, both of which control several cellular metabolic pathways (Sato et al. 2013). Thus, we speculate that additional mutations in *Vhl/Trp53* negative cells that affect cellular metabolism could lead to their transformation. Indeed, unpublished studies in our laboratory show that c-Myc overexpression in *Vhl/Trp53* deficient MEFs and primary kidney cells causes their transformation (Tomas Hejhal, unpublished observations). In this context, a very recent publication showed that FBP1 (fructose-1,6-bisphosphatase 1) is inhibited in almost 100% of analysed ccRCC tumour samples at the level of protein accumulation. FBP1 is the main enzyme of

gluconeogenesis, converting fructose-1,6-bisphosphate to fructose-6-phosphate, thus counteracting PFK1 (phosphofructokinase 1) (see also Figure 1.2). In addition, FBP1 was shown to antagonize glycolytic flux and can directly inhibit HIF by interacting with the HIF inhibitory domain and thereby inhibiting glucose metabolism (Li et al. 2014). We speculate that FBP1 may counteract HIF activity in *Vhl* and *Vhl/Trp53* deficient MEFs and therefore limit glycolytic flux, causing ATP deficiency. Selection for low levels of FBP1 may therefore overcome the potential barrier to tumour formation imposed by Hif1α. It would be very interesting to analyse glycolytic flux, oxidative phosphorylation, ATP production, proliferation and transformation in *Vhl/Trp53* null MEFs with knockdown of *Fbp1*.

Another interesting finding in *Vhl* and *Vhl/Trp53* MEFs was increased levels of activated AMPK (Figure 4.5). This kinase is the energy sensor of cells that is activated by stress situations and maintains the energy balance in cells in response to changes in the ratio of AMP/ATP (Hardie 2011). One function of AMPK is to antagonize the mTORC1 complex, a key regulator of cell growth and proliferation (Inoki et al. 2003; Gwinn et al. 2008). In cancer cell lines, AMPK may function as a negative regulator of aerobic glycolysis and cellular biosynthesis as the downregulation of its activity promoted the Warburg effect and AMPK activation suppressed HIF1α translation by inhibiting mTORC1 (Faubert et al. 2013). An attractive hypothesis that we investigated was that AMPK exhibits tumour suppressor functions in MEFs with a deletion of *Vhl/Trp53* which contributes to this mild Warburg effect and the proliferative deficiency. Indeed, in some experiments we could detect decreased phosphorylation levels of mTORC1 targets (Figure 4.9) suggesting that AMPK might regulate mTORC1 in response to energy stress following *Vhl* deletion (Inoki et al. 2003; Shaw et al. 2004; Liu et al. 2006). Unfortunately, these experimental findings proved difficult to reproduce, potentially because they occur only in a restricted time window after gene deletion or because other factors that we were not able to control in our experimental setup also influence AMPK activity, for example increased lactate concentrations in the medium or depletion of amino acids.

We wondered whether Hif1α-mediated metabolic changes could cause energy stress, AMPK activation and downregulation of the mTORC1 pathway, leading to lowered rates of proliferation. Thus, a selection against AMPK and/or mTORC1 may represent the additional step for tumour initiation and progression in *Vhl/Trp53* deficient cells. As already mentioned the PI3K-AKT-mTORC1 pathway is mutationally activated in a subset of sporadic ccRCC (Sato et al. 2013). Reduced AMPK activity or reduced expression of *Prkaa2*, the gene encoding AMPK, was found in human breast, ovarian and gastric

cancer (Hallstrom et al. 2008; Hadad et al. 2009; Kim et al. 2012). In sporadic ccRCC, decreased AMPK activity has been proposed to be involved in a metabolic shift that correlates with disease aggressiveness (TCGA 2013). Furthermore, for LKB1, the kinase upstream of AMPK, a tumour suppressor function in sporadic cases of ccRCC was predicted whereas its underexpression seems to be important for cancer progression, at least in cultured ccRCC cells (Duivenvoorden et al. 2013). Thus, there could be several possibilities by which AMPK function could be suppressed during the progression of ccRCC and the resulting cell signalling and metabolic changes may provide a growth advantage for cells. Different experiments with knockdowns of *Tsc1*, *Tsc2*, *Stk11* or *Prkaa1* in *Vhl/Trp53* deficient MEFs could not further confirm this hypothesis as none of these knockdowns promoted enhanced proliferation or transformation of these cells (Figure 4.10A, 4.11A, 4.11E and 4.13A). Although all knockdown experiments showed increased phosphorylation levels of mTORC1 targets (Figure 4.10C, 4.11B, 4.11F and 4.13F), it seems that other pathways which are affected by the loss of *Vhl* may have a stronger restriction on accelerated proliferation and transformation than the loss of AMPK and the resulting induction of mTORC1. Another interesting aspect in those experiments was that none of the knockdowns rescued ATP levels (Figure 4.10E, 4.13E). In conclusion, it seems that on top of *Vhl* and *Trp53* mutation and an activation of the mTORC1 pathway additional mutations are required for tumour initiation.

5 Glutamine metabolism in *Vhl*-deficient cells

5.1 Introduction and Aims

Highly proliferating cells as well as cancer cells have special requirements: maintenance of their energy status through rapid ATP generation and of cellular redox status as well as an increase of macromolecule biosynthesis (Cairns et al. 2011). Glutamine is, besides glucose, the main bioenergetic substrate, providing carbon and nitrogen for cell growth and viability. Many cancer cells are critically dependent on glutamine for proliferation and survival (Wise and Thompson 2010). Hypoxic or *VHL*-deficient cancer cells almost exclusively use reductive carboxylation to metabolise glutamine-derived α-ketoglutarate to produce citrate for lipid biosynthesis (Metallo et al. 2011). The first step in glutaminolysis is the metabolism of glutamine to glutamate which is conducted by glutaminases. So far, four different isoforms have been identified in mammalian cells. They are encoded by two different genes, *GLS1* with its two splicing forms *KGA* and *GAC*, as well as *GLS2* with the two transcript variants *GAB* and *LGA*. Quite often only one of the four glutaminases is found in a specific organ or cancer cell line but also a co-expression is possible (Aledo et al. 2000). In tumourigenesis the glutaminases have been shown to have contrasting roles. In contrast to GLS2, c-Myc regulated GLS1 promotes tumour progression when overexpressed (Gao et al. 2009; Hu et al. 2010). The loss of *GLS1* prevents accelerated cell growth whereas decreased levels of *GLS2*, a p53 target gene, could be found in hepatocellular carcinomas (Lobo et al. 2000; Liu et al. 2014).

Vhl/Trp53 negative cells show a similar metabolic phenotype to *Vhl* deficient cells in terms of a shift from oxidative phosphorylation towards glycolysis and decreased ATP levels. Interestingly however, these cells have overcome *Vhl*-induced senescence. We wondered if the senescence-rescued *Vhl/Trp53* null cells might rely more on glutamine for anapleurosis to fuel their demands for energy and metabolic intermediates since glucose preferentially is converted to lactate and therefore cannot be metabolised in the oxidative TCA cycle.

5.2 Results

5.2.1 Hif1α-dependent regulation of glutaminase

In a first step to investigate this idea, glutamine uptake was analysed by measuring the incorporation of radioactive labelled glutamine ($^{14}C_5$) in wild-type, $Vhl^{fl/fl}$, $Vhl^{fl/fl}$ $Trp53^{fl/fl}$ and

Trp53$^{fl/fl}$ MEFs treated with Adeno-GFP or Adeno-Cre. However, no differences in the rate of glutamine uptake could be observed (Figure 5.1).

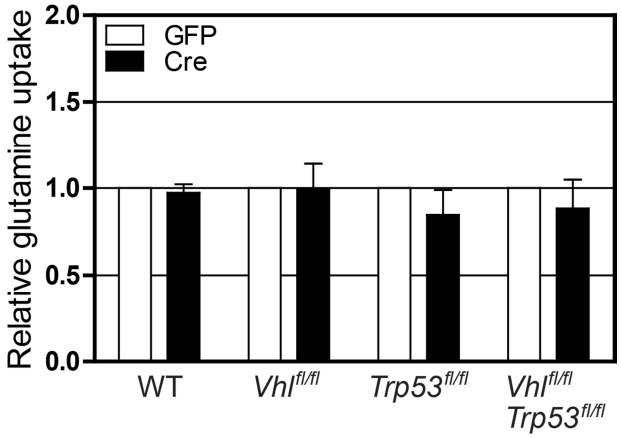

Figure 5.1: *Vhl* deficiency does not affect glutamine uptake.
Glutamine uptake was measured by incorporation of $^{14}C_5$-labeled glutamine in wild-type, *Vhl*$^{fl/fl}$, *Vhl*$^{fl/fl}$ *Trp53*$^{fl/fl}$ and *Trp53*$^{fl/fl}$ MEFs infected with adenoviruses expressing GFP or Cre.

In a parallel experimental approach, genes were examined that are directly involved in glutamine uptake (*Asct2)*, conversion (*Gls1*, *Gls2*, *Glud1*, *Got1*, *Got2*) and the TCA cycle (*Idh1*, *Idh2*, *Aco1*, *Aco2*) (see also Figure 1.2). No changes could be observed in the transcript levels of *Asct2*, *Gls1*, *Glud1*, *Got1*, *Got2*, *Idh1*, *Idh2*, *Aco1* or *Aco2* neither in *Vhl* nor in *Vhl/Trp53* depleted MEFs (Figure 5.2A-D). However, the levels of *Gls2* were significantly increased in *Vhl* and *Vhl/Trp53* knockout MEFs (Figure 5.3A, B) and primary kidney cells (Figure 5.4A, B). Cells harbour four different forms of the enzyme glutaminase. To test which forms are expressed in primary MEFs and kidney cells primers specific for the different forms were tested. The used primer pair for Gls1 could detect both forms, *Kga* and *Gac*. Interestingly, the Gls2 isozyme *Lga* could not be detected in MEFs or in kidney cells (data not shown). The primer pairs *Gls2 A* and *Gls2 B* specifically recognised *Gab*, *Gls2 C* and *Gls2 D* were able to detect *Gab* and *Lga*. As the changes in the expression levels with all four *Gls2* primer pairs were similar, this confirmed that *Lga* was not expressed in primary MEFs and kidney cells (Figure 5.3A, B and 5.4A, B). In general in both cell types the transcript levels of *Gls2* were lower compared to *Gls1*. Even with induced *Gls2* in *Vhl* negative cells these levels were still lower than the levels of *Gls1*.

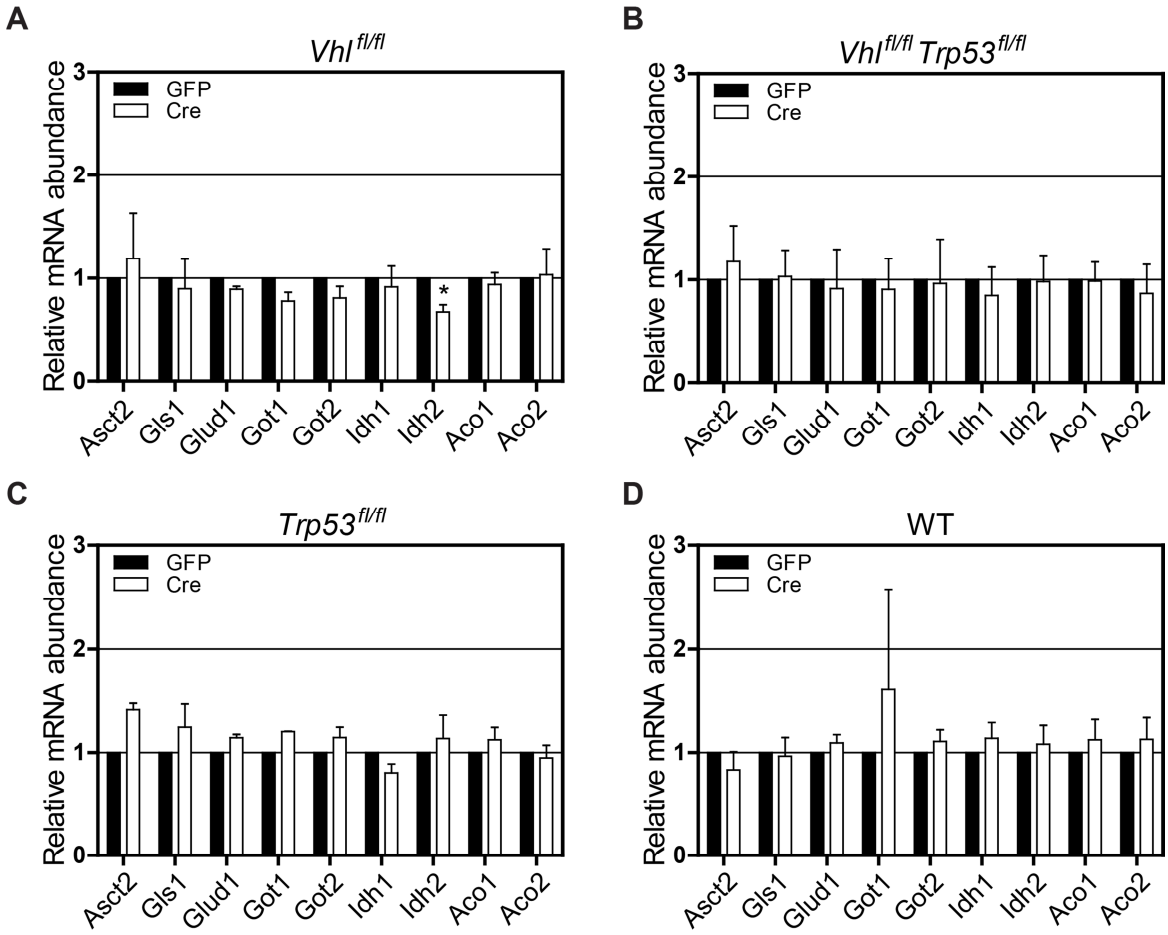

Figure 5.2: No induction of genes involved in reductive TCA cycle in *Vhl* or *Vhl/Trp53* deficient MEFs.

A-D Real-time quantitative PCR analysis of different genes that are involved in glutaminolysis in *Vhl*$^{fl/fl}$ (A), *Vhl*$^{fl/fl}$ *Trp53*$^{fl/fl}$ (B), *Trp53*$^{fl/fl}$ (C) and wild-type (D) MEFs infected with adenoviruses expressing GFP or Cre (Student´s t-test, *$p < 0.05$).

So far very little is known about the regulation of *Gls2*. Two independent studies revealed that p53 associates with the *GLS2* promoter and thus increases its expression in stressed and non-stressed conditions (Hu et al. 2010; Suzuki et al. 2010). In primary MEFs the levels of *Gls2* were not reduced by the loss of *Trp53* (Figure 5.3C). Moreover, since *Vhl/Trp53* double knockout MEFs and primary kidney epithelial cells exhibit high levels of *Gls2*, we conclude that the induction of *Gls2* following *Vhl* deletion is independent of p53. Since *Gls2* was upregulated in *Vhl* and *Vhl/Trp53* deleted cells, with stabilised Hif1α transcription factors (Albers et al. 2013), *Vhl*$^{fl/fl}$ *Hif1a*$^{fl/fl}$ and *Vhl*$^{fl/fl}$ *Hif2a*$^{fl/fl}$ cells were analysed. The deletion of *Hif1a* rescued the increased expression levels of *Gls2* in a *Vhl* negative background (Figure 5.3E, 5.4D), whereas the loss of *Hif2a* in *Vhl* negative cells showed no effect (Figure 5.3F). This could be confirmed with the triple knockout MEFs *Vhl*$^{fl/fl}$ *Hif1a*$^{fl/fl}$ *Hif2a*$^{fl/fl}$ with rescued transcript levels of *Gls2* (Figure 5.3G). The results indicate that a Hif1α-dependent mechanism is responsible for the regulation of *Gls2* transcription.

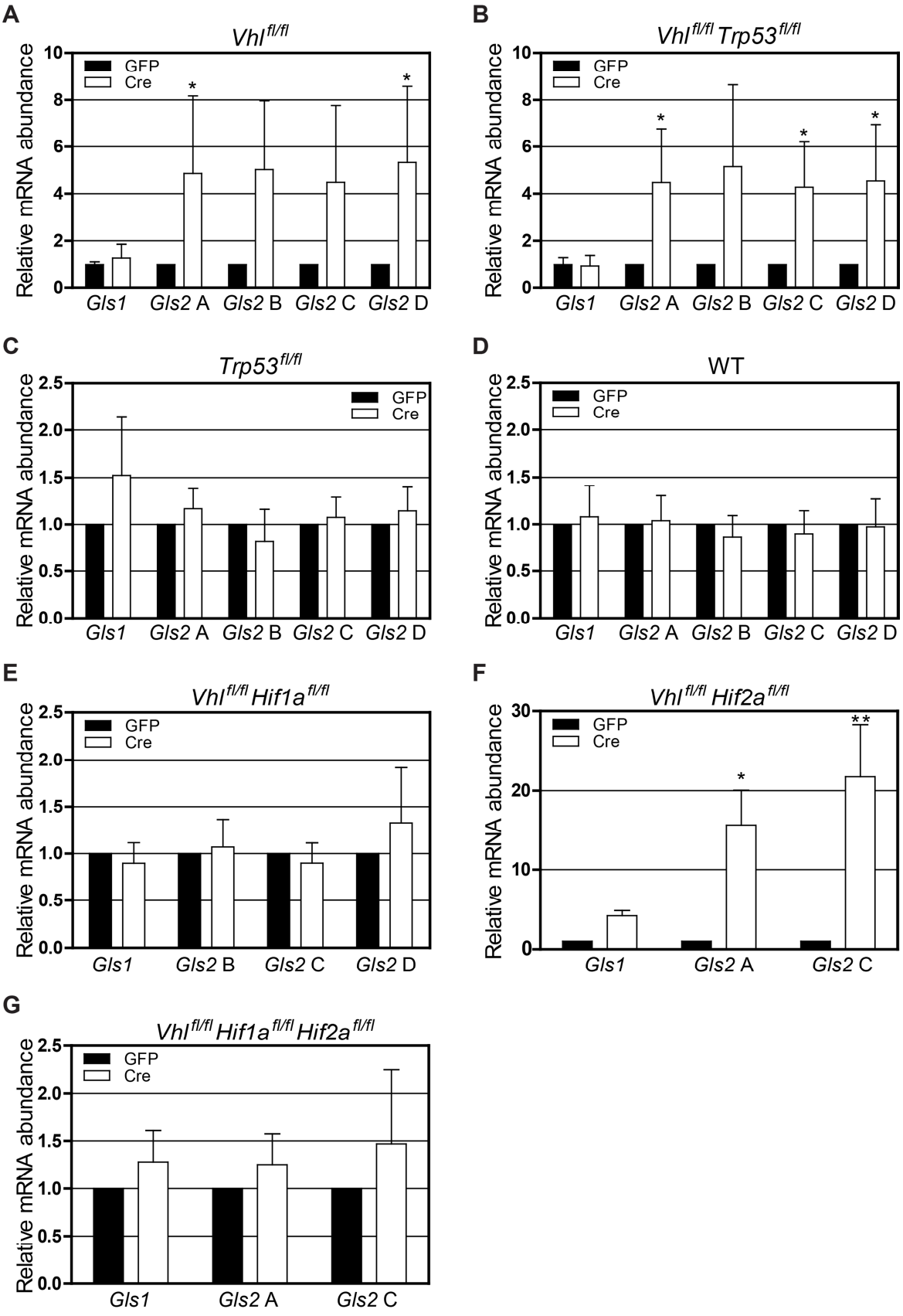

Figure 5.3: Upregulation of *Gls2* mRNA levels in *Vhl* and *Vhl/Trp53* null MEFs.

A-G Real-time quantitative PCR analysis of *Gls1* and *Gls2* mRNA abundance normalized to *S12* mRNA abundance in $Vhl^{fl/fl}$ (A), $Vhl^{fl/fl}$ $Trp53^{fl/fl}$ (B), $Trp53^{fl/fl}$ (C), wild-type (D), $Vhl^{fl/fl}$ $Hif1a^{fl/fl}$ (E), $Vhl^{fl/fl}$ $Hif2a^{fl/fl}$ (F) and $Vhl^{fl/fl}$ $Hif1a^{fl/fl}$ $Hif2a^{fl/fl}$ (G) MEFs infected with adenoviruses expressing GFP or Cre. For the detection of *Gls2* mRNA four different primer pairs were used labelled with *Gls2* A-D (Student´s t-test, *$p < 0.05$, **$p < 0.01$).

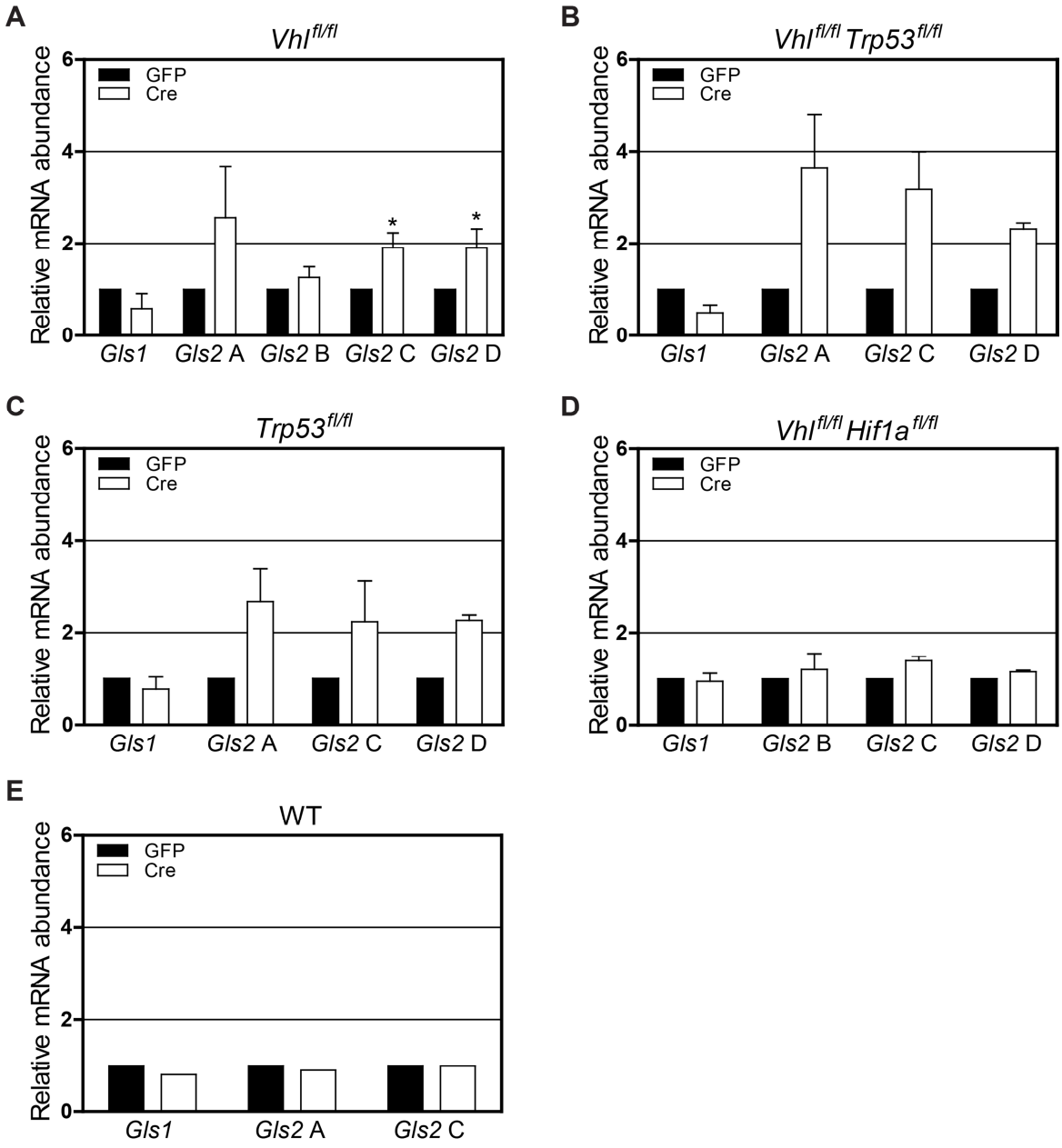

Figure 5.4: Elevated *Gls2* transcript levels in *Vhl* and *Vhl/Trp53* deficient kidney cells.

A-E Real-time quantitative PCR analysis of *Gls1* and *Gls2* mRNA abundance normalized to *S12* mRNA abundance in $Vhl^{fl/fl}$ (A), $Vhl^{fl/fl}$ $Trp53^{fl/fl}$ (B), $Trp53^{fl/fl}$ (C), $Vhl^{fl/fl}$ $Hif1a^{fl/fl}$ (D), and wild-type (E) kidney cells infected with adenoviruses expressing GFP or Cre. For *Gls2* four different primer pairs were used labelled with *Gls2* A-D (Student´s t-test, $*p < 0.05$).

To further investigate the role of Hif1α in the modulation of *Gls2* we treated cells for several hours with hypoxia as low oxygen levels stabilise the Hifα transcription factors. The treatment of cells with 1% oxygen for four, six or 30 hours had no effect on *Gls2* levels in wild-type cells (Figure 5.5A) and only in *Vhl* null cells a further induction could be observed after long-term hypoxia (Figure 5.5B-D). Hypoxia treatment had no effect on *Gls1* levels in any of the cell types (Figure 5.6A-D). Taking these results together, the loss of *Vhl* causes an increase of the *Gls2* transcript, which is Hif1α-dependent but not

hypoxia inducible. Unfortunately, it was not possible to confirm these observations at the protein expression level as several commercially available anti-Gls2 antibodies did not give any specific bands in western blotting experiments.

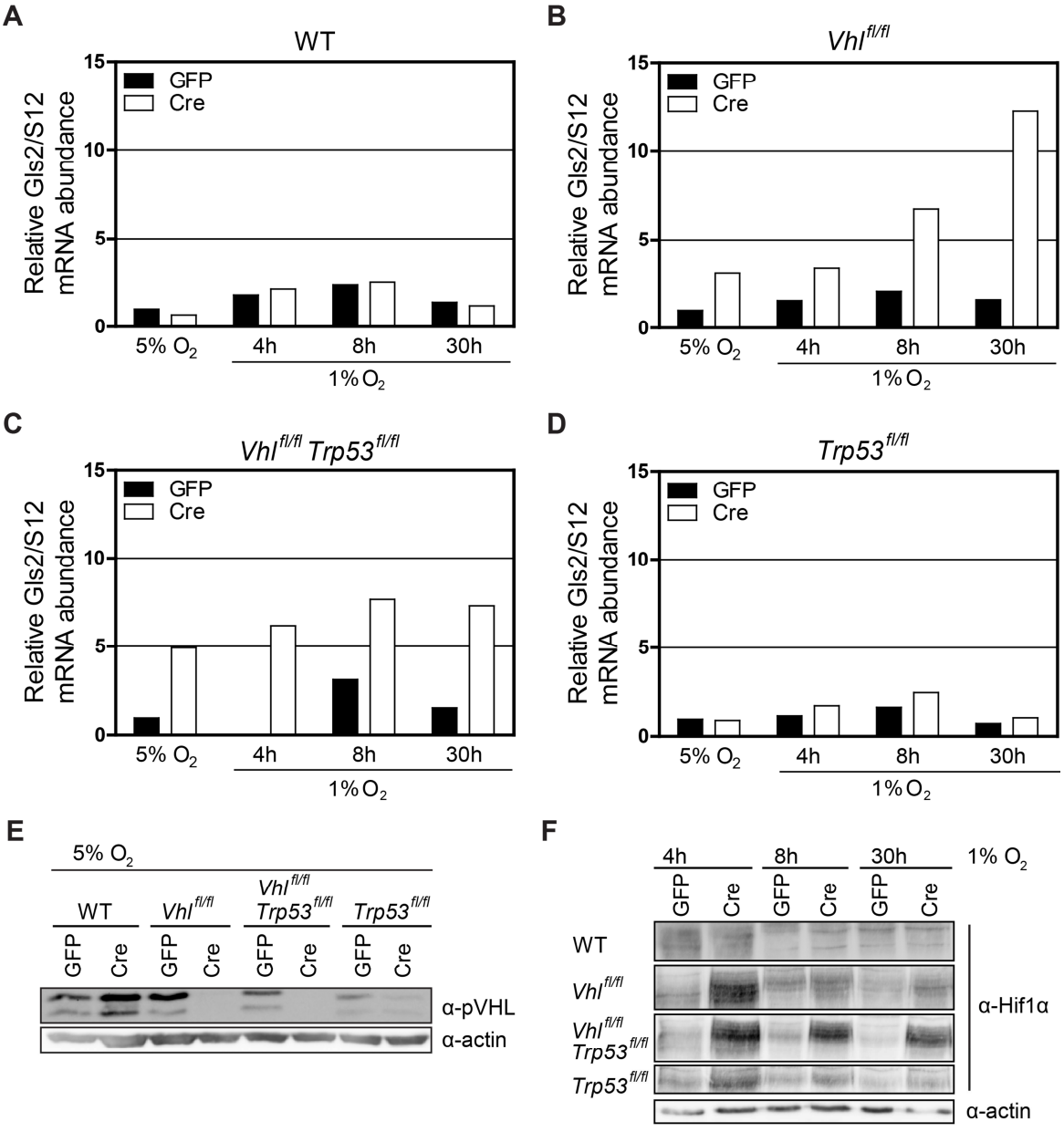

Figure 5.5: *Gls2* transcript levels are not hypoxia-inducible.

A-D Real-time quantitative PCR analysis of *Gls2* mRNA abundance normalized to *S12* mRNA abundance in wild-type (A), *Vhl*$^{fl/fl}$ (B), *Vhl*$^{fl/fl}$ *Trp53*$^{fl/fl}$ (C) and *Trp53*$^{fl/fl}$ (D) MEFs infected with adenoviruses expressing GFP or Cre in 5% O_2 or 1% O_2 for 4h, 8h or 30h.

E, F Western blotting analysis of cells from (A-D) with indicated O_2 levels.

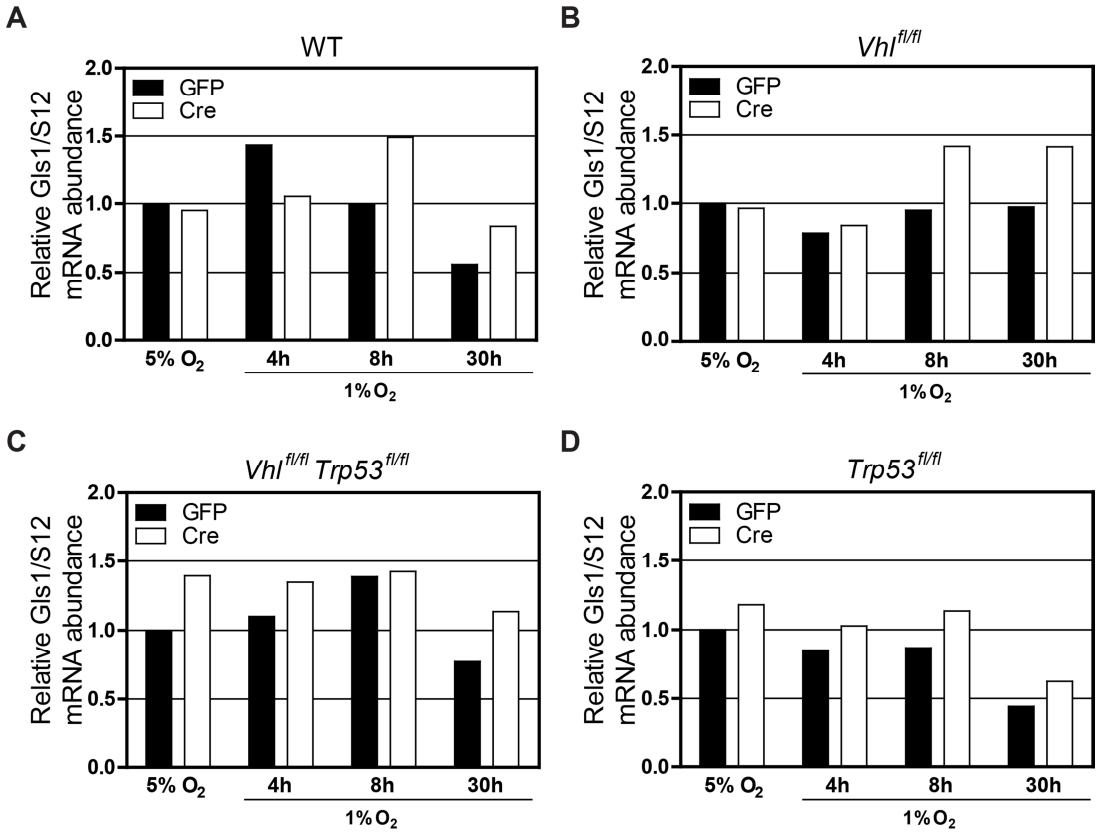

Figure 5.6: Hypoxia has no effect on *Gls1* transcript levels.

A-D Real-time quantitative PCR analysis of *Gls1* mRNA abundance normalized to *S12* mRNA abundance in wild-type (A), *Vhl*$^{fl/fl}$ (B), *Vhl*$^{fl/fl}$ *Trp53*$^{fl/fl}$ (C) and *Trp53*$^{fl/fl}$ (D) MEFs infected with adenoviruses expressing GFP or Cre in 5% O_2 or 1% O_2 for 4h, 8h or 30h.

5.2.2 Loss of *Gls2* provides a growth advantage for cells

To further investigate the role of the Gls1 and Gls2 glutaminases in *Vhl* depleted cells, knockdown experiments using shRNAs directed against *Gls1* and *Gls2* were performed in *Vhl/Trp53* null MEFs. The knockdown of *Gls1* had no effect on the proliferation of *Vhl/Trp53* negative cells but control cells (Adeno-GFP treated) grew marginally better than cells infected with non-silencing shRNA (Figure 5.7A). Interestingly, silencing of *Gls2* caused a minor growth advantage for *Vhl/Trp53* deficient MEFs as well as for control cells (Adeno-GFP treated) (Figure 5.7B). In immortalisation assays the *Vhl/Trp53* deleted MEFs with a *Gls2* knockdown also formed more colonies (Figure 5.7F) and these cells were able to grow in an anchorage independent manner (Figure 5.7G). As an additional control, we investigated whether the knockdown of *Gls2* could be compensated by an increased expression of *Gls1* and *vice versa*. Real time quantitative PCR analysis revealed that no compensatory events took place (Figure 5.7D, E). These preliminary experiments suggest that Gls2 activation prevents the efficient transformation of *Vhl/Trp53* double mutant cells. More experiments are now necessary to further investigate the role of *Gls2* and its effects on the transformation of *Vhl* negative cells.

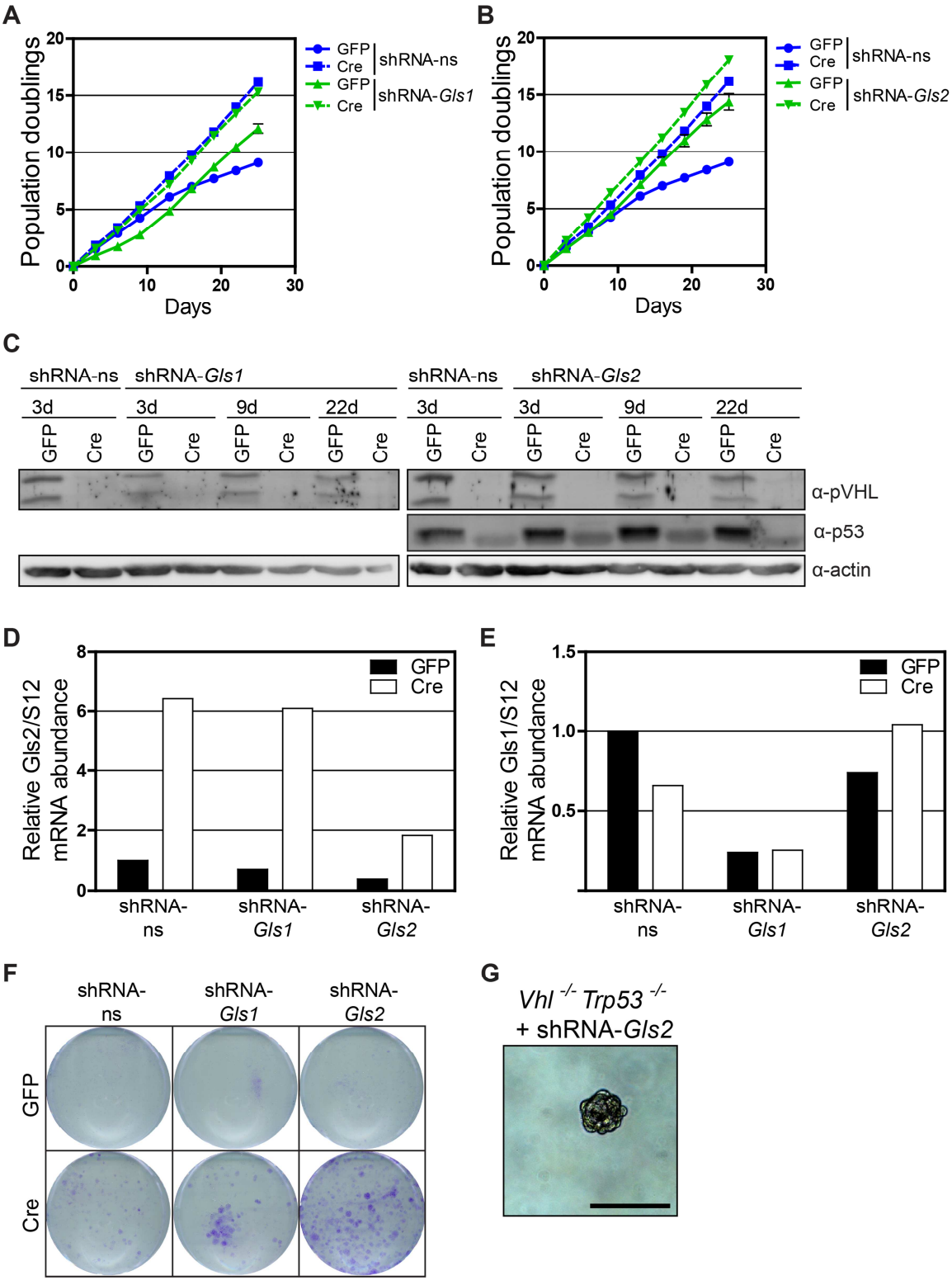

Figure 5.7: Anchorage independent growth after deletion of *Gls2* in *Vhl/Trp53* negative MEFs.

A, B Proliferation assay of *Vhl*$^{fl/fl}$ *Trp53*$^{fl/fl}$ MEFs infected with adenoviruses expressing GFP or Cre and lentiviruses expressing an empty pLKO.1 shRNA (shRNA-ns) or pLKO.1 shRNA directed against *Gls1* (A) or *Gls2* (B) (shRNA-*Gls1* or *Gls2*).

C Western blotting analysis of cells from (A) and (B) at indicated time points.

D, E Real-time quantitative PCR analysis of *Gls1* (D) and *Gls2* (E) mRNA abundance normalized to *S12* mRNA abundance in cells from (A) and (B).

F Immortalisation assay of cells from (A) and (B).

G Anchorage independent growth of cells from (B). Scale bar 50 µm.

5.3 Discussion

In proliferating tumour cells glutamine is an essential nutrient, participating in oxidative stress responses, in the maintenance of the cellular energy status and in complementing macromolecular biosynthesis by providing a source of carbon and nitrogen (DeBerardinis and Cheng 2010). Interestingly, many cancer cells are critically dependent on glutamine for proliferation and survival (Wise and Thompson 2010). Proliferating cells in normoxia use glucose-derived acetyl-CoA or oxidative metabolism of glutamine to support citrate production, whereas hypoxic or *VHL*-deficient cancer cells almost exclusively use reductive carboxylation to metabolise glutamine-derived α-ketoglutarate to produce citrate for lipid biosynthesis (Metallo et al. 2011; Wise et al. 2011; Gameiro et al. 2013). This pathway is dependent on HIF1 activity and results in the reduction of the activity of α-KGDH (α-ketoglutarate dehydrogenase) which normally acts to convert α-ketoglutarate to succinyl-CoA, supplying carbons for anapleurotic glutamine metabolism via the TCA cycle. Shutting down this anapleurotic oxidative glutamine metabolism is proposed to enhance reductive glutamine metabolism (Sun and Denko 2014). We tried to answer the question if the senescence-rescued *Vhl/Trp53* null cells might use carbons derived from glutamine to fuel their demands for energy and metabolic intermediates. The mRNA levels of genes that are responsible for glutaminolysis and reductive carboxylation, including *Asct2*, *Gls1*, *Glud1*, *Got1*, *Got2*, *Idh1*, *Idh2*, *Aco1* or *Aco2*, were not changed in MEFs deficient for *Vhl* and *Vhl/Trp53* (Figure 5.2), suggesting that they are not responsive to stabilisation of Hifα proteins. A similar result was shown in UMRC2 cells, a kidney carcinoma cell line negative for VHL, which uses reductive carboxylation of glutamine, where these genes were also not more highly expressed than in a VHL rescued cell line (Gameiro et al. 2013). However, it cannot be ruled out that Hifα protein stabilisation might still have an effect on the activity of these enzymes possibly via post-transcriptional modifications or by effecting other metabolic changes that alter the availability of cofactors. Metabolomic analysis of cells negative for *Vhl* and *Vhl/Trp53* did not show any accumulation of glutaminolytic metabolites (Figure 3.4). To find convincing answers to the question if *Vhl/Trp53* negative cells use reductive carboxylation, metabolic flux analysis would be necessary to fully trace the metabolism of glutamine. Also, to exactly determine the intracellular pathways of glucose metabolism this would be a helpful tool. For these experiments, cells would be starved for a short time period for glucose or glutamine before radioactive labelled glucose or glutamine is introduced to the cells. Dependent on the way glucose or glutamine are metabolised in the cell different metabolites accumulate. These radioactive labelled metabolites can then be determined by GC-MS. For example, with the tracing of labelled glucose we could determine if

glucose is more metabolised in the pentose phosphate pathway or is preferentially metabolised directly via glycolysis to lactate.

An interesting finding in MEFs and kidney cells deficient for *Vhl* and *Vhl/Trp53* was that *Gls2* transcript levels were elevated in a Hif1α-dependent manner (Figures 5.3 and 5.4). We could not detect a consensus hypoxia-response element (HRE) in the promoter region of *Gls2*, suggesting that *Gls2* is not a direct transcriptional target of Hif1α. The levels of *Gls2* were also not hypoxia inducible (Figure 5.5) suggesting that other mechanisms caused by the loss of *Vhl* might be important. *Gls2* is expressed due to p53 activation in MEFs and human colon, breast and lung cancer cell lines. Also the p53 family members p63 and p73 regulate *Gls2* expression in keratinocyte differentiation or during neuronal differentiation, respectively (Hu et al. 2010; Suzuki et al. 2010; Giacobbe et al. 2013; Velletri et al. 2013). Upon p53 activation, Gls2 contributes to reduced ROS levels and enhanced oxygen consumption, mitochondrial respiration and ATP generation (Hu et al. 2010; Suzuki et al. 2010). In the context of *Vhl*-deficiency, p53 has no influence on *Gls2* levels as p53 is not activated in those cells (Figure 4.5) and *Vhl/Trp53* negative cells still show elevated *Gls2* levels (Figure 5.3B and 5.4B).

As the upregulation is seen in *Vhl* negative cells and in the senescence-rescued *Vhl/Trp53* deficient cells, which still proliferate less than cells that lost *Trp53* alone, we speculated that Gls2 might negatively influence proliferation. Preliminary knockdown experiments of *Gls2* in *Vhl/Trp53* deficient MEFs suggest that this hypothesis might be correct as these cells proliferated better than *Vhl/Trp53* negative cells alone and they could grow in an anchorage independent manner (Figure 5.7). Further experiments using multiple independent shRNAs targeting *Gls2* are now underway to further support this unexpected finding that elevated *Gls2* expression may exert a tumour suppressor-like activity in *Vhl* mutant cells. It would be interesting to investigate whether *Vhl/Trp53* negative cells with a knockdown of *Gls2* could grow as xenografts. Consistent with our preliminary findings, different studies have predicted a potential role for GLS2 in tumour suppression. In hepatocellular carcinoma and many brain tumours the levels of *GLS2* were decreased or lost and re-expression reduced or inhibited tumour cell proliferation (Szeliga et al. 2009; Hu et al. 2010; Suzuki et al. 2010).

Cells with stabilised Hif1α (hypoxic or VHL-deficient) use glutamine-dependent reductive carboxylation to support citrate and lipid biosynthesis (Metallo et al. 2011). The kinetic properties of the different glutaminases are diverse. GLS2 shows, in contrast to GLS1, no inhibition by glutamate, the product of its enzymatic reaction (Curthoys and Watford

1995). Thus, it might be speculated that an increase in *GLS2* expression might allow higher levels of glutaminolysis, which could be needed for reductive carboxylation. As HIF promotes reductive glutamine metabolism a potential regulatory mechanism between Hif1α and Gls2 would be conceivable. Further analyses are necessary to investigate the mechanism of Hif1α-dependent regulation of *Gls2* and the functional implications of the change in expression of this enzyme.

To date, no research was conducted on *GLS2* expression or function in kidney tumours or renal cancer cell lines. Aledo and colleagues could not detect *GLS2* levels in human kidneys (Aledo et al. 2000). One possibility therefore could be that in unstressed conditions *GLS2* expression is extremely low and an increase of *GLS2* levels represents a mechanism that follows *VHL* mutation and suppresses early tumour development that needs to be overcome for further tumour progression. In contrast, in diverse mouse genetic backgrounds we found that mRNA levels of *Gls2* were detectable in the kidney at levels similar to levels seen in MEFs (data not shown). It will be now interesting to investigate if there is a role for Gls2 in tumour prevention in renal cancer by investigating the dependency of *GLS2* expression in *VHL* deficient and *VHL* rescued ccRCC cell lines on HIF1α and HIF2α. Another question that has to be answered is whether early lesions in mouse and human kidneys exhibit elevated Gls2/GLS2 protein levels and whether *GLS2* expression might be reduced or lost in a subset of human ccRCC.

6 Cooperation of loss of *Vhl* and *Rb1* in tumour initiation

6.1 Introduction and Aims

An important tumour suppressor that is involved in cell cycle and senescence regulation is the retinoblastoma protein. During cell cycle pRB is phosphorylated and inactivated by cyclin/Cdk complexes. Thereby, E2F proteins are released from pRB and can function as transcription regulators. The cyclin/Cdk complexes are in turn regulated by CDK inhibitors such as $p21^{Cip}$ and $p27^{Kip}$. These two proteins exhibit elevated levels upon deletion of *Vhl* in transformed MEFs (Mack et al. 2005). pRb also has been implicated in the regulation of senescence following loss of *Vhl* in primary MEFs (Young et al. 2008). Loss of function mutation of *RB1* is a common event in the development of many tumour types. In a sub-fraction of human ccRCC, genetic alterations of the *RB1* gene have been detected (Ishikawa et al. 1991; Shuin et al. 1995; Lai et al. 1997). Recent studies in sporadic ccRCC revealed multiple alterations in components of senescence and cell cycle machinery pathways including RB1 and its direct target E2F3 (Sato et al. 2013).

Our aim was to generate an inducible kidney epithelial cell-specific combined deletion of *Vhl* and *Rb1* to study potential cooperative effects of loss of function of these genes on ccRCC development. Furthermore, primary cell culture studies with cells derived from $Vhl^{fl/fl}Rb1^{fl/fl}$ mice were utilised to examine the role of *Rb1* deletion in a *Vhl* negative background.

6.2 Results

6.2.1 Deletion of *Rb1* rescues *Vhl* induced senescence and ATP deficiency in mouse embryonic fibroblasts

For *ex vivo* studies we generated primary mouse embryonic fibroblast from the mice described in 6.2.2. Since pRb seems to be important for the regulation of cell cycle and senescence pathways, we tested whether the loss of protein expression is beneficial for *Vhl* deficient cells. The growth disadvantage of *Vhl* null cells was partially rescued due to combined deletion of *Vhl* and *Rb1* but these cells proliferated less than *Rb1* knockout cells alone (Figure 6.1A), a similar phenotype to that observed in *Vhl/Trp53* double mutant cells. Both, *Vhl/Rb1* and *Rb1* negative cells were immortalised (Figure 6.1E) but only *Vhl/Rb1* deficient MEFs were able to grow in an anchorage independent manner (Figure 6.1C). Cells deficient for *Vhl* undergo senescence and activate a Warburg-like metabolic phenotype with shifted glucose utilisation and decreased ATP levels.

Senescence-rescued *Vhl/Trp53* negative cells still exhibit reduced ATP levels (Figure 4.2F). The loss of *Vhl* also gives rise to elevated glycolytic genes and a shift form oxidative phosphorylation to glycolysis (Figure 4.1A, B). Interestingly, the combined loss of *Vhl* and *Rb1* restored the ATP levels in primary MEFs (Figure 6.1D). However, glycolytic genes like *Glut1* and *Pfkfb3* were still upregulated (Figure 6.2B). Further experiments are now required to understand how these metabolic changes arise and what their influence is on cell transformation. Comparison of *Vhl/Trp53* and *Vhl/Rb1* negative cells reveals that senescence induced by loss of *Vhl* is rescued in both, and both exhibited elevated glycolytic genes, yet only *Vhl/Rb1* deficient MEFs display rescued ATP levels and were able to grow anchorage independently.

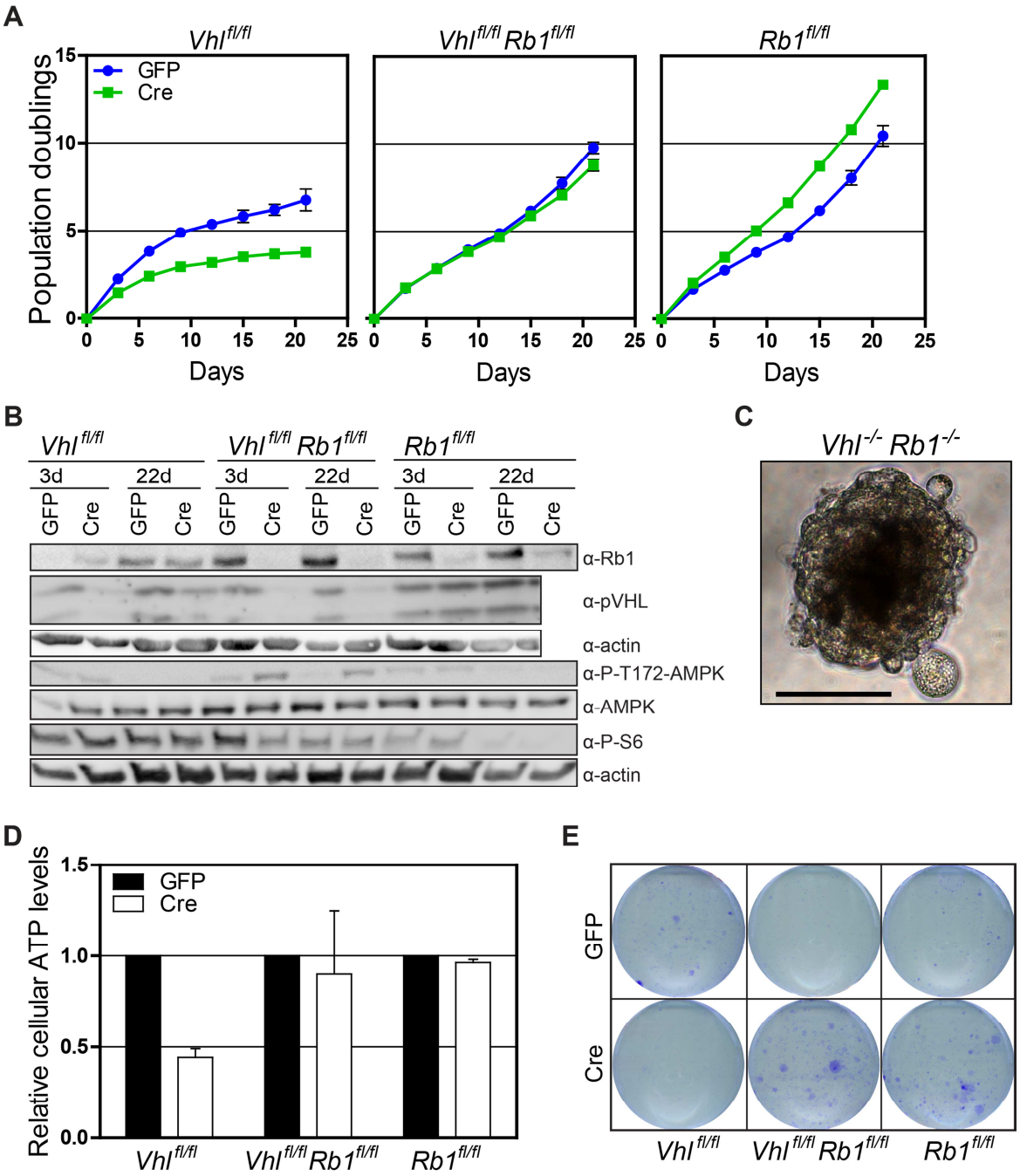

Figure 6.1: Deletion of *Rb1* rescues senescence and ATP levels in *Vhl* negative MEFs.

A Proliferation assay of *Vhl*$^{fl/fl}$, *Vhl*$^{fl/fl}$ *Rb1*$^{fl/fl}$ and *Rb1*$^{fl/fl}$ MEFs infected with adenoviruses expressing GFP or Cre.

B Western blotting analysis of cells from (A) at indicated time points.

C Anchorage independent growth of *Vhl*$^{-/-}$ *Rb1*$^{-/-}$ cells from (A). Scale bar 50 µm.

D Cellular ATP levels of cells from (A) 5 days after adenovirus infection.

E Immortalisation assay of cells from (A).

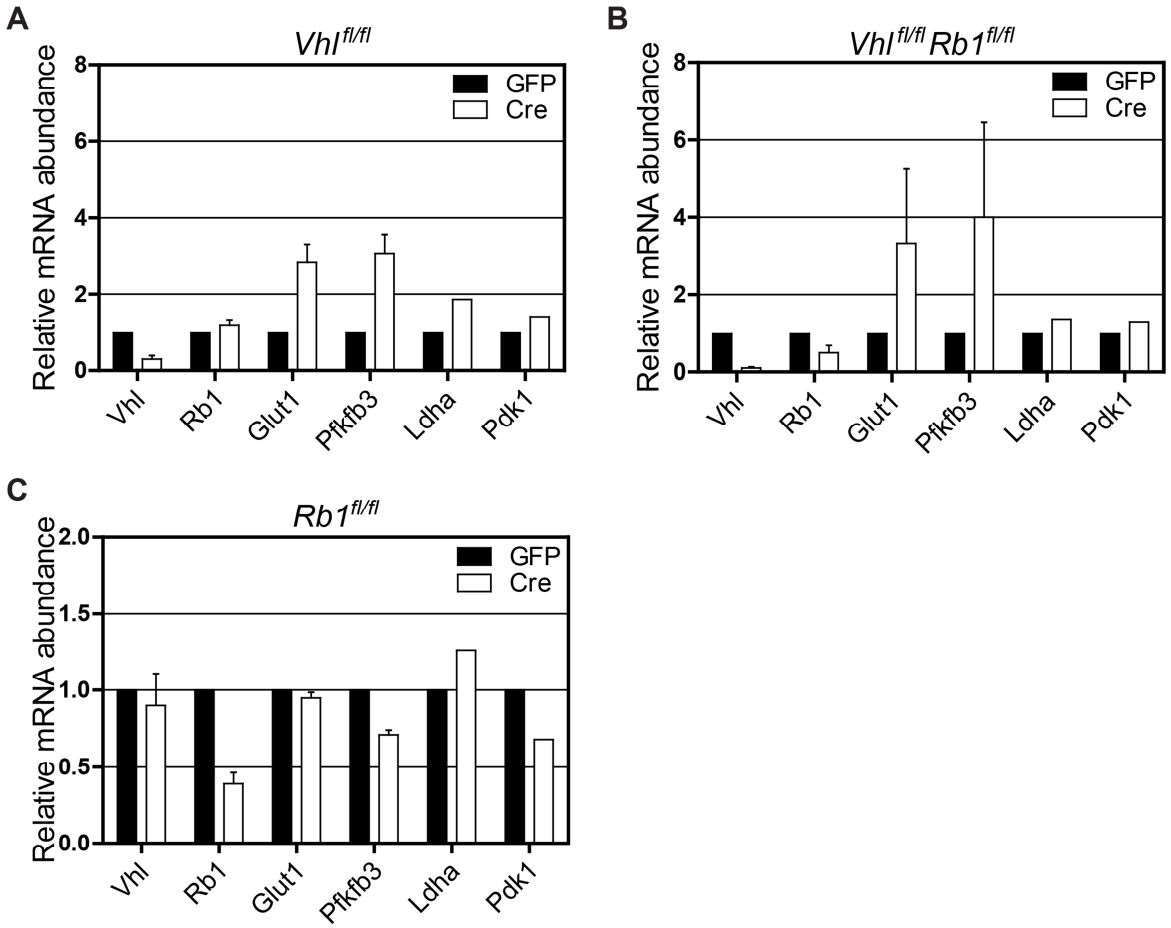

Figure 6.2: Glycolytic genes are also upregulated in *Vhl/Rb1* negative MEFs.

A-C Real-time quantitative PCR analysis of *Vhl*$^{fl/fl}$ (A), *Vhl*$^{fl/fl}$ *Rb1*$^{fl/fl}$ (B) and *Rb1*$^{fl/fl}$ (C) MEFs infected with adenoviruses expressing GFP or Cre. mRNA abundance of shown genes was normalized to *S12*.

A recent study from (Reynolds et al. 2014) revealed that glutamine metabolism is controlled by the retinoblastoma protein family. The combined loss of *Rb1*/*p130*/*p107* in MEFs resulted in increased glutamine uptake caused by higher expression of the glutamine transporter *Asct2* via releasing E2F3 from Rb. Furthermore, the activity of Gls1 was elevated and glutathione synthesis was increased in these cells. Therefore, we investigated whether the *Vhl*/*Rb1* deficient cells with rescued ATP levels exhibit changes in glutamine metabolism. Genes were analysed that are involved in glutaminolysis such as *Asct2*, *Gls1*, *Gls2*, *Glud1*, *Got1* and *Got2*. The levels of *Asct2* were neither in *Vhl*/*Rb1* nor in *Rb1* negative MEFs changed (Figure 6.3B, C) and also none of the other glutaminolytic genes showed any differences compared to control cells. Interestingly, *Gls2* levels were elevated in *Vhl*/*Rb1* knockout cells (Figure 6.3B) but not in *Rb1* deficient MEFs (Figure 6.3C). Since we also observed elevated *Gls2* levels in *Vhl* and *Vhl*/*Trp53* negative cells, both with deficient ATP levels and since the loss of *Gls2* provided a growth advantage for *Vhl*/*p53* negative cells and allowed them to grow anchorage

independently, further experiments are now necessary to define the function of *Gls2* in transformed *Vhl/Rb1* negative cells.

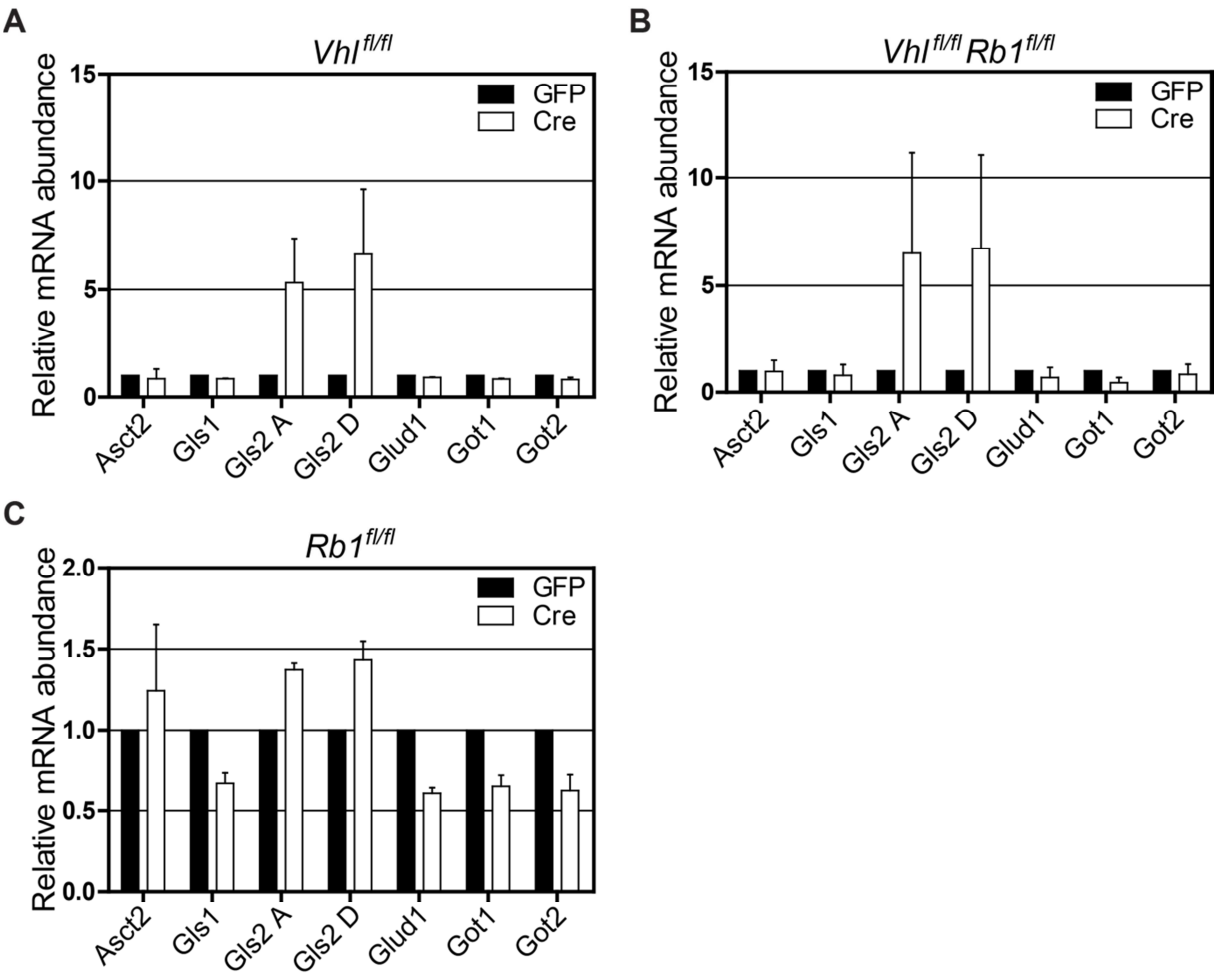

Figure 6.3: Transcript levels of *Gls2* elevated in *Vhl/Rb1* deficient cells.

A-C Real-time quantitative PCR analysis of *Vhl*$^{fl/fl}$ (A), *Vhl*$^{fl/fl}$ *Rb1*$^{fl/fl}$ (B) and *Rb1*$^{fl/fl}$ (C) MEFs infected with adenoviruses expressing GFP or Cre. mRNA abundance of shown genes was normalized to *S12*.

6.2.2 Kidney cancer model

Given our observation of genetic cooperation between Vhl and Rb1 in cell culture and the presence of RB1 pathway alterations in ccRCC, we generated mice with a tamoxifen-inducible kidney-specific deletion of *Rb1* alone (Ksp1.3-Cre-ER$^{T2\ Tg/+}$; *Rb1*$^{fl/fl}$) as well as in combination with *Vhl* (Ksp1.3-Cre-ER$^{T2\ Tg/+}$; *Vhl*$^{fl/fl}$; *Rb1*$^{fl/fl}$). As control animals littermate mice that were negative for the Ksp1.3-Cre-ER^{T2} transgene were used (Ksp1.3-Cre-ER$^{T2\ +/+}$). Therefore, Ksp1.3-Cre-ER^{T2} mice were crossed with *Rb1*$^{fl/fl}$ and *Vhl*$^{fl/fl}$ *Rb1*$^{fl/fl}$ mice containing loxP sites inserted in the genomic DNA. Transgenic Ksp1.3-Cre-ER^{T2} mice contain the fusion protein Cre-ER^{T2} that is under the control of the Ksp-cadherin gene promoter. The Cre-ER^{T2} protein is retained in its inactivated form in the cytosol and

is activated upon binding of 4-hydroxytamoxifen, translocated to the nucleus and mediates Cre/loxP recombination. The Ksp1.3-Cre promoter is a kidney specific transgene that generates a deletion of floxed genes in the epithelial cells at the urinary pole of the glomerulus, distal tubules, loops of Henle, collecting ducts and also more rarely in proximal tubular cells (Feil et al. 1997; Shao et al. 2002; Shao et al. 2002). To study the effects of inactivation of *Rb1* and *Vhl/Rb1* in mice, control and Cre-expressing *Rb1*$^{fl/fl}$ and *Vhl*$^{fl/fl}$ *Rb1*$^{fl/fl}$ mutant mice were exposed to tamoxifen. Nursing dams were injected intra peritoneal with tamoxifen two days after giving birth (P2) or animals were directly injected eleven days after birth (P11) or at four weeks of age (4W). The different injection time points were chosen to test whether there is a difference in the onset of cyst and tumour development caused by decreased cell proliferation in older mice. Several studies revealed that cyst progression was dependent on the time point when the deletion of *Kif3a*, a kinesin II subunit important for ciliogenesis, was initiated. Animals injected before P11 had a fast cyst progression within four weeks, whereas after P11 cyst development occurred after six month of age (Davenport et al. 2007; Patel et al. 2008). Treated animals are hereafter referred to as Rb1$^{\Delta/\Delta}$, Vhl$^{\Delta/\Delta}$Rb1$^{\Delta/\Delta}$ and controls as Rb1$^{fl/fl}$, Vhl$^{fl/fl}$ Rb1$^{fl/fl}$, respectively. Animals were analysed at the age of 2-3 months (Rb1$^{\Delta/\Delta}$: P2: *n* = 2; Vhl$^{\Delta/\Delta}$Rb1$^{\Delta/\Delta}$: 4W: *n* = 4), 5-8 months (Rb1$^{\Delta/\Delta}$: 4W: *n* = 5, P2: *n* = 4; Vhl$^{\Delta/\Delta}$Rb1$^{\Delta/\Delta}$: 4W: *n* = 5, P2: *n* = 4) and 11-13 months (Rb1$^{\Delta/\Delta}$: 4W: *n* = 3, P2: *n* = 17, P11: *n* = 6; Vhl$^{\Delta/\Delta}$Rb1$^{\Delta/\Delta}$: 4W: *n* = 1, P2: *n* = 9). Control, Rb1$^{\Delta/\Delta}$ and Vhl$^{\Delta/\Delta}$Rb1$^{\Delta/\Delta}$ mice exhibited normal kidney histology within three months after tamoxifen treatment (data not shown). It could be clearly shown that the recombination of *Vhl* and *Rb1* occurred but with high variance between different animals (Figure 6.4M-R). However, at the age of five months small clusters of disorganised cells could infrequently be observed in Rb1$^{\Delta/\Delta}$ and Vhl$^{\Delta/\Delta}$Rb1$^{\Delta/\Delta}$ animals but not in control animals (Figure 6.4A-C). At the age of one year, Rb1$^{\Delta/\Delta}$ mutant animals infrequently displayed micro-cysts but this could only be observed in less than 50% of analysed animals (Rb1$^{\Delta/\Delta}$: 4W: *n* = 3; P2: *n* = 17; P11: *n* = 6) (Figure 6.4D-I). Interestingly, the double knockout mice had an almost normal histological appearance aside from very infrequent clusters of disorganised cells that already could be seen in younger mice and atypical nuclei (Vhl$^{\Delta/\Delta}$Rb1$^{\Delta/\Delta}$: 4W: *n* = 1; P2: *n* = 9) (Figure 6.4J-L). Thus, no neoplastic transformation took place with advanced age. In summary, these mouse studies with combined loss of *Vhl* and *Rb1* in kidney epithelial cells revealed no cyst or tumour formation, suggesting that additional mutations might have to occur to initiate enhanced cell proliferation. However, as the Rb1$^{\Delta/\Delta}$ mice display micro-cysts and this phenotype is completely gone in Vhl$^{\Delta/\Delta}$Rb1$^{\Delta/\Delta}$ animals it seems that the loss of *Vhl* prevents rather than accelerates growth of hyperplastic lesions.

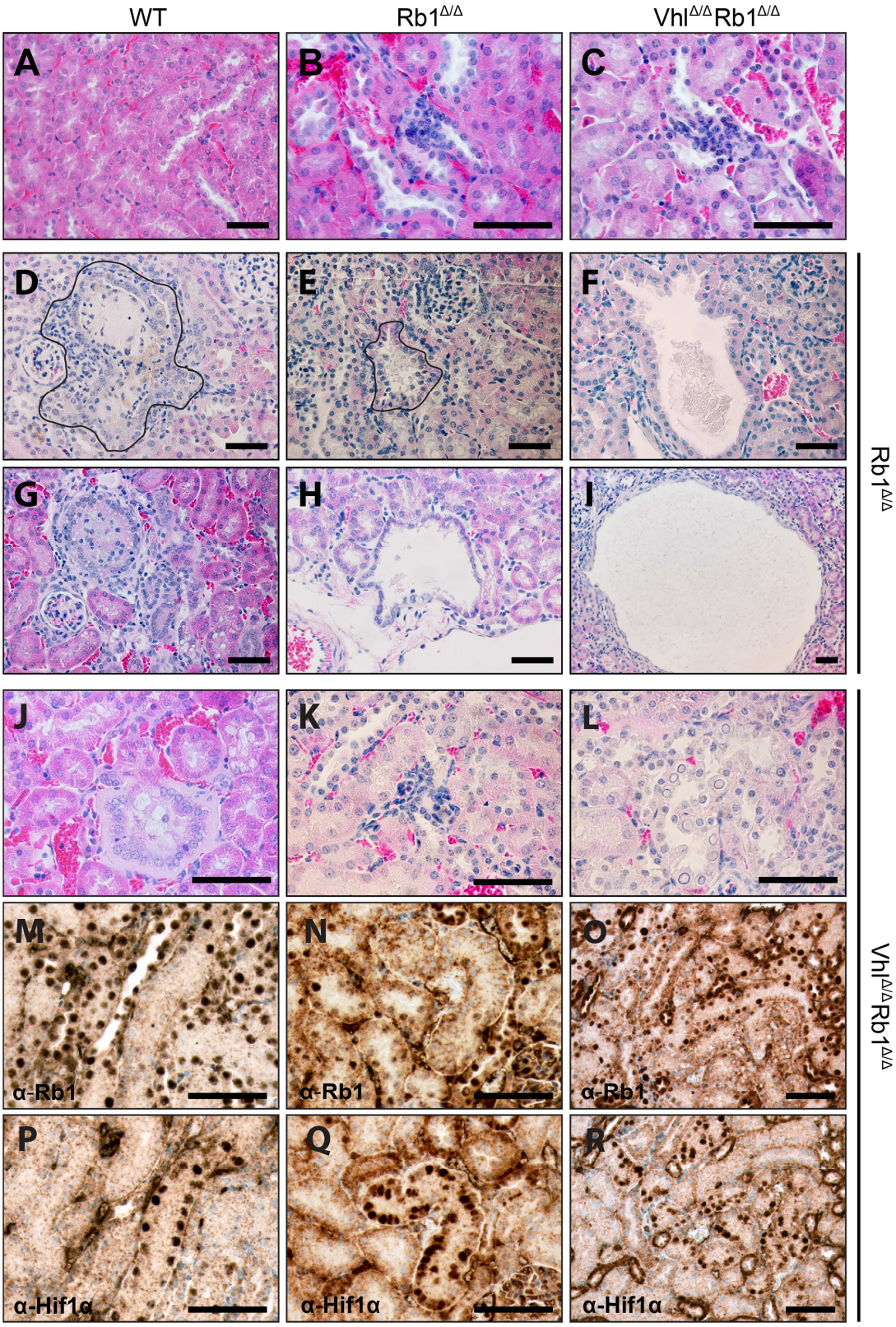

Figure 6.4: $Rb1^{\Delta/\Delta}$ and $Vhl^{\Delta/\Delta}Rb1^{\Delta/\Delta}$ mice display no cyst or tumour formation in kidneys.

Scale bars depict 50 µm. A, D-H, O, R are the same magnification. B-C, J-N, P-Q are the same magnification.

A-C Histological appearance of cortex of kidneys from 5-8 month-old wild-type (A), $Rb1^{\Delta/\Delta}$ (B) and $Vhl^{\Delta/\Delta}Rb1^{\Delta/\Delta}$ (C) mice.

D-I Examples of micro-cysts found in kidneys of 1-year-old $Rb1^{\Delta/\Delta}$ mice.

J-L Histological appearance of cortex of kidneys from 1-year-old $Vhl^{\Delta/\Delta}Rb1^{\Delta/\Delta}$ mice.

M-R anti-Rb1 and anti-Hif1α immunohistochemistry of 1-year-old $Vhl^{\Delta/\Delta}Rb1^{\Delta/\Delta}$ mice.

We showed that $Vhl^{\Delta/\Delta}Trp53^{\Delta/\Delta}$ mice exhibit a dysregulation of epithelial cell proliferation, thus developing simple cysts, atypical cysts and neoplasms in the kidneys (Albers et al. 2013). However, the latency for development of cysts and tumours was one year, indicating that other mutations are most likely necessary for initiation of these lesions. Given our cell culture data indicating a cooperative effect of combined *Vhl* and *Rb1* mutation in senescence-rescue, ATP-rescue and induction of anchorage-independent growth we also generated mice with a tamoxifen-inducible kidney-specific deletion of *Vhl*, *Rb1* and *Trp53* (Ksp1.3-Cre-$ER^{T2\ Tg/+}$; $Vhl^{fl/fl}$; $Rb1^{fl/fl}$; $Trp53^{fl/fl}$) as well as of *Rb1* and *Trp53* (Ksp1.3-Cre-$ER^{T2\ Tg/+}$; $Rb1^{fl/fl}$; $Trp53^{fl/fl}$). Littermate mice negative for the Ksp1.3-Cre-ER^{T2} transgene were used as control animals (Ksp1.3-Cre-$ER^{T2\ +/+}$). The breeding for Ksp1.3-Cre-$ER^{T2\ Tg/+}$; $Rb1^{fl/fl}$; $Trp53^{fl/fl}$ animals is still ongoing. To generate knockout animals, nursing dams were injected with tamoxifen two days after giving birth (P2). Treated animals are hereafter referred to as $Vhl^{\Delta/\Delta}Rb1^{\Delta/\Delta}Trp53^{\Delta/\Delta}$ and controls as $Vhl^{fl/fl}\ Rb1^{fl/fl}\ Trp53^{fl/fl}$, respectively. The first $Vhl^{\Delta/\Delta}Rb1^{\Delta/\Delta}Trp53^{\Delta/\Delta}$ animals were analysed at the age of three months (P2: 3 littermates). $Vhl^{fl/fl}\ Rb1^{fl/fl}\ Trp53^{fl/fl}$ control mice and one $Vhl^{\Delta/\Delta}Rb1^{\Delta/\Delta}Trp53^{\Delta/\Delta}$ animal did not show any histological abnormalities (Figure 6.5A). The other two $Vhl^{\Delta/\Delta}Rb1^{\Delta/\Delta}Trp53^{\Delta/\Delta}$ animals exhibited neoplasms, which grew in a solid or cystic pattern, some with clear cell appearance and some with nuclear atypia, suggestive of precursor lesions of ccRCC (Figure 6.5B-O). In ongoing experiments, aged cohorts of $Vhl^{\Delta/\Delta}Rb1^{\Delta/\Delta}Trp53^{\Delta/\Delta}$ and $Rb1^{\Delta/\Delta}Trp53^{\Delta/\Delta}$ mice will be analysed to determine whether these precursor lesions can progress to form ccRCC and if these are dependent on loss of pVhl function.

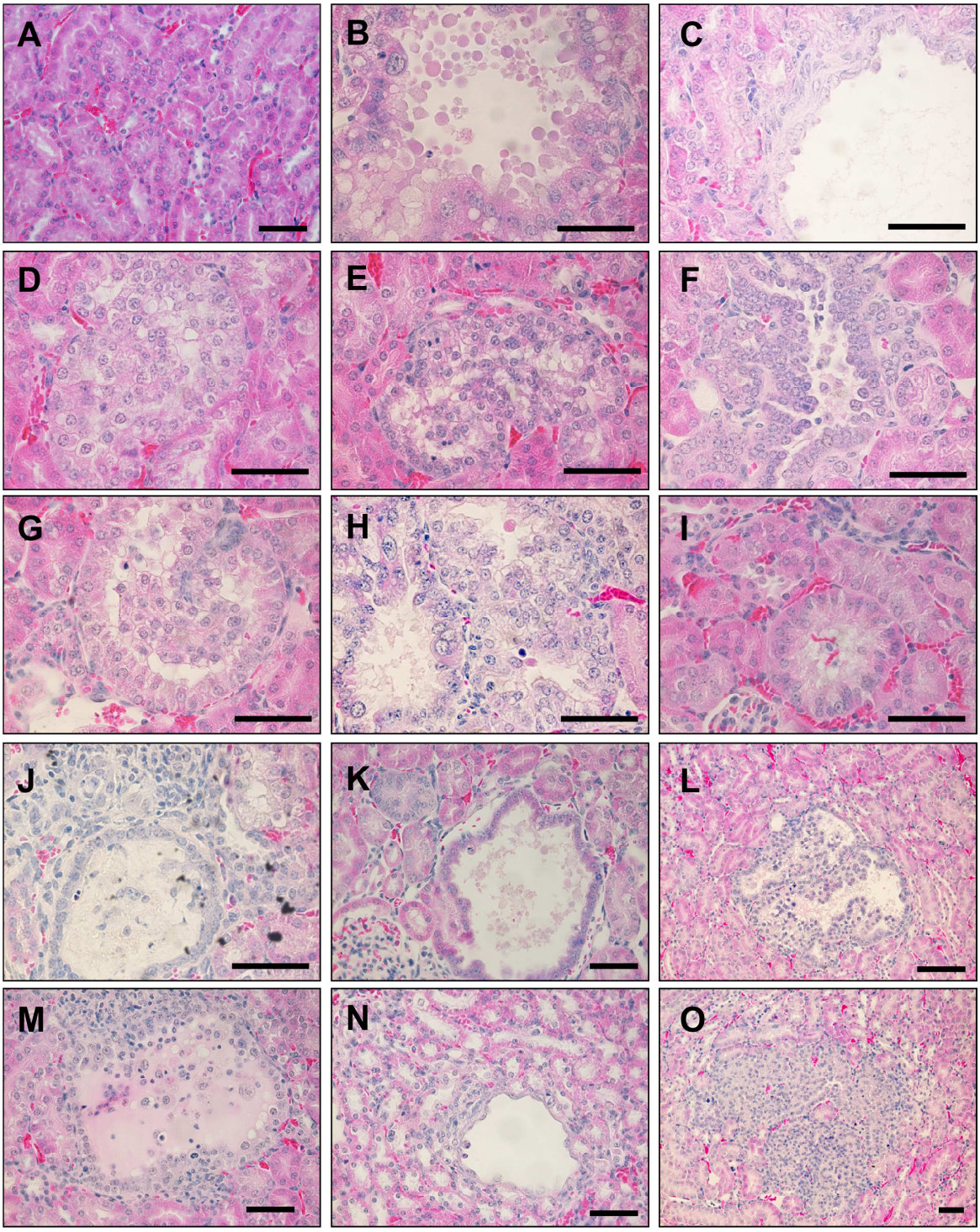

Figure 6.5: Precursor lesions of ccRCC in kidneys of $Vhl^{\Delta/\Delta}Rb1^{\Delta/\Delta}Trp53^{\Delta/\Delta}$ mice.

Scale bars depict 50 µm. B-J are the same magnification. A, K-N are the same magnification.

A Histological appearance of cortex of kidneys from 3 month-old wild-type mice.

B-O Examples of lesions found in kidneys of 3 month-old $Vhl^{\Delta/\Delta}Rb1^{\Delta/\Delta}Trp53^{\Delta/\Delta}$ mice.

6.3 Discussion

The cell cycle and senescence regulator pRb has been indirectly implicated in the regulation of senescence following loss of *Vhl* in primary MEFs (Young et al. 2008). Recent studies in sporadic ccRCC revealed multiple alterations in components of the senescence and cell cycle machinery pathways, including RB1 and its direct target E2F3 (Sato et al. 2013). We therefore examined the effect of combined loss of *Vhl* and *Rb1* on cellular senescence and cellular metabolism following loss of pVhl function. In proliferation assays, *Vhl/Rb1* negative MEFs showed a similar phenotype to *Vhl/Trp53* deficient MEFs. In both genotypes the senescence induced by loss of *Vhl* was rescued (Figure 6.1A) (Albers et al. 2013), but unlike *Vhl/Trp53* negative cells, *Vhl/Rb1* deficient MEFs showed rescued ATP levels and were able to grow in an anchorage independent manner, a hallmark of cellular transformation (Figure 6.1C and D). A recent study with *Rb1/Rbl-1/Rbl-2* knockout MEFs could show a control function of Rb in glutamine metabolism (Reynolds et al. 2014). Therefore, it might be possible that *Vhl/Rb1* deficient cells use glutamine to fuel the TCA cycle with carbons and thus can restore ATP. However, analyses of mRNA levels of glutaminolytic genes provided no further insights in this respect (Figure 6.3). As in the *Vhl* MEFs, *Vhl/Rb1* cells also showed increased *Gls2* transcript levels (Figure 6.3). Further analysis will now be necessary to detect whether these cells take up more glutamine and to determine how it is metabolised. It will also be interesting to see if the oxygen consumption is rescued in *Vhl/Rb1* deficient cells and whether this in turn influences cellular ATP levels. Furthermore, starvation assays are another experimental possibility to detect whether glutamine is necessary for the enhanced proliferation of *Vhl/Rb1* negative cells. Another cause for the rescued ATP levels could be that the loss of *Rb1* enhances glycolytic flux. A recent publication showed that Rb is part of the Rb-TRIP230-ARNT complex that mediates Hif1-activated gene expression and the loss of *Rb* enhanced Hif1-regulated transcription (Labrecque et al. 2014). However, in contrast to this idea the analysed glycolytic genes in *Vhl/Rb1* deficient cells did not indicate a connection between Rb1 and Hif1 as their mRNA levels were not more elevated than in *Vhl* negative cells (Figure 6.2). Another question that has to be elucidated is why the *Vhl/Rb1* negative MEFs can grow anchorage independently. Could the rescued ATP levels play a role in this phenotype? Detached epithelial cells exhibit reduced glucose transport and decreased ATP levels in comparison to attached cells and this has been proposed to prevent their proliferation in a type of attachment-sensitive metabolic checkpoint (Schafer et al. 2009). This could be either rescued through overexpression of Erbb2 which enhanced glucose flux through stabilisation of PI3K and EGFR in a pentose phosphate pathway-dependent manner or via antioxidant treatment dependent on enhanced fatty acid oxidation without a rescue of glucose flux.

Both treatments enabled these cells to grow anchorage independently after rescuing ATP levels (Schafer et al. 2009). It will be now interesting to explore if *Rb1* deletion has similar effects on *Vhl* deficient MEFs.

Given our observation of genetic cooperation between *Vhl* and *Rb1* in cell culture and the presence of RB1 pathway alterations in ccRCC, another aim of this thesis was to generate kidney-specific combined deletion of *Rb1* and *Vhl* to study potential cooperative effects of loss of function of these genes on ccRCC development. Despite promising results from cell culture studies, the kidney-specific deletion of *Vhl* and *Rb1* did not lead to the breakdown of normal proliferation in mice. While $Rb1^{\Delta/\Delta}$ animals showed micro-cysts and small foci of tubular dysplasia, the additional loss of *Vhl* in fact prevented the growth of hyperplastic lesions (Figure 6.4). Potentially, additional mutations might be necessary to initiate tumour development. In this context, our first analyses of mice harbouring combined deletion of *Vhl*, *Trp53* and *Rb1* provide very promising results. Already at the age of three months neoplasms could be found, which grew in a solid or cystic pattern, some with clear cell appearance and some with nuclear atypia (Figure 6.5). This histological appearance could potentially indicate precursor lesions of ccRCC. These lesions are already larger and occur at a much higher frequency about nine months earlier than the lesions that were observed in *Vhl/Trp53* null mice. The analysis of aged cohorts of $Vhl^{\Delta/\Delta}Rb1^{\Delta/\Delta}Trp53^{\Delta/\Delta}$ mice will show whether these precursor lesions can progress to form ccRCC. The use of control $Rb1^{\Delta/\Delta}Trp53^{\Delta/\Delta}$ mice will allow us to answer the question if the loss of *Vhl* is necessary for the development of these lesions and ccRCC. The Ksp1.3-Cre promoter is active in different kidney epithelial cells such as urinary pole of the glomerulus, distal tubules, loops of Henle, collecting ducts and also in proximal tubular cells. The exact determination of the cells of origin that gave rise to the different kinds of precursor lesions will be quite important, especially as the cell type(s) that gives rise to ccRCC is still unknown. Co-stainings with specific tubule markers and Hif target genes, to confirm *Vhl* deletion, will be helpful tools. Furthermore, it will be important to elucidate the status of primary cilia in these lesions. pVHL is involved in the suppression of cyst formation through the maintenance of primary cilia. In human VHL patients, as well as in the $Vhl^{\Delta/\Delta}Trp53^{\Delta/\Delta}$ mouse model, reduced cilia frequencies were seen in simple cystic lesions (Thoma et al. 2007; Albers et al. 2013). Thus, it would be interesting to confirm this initial cyst formation model with the triple knockout animals. The development of the neoplastic state observed in *Vhl/Trp53* mutant mice correlated with upregulated c-Myc expression and hyperactivation of mTORC1 signalling (Albers et al. 2013). As the upregulation of mTORC1 or C-MYC predict poor patient outcome in human ccRCC patients it would be interesting to elucidate the levels of these proteins

and their associated signalling pathways in the triple knockout animals as it may be that these cooperating mutations could act to initiate and promote tumour formation.

7 General Discussion and Outlook

The overall aim of this thesis was to begin to close some of the large knowledge gaps in understanding the molecular and cellular mechanisms that cause clear cell renal cell carcinoma. We used mice and primary cell culture systems to pursue the question of which mechanisms when disrupted can cause dysregulation of cell proliferation. This knowledge of the signalling pathways that underlie ccRCC development and progression is essential for thinking about rationally designed potential therapeutic targets. To approach this question we chose primary mouse embryonic fibroblasts as a culture system due to their ease of culturing and genetic manipulation. Compared to cancer cell lines which have an unknown variety of mutations we are able to specifically introduce defined mutations. We could prove that *Vhl* deficient cells show a Warburg-like phenotype. Even with a mutated second tumour suppressor gene such as *Trp53* the Warburg effect was not fully developed in that there was only a relatively modest increase in glucose uptake that lead to a state of cellular energy stress, which potentially limits further transformation of these cells. However, in this project we were unable to identify the additional mutations that are necessary to initiate transformation of these cells.

Another faster approach to identify pro-proliferative mutations on top of *Vhl* and *Trp53* could be to employ loss and gain of representation screenings. Thereby, shRNA-based screenings can be used to knockdown either the whole genome or selected sets of genes, like the kinome, or genes that regulate different signalling pathways, for example cell cycle controlling genes. With deep sequencing approaches we are then able to simultaneously discover the effects of knockdown of several hundred genes on proliferation of cells of the *Vhl/Trp53* deficient background. In these experiments the cells would be infected with the desired library of shRNAs and either infected with adenovirus expressing GFP or Cre. During culturing of the knockout cells shRNA vectors of genes whose knockdowns cause inhibition of proliferation or cell death will rapidly be lost and are therefore under-represented in the deep-sequencing of the entire population of integrated shRNAs. shRNA vectors that are over-represented in the sequencing results indicate that the knockdown of these genes induces a proliferative advantage. Besides shRNAs, it would be also possible to use other systems like libraries based on the RNA-guided CRISPR-Cas9 nuclease system that allows generation of gene knockouts in mammalian cells (Ran et al. 2013). In follow up experiments, any hits obtained could be individually validated in MEFs or primary epithelial kidney cells. A special interest focuses on their influence on the metabolism as we hope to clarify if the reduced ATP levels in *Vhl/Trp53* deficient MEFs inhibit further proliferation. To further validate the results in a

more physiological setting, mutated MEFs or kidney cells could be injected into mice for xenograft assays. Another possibility would be to directly introduce the desired mutations into mouse kidneys. In our lab a lentiviral-based vector system, called MuLE (Multiple Lentiviral Expression), was developed which allows us to simultaneously introduce multiple genetic alterations into mammalian cells in vivo and ex vivo. This system enables us to generate complex polycistronic lentiviruses, which can combine constitutive or inducible gene knockdown, deletion or overexpression. In addition, fluorescent (eGFP, tdTomato, mCherry, iRFP) or enzymatic reporters (lacZ, luciferase) which can be used for animal imaging studies or cellular assays can be expressed as well (Albers et al. 2014). With this system we are able to combine shRNAs against *Vhl* and *Trp53* with the shRNAs found in the screening described above and an enzymatic reporter such as luciferase and can directly inject the produced virus in mouse kidneys. With the enzymatic reporter, we would then be able to follow potential tumour development over time. Furthermore, the potential ability to generate different types of genetically defined mouse ccRCC tumour models using this system would also allow us to exactly monitor the process and efficacy of administered therapeutics.

ccRCC remains one of the few major human cancer types for which no autochthonous mouse model exists. With the generated triple *Vhl/Rb1/Trp53* knockout mouse model we hope that we will be able to specifically examine the different phases of tumour initiation and progression. The development of an accurate mouse model of ccRCC would be of high value as the current treatment options for ccRCC patients are quite limited and largely ineffective. The primary treatment modality of ccRCC confined to the kidney and its regional lymph nodes and vasculature is nephrectomy or if possible nephron-sparing surgery. However, at the time of diagnosis metastatic ccRCCs were found in 30% of patients. A similar percentage of patients develop metastasis during further cancer progression (Motzer et al. 1996; Leibovich et al. 2003). The symptom burden of metastatic ccRCC is extremely high and it is a rapidly fatal disease. So far, different tested treatment strategies, such as cytotoxic and hormonal therapy, had little success (Harris 1983; Yagoda and Bander 1989). In contrast, cytokine therapy with interferon-α and interleukin-2 promised at least for a sub-fraction of patients a positive effect (Motzer et al. 2002). The latest systemic therapies for ccRCC are based on new insights into signalling pathways that are affected in this disease such as VHL and mTORC1 pathways. Their main aim is to target VEGF-mediated angiogenesis either via tyrosine kinase inhibitors, monoclonal antibodies or mTOR inhibitors. However, the therapeutic efficacy of these “new” agents is also not high and it is almost always non-curative and

associated with significant side effects (Fisher et al. 2013). With the generation of a mouse model we hope to be able to provide a better tool to test new therapeutic agents.

We have developed a micro-computed tomography (µCT) imaging system that will be useful for the study of tumour development in our mouse model. The CT is a 3D x-ray imaging technique which is used to obtain x-ray projection images around the axis of an object. It generates a pile of thin tomographic images of adjacent slices through the body. This method can be applied to follow *in vivo* processes in animals such as myocardial infarction (Badea et al. 2008), metastasis (Ohta et al. 2006) and kidney volume (Almajdub et al. 2008). In our lab it also could be shown to be an efficient tool to follow longitudinal studies of cyst formation and progression in mouse kidneys using an injected contrast agent (Lehmann et al. 2014). We will employ our *Vhl/Rb1/Trp53* mouse model and utilise µCT imaging at different time points to determine how and when tumours are initiated and how rapidly they progress in this model. If it is possible in living mice to quantitatively follow the tumour progression with the µCT, we would then aim to apply specific therapeutic agents at different tumour stages and the efficacy of the treatment could easily be traced via non-invasive imaging.

Using whole genome DNA sequencing analyses of lesions that arise in *Vhl/Rb1/Trp53* mice we would be able to detect other genetic alterations, which potentially cooperate at different tumour stages with the induced mutations, possibly promoting tumour progression. Alternatively or additionally, sequencing platforms could be used which amplify based on PCR analyses discrete regions of the genome. The genomic DNA can be isolated by laser capture microdissection from formalin-fixed paraffin-embedded tumour tissue. As this system can work with a low amount of DNA, specific tumour regions can be isolated and analysed separately for mutations in sets of genes to investigate questions of intratumoural heterogeneity.

Cell lines derived from different tumour stages of triple knockout mice could provide another useful tool for new therapeutic strategies. These cell lines could be used to screen chemical libraries to search for new therapeutic targets. Furthermore, the above described genetic sequencing analyses could also be conducted in these cell lines and the obtained results may help to develop better treatment strategies. Thus, a ccRCC mouse model that accurately reproduces the genetic and cellular features of the human disease would tremendously contribute to the understanding of the mechanisms underlying ccRCC initiation and progression and to the development of new therapeutic strategies.

8 References

Albers J., Brandt S., Bode P. K., Bode-Lesniewska B., Wild P. J. and Frew I. J. (2014). The MuLE lentiviral vector system facilitates combinatorial genetics and reveals genetic cooperation between H-Ras and Cdkn2a in rhabdomyosarcomas. Unpublished data.

Albers J., Rajski M., Schonenberger D., Harlander S., Schraml P., von Teichman A., Georgiev S., Wild P. J., Moch H., Krek W. and Frew I. J. (2013) "Combined mutation of Vhl and Trp53 causes renal cysts and tumours in mice." EMBO Mol Med **5**(6): 949-964.

Aledo J. C., Gomez-Fabre P. M., Olalla L. and Marquez J. (2000) "Identification of two human glutaminase loci and tissue-specific expression of the two related genes." Mamm Genome **11**(12): 1107-1110.

Almajdub M., Magnier L., Juillard L. and Janier M. (2008) "Kidney volume quantification using contrast-enhanced in vivo X-ray micro-CT in mice." Contrast Media Mol Imaging **3**(3): 120-126.

Baas A. F., Boudeau J., Sapkota G. P., Smit L., Medema R., Morrice N. A., Alessi D. R. and Clevers H. C. (2003) "Activation of the tumour suppressor kinase LKB1 by the STE20-like pseudokinase STRAD." EMBO J **22**(12): 3062-3072.

Baba M., Hirai S., Kawakami S., Kishida T., Sakai N., Kaneko S., Yao M., Shuin T., Kubota Y., Hosaka M. and Ohno S. (2001) "Tumor suppressor protein VHL is induced at high cell density and mediates contact inhibition of cell growth." Oncogene **20**(22): 2727-2736.

Baba M., Hirai S., Yamada-Okabe H., Hamada K., Tabuchi H., Kobayashi K., Kondo K., Yoshida M., Yamashita A., Kishida T., Nakaigawa N., Nagashima Y., Kubota Y., Yao M. and Ohno S. (2003) "Loss of von Hippel-Lindau protein causes cell density dependent deregulation of CyclinD1 expression through hypoxia-inducible factor." Oncogene **22**(18): 2728-2738.

Badea C. T., Drangova M., Holdsworth D. W. and Johnson G. A. (2008) "In vivo small-animal imaging using micro-CT and digital subtraction angiography." Phys Med Biol **53**(19): R319-350.

Barnes K., Ingram J. C., Porras O. H., Barros L. F., Hudson E. R., Fryer L. G., Foufelle F., Carling D., Hardie D. G. and Baldwin S. A. (2002) "Activation of GLUT1 by metabolic and osmotic stress: potential involvement of AMP-activated protein kinase (AMPK)." J Cell Sci **115**(Pt 11): 2433-2442.

Bindra R. S., Vasselli J. R., Stearman R., Linehan W. M. and Klausner R. D. (2002) "VHL-mediated hypoxia regulation of cyclin D1 in renal carcinoma cells." Cancer Res **62**(11): 3014-3019.

Blankenship C., Naglich J. G., Whaley J. M., Seizinger B. and Kley N. (1999) "Alternate choice of initiation codon produces a biologically active product of the von Hippel Lindau gene with tumor suppressor activity." Oncogene **18**(8): 1529-1535.

Boudeau J., Baas A. F., Deak M., Morrice N. A., Kieloch A., Schutkowski M., Prescott A. R., Clevers H. C. and Alessi D. R. (2003) "MO25alpha/beta interact with STRADalpha/beta enhancing their ability to bind, activate and localize LKB1 in the cytoplasm." EMBO J **22**(19): 5102-5114.

Bringold F. and Serrano M. (2000) "Tumor suppressors and oncogenes in cellular senescence." Exp Gerontol **35**(3): 317-329.

Brugarolas J., Lei K., Hurley R. L., Manning B. D., Reiling J. H., Hafen E., Witters L. A., Ellisen L. W. and Kaelin W. G., Jr. (2004) "Regulation of mTOR function in response to hypoxia by REDD1 and the TSC1/TSC2 tumor suppressor complex." Genes Dev **18**(23): 2893-2904.

Buchkovich K., Duffy L. A. and Harlow E. (1989) "The retinoblastoma protein is phosphorylated during specific phases of the cell cycle." Cell **58**(6): 1097-1105.

Budanov A. V. and Karin M. (2008) "p53 target genes sestrin1 and sestrin2 connect genotoxic stress and mTOR signaling." Cell **134**(3): 451-460.

Burkhart D. L. and Sage J. (2008) "Cellular mechanisms of tumour suppression by the retinoblastoma gene." Nat Rev Cancer **8**(9): 671-682.
Cairns R. A., Harris I. S. and Mak T. W. (2011) "Regulation of cancer cell metabolism." Nat Rev Cancer **11**(2): 85-95.
Campisi J. (2001) "Cellular senescence as a tumor-suppressor mechanism." Trends in Cell Biology **11**(11): S27-S31.
Canto C., Gerhart-Hines Z., Feige J. N., Lagouge M., Noriega L., Milne J. C., Elliott P. J., Puigserver P. and Auwerx J. (2009) "AMPK regulates energy expenditure by modulating NAD+ metabolism and SIRT1 activity." Nature **458**(7241): 1056-1060.
Carnero A. and Hannon G. J. (1998) "The INK4 family of CDK inhibitors." Curr Top Microbiol Immunol **227**: 43-55.
Chan D. A., Sutphin P. D., Nguyen P., Turcotte S., Lai E. W., Banh A., Reynolds G. E., Chi J.-T., Wu J., Solow-Cordero D. E., Bonnet M., Flanagan J. U., Bouley D. M., Graves E. E., Denny W. A., Hay M. P. and Giaccia A. J. (2011) "Targeting GLUT1 and the Warburg Effect in Renal Cell Carcinoma by Chemical Synthetic Lethality." Science Translational Medicine **3**(94): 94ra70.
Chan E. Y. (2009) "mTORC1 phosphorylates the ULK1-mAtg13-FIP200 autophagy regulatory complex." Sci Signal **2**(84): pe51.
Chitalia V. C., Foy R. L., Bachschmid M. M., Zeng L., Panchenko M. V., Zhou M. I., Bharti A., Seldin D. C., Lecker S. H., Dominguez I. and Cohen H. T. (2008) "Jade-1 inhibits Wnt signalling by ubiquitylating beta-catenin and mediates Wnt pathway inhibition by pVHL." Nat Cell Biol **10**(10): 1208-1216.
Claudio P. P., Tonini T. and Giordano A. (2002) "The retinoblastoma family: twins or distant cousins?" Genome Biol **3**(9): reviews3012.
Curthoys N. P., Kuhlenschmidt T., Godfrey S. S. and Weiss R. F. (1976) "Phosphate-dependent glutaminase from rat kidney. Cause of increased activity in response to acidosis and identity with glutaminase from other tissues." Arch Biochem Biophys **172**(1): 162-167.
Curthoys N. P. and Watford M. (1995) "Regulation of glutaminase activity and glutamine metabolism." Annu Rev Nutr **15**: 133-159.
Davenport J. R., Watts A. J., Roper V. C., Croyle M. J., van Groen T., Wyss J. M., Nagy T. R., Kesterson R. A. and Yoder B. K. (2007) "Disruption of intraflagellar transport in adult mice leads to obesity and slow-onset cystic kidney disease." Curr Biol **17**(18): 1586-1594.
Davies S. P., Helps N. R., Cohen P. T. and Hardie D. G. (1995) "5'-AMP inhibits dephosphorylation, as well as promoting phosphorylation, of the AMP-activated protein kinase. Studies using bacterially expressed human protein phosphatase-2C alpha and native bovine protein phosphatase-2AC." FEBS Lett **377**(3): 421-425.
Dayan F., Roux D., Brahimi-Horn M. C., Pouyssegur J. and Mazure N. M. (2006) "The oxygen sensor factor-inhibiting hypoxia-inducible factor-1 controls expression of distinct genes through the bifunctional transcriptional character of hypoxia-inducible factor-1alpha." Cancer Res **66**(7): 3688-3698.
de la Rosa V., Campos-Sandoval J. A., Martín-Rufián M., Cardona C., Matés J. M., Segura J. A., Alonso F. J. and Márquez J. (2009) "A novel glutaminase isoform in mammalian tissues." Neurochemistry International **55**(1-3): 76-84.
DeBerardinis R. J. and Cheng T. (2010) "Q's next: the diverse functions of glutamine in metabolism, cell biology and cancer." Oncogene **29**(3): 313-324.
DeBerardinis R. J., Lum J. J., Hatzivassiliou G. and Thompson C. B. (2008) "The biology of cancer: metabolic reprogramming fuels cell growth and proliferation." Cell Metab **7**(1): 11-20.
Denison F. C., Hiscock N. J., Carling D. and Woods A. (2009) "Characterization of an Alternative Splice Variant of LKB1." Journal of Biological Chemistry **284**(1): 67-76.
DeYoung M. P., Horak P., Sofer A., Sgroi D. and Ellisen L. W. (2008) "Hypoxia regulates TSC1/2-mTOR signaling and tumor suppression through REDD1-mediated 14-3-3 shuttling." Genes Dev **22**(2): 239-251.

Dirac A. M. and Bernards R. (2003) "Reversal of senescence in mouse fibroblasts through lentiviral suppression of p53." J Biol Chem **278**(14): 11731-11734.
Droz D., Zachar D., Charbit L., Gogusev J., Chretein Y. and Iris L. (1990) "Expression of the human nephron differentiation molecules in renal cell carcinomas." Am J Pathol **137**(4): 895-905.
Duivenvoorden W. C., Beatty L. K., Lhotak S., Hill B., Mak I., Paulin G., Gallino D., Popovic S., Austin R. C. and Pinthus J. H. (2013) "Underexpression of tumour suppressor LKB1 in clear cell renal cell carcinoma is common and confers growth advantage in vitro and in vivo." British Journal of Cancer **108**(2): 327-333.
Eble J., Sauter G., Epstein J. and Sesterhenn I., Eds. (2004) Tumours of the Kidney, World Health Organization Classification of Tumours. Pathology and Genetics of Tumours of the Urinary System and Male Genital Organs. Lyon, IARC Press.
Eble J. N. and Bonsib S. M. (1998) "Extensively cystic renal neoplasms: cystic nephroma, cystic partially differentiated nephroblastoma, multilocular cystic renal cell carcinoma, and cystic hamartoma of renal pelvis." Semin Diagn Pathol **15**(1): 2-20.
Egan D. F., Shackelford D. B., Mihaylova M. M., Gelino S., Kohnz R. A., Mair W., Vasquez D. S., Joshi A., Gwinn D. M., Taylor R., Asara J. M., Fitzpatrick J., Dillin A., Viollet B., Kundu M., Hansen M. and Shaw R. J. (2010) "Phosphorylation of ULK1 (hATG1) by AMP-Activated Protein Kinase Connects Energy Sensing to Mitophagy." Science **331**(6016): 456-461.
Elgadi K. M., Meguid R. A., Qian M., Souba W. W. and Abcouwer S. F. (1999) "Cloning and analysis of unique human glutaminase isoforms generated by tissue-specific alternative splicing." Physiol Genomics **1**(2): 51-62.
Epstein A. C., Gleadle J. M., McNeill L. A., Hewitson K. S., O'Rourke J., Mole D. R., Mukherji M., Metzen E., Wilson M. I., Dhanda A., Tian Y. M., Masson N., Hamilton D. L., Jaakkola P., Barstead R., Hodgkin J., Maxwell P. H., Pugh C. W., Schofield C. J. and Ratcliffe P. J. (2001) "C. elegans EGL-9 and mammalian homologs define a family of dioxygenases that regulate HIF by prolyl hydroxylation." Cell **107**(1): 43-54.
Esteban M. A., Tran M. G., Harten S. K., Hill P., Castellanos M. C., Chandra A., Raval R., O'Brien T S. and Maxwell P. H. (2006) "Regulation of E-cadherin expression by VHL and hypoxia-inducible factor." Cancer Res **66**(7): 3567-3575.
Faubert B., Boily G., Izreig S., Griss T., Samborska B., Dong Z., Dupuy F., Chambers C., Fuerth Benjamin J., Viollet B., Mamer Orval A., Avizonis D., DeBerardinis Ralph J., Siegel Peter M. and Jones Russell G. (2013) "AMPK Is a Negative Regulator of the Warburg Effect and Suppresses Tumor Growth In Vivo." Cell Metabolism **17**(1): 113-124.
Feil R., Wagner J., Metzger D. and Chambon P. (1997) "Regulation of Cre Recombinase Activity by Mutated Estrogen Receptor Ligand-Binding Domains." Biochemical and Biophysical Research Communications **237**(3): 752-757.
Filipp F. V., Scott D. A., Ronai Z. A., Osterman A. L. and Smith J. W. (2012) "Reverse TCA cycle flux through isocitrate dehydrogenases 1 and 2 is required for lipogenesis in hypoxic melanoma cells." Pigment Cell Melanoma Res **25**(3): 375-383.
Fisher R., Gore M. and Larkin J. (2013) "Current and future systemic treatments for renal cell carcinoma." Semin Cancer Biol **23**(1): 38-45.
Foster K., Prowse A., van den Berg A., Fleming S., Hulsbeek M. M., Crossey P. A., Richards F. M., Cairns P., Affara N. A., Ferguson-Smith M. A. and et al. (1994) "Somatic mutations of the von Hippel-Lindau disease tumour suppressor gene in non-familial clear cell renal carcinoma." Hum Mol Genet **3**(12): 2169-2173.
Freedman D. A., Wu L. and Levine A. J. (1999) "Functions of the MDM2 oncoprotein." Cell Mol Life Sci **55**(1): 96-107.
Frew I. J. and Krek W. (2007) "Multitasking by pVHL in tumour suppression." Current Opinion in Cell Biology **19**(6): 685-690.

Frew I. J., Thoma C. R., Georgiev S., Minola A., Hitz M., Montani M., Moch H. and Krek W. (2008) "pVHL and PTEN tumour suppressor proteins cooperatively suppress kidney cyst formation." EMBO J **27**(12): 1747-1757.

Fu L., Wang G., Shevchuk M. M., Nanus D. M. and Gudas L. J. (2011) "Generation of a mouse model of Von Hippel-Lindau kidney disease leading to renal cancers by expression of a constitutively active mutant of HIF1alpha." Cancer Res **71**(21): 6848-6856.

Fu L., Wang G., Shevchuk M. M., Nanus D. M. and Gudas L. J. (2013) "Activation of HIF2alpha in kidney proximal tubule cells causes abnormal glycogen deposition but not tumorigenesis." Cancer Res **73**(9): 2916-2925.

Fuhrer T., Heer D., Begemann B. and Zamboni N. (2011) "High-throughput, accurate mass metabolome profiling of cellular extracts by flow injection-time-of-flight mass spectrometry." Anal Chem **83**(18): 7074-7080.

Fukuda R., Zhang H., Kim J. W., Shimoda L., Dang C. V. and Semenza G. L. (2007) "HIF-1 regulates cytochrome oxidase subunits to optimize efficiency of respiration in hypoxic cells." Cell **129**(1): 111-122.

Gameiro Paulo A., Yang J., Metelo Ana M., Pérez-Carro R., Baker R., Wang Z., Arreola A., Rathmell W. K., Olumi A., López-Larrubia P., Stephanopoulos G. and Iliopoulos O. (2013) "In Vivo HIF-Mediated Reductive Carboxylation Is Regulated by Citrate Levels and Sensitizes VHL-Deficient Cells to Glutamine Deprivation." Cell Metabolism **17**(3): 372-385.

Gao P., Tchernyshyov I., Chang T.-C., Lee Y.-S., Kita K., Ochi T., Zeller K. I., De Marzo A. M., Van Eyk J. E., Mendell J. T. and Dang C. V. (2009) "c-Myc suppression of miR-23a/b enhances mitochondrial glutaminase expression and glutamine metabolism." Nature **458**(7239): 762-765.

Gao P., Tchernyshyov I., Chang T. C., Lee Y. S., Kita K., Ochi T., Zeller K. I., De Marzo A. M., Van Eyk J. E., Mendell J. T. and Dang C. V. (2009) "c-Myc suppression of miR-23a/b enhances mitochondrial glutaminase expression and glutamine metabolism." Nature **458**(7239): 762-765.

Garcia-Martinez J. M. and Alessi D. R. (2008) "mTOR complex 2 (mTORC2) controls hydrophobic motif phosphorylation and activation of serum- and glucocorticoid-induced protein kinase 1 (SGK1)." Biochem J **416**(3): 375-385.

Giacobbe A., Bongiorno-Borbone L., Bernassola F., Terrinoni A., Markert E. K., Levine A. J., Feng Z., Agostini M., Zolla L., Agrò A. F., Notterman D. A., Melino G. and Peschiaroli A. (2013) "p63 regulates glutaminase 2 expression." Cell Cycle **12**(9): 1395-1405.

Giardiello F. M., Welsh S. B., Hamilton S. R., Offerhaus G. J., Gittelsohn A. M., Booker S. V., Krush A. J., Yardley J. H. and Luk G. D. (1987) "Increased risk of cancer in the Peutz-Jeghers syndrome." N Engl J Med **316**(24): 1511-1514.

Ginsberg D., Mechta F., Yaniv M. and Oren M. (1991) "Wild-type p53 can down-modulate the activity of various promoters." Proc Natl Acad Sci U S A **88**(22): 9979-9983.

Gnarra J. R., Tory K., Weng Y., Schmidt L., Wei M. H., Li H., Latif F., Liu S., Chen F., Duh F. M. and et al. (1994) "Mutations of the VHL tumour suppressor gene in renal carcinoma." Nat Genet **7**(1): 85-90.

Gnarra J. R., Ward J. M., Porter F. D., Wagner J. R., Devor D. E., Grinberg A., Emmert-Buck M. R., Westphal H., Klausner R. D. and Linehan W. M. (1997) "Defective placental vasculogenesis causes embryonic lethality in VHL-deficient mice." Proc Natl Acad Sci U S A **94**(17): 9102-9107.

Gomez-Fabre P. M., Aledo J. C., Del Castillo-Olivares A., Alonso F. J., Nunez De Castro I., Campos J. A. and Marquez J. (2000) "Molecular cloning, sequencing and expression studies of the human breast cancer cell glutaminase." Biochem J **345 Pt 2**: 365-375.

Gordan J. D., Bertout J. A., Hu C. J., Diehl J. A. and Simon M. C. (2007) "HIF-2alpha promotes hypoxic cell proliferation by enhancing c-myc transcriptional activity." Cancer Cell **11**(4): 335-347.

Gordan J. D. and Simon M. C. (2007) "Hypoxia-inducible factors: central regulators of the tumor phenotype." Curr Opin Genet Dev **17**(1): 71-77.
Grignon D. J. and Che M. (2005) "Clear cell renal cell carcinoma." Clin Lab Med **25**(2): 305-316.
Gwinn D. M., Shackelford D. B., Egan D. F., Mihaylova M. M., Mery A., Vasquez D. S., Turk B. E. and Shaw R. J. (2008) "AMPK phosphorylation of raptor mediates a metabolic checkpoint." Mol Cell **30**(2): 214-226.
Haase V. H., Glickman J. N., Socolovsky M. and Jaenisch R. (2001) "Vascular tumors in livers with targeted inactivation of the von Hippel-Lindau tumor suppressor." Proc Natl Acad Sci U S A **98**(4): 1583-1588.
Hadad S., Baker L., Quinlan P., Robertson K., Bray S., Thomson G., Kellock D., Jordan L., Purdie C., Hardie D., Fleming S. and Thompson A. (2009) "Histological evaluation of AMPK signalling in primary breast cancer." BMC Cancer **9**(1): 307.
Hallstrom T. C., Mori S. and Nevins J. R. (2008) "An E2F1-Dependent Gene Expression Program that Determines the Balance between Proliferation and Cell Death." Cancer Cell **13**(1): 11-22.
Hara K., Maruki Y., Long X., Yoshino K., Oshiro N., Hidayat S., Tokunaga C., Avruch J. and Yonezawa K. (2002) "Raptor, a binding partner of target of rapamycin (TOR), mediates TOR action." Cell **110**(2): 177-189.
Hara K., Yonezawa K., Weng Q. P., Kozlowski M. T., Belham C. and Avruch J. (1998) "Amino acid sufficiency and mTOR regulate p70 S6 kinase and eIF-4E BP1 through a common effector mechanism." J Biol Chem **273**(23): 14484-14494.
Hardie D. G. (2004) "The AMP-activated protein kinase pathway - new players upstream and downstream." Journal of Cell Science **117**(23): 5479-5487.
Hardie D. G. (2011) "Signal transduction: How cells sense energy." Nature **472**(7342): 176-177.
Hardie D. G. and Pan D. A. (2002) "Regulation of fatty acid synthesis and oxidation by the AMP-activated protein kinase." Biochem Soc Trans **30**(Pt 6): 1064-1070.
Harris D. T. (1983) "Hormonal therapy and chemotherapy of renal-cell carcinoma." Semin Oncol **10**(4): 422-430.
Hartwell L. H. and Weinert T. A. (1989) "Checkpoints: controls that ensure the order of cell cycle events." Science **246**(4930): 629-634.
Hawley S. A., Boudeau J., Reid J. L., Mustard K. J., Udd L., Makela T. P., Alessi D. R. and Hardie D. G. (2003) "Complexes between the LKB1 tumor suppressor, STRAD alpha/beta and MO25 alpha/beta are upstream kinases in the AMP-activated protein kinase cascade." J Biol **2**(4): 28.
Hawley S. A., Pan D. A., Mustard K. J., Ross L., Bain J., Edelman A. M., Frenguelli B. G. and Hardie D. G. (2005) "Calmodulin-dependent protein kinase kinase-beta is an alternative upstream kinase for AMP-activated protein kinase." Cell Metab **2**(1): 9-19.
Hawley S. A., Selbert M. A., Goldstein E. G., Edelman A. M., Carling D. and Hardie D. G. (1995) "5'-AMP activates the AMP-activated protein kinase cascade, and Ca2+/calmodulin activates the calmodulin-dependent protein kinase I cascade, via three independent mechanisms." J Biol Chem **270**(45): 27186-27191.
Hayden M. S. and Ghosh S. (2008) "Shared Principles in NF-κB Signaling." Cell **132**(3): 344-362.
Hemminki A. (1999) "The molecular basis and clinical aspects of Peutz-Jeghers syndrome." Cellular and Molecular Life Sciences CMLS **55**(5): 735-750.
Hemminki A., Markie D., Tomlinson I., Avizienyte E., Roth S., Loukola A., Bignell G., Warren W., Aminoff M., Hoglund P., Jarvinen H., Kristo P., Pelin K., Ridanpaa M., Salovaara R., Toro T., Bodmer W., Olschwang S., Olsen A. S., Stratton M. R., de la Chapelle A. and Aaltonen L. A. (1998) "A serine/threonine kinase gene defective in Peutz-Jeghers syndrome." Nature **391**(6663): 184-187.
Hemminki A., Markie D., Tomlinson I., Avizienyte E., Roth S., Loukola A., Bignell G., Warren W., Aminoff M., Hoglund P., Jarvinen H., Kristo P., Pelin K., Ridanpaa M., Salovaara R., Toro T., Bodmer W., Olschwang S., Olsen A. S., Stratton M. R., de

la Chapelle A. and Aaltonen L. A. (1998) "A serine/threonine kinase gene defective in Peutz-Jeghers syndrome." Nature **391**(6663): 184-187.
Hergovich A., Lisztwan J., Barry R., Ballschmieter P. and Krek W. (2003) "Regulation of microtubule stability by the von Hippel-Lindau tumour suppressor protein pVHL." Nat Cell Biol **5**(1): 64-70.
Herman J. G., Latif F., Weng Y., Lerman M. I., Zbar B., Liu S., Samid D., Duan D. S., Gnarra J. R., Linehan W. M. and et al. (1994) "Silencing of the VHL tumor-suppressor gene by DNA methylation in renal carcinoma." Proc Natl Acad Sci U S A **91**(21): 9700-9704.
Hervouet E., Simonnet H. and Godinot C. (2007) "Mitochondria and reactive oxygen species in renal cancer." Biochimie **89**(9): 1080-1088.
Hes F., Zewald R., Peeters T., Sijmons R., Links T., Verheij J., Matthijs G., Leguis E., Mortier G., van der Torren K., Rosman M., Lips C., Pearson P. and van der Luijt R. (2000) "Genotype-phenotype correlations in families with deletions in the von Hippel-Lindau (VHL) gene." Hum Genet **106**(4): 425-431.
Holz M. K., Ballif B. A., Gygi S. P. and Blenis J. (2005) "mTOR and S6K1 mediate assembly of the translation preinitiation complex through dynamic protein interchange and ordered phosphorylation events." Cell **123**(4): 569-580.
Hsu P. P., Kang S. A., Rameseder J., Zhang Y., Ottina K. A., Lim D., Peterson T. R., Choi Y., Gray N. S., Yaffe M. B., Marto J. A. and Sabatini D. M. (2011) "The mTOR-regulated phosphoproteome reveals a mechanism of mTORC1-mediated inhibition of growth factor signaling." Science **332**(6035): 1317-1322.
Hsu T., Adereth Y., Kose N. and Dammai V. (2006) "Endocytic function of von Hippel-Lindau tumor suppressor protein regulates surface localization of fibroblast growth factor receptor 1 and cell motility." J Biol Chem **281**(17): 12069-12080.
Hu W., Zhang C., Wu R., Sun Y., Levine A. and Feng Z. (2010) "Glutaminase 2, a novel p53 target gene regulating energy metabolism and antioxidant function." Proceedings of the National Academy of Sciences **107**(16): 7455-7460.
Hudson C. C., Liu M., Chiang G. G., Otterness D. M., Loomis D. C., Kaper F., Giaccia A. J. and Abraham R. T. (2002) "Regulation of Hypoxia-Inducible Factor 1α Expression and Function by the Mammalian Target of Rapamycin." Molecular and Cellular Biology **22**(20): 7004-7014.
Hurley R. L., Anderson K. A., Franzone J. M., Kemp B. E., Means A. R. and Witters L. A. (2005) "The Ca2+/calmodulin-dependent protein kinase kinases are AMP-activated protein kinase kinases." J Biol Chem **280**(32): 29060-29066.
Ikenoue T., Inoki K., Yang Q., Zhou X. and Guan K. L. (2008) "Essential function of TORC2 in PKC and Akt turn motif phosphorylation, maturation and signalling." EMBO J **27**(14): 1919-1931.
Iliopoulos O., Ohh M. and Kaelin W. G., Jr. (1998) "pVHL19 is a biologically active product of the von Hippel-Lindau gene arising from internal translation initiation." Proc Natl Acad Sci U S A **95**(20): 11661-11666.
Inoki K., Li Y., Zhu T., Wu J. and Guan K. L. (2002) "TSC2 is phosphorylated and inhibited by Akt and suppresses mTOR signalling." Nat Cell Biol **4**(9): 648-657.
Inoki K., Ouyang H., Zhu T., Lindvall C., Wang Y., Zhang X., Yang Q., Bennett C., Harada Y., Stankunas K., Wang C. Y., He X., MacDougald O. A., You M., Williams B. O. and Guan K. L. (2006) "TSC2 integrates Wnt and energy signals via a coordinated phosphorylation by AMPK and GSK3 to regulate cell growth." Cell **126**(5): 955-968.
Inoki K., Zhu T. and Guan K. L. (2003) "TSC2 mediates cellular energy response to control cell growth and survival." Cell **115**(5): 577-590.
Ishikawa J., Xu H.-J., Hu S.-X., Yandell D. W., Maeda S., Kamidono S., Benedict W. F. and Takahashi R. (1991) "Inactivation of the Retinoblastoma Gene in Human Bladder and Renal Cell Carcinomas." Cancer Research **51**(20): 5736-5743.
Ivan M., Kondo K., Yang H., Kim W., Valiando J., Ohh M., Salic A., Asara J. M., Lane W. S. and Kaelin W. G., Jr. (2001) "HIFalpha targeted for VHL-mediated destruction

by proline hydroxylation: implications for O2 sensing." Science **292**(5516): 464-468.
Jenne D. E., Reimann H., Nezu J., Friedel W., Loff S., Jeschke R., Muller O., Back W. and Zimmer M. (1998) "Peutz-Jeghers syndrome is caused by mutations in a novel serine threonine kinase." Nat Genet **18**(1): 38-43.
Jones R. G., Plas D. R., Kubek S., Buzzai M., Mu J., Xu Y., Birnbaum M. J. and Thompson C. B. (2005) "AMP-Activated Protein Kinase Induces a p53-Dependent Metabolic Checkpoint." Molecular Cell **18**(3): 283-293.
Jonkers J., Meuwissen R., van der Gulden H., Peterse H., van der Valk M. and Berns A. (2001) "Synergistic tumor suppressor activity of BRCA2 and p53 in a conditional mouse model for breast cancer." Nat Genet **29**(4): 418-425.
Kaelin W. G. (2002) "Molecular basis of the VHL hereditary cancer syndrome." Nature Reviews Cancer **2**(9): 673-682.
Kamura T., Koepp D. M., Conrad M. N., Skowyra D., Moreland R. J., Iliopoulos O., Lane W. S., Kaelin W. G., Jr., Elledge S. J., Conaway R. C., Harper J. W. and Conaway J. W. (1999) "Rbx1, a component of the VHL tumor suppressor complex and SCF ubiquitin ligase." Science **284**(5414): 657-661.
Keith B., Johnson R. S. and Simon M. C. (2012) "HIF1alpha and HIF2alpha: sibling rivalry in hypoxic tumour growth and progression." Nat Rev Cancer **12**(1): 9-22.
Kelly T. J. and Brown G. W. (2000) "Regulation of chromosome replication." Annu Rev Biochem **69**: 829-880.
Kim D. H., Sarbassov D. D., Ali S. M., Latek R. R., Guntur K. V., Erdjument-Bromage H., Tempst P. and Sabatini D. M. (2003) "GbetaL, a positive regulator of the rapamycin-sensitive pathway required for the nutrient-sensitive interaction between raptor and mTOR." Mol Cell **11**(4): 895-904.
Kim J. W., Tchernyshyov I., Semenza G. L. and Dang C. V. (2006) "HIF-1-mediated expression of pyruvate dehydrogenase kinase: a metabolic switch required for cellular adaptation to hypoxia." Cell Metab **3**(3): 177-185.
Kim Y. H., Liang H., Liu X., Lee J.-S., Cho J. Y., Cheong J.-H., Kim H., Li M., Downey T. J., Dyer M. D., Sun Y., Sun J., Beasley E. M., Chung H. C., Noh S. H., Weinstein J. N., Liu C.-G. and Powis G. (2012) "AMPKα Modulation in Cancer Progression: Multilayer Integrative Analysis of the Whole Transcriptome in Asian Gastric Cancer." Cancer Research **72**(10): 2512-2521.
Kleymenova E., Everitt J. I., Pluta L., Portis M., Gnarra J. R. and Walker C. L. (2004) "Susceptibility to vascular neoplasms but no increased susceptibility to renal carcinogenesis in Vhl knockout mice." Carcinogenesis **25**(3): 309-315.
Koshiji M., Kageyama Y., Pete E. A., Horikawa I., Barrett J. C. and Huang L. E. (2004) "HIF-1alpha induces cell cycle arrest by functionally counteracting Myc." EMBO J **23**(9): 1949-1956.
Kurban G., Duplan E., Ramlal N., Hudon V., Sado Y., Ninomiya Y. and Pause A. (2008) "Collagen matrix assembly is driven by the interaction of von Hippel-Lindau tumor suppressor protein with hydroxylated collagen IV alpha 2." Oncogene **27**(7): 1004-1012.
Kurth-Kraczek E. J., Hirshman M. F., Goodyear L. J. and Winder W. W. (1999) "5' AMP-activated protein kinase activation causes GLUT4 translocation in skeletal muscle." Diabetes **48**(8): 1667-1671.
Kuznetsova A. V., Meller J., Schnell P. O., Nash J. A., Ignacak M. L., Sanchez Y., Conaway J. W., Conaway R. C. and Czyzyk-Krzeska M. F. (2003) "von Hippel-Lindau protein binds hyperphosphorylated large subunit of RNA polymerase II through a proline hydroxylation motif and targets it for ubiquitination." Proc Natl Acad Sci U S A **100**(5): 2706-2711.
Labrecque M. P., Takhar M. K., Jagdeo J. M., Tam K. J., Chiu C., Wang T. Y., Prefontaine G. G., Cox M. E. and Beischlag T. V. (2014) "A TRIP230-retinoblastoma protein complex regulates hypoxia-inducible factor-1alpha-mediated transcription and cancer cell invasion." PLoS One **9**(6): e99214.

Lai S., Benedict W. F., Silver S. A. and El-Naggar A. K. (1997) "Loss of retinoblastoma gene function and heterozygosity at the RB locus in renal cortical neoplasms." Hum Pathol **28**(6): 693-697.

Langbein S., Frederiks W. M., zur Hausen A., Popa J., Lehmann J., Weiss C., Alken P. and Coy J. F. (2008) "Metastasis is promoted by a bioenergetic switch: New targets for progressive renal cell cancer." International Journal of Cancer **122**(11): 2422-2428.

Latif F., Tory K., Gnarra J., Yao M., Duh F. M., Orcutt M. L., Stackhouse T., Kuzmin I., Modi W., Geil L. and et al. (1993) "Identification of the von Hippel-Lindau disease tumor suppressor gene." Science **260**(5112): 1317-1320.

Lee S., Nakamura E., Yang H., Wei W., Linggi M. S., Sajan M. P., Farese R. V., Freeman R. S., Carter B. D., Kaelin W. G., Jr. and Schlisio S. (2005) "Neuronal apoptosis linked to EglN3 prolyl hydroxylase and familial pheochromocytoma genes: developmental culling and cancer." Cancer Cell **8**(2): 155-167.

Lehmann H., Vicari D. and Frew I. J. (2014). Combined deletion of Vhl and loss of the primary cilium dysregulates planar cell division and causes simple and atypical renal cysts. Unpublished data.

Leibovich B. C., Blute M. L., Cheville J. C., Lohse C. M., Frank I., Kwon E. D., Weaver A. L., Parker A. S. and Zincke H. (2003) "Prediction of progression after radical nephrectomy for patients with clear cell renal cell carcinoma." Cancer **97**(7): 1663-1671.

Levine A. J. and Oren M. (2009) "The first 30 years of p53: growing ever more complex." Nat Rev Cancer **9**(10): 749-758.

Li B., Qiu B., Lee D. S., Walton Z. E., Ochocki J. D., Mathew L. K., Mancuso A., Gade T. P., Keith B., Nissim I. and Simon M. C. (2014) "Fructose-1,6-bisphosphatase opposes renal carcinoma progression." Nature.

Liang J., Shao S. H., Xu Z.-X., Hennessy B., Ding Z., Larrea M., Kondo S., Dumont D. J., Gutterman J. U., Walker C. L., Slingerland J. M. and Mills G. B. (2007) "The energy sensing LKB1–AMPK pathway regulates p27kip1 phosphorylation mediating the decision to enter autophagy or apoptosis." Nature Cell Biology **9**(2): 218-224.

Lisztwan J., Imbert G., Wirbelauer C., Gstaiger M. and Krek W. (1999) "The von Hippel-Lindau tumor suppressor protein is a component of an E3 ubiquitin-protein ligase activity." Genes Dev **13**(14): 1822-1833.

Liu J., Zhang C., Lin M., Zhu W., Liang Y., Hong X., Zhao Y., Young K. H., Hu W. and Feng Z. (2014). Glutaminase 2 negatively regulates the PI3K/AKT signaling and shows tumor suppression activity in human hepatocellular carcinoma.

Liu L., Cash T. P., Jones R. G., Keith B., Thompson C. B. and Simon M. C. (2006) "Hypoxia-induced energy stress regulates mRNA translation and cell growth." Mol Cell **21**(4): 521-531.

Liu P., Gan W., Inuzuka H., Lazorchak A. S., Gao D., Arojo O., Liu D., Wan L., Zhai B., Yu Y., Yuan M., Kim B. M., Shaik S., Menon S., Gygi S. P., Lee T. H., Asara J. M., Manning B. D., Blenis J., Su B. and Wei W. (2013) "Sin1 phosphorylation impairs mTORC2 complex integrity and inhibits downstream Akt signalling to suppress tumorigenesis." Nature Cell Biology **15**(11): 1340-1350.

Lizcano J. M., Goransson O., Toth R., Deak M., Morrice N. A., Boudeau J., Hawley S. A., Udd L., Makela T. P., Hardie D. G. and Alessi D. R. (2004) "LKB1 is a master kinase that activates 13 kinases of the AMPK subfamily, including MARK/PAR-1." EMBO J **23**(4): 833-843.

Lobo C., Ruiz-Bellido M. A., Aledo J. C., Marquez J., Nunez De Castro I. and Alonso F. J. (2000) "Inhibition of glutaminase expression by antisense mRNA decreases growth and tumourigenicity of tumour cells." Biochem J **348 Pt 2**: 257-261.

Locasale J. W. and Cantley L. C. (2011) "Metabolic flux and the regulation of mammalian cell growth." Cell Metab **14**(4): 443-451.

Lonergan K. M., Iliopoulos O., Ohh M., Kamura T., Conaway R. C., Conaway J. W. and Kaelin W. G., Jr. (1998) "Regulation of hypoxia-inducible mRNAs by the von

Hippel-Lindau tumor suppressor protein requires binding to complexes containing elongins B/C and Cul2." Mol Cell Biol **18**(2): 732-741.
Loonstra A., Vooijs M., Beverloo H. B., Allak B. A., van Drunen E., Kanaar R., Berns A. and Jonkers J. (2001) "Growth inhibition and DNA damage induced by Cre recombinase in mammalian cells." Proceedings of the National Academy of Sciences **98**(16): 9209-9214.
Lowe S. W. and Sherr C. J. (2003) "Tumor suppression by Ink4a-Arf: progress and puzzles." Curr Opin Genet Dev **13**(1): 77-83.
Ma L., Chen Z., Erdjument-Bromage H., Tempst P. and Pandolfi P. P. (2005) "Phosphorylation and functional inactivation of TSC2 by Erk implications for tuberous sclerosis and cancer pathogenesis." Cell **121**(2): 179-193.
Ma X. M., Yoon S. O., Richardson C. J., Julich K. and Blenis J. (2008) "SKAR links pre-mRNA splicing to mTOR/S6K1-mediated enhanced translation efficiency of spliced mRNAs." Cell **133**(2): 303-313.
Mack F. A., Patel J. H., Biju M. P., Haase V. H. and Simon M. C. (2005) "Decreased Growth of Vhl-/- Fibrosarcomas Is Associated with Elevated Levels of Cyclin Kinase Inhibitors p21 and p27." Molecular and Cellular Biology **25**(11): 4565-4578.
Mack F. A., Rathmell W. K., Arsham A. M., Gnarra J., Keith B. and Simon M. C. (2003) "Loss of pVHL is sufficient to cause HIF dysregulation in primary cells but does not promote tumor growth." Cancer Cell **3**(1): 75-88.
Maddocks O. D. and Vousden K. H. (2011) "Metabolic regulation by p53." J Mol Med (Berl) **89**(3): 237-245.
Maher E. R. and Kaelin W. G., Jr. (1997) "von Hippel-Lindau disease." Medicine (Baltimore) **76**(6): 381-391.
Malumbres M., Harlow E., Hunt T., Hunter T., Lahti J. M., Manning G., Morgan D. O., Tsai L.-H. and Wolgemuth D. J. (2009) "Cyclin-dependent kinases: a family portrait." Nat Cell Biol **11**(11): 1275-1276.
Mandriota S. J., Turner K. J., Davies D. R., Murray P. G., Morgan N. V., Sowter H. M., Wykoff C. C., Maher E. R., Harris A. L., Ratcliffe P. J. and Maxwell P. H. (2002) "HIF activation identifies early lesions in VHL kidneys: evidence for site-specific tumor suppressor function in the nephron." Cancer Cell **1**(5): 459-468.
Manning B. D., Tee A. R., Logsdon M. N., Blenis J. and Cantley L. C. (2002) "Identification of the tuberous sclerosis complex-2 tumor suppressor gene product tuberin as a target of the phosphoinositide 3-kinase/akt pathway." Mol Cell **10**(1): 151-162.
Marino S., Vooijs M., van Der Gulden H., Jonkers J. and Berns A. (2000) "Induction of medulloblastomas in p53-null mutant mice by somatic inactivation of Rb in the external granular layer cells of the cerebellum." Genes Dev **14**(8): 994-1004.
Márquez J., López de la Oliva A. R., Matés J. M., Segura J. A. and Alonso F. J. (2006) "Glutaminase: A multifaceted protein not only involved in generating glutamate." Neurochemistry International **48**(6-7): 465-471.
Marsin A. S., Bertrand L., Rider M. H., Deprez J., Beauloye C., Vincent M. F., Van den Berghe G., Carling D. and Hue L. (2000) "Phosphorylation and activation of heart PFK-2 by AMPK has a role in the stimulation of glycolysis during ischaemia." Curr Biol **10**(20): 1247-1255.
Marsin A. S., Bouzin C., Bertrand L. and Hue L. (2002) "The stimulation of glycolysis by hypoxia in activated monocytes is mediated by AMP-activated protein kinase and inducible 6-phosphofructo-2-kinase." J Biol Chem **277**(34): 30778-30783.
Martin-Rufian M., Tosina M., Campos-Sandoval J. A., Manzanares E., Lobo C., Segura J. A., Alonso F. J., Mates J. M. and Marquez J. (2012) "Mammalian glutaminase Gls2 gene encodes two functional alternative transcripts by a surrogate promoter usage mechanism." PLoS One **7**(6): e38380.
Mathia S., Paliege A., Koesters R., Peters H., Neumayer H. H., Bachmann S. and Rosenberger C. (2013) "Action of hypoxia-inducible factor in liver and kidney from

mice with Pax8-rtTA-based deletion of von Hippel-Lindau protein." Acta Physiologica **207**(3): 565-576.
Maxwell P. H., Wiesener M. S., Chang G. W., Clifford S. C., Vaux E. C., Cockman M. E., Wykoff C. C., Pugh C. W., Maher E. R. and Ratcliffe P. J. (1999) "The tumour suppressor protein VHL targets hypoxia-inducible factors for oxygen-dependent proteolysis." Nature **399**(6733): 271-275.
Meierhofer D., Mayr J. A., Foetschl U., Berger A., Fink K., Schmeller N., Hacker G. W., Hauser-Kronberger C., Kofler B. and Sperl W. (2004) "Decrease of mitochondrial DNA content and energy metabolism in renal cell carcinoma." Carcinogenesis **25**(6): 1005-1010.
Menendez D., Inga A. and Resnick M. A. (2009) "The expanding universe of p53 targets." Nat Rev Cancer **9**(10): 724-737.
Merrill G. F., Kurth E. J., Hardie D. G. and Winder W. W. (1997) "AICA riboside increases AMP-activated protein kinase, fatty acid oxidation, and glucose uptake in rat muscle." Am J Physiol **273**(6 Pt 1): E1107-1112.
Metallo C. M., Gameiro P. A., Bell E. L., Mattaini K. R., Yang J., Hiller K., Jewell C. M., Johnson Z. R., Irvine D. J., Guarente L., Kelleher J. K., Vander Heiden M. G., Iliopoulos O. and Stephanopoulos G. (2011) "Reductive glutamine metabolism by IDH1 mediates lipogenesis under hypoxia." Nature.
Moch H. (2013) "An overview of renal cell cancer: Pathology and genetics." Seminars in Cancer Biology **23**(1): 3-9.
Montani M., Heinimann K., von Teichman A., Rudolph T., Perren A. and Moch H. (2010) "VHL-gene deletion in single renal tubular epithelial cells and renal tubular cysts: further evidence for a cyst-dependent progression pathway of clear cell renal carcinoma in von Hippel-Lindau disease." Am J Surg Pathol **34**(6): 806-815.
Moreno-Sánchez R., Rodríguez-Enríquez S., Marín-Hernández A. and Saavedra E. (2007) "Energy metabolism in tumor cells." FEBS Journal **274**(6): 1393-1418.
Morita S., Kojima T. and Kitamura T. (2000) "Plat-E: an efficient and stable system for transient packaging of retroviruses." Gene Ther **7**(12): 1063-1066.
Motzer R. J., Bacik J., Murphy B. A., Russo P. and Mazumdar M. (2002) "Interferon-alfa as a comparative treatment for clinical trials of new therapies against advanced renal cell carcinoma." J Clin Oncol **20**(1): 289-296.
Motzer R. J., Bander N. H. and Nanus D. M. (1996) "Renal-Cell Carcinoma." New England Journal of Medicine **335**(12): 865-875.
Mullen A. R., Wheaton W. W., Jin E. S., Chen P.-H., Sullivan L. B., Cheng T., Yang Y., Linehan W. M., Chandel N. S. and DeBerardinis R. J. (2011) "Reductive carboxylation supports growth in tumour cells with defective mitochondria." Nature.
Ohh M., Park C. W., Ivan M., Hoffman M. A., Kim T. Y., Huang L. E., Pavletich N., Chau V. and Kaelin W. G. (2000) "Ubiquitination of hypoxia-inducible factor requires direct binding to the beta-domain of the von Hippel-Lindau protein." Nat Cell Biol **2**(7): 423-427.
Ohh M., Yauch R. L., Lonergan K. M., Whaley J. M., Stemmer-Rachamimov A. O., Louis D. N., Gavin B. J., Kley N., Kaelin W. G., Jr. and Iliopoulos O. (1998) "The von Hippel-Lindau tumor suppressor protein is required for proper assembly of an extracellular fibronectin matrix." Mol Cell **1**(7): 959-968.
Ohta S., Lai E. W., Morris J. C., Bakan D. A., Klaunberg B., Cleary S., Powers J. F., Tischler A. S., Abu-Asab M., Schimel D. and Pacak K. (2006) "MicroCT for high-resolution imaging of ectopic pheochromocytoma tumors in the liver of nude mice." Int J Cancer **119**(9): 2236-2241.
Olalla L., Gutierrez A., Campos J. A., Khan Z. U., Alonso F. J., Segura J. A., Marquez J. and Aledo J. C. (2002) "Nuclear localization of L-type glutaminase in mammalian brain." J Biol Chem **277**(41): 38939-38944.
Orlova K. A. and Crino P. B. (2010) "The tuberous sclerosis complex." Annals of the New York Academy of Sciences **1184**(1): 87-105.

Pantuck A. J., An J., Liu H. and Rettig M. B. (2010) "NF-kappaB-dependent plasticity of the epithelial to mesenchymal transition induced by Von Hippel-Lindau inactivation in renal cell carcinomas." Cancer Res **70**(2): 752-761.

Papandreou I., Cairns R. A., Fontana L., Lim A. L. and Denko N. C. (2006) "HIF-1 mediates adaptation to hypoxia by actively downregulating mitochondrial oxygen consumption." Cell Metab **3**(3): 187-197.

Paraf F., Chauveau D., Chretien Y., Richard S., Grunfeld J. P. and Droz D. (2000) "Renal lesions in von Hippel-Lindau disease: immunohistochemical expression of nephron differentiation molecules, adhesion molecules and apoptosis proteins." Histopathology **36**(5): 457-465.

Patel V., Li L., Cobo-Stark P., Shao X., Somlo S., Lin F. and Igarashi P. (2008) "Acute kidney injury and aberrant planar cell polarity induce cyst formation in mice lacking renal cilia." Hum Mol Genet **17**(11): 1578-1590.

Pause A., Lee S., Worrell R. A., Chen D. Y., Burgess W. H., Linehan W. M. and Klausner R. D. (1997) "The von Hippel-Lindau tumor-suppressor gene product forms a stable complex with human CUL-2, a member of the Cdc53 family of proteins." Proc Natl Acad Sci U S A **94**(6): 2156-2161.

Pearce L. R., Huang X., Boudeau J., Pawlowski R., Wullschleger S., Deak M., Ibrahim A. F., Gourlay R., Magnuson M. A. and Alessi D. R. (2007) "Identification of Protor as a novel Rictor-binding component of mTOR complex-2." Biochem J **405**(3): 513-522.

Perez-Gomez C., Campos-Sandoval J. A., Alonso F. J., Segura J. A., Manzanares E., Ruiz-Sanchez P., Gonzalez M. E., Marquez J. and Mates J. M. (2005) "Co-expression of glutaminase K and L isoenzymes in human tumour cells." Biochem J **386**(Pt 3): 535-542.

Peterson T. R., Laplante M., Thoreen C. C., Sancak Y., Kang S. A., Kuehl W. M., Gray N. S. and Sabatini D. M. (2009) "DEPTOR is an mTOR inhibitor frequently overexpressed in multiple myeloma cells and required for their survival." Cell **137**(5): 873-886.

Phoenix K. N., Devarakonda C. V., Fox M. M., Stevens L. E. and Claffey K. P. (2012) "AMPKalpha2 Suppresses Murine Embryonic Fibroblast Transformation and Tumorigenesis." Genes Cancer **3**(1): 51-62.

Porter L. D., Ibrahim H., Taylor L. and Curthoys N. P. (2002) "Complexity and species variation of the kidney-type glutaminase gene." Physiol Genomics **9**(3): 157-166.

Prasanth S. G., Mendez J., Prasanth K. V. and Stillman B. (2004) "Dynamics of pre-replication complex proteins during the cell division cycle." Philos Trans R Soc Lond B Biol Sci **359**(1441): 7-16.

Ran F. A., Hsu P. D., Wright J., Agarwala V., Scott D. A. and Zhang F. (2013) "Genome engineering using the CRISPR-Cas9 system." Nat. Protocols **8**(11): 2281-2308.

Rankin E. B., Tomaszewski J. E. and Haase V. H. (2006) "Renal Cyst Development in Mice with Conditional Inactivation of the von Hippel-Lindau Tumor Suppressor." Cancer Research **66**(5): 2576-2583.

Raval R. R., Lau K. W., Tran M. G., Sowter H. M., Mandriota S. J., Li J. L., Pugh C. W., Maxwell P. H., Harris A. L. and Ratcliffe P. J. (2005) "Contrasting properties of hypoxia-inducible factor 1 (HIF-1) and HIF-2 in von Hippel-Lindau-associated renal cell carcinoma." Mol Cell Biol **25**(13): 5675-5686.

Reynolds M. R., Lane A. N., Robertson B., Kemp S., Liu Y., Hill B. G., Dean D. C. and Clem B. F. (2014) "Control of glutamine metabolism by the tumor suppressor Rb." Oncogene **33**(5): 556-566.

Roe J. S., Kim H., Lee S. M., Kim S. T., Cho E. J. and Youn H. D. (2006) "p53 stabilization and transactivation by a von Hippel-Lindau protein." Mol Cell **22**(3): 395-405.

Roux P. P., Ballif B. A., Anjum R., Gygi S. P. and Blenis J. (2004) "Tumor-promoting phorbol esters and activated Ras inactivate the tuberous sclerosis tumor suppressor complex via p90 ribosomal S6 kinase." Proc Natl Acad Sci U S A **101**(37): 13489-13494.

Ruvinsky I., Sharon N., Lerer T., Cohen H., Stolovich-Rain M., Nir T., Dor Y., Zisman P. and Meyuhas O. (2005) "Ribosomal protein S6 phosphorylation is a determinant of cell size and glucose homeostasis." Genes Dev **19**(18): 2199-2211.

Salt I. P., Johnson G., Ashcroft S. J. and Hardie D. G. (1998) "AMP-activated protein kinase is activated by low glucose in cell lines derived from pancreatic beta cells, and may regulate insulin release." Biochem J **335 (Pt 3)**: 533-539.

Sancak Y., Thoreen C. C., Peterson T. R., Lindquist R. A., Kang S. A., Spooner E., Carr S. A. and Sabatini D. M. (2007) "PRAS40 is an insulin-regulated inhibitor of the mTORC1 protein kinase." Mol Cell **25**(6): 903-915.

Sanchez-Cespedes M., Parrella P., Esteller M., Nomoto S., Trink B., Engles J. M., Westra W. H., Herman J. G. and Sidransky D. (2002) "Inactivation of LKB1/STK11 is a common event in adenocarcinomas of the lung." Cancer Res **62**(13): 3659-3662.

Sarbassov D. D., Ali S. M., Kim D. H., Guertin D. A., Latek R. R., Erdjument-Bromage H., Tempst P. and Sabatini D. M. (2004) "Rictor, a novel binding partner of mTOR, defines a rapamycin-insensitive and raptor-independent pathway that regulates the cytoskeleton." Curr Biol **14**(14): 1296-1302.

Sarbassov D. D., Guertin D. A., Ali S. M. and Sabatini D. M. (2005) "Phosphorylation and regulation of Akt/PKB by the rictor-mTOR complex." Science **307**(5712): 1098-1101.

Sato Y., Yoshizato T., Shiraishi Y., Maekawa S., Okuno Y., Kamura T., Shimamura T., Sato-Otsubo A., Nagae G., Suzuki H., Nagata Y., Yoshida K., Kon A., Suzuki Y., Chiba K., Tanaka H., Niida A., Fujimoto A., Tsunoda T., Morikawa T., Maeda D., Kume H., Sugano S., Fukayama M., Aburatani H., Sanada M., Miyano S., Homma Y. and Ogawa S. (2013) "Integrated molecular analysis of clear-cell renal cell carcinoma." Nat Genet **45**(8): 860-867.

Saucedo L. J., Gao X., Chiarelli D. A., Li L., Pan D. and Edgar B. A. (2003) "Rheb promotes cell growth as a component of the insulin/TOR signalling network." Nat Cell Biol **5**(6): 566-571.

Schafer Z. T., Grassian A. R., Song L., Jiang Z., Gerhart-Hines Z., Irie H. Y., Gao S., Puigserver P. and Brugge J. S. (2009) "Antioxidant and oncogene rescue of metabolic defects caused by loss of matrix attachment." Nature **461**(7260): 109-113.

Schietke R. E., Hackenbeck T., Tran M., Gunther R., Klanke B., Warnecke C. L., Knaup K. X., Shukla D., Rosenberger C., Koesters R., Bachmann S., Betz P., Schley G., Schodel J., Willam C., Winkler T., Amann K., Eckardt K. U., Maxwell P. and Wiesener M. S. (2012) "Renal tubular HIF-2alpha expression requires VHL inactivation and causes fibrosis and cysts." PLoS One **7**(1): e31034.

Schley G., Klanke B., Schödel J., Forstreuter F., Shukla D., Kurtz A., Amann K., Wiesener M. S., Rosen S., Eckardt K.-U., Maxwell P. H. and Willam C. (2011) "Hypoxia-Inducible Transcription Factors Stabilization in the Thick Ascending Limb Protects against Ischemic Acute Kidney Injury." Journal of the American Society of Nephrology **22**(11): 2004-2015.

Seizinger B. R., Rouleau G. A., Ozelius L. J., Lane A. H., Farmer G. E., Lamiell J. M., Haines J., Yuen J. W., Collins D., Majoor-Krakauer D. and et al. (1988) "Von Hippel-Lindau disease maps to the region of chromosome 3 associated with renal cell carcinoma." Nature **332**(6161): 268-269.

Semenza G. L., Roth P. H., Fang H. M. and Wang G. L. (1994) "Transcriptional regulation of genes encoding glycolytic enzymes by hypoxia-inducible factor 1." Journal of Biological Chemistry **269**(38): 23757-23763.

Serrano M., Hannon G. J. and Beach D. (1993) "A new regulatory motif in cell-cycle control causing specific inhibition of cyclin D/CDK4." Nature **366**(6456): 704-707.

Shackelford D. B. and Shaw R. J. (2009) "The LKB1-AMPK pathway: metabolism and growth control in tumour suppression." Nat Rev Cancer **9**(8): 563-575.

Shao X., Johnson J. E., Richardson J. A., Hiesberger T. and Igarashi P. (2002) "A Minimal Ksp-Cadherin Promoter Linked to a Green Fluorescent Protein Reporter

Gene Exhibits Tissue-Specific Expression in the Developing Kidney and Genitourinary Tract." Journal of the American Society of Nephrology **13**(7): 1824-1836.

Shao X., Somlo S. and Igarashi P. (2002) "Epithelial-Specific Cre/lox Recombination in the Developing Kidney and Genitourinary Tract." Journal of the American Society of Nephrology **13**(7): 1837-1846.

Shapiro R. A., Farrell L., Srinivasan M. and Curthoys N. P. (1991) "Isolation, characterization, and in vitro expression of a cDNA that encodes the kidney isoenzyme of the mitochondrial glutaminase." J Biol Chem **266**(28): 18792-18796.

Shaw R. J., Bardeesy N., Manning B. D., Lopez L., Kosmatka M., DePinho R. A. and Cantley L. C. (2004) "The LKB1 tumor suppressor negatively regulates mTOR signaling." Cancer Cell **6**(1): 91-99.

Shaw R. J., Kosmatka M., Bardeesy N., Hurley R. L., Witters L. A., DePinho R. A. and Cantley L. C. (2004) "The tumor suppressor LKB1 kinase directly activates AMP-activated kinase and regulates apoptosis in response to energy stress." Proceedings of the National Academy of Sciences **101**(10): 3329-3335.

Sherr C. J. and Roberts J. M. (1995) "Inhibitors of mammalian G1 cyclin-dependent kinases." Genes & Development **9**(10): 1149-1163.

Sherr C. J. and Roberts J. M. (1999) "CDK inhibitors: positive and negative regulators of G1-phase progression." Genes & Development **13**(12): 1501-1512.

Short J. D., Dere R., Houston K. D., Cai S.-L., Kim J., Bergeron J. M., Shen J., Liang J., Bedford M. T., Mills G. B. and Walker C. L. (2010) "AMPK-mediated phosphorylation of murine p27 at T197 promotes binding of 14-3-3 proteins and increases p27 stability." Molecular Carcinogenesis: n/a-n/a.

Short J. D., Houston K. D., Dere R., Cai S. L., Kim J., Johnson C. L., Broaddus R. R., Shen J., Miyamoto S., Tamanoi F., Kwiatkowski D., Mills G. B. and Walker C. L. (2008) "AMP-Activated Protein Kinase Signaling Results in Cytoplasmic Sequestration of p27." Cancer Research **68**(16): 6496-6506.

Shuin T., Torigoe S., Kubota Y., Kishida T., Hosaka M., Horikoshi T., Yao M., Kondo K., Sakai N., Danenberg K. and et al. (1995) "Retinoblastoma gene mutation in primary human renal cell carcinoma." Oncol Res **7**(2): 63-66.

Simonnet H., Alazard N., Pfeiffer K., Gallou C., Béroud C., Demont J., Bouvier R., Schägger H. and Godinot C. (2002) "Low mitochondrial respiratory chain content correlates with tumor aggressiveness in renal cell carcinoma." Carcinogenesis **23**(5): 759-768.

Srigley J. R., Delahunt B., Eble J. N., Egevad L., Epstein J. I., Grignon D., Hes O., Moch H., Montironi R., Tickoo S. K., Zhou M., Argani P. and Panel T. I. R. T. (2013) "The International Society of Urological Pathology (ISUP) Vancouver Classification of Renal Neoplasia." The American Journal of Surgical Pathology **37**(10): 1469-1489 1410.1097/PAS.1460b1013e318299f318292d318291.

Stapleton D., Mitchelhill K. I., Gao G., Widmer J., Michell B. J., Teh T., House C. M., Fernandez C. S., Cox T., Witters L. A. and Kemp B. E. (1996) "Mammalian AMP-activated protein kinase subfamily." J Biol Chem **271**(2): 611-614.

Stebbins C. E., Kaelin W. G., Jr. and Pavletich N. P. (1999) "Structure of the VHL-ElonginC-ElonginB complex: implications for VHL tumor suppressor function." Science **284**(5413): 455-461.

Stolle C., Glenn G., Zbar B., Humphrey J. S., Choyke P., Walther M., Pack S., Hurley K., Andrey C., Klausner R. and Linehan W. M. (1998) "Improved detection of germline mutations in the von Hippel-Lindau disease tumor suppressor gene." Hum Mutat **12**(6): 417-423.

Straube T., Elli A. F., Greb C., Hegele A., Elsasser H. P., Delacour D. and Jacob R. (2011) "Changes in the expression and subcellular distribution of galectin-3 in clear cell renal cell carcinoma." J Exp Clin Cancer Res **30**: 89.

Sun A., Bagella L., Tutton S., Romano G. and Giordano A. (2007) "From G0 to S phase: a view of the roles played by the retinoblastoma (Rb) family members in the Rb-E2F pathway." J Cell Biochem **102**(6): 1400-1404.

Sun R. C. and Denko N. C. (2014) "Hypoxic regulation of glutamine metabolism through HIF1 and SIAH2 supports lipid synthesis that is necessary for tumor growth." Cell Metab **19**(2): 285-292.

Suter M., Riek U., Tuerk R., Schlattner U., Wallimann T. and Neumann D. (2006) "Dissecting the role of 5'-AMP for allosteric stimulation, activation, and deactivation of AMP-activated protein kinase." J Biol Chem **281**(43): 32207-32216.

Suzuki S., Tanaka T., Poyurovsky M. V., Nagano H., Mayama T., Ohkubo S., Lokshin M., Hosokawa H., Nakayama T., Suzuki Y., Sugano S., Sato E., Nagao T., Yokote K., Tatsuno I. and Prives C. (2010) "Phosphate-activated glutaminase (GLS2), a p53-inducible regulator of glutamine metabolism and reactive oxygen species." Proceedings of the National Academy of Sciences **107**(16): 7461-7466.

Szeliga M., Obara-Michlewska M., Matyja E., Lazarczyk M., Lobo C., Hilgier W., Alonso F. J., Marquez J. and Albrecht J. (2009) "Transfection with liver-type glutaminase cDNA alters gene expression and reduces survival, migration and proliferation of T98G glioma cells." Glia **57**(9): 1014-1023.

Tanimoto K., Makino Y., Pereira T. and Poellinger L. (2000) "Mechanism of regulation of the hypoxia-inducible factor-1 alpha by the von Hippel-Lindau tumor suppressor protein." EMBO J **19**(16): 4298-4309.

TCGA (2013) "Comprehensive molecular characterization of clear cell renal cell carcinoma." Nature **499**(7456): 43-49.

Tee A. R., Fingar D. C., Manning B. D., Kwiatkowski D. J., Cantley L. C. and Blenis J. (2002) "Tuberous sclerosis complex-1 and -2 gene products function together to inhibit mammalian target of rapamycin (mTOR)-mediated downstream signaling." Proc Natl Acad Sci U S A **99**(21): 13571-13576.

Tello D., Balsa E., Acosta-Iborra B., Fuertes-Yebra E., Elorza A., Ordonez A., Corral-Escariz M., Soro I., Lopez-Bernardo E., Perales-Clemente E., Martinez-Ruiz A., Enriquez J. A., Aragones J., Cadenas S. and Landazuri M. O. (2011) "Induction of the mitochondrial NDUFA4L2 protein by HIF-1alpha decreases oxygen consumption by inhibiting Complex I activity." Cell Metab **14**(6): 768-779.

Thoma C. R., Frew I. J., Hoerner C. R., Montani M., Moch H. and Krek W. (2007) "pVHL and GSK3beta are components of a primary cilium-maintenance signalling network." Nat Cell Biol **9**(5): 588-595.

Thoma C. R., Frew I. J. and Krek W. (2007) "The VHL tumor suppressor: riding tandem with GSK3beta in primary cilium maintenance." Cell Cycle **6**(15): 1809-1813.

Thoma C. R., Toso A., Gutbrodt K. L., Reggi S. P., Frew I. J., Schraml P., Hergovich A., Moch H., Meraldi P. and Krek W. (2009) "VHL loss causes spindle misorientation and chromosome instability." Nat Cell Biol **11**(8): 994-1001.

Towler M. C., Fogarty S., Hawley S. A., Pan D. A., Martin D. M. A., Morrice N. A., McCarthy A., Galardo M. N., Meroni S. B., Cigorraga S. B., Ashworth A., Sakamoto K. and Hardie D. G. (2008) "A novel short splice variant of the tumour suppressor LKB1 is required for spermiogenesis." Biochem J **416**(1): 1-14.

Um S. H., Frigerio F., Watanabe M., Picard F., Joaquin M., Sticker M., Fumagalli S., Allegrini P. R., Kozma S. C., Auwerx J. and Thomas G. (2004) "Absence of S6K1 protects against age- and diet-induced obesity while enhancing insulin sensitivity." Nature **431**(7005): 200-205.

Unwin R. D., Craven R. A., Harnden P., Hanrahan S., Totty N., Knowles M., Eardley I., Selby P. J. and Banks R. E. (2003) "Proteomic changes in renal cancer and co-ordinate demonstration of both the glycolytic and mitochondrial aspects of the Warburg effect." PROTEOMICS **3**(8): 1620-1632.

Vander Heiden M. G., Cantley L. C. and Thompson C. B. (2009) "Understanding the Warburg effect: the metabolic requirements of cell proliferation." Science **324**(5930): 1029-1033.

Velletri T., Romeo F., Tucci P., Peschiaroli A., Annicchiarico-Petruzzelli M., Niklison-Chirou M. V., Amelio I., Knight R. A., Mak T. W., Melino G. and Agostini M. (2013)

"GLS2 is transcriptionally regulated by p73 and contributes to neuronal differentiation." Cell Cycle **12**(22): 3564-3573.
Vermeulen K., Van Bockstaele D. R. and Berneman Z. N. (2003) "The cell cycle: a review of regulation, deregulation and therapeutic targets in cancer." Cell Prolif **36**(3): 131-149.
Vichai V. and Kirtikara K. (2006) "Sulforhodamine B colorimetric assay for cytotoxicity screening." Nat Protoc **1**(3): 1112-1116.
von Teichman A., Comperat E., Behnke S., Storz M., Moch H. and Schraml P. (2011) "VHL mutations and dysregulation of pVHL- and PTEN-controlled pathways in multilocular cystic renal cell carcinoma." Mod Pathol **24**(4): 571-578.
Wang X., Li W., Williams M., Terada N., Alessi D. R. and Proud C. G. (2001) "Regulation of elongation factor 2 kinase by p90(RSK1) and p70 S6 kinase." EMBO J **20**(16): 4370-4379.
Warburg O. (1956) "On the origin of cancer cells." Science **123**(3191): 309-314.
Warburg O., Posener K. and Negelein E. (1924) "Ueber den stoffwechsel der tumoren." Biochemische Zeitschrift **152**(1): 319-344.
Welford S. M., Dorie M. J., Li X., Haase V. H. and Giaccia A. J. (2010) "Renal Oxygenation Suppresses VHL Loss-Induced Senescence That Is Caused by Increased Sensitivity to Oxidative Stress." Molecular and Cellular Biology **30**(19): 4595-4603.
Wenger R. H., Stiehl D. P. and Camenisch G. (2005) "Integration of oxygen signaling at the consensus HRE." Sci STKE **2005**(306): re12.
Whillier S., Garcia B., Chapman B. E., Kuchel P. W. and Raftos J. E. (2011) "Glutamine and alpha-ketoglutarate as glutamate sources for glutathione synthesis in human erythrocytes." FEBS J **278**(17): 3152-3163.
Wild P. J., Ikenberg K., Fuchs T. J., Rechsteiner M., Georgiev S., Fankhauser N., Noske A., Roessle M., Caduff R., Dellas A., Fink D., Moch H., Krek W. and Frew I. J. (2012) "p53 suppresses type II endometrial carcinomas in mice and governs endometrial tumour aggressiveness in humans." EMBO Mol Med **4**(8): 808-824.
Wilson K. F., Wu W. J. and Cerione R. A. (2000) "Cdc42 stimulates RNA splicing via the S6 kinase and a novel S6 kinase target, the nuclear cap-binding complex." J Biol Chem **275**(48): 37307-37310.
Wingo S. N., Gallardo T. D., Akbay E. A., Liang M. C., Contreras C. M., Boren T., Shimamura T., Miller D. S., Sharpless N. E., Bardeesy N., Kwiatkowski D. J., Schorge J. O., Wong K. K. and Castrillon D. H. (2009) "Somatic LKB1 mutations promote cervical cancer progression." PLoS One **4**(4): e5137.
Wise D. R. and Thompson C. B. (2010) "Glutamine addiction: a new therapeutic target in cancer." Trends in Biochemical Sciences **35**(8): 427-433.
Wise D. R., Ward P. S., Shay J. E. S., Cross J. R., Gruber J. J., Sachdeva U. M., Platt J. M., DeMatteo R. G., Simon M. C. and Thompson C. B. (2011) "Hypoxia promotes isocitrate dehydrogenase-dependent carboxylation of -ketoglutarate to citrate to support cell growth and viability." Proceedings of the National Academy of Sciences **108**(49): 19611-19616.
Woods A., Cheung P. C., Smith F. C., Davison M. D., Scott J., Beri R. K. and Carling D. (1996) "Characterization of AMP-activated protein kinase beta and gamma subunits. Assembly of the heterotrimeric complex in vitro." J Biol Chem **271**(17): 10282-10290.
Woods A., Dickerson K., Heath R., Hong S. P., Momcilovic M., Johnstone S. R., Carlson M. and Carling D. (2005) "Ca2+/calmodulin-dependent protein kinase kinase-beta acts upstream of AMP-activated protein kinase in mammalian cells." Cell Metab **2**(1): 21-33.
Woods A., Johnstone S. R., Dickerson K., Leiper F. C., Fryer L. G., Neumann D., Schlattner U., Wallimann T., Carlson M. and Carling D. (2003) "LKB1 is the upstream kinase in the AMP-activated protein kinase cascade." Curr Biol **13**(22): 2004-2008.

Wu X., Bayle J. H., Olson D. and Levine A. J. (1993) "The p53-mdm-2 autoregulatory feedback loop." Genes Dev **7**(7A): 1126-1132.
Wullschleger S., Loewith R. and Hall M. N. (2006) "TOR signaling in growth and metabolism." Cell **124**(3): 471-484.
Xiao B., Heath R., Saiu P., Leiper F. C., Leone P., Jing C., Walker P. A., Haire L., Eccleston J. F., Davis C. T., Martin S. R., Carling D. and Gamblin S. J. (2007) "Structural basis for AMP binding to mammalian AMP-activated protein kinase." Nature **449**(7161): 496-500.
Xiao B., Sanders M. J., Underwood E., Heath R., Mayer F. V., Carmena D., Jing C., Walker P. A., Eccleston J. F., Haire L. F., Saiu P., Howell S. A., Aasland R., Martin S. R., Carling D. and Gamblin S. J. (2011) "Structure of mammalian AMPK and its regulation by ADP." Nature **472**(7342): 230-233.
Xie L., Xiao K., Whalen E. J., Forrester M. T., Freeman R. S., Fong G., Gygi S. P., Lefkowitz R. J. and Stamler J. S. (2009) "Oxygen-regulated beta(2)-adrenergic receptor hydroxylation by EGLN3 and ubiquitylation by pVHL." Sci Signal **2**(78): ra33.
Yagoda A. and Bander N. H. (1989) "Failure of Cytotoxic Chemotherapy, 1983–1988, and the Emerging Role of Monoclonal Antibodies for Renal Cancer." Urologia Internationalis **44**(6): 338-345.
Yang H., Minamishima Y. A., Yan Q., Schlisio S., Ebert B. L., Zhang X., Zhang L., Kim W. Y., Olumi A. F. and Kaelin Jr W. G. (2007) "pVHL Acts as an Adaptor to Promote the Inhibitory Phosphorylation of the NF-κB Agonist Card9 by CK2." Molecular Cell **28**(1): 15-27.
Young A. P., Schlisio S., Minamishima Y. A., Zhang Q., Li L., Grisanzio C., Signoretti S. and Kaelin W. G. (2008) "VHL loss actuates a HIF-independent senescence programme mediated by Rb and p400." Nature Cell Biology **10**(3): 361-369.
Zbar B., Brauch H., Talmadge C. and Linehan M. (1987) "Loss of alleles of loci on the short arm of chromosome 3 in renal cell carcinoma." Nature **327**(6124): 721-724.
Zbar B., Kishida T., Chen F., Schmidt L., Maher E. R., Richards F. M., Crossey P. A., Webster A. R., Affara N. A., Ferguson-Smith M. A., Brauch H., Glavac D., Neumann H. P., Tisherman S., Mulvihill J. J., Gross D. J., Shuin T., Whaley J., Seizinger B., Kley N., Olschwang S., Boisson C., Richard S., Lips C. H., Lerman M. and et al. (1996) "Germline mutations in the Von Hippel-Lindau disease (VHL) gene in families from North America, Europe, and Japan." Hum Mutat **8**(4): 348-357.
Zhang H., Gao P., Fukuda R., Kumar G., Krishnamachary B., Zeller K. I., Dang Chi V. and Semenza G. L. (2007) "HIF-1 Inhibits Mitochondrial Biogenesis and Cellular Respiration in VHL-Deficient Renal Cell Carcinoma by Repression of C-MYC Activity." Cancer Cell **11**(5): 407-420.
Zhang Y., Gao X., Saucedo L. J., Ru B., Edgar B. A. and Pan D. (2003) "Rheb is a direct target of the tuberous sclerosis tumour suppressor proteins." Nat Cell Biol **5**(6): 578-581.
Zmijewski J. W., Banerjee S., Bae H., Friggeri A., Lazarowski E. R. and Abraham E. (2010) "Exposure to Hydrogen Peroxide Induces Oxidation and Activation of AMP-activated Protein Kinase." Journal of Biological Chemistry **285**(43): 33154-33164.